Novel approaches to aromatic C–H borylation

Matthew Cross

A thesis presented to

UNIVERSITY COLLEGE LONDON

In partial fulfilment of the requirements for the degree of

DOCTOR OF PHILOSOPHY

UCL Department of Chemistry
20 Gordon Street
London
WC1H 0AJ

Declaration

I, Matthew J Cross, confirm that the work presented in this thesis is my own. Where information has been derived from other sources, I confirm this has been acknowledged in the thesis.

……..

Abstract

This thesis primarily explores novel approaches to C–H borylation in substrates containing (hetero)arenes.

Chapter 1 provides an overview of the recent advances in aromatic C–H borylation, as well as free radical C–X borylation.

Chapter 2 sets out our objectives for this research programme.

Chapter 3.1 describes our attempts at performing the free radical borylation of aryl halides. The hypothesised protocol was to proceed *via* a base-free setup in the presence of an unsymmetrical diboron compound.

Chapter 3.2 explores the limitations of iridium-catalysed borylation by screening an array of complex, 'drug-like' molecules. Our results give insight into the compatibility of various heterocycles and functional groups with this methodology, where previously unknown. The details of a study are reported into the regioselectivity observed when 4-substituted quinolines are subjected to standard iridium-catalysed borylation conditions. The investigation aimed to determine if the product regioisomer distribution is governed by the nature of the 4-substituent.

Chapter 3.3 describes our attempts to devise a novel electrophilic borylation procedure mediated *via* the use of a late transition metal (Cu, Au). We report a simple and efficient method to transmetallate boron moieties (Bpin and Bdan) onto gold in high yields. A novel sp^2-sp^3 hybridised diboron compound is also reported (DIPA-dan diboron). However, its synthesis and isolation require optimisation in order to obtain sufficient quantities to probe reactivity.

Chapter 3.4 reports a novel method to mono-*N*-methylate primary amines *via* the use of a halomethylboronate reagent. A boron-centred spiro compound was detected as a side product, thought to form *via* the activation of nitrile solvent. A series of novel structural analogues are reported, including an X-ray crystal structure.

Impact statement

(Hetero)arenes are used in abundance as agrochemicals, pharmaceuticals and dyes. But, modifying aromatic compounds into closely related analogues is challenging, given the ubiquitous and inert nature of C–H bonds. Thus, aromatic C–H borylation represents a huge field of research in synthetic chemistry.

Our work on iridium-catalysed borylation highlighted the limitations of this methodology when larger substrates are employed with basic heterocycles and polar functional groups. Our results can lead to more informed synthetic strategies being devised in an academic setting.

Our work with copper and gold complexes found simple and efficient routes to forming M–B bonds (M = metal). This lays the foundation for the development of a novel C–H borylation protocol that doesn't require the use of a glovebox.

We also report a novel method to selectively mono-*N*-methylate primary amines with a cheap and non-toxic boron reagent. An analysis of reactions used in medicinal chemistry at GSK, Pfizer and AstraZeneca in 2011 identified heteroatom alkylation as the most common class of reaction.[†] Thus, we anticipate our work being of great interest to the pharmaceutical industry. Moreover, the diazaborole side products we identified during this work hold potential for use as chiral auxiliaries or drug analogues.

[†]Roughley, S. D. & Jordan, A. M. The medicinal chemist's toolbox: an analysis of reactions used in the pursuit of drug candidates. *J. Med. Chem.* **54**, 3451–3471 (2011).

Acknowledgements

My foremost thanks go to Tom Sheppard for his excellent supervision over the course of my PhD, particularly during the Covid-19 pandemic. I found his enthusiasm and glass-half-full approach uplifting, which was often just what I needed when dealing with a series of failed reactions! It is unfortunate to be leaving in the midst of my most productive and exciting project to date, but I hope I've made a helpful contribution to what should be an interesting paper.

Thank you also to my industrial supervisor, Rob Law, for his guidance during my placement at GSK, not least because I stayed three months longer than I was contractually obliged to. I am very grateful for the time he gave up to show me around the site and make the experience as enriching as possible.

The KLB lab I leave with a very heavy heart, despite its wildly fluctuating temperatures, beeping fumehoods and culture of petty theft. Of my day-to-day colleagues, my first thanks go to Marco, who helped me find my feet at the start of my project and inducted me into the world of boron. I also enjoyed getting to know Cal and Joe, despite not having the chance to work directly alongside either of them.

Victor was an excellent colleague, lovely bloke and a remarkably productive worker – I'm sure he'll go far. Same too with Rachel, who was an absolute pleasure to work alongside in the little alcove of Sheppard desks – laidback, helpful and a great taste in music – not to mention, an enviably high number of strings to her bow, beyond chemistry!

I'll miss, too, my boron comrade, Usman and his mischievous sense of humour. Unfortunately, despite overlapping for two years, I feel like we only worked alongside one another for a few months because of our respective placements, lab closure and being in alternate cohorts. I hope he doesn't run into too many obstacles finishing off the work that I passed to him.

Titan of the KLB, Dave, is the colleague every workplace needs. Generous with his time, chilled out, tidy and always has an inventive DIY solution to a practical issue. It's no wonder lab members would traverse great distances to seek his wisdom and advice. As I write this, he has recently moved on from the KLB, much to the loss of the lab.

Arriving later on my PhD timeline, Sahra was a kind and thoughtful soul who brought a whole new level of standards to the KLB. The shake-up she gave the lab upon arriving revolutionised our day-to-day practices and made for a safer, more organised and less cluttered workplace. I wish, too, that I could've overlapped for longer with Richard Procter – not just for the dry wit and late-working companionship but the expert knowledge of boron and air-sensitive techniques. He often had smart suggestions to try when my chemistry was letting me down.

Will was good fun to have around and always had interesting conversation to offer at the lunch table. Same too with Phyllida – a real bundle of joy with remarkable energy for someone who spends several hours a day swimming. It was a pleasure, also, to share a desk with Matt for the last few months. I hope he doesn't mind that I took the paper tray away with me, but I promise I bought it with my own money.

I must also give a nod to members of the Baker and Chudasama groups, of whom there are far too many to list. However, I particularly enjoyed the company of Archie, Nehaal, Calise and Richard Spears. There was also a nice trickle of Masters students – my personal favourite being Kathy, despite her horrifying disregard for health and safety. I enjoyed collaborating very briefly with Helen Allan towards the end of my PhD and I'm extremely grateful for her assistance in structure elucidation. Beyond the KLB, Eve and Esther, were a delight to catch up with every now and then and I wish them well.

Thanks also to the technical staff, Abil Aliev and Kersti Karu, for their efficient and dedicated upkeep of the NMR and mass spectrometry services, respectively. Same too, to Krešo Bučar for providing a lovely crystal structure of one of my compounds. I should also acknowledge Tony Field for managing chemical stores efficiently.

Away from Chemistry, I loved having two old school friends, Harry and Dave, also doing PhDs nearby for my final two years. Whether it was Pint Club® or Coffee Club®, meeting up was always a laugh and I will greatly miss it.

Thank you also to my parents, Richard and Vicky, for their unwavering support over the course of my PhD. I'm particularly grateful for when they rescued me with a quickfire loan when my cash flow was interrupted due to an administrative oversight.

Lastly, thanks to my rock, Jacky, who I met three-and-a-half months into my PhD and so has been a defining figure of the journey. When she asked me on our first date what my PhD was about, she had to sit down on the floor of the pub as I was explaining because she thought she was going to faint. Make of that what you will. But she has always been my number one fan throughout and helped me to escape the sometimes-cruel reality of my PhD when I got home each night.

Dedicated to my maternal grandmother, Sheila Margaret Bentley (1937 – 2022), who passed away shortly before the submission of this thesis. She wouldn't have cared much for the contents but would have probably still requested a copy.

Contents

Abbreviations

Ac = Acyl

acac = Acetylacetonate

aq = Aqueous

Ar = Aryl

BBN = Borabicyclo[3.3.1]nonane

Boc = *tert*-Butyloxycarbonyl

bpy = 2,2’-Bipyridine

cat = Catecholato

cat. = Catalyst

Cbz = Benzyl carbamate

COD = 1,5-Cyclooctadiene

COE = Cyclooctene

conc. = Concentrated

Conv = Conversion

COSY = Correlation Spectroscopy

Cp = Cyclopentadienyl

CPME = Cyclopentyl methyl ether

Cy = Cyclohexyl

d = Days

dan = 1,8-Naphthalenediaminato

DBN = 1,5-Diazabicyclo[4.3.0]non-5-ene

DBU = 1,8-Diazabicyclo[5.4.0]undec-7-ene

DCE = 1,2-Dichloroethane

DCM = Dichloromethane

DFT = Density Functional Theory

Dioxane = 1,4-Dioxane

dil = Dilute

DIPA = Diisopropanolaminato

DIPEA = *N*,*N*-Diisopropylethylamine

dmabpy = 4,4’-Bis(dimethylamino)-2,2’-bipyridine

DME = 1,2-Dimethoxyethane

DMF = *N*,*N*-Dimethylformamide

DMSO = Dimethylsulphoxide

dtbpy = 4,4’-Di-*tert*-butyl-2,2’-dipyridyl

EDG = Electron-donating group

EPR = Electron paramagnetic resonance

eq. = Equivalents

Et = Ethyl

EWG = Electron-withdrawing group

h = Hours

HBX = 1-Hydroxy-1,2-benziodoxol-3(1*H*)-one

Het = Hetero

HMBC = Heteronuclear multiple bond correlation

HOMO = Highest occupied molecular orbital

HSQC = Heteronuclear single quantum coherence

HRMS = High resolution mass spectrometry

i = *iso*

^{i}Pr = *iso*-Propyl

IPr = 1,3-Bis(2,6-diisopropylphenyl)imidazol-2-ylidene

LRMS = Low resolution mass spectrometry

m = *meta*

Me = Methyl

Mesyl = Methanesulphonyl

min = Minutes

mL = Millilitre

m.p. = Melting point

mTBD = 7-Methyl-1,5,7-triazabicyclo[4.4.0]dec-5-ene

MTBE = Methyl *tert*-butyl ether

n-Bu = Normal butyl

neop = Neopentyl glycolato

NHC = *N*-heterocyclic carbene

NOE = Nuclear Overhauser effect

NOESY = Nuclear Overhauser Effect Spectroscopy

NMR = Nuclear magnetic resonance

p = *para*

PBX = 1-Pivaloyloxy-1,2-benziodoxol-3(1*H*)-one

PDIPA = Pinacolato diisopropanolaminato

Ph = Phenyl

phen = Phenanthroline

pin = Pinacolato

Piv = Pivaloyl

ppm = Parts per million

Protac = Proteolysis Targeting Chimera

Py = Pyridine

R = Generic substituent

r.t. = Room temperature

s = Seconds

sat = Saturated

S_EAr = Electrophilic aromatic substitution

SED = Super electron donor

SET = Single electron transfer

SM = Starting material

TAME = *tert*-Amyl methyl ether

^tBu = *tert*-Butyl

Temp = Temperature

THF = Tetrahydrofuran

THQ = 1,2,3,4-Tetrahydroquinoline

TIPS = Triisopropylsilyl

TLC = Thin layer chromatography

TMDAM = *N*,*N*,*N'*,*N'*-Tetramethyldiaminomethane

TMEDA = *N,N,N',N'*-Tetramethylethylenediamine

TMG = *N*,*N*,*N'*,*N'*-Tetramethylguanidine

tmphen = 3,4,7,8-Tetramethyl-1,10-phenanthroline

tol = Tolyl

Tosyl; Tos = *para*-Toluenesulphonyl

OTf = Trifluoromethanesulphonate

UFF = Universal Force Field

US = United States (of America)

UV = Ultraviolet

XS = Excess

1 Introduction

1.1 Aromatic C–H borylation

Aromatic heterocycles are abundant in a vast range of synthetic compounds with commercial value. This includes herbicides (*e.g.* **1**), fungicides (*e.g.* **2**), insecticides (*e.g.* **3**), dyes (*e.g.* **4**), organic conductors (*e.g.* **5**) and, of course, many pharmaceuticals on the market today, such as hydroxychloroquine **6** (**Figure 1.1**).[1,2]

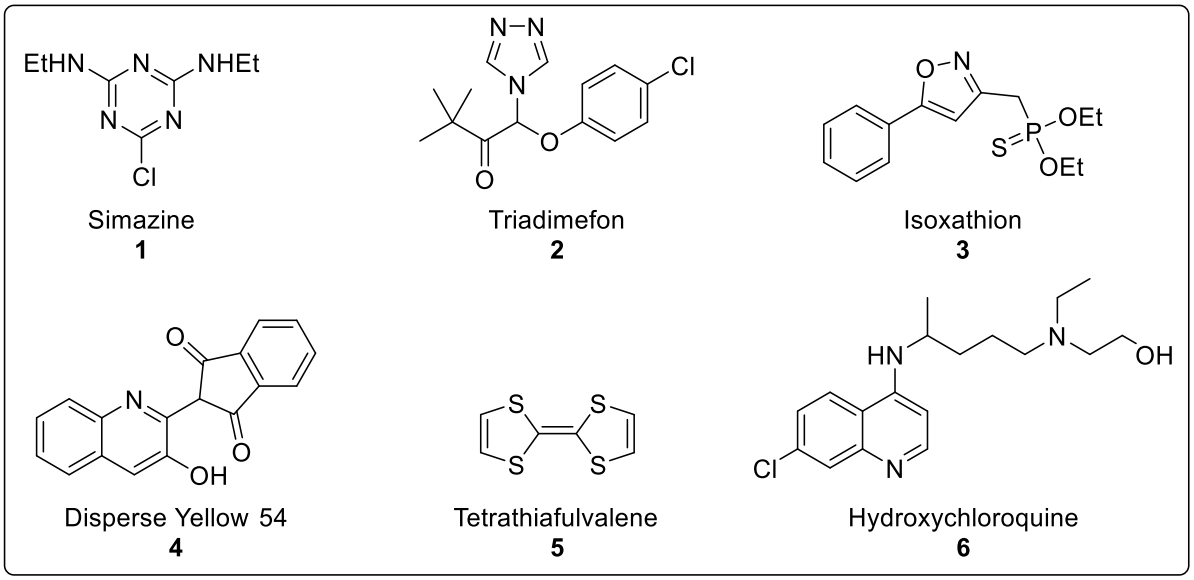

Figure 1.1: Synthetic heterocycles available commercially.

There has been intense research interest in the development of late-stage aromatic C–H functionalisation techniques, which allow for the direct modification of existing compounds into closely related analogues. The major advantage of this approach is that it avoids the need to revise existing synthetic routes. However, the regioselective functionalisation of structurally complex molecules can be exacerbated by nitrogen-containing heterocycles and polar functional groups. Finding methods to overcome these challenges represents a major goal in synthetic chemistry, although good progress has been made,[3] particularly in the field of drug discovery.[4,5]

One facet of aromatic C–H activation that has seen a particular explosion of interest over the last two decades has been C–B bond forming reactions. Replacing an aromatic C–H bond with a boryl group (–$B(OR)_2$) provides non-toxic, bench-stable aryl boronate esters. Traditionally, this would proceed in a multi-step fashion *via* halogenated and moisture sensitive intermediates.[6,7] However, direct methods are

more atom and step efficient, and represent the ideal for green and sustainable processes (**Scheme 1.1**).

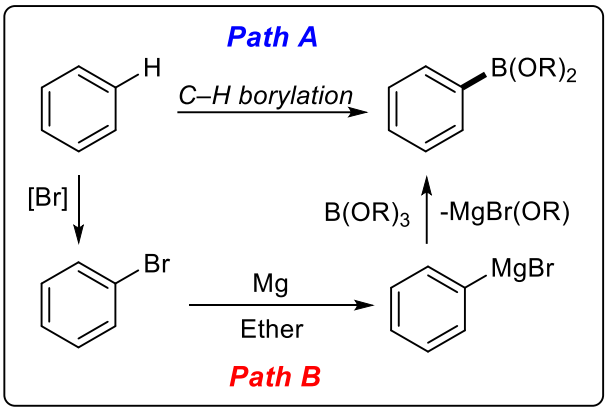

Scheme 1.1: Direct (Path A) and traditional (Path B) routes to aryl boronate esters from aromatic substrates.

Borylated (hetero)aromatic compounds are highly versatile intermediates that can undergo a broad scope of further derivatisation *via* techniques such as Suzuki coupling,[8] Chan-Lam Evans coupling,[9] trifluoromethylation,[10] oxidation,[11] halogenation[12] and cyanation[13] (**Scheme1.2**).

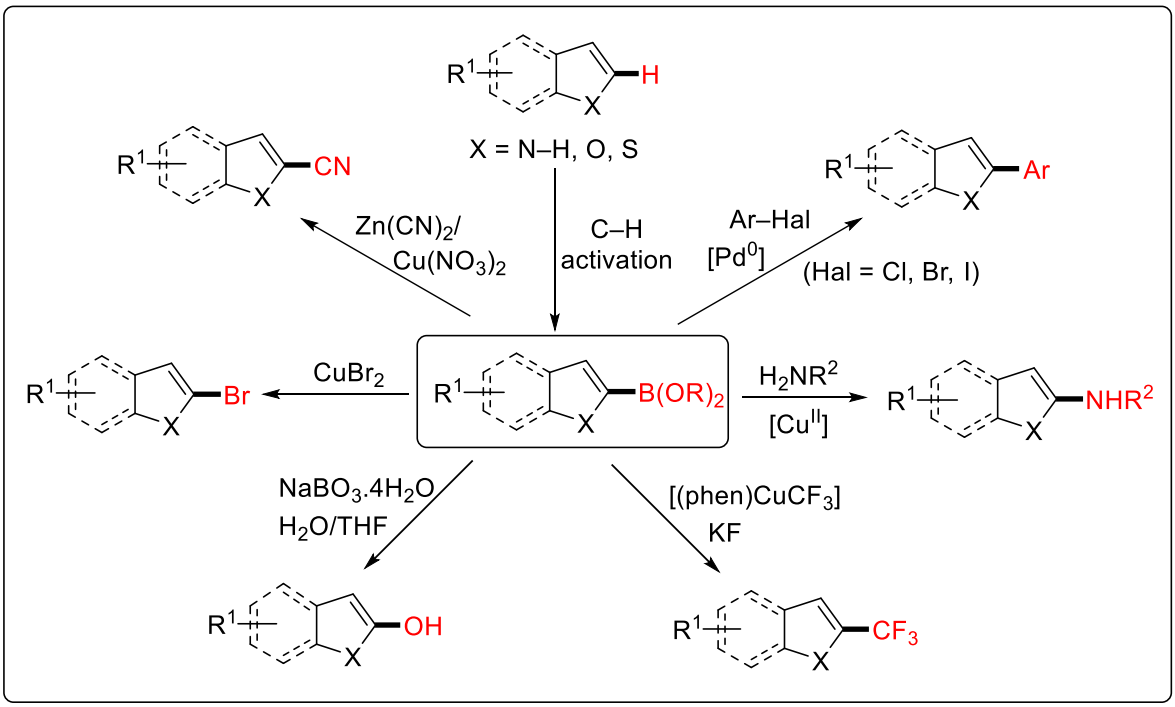

Scheme 1.2: Divergent scheme illustrating the synthetic versatility of (hetero)aryl boronate esters.

Since the turn of the century, significant advances in C–H borylation have been made *via* the use of iridium catalysis,[14–21] although catalytic methods using a wide array of other late transition metals have been reported. This includes other precious

metals such as ruthenium,[22] rhodium,[23] and platinum,[24] but also first-row d-block elements such as cobalt,[25] iron,[26] nickel[27] and zinc.[28] Considerable progress has also been made in developing C–H borylation methods that generate boron cations *in situ* and proceed *via* electrophilic aromatic substitution (hereafter S_EAr).[29,30]

In the last few years, techniques have been developed which are thought to develop boron radicals under mild conditions *via* homolytic cleavage of a B–B bond. Upon the outset of this project, aromatic C–X borylation had been reported (X = F, Cl, Br, I, OTf, N_2^+) proceeding *via* a free radical-initiated pathway.[31,32] This sub-field is undergoing rapid development and looks poised to enter the realm of C–H borylation.

This introduction aims to give a critical overview of the recent advances in iridium-catalysed and electrophilic C–H borylation, as well as recent progress in the burgeoning area of free radical borylation. In each case, particular attention will be paid to the scope, regioselectivity and functional group tolerance of reaction methodology with respect to aromatic and heteroaromatic substrates. In the interests of conciseness, other transition metal-catalysed techniques, will not be discussed, but an excellent summary of these methods can be found in a review by Li *et al*.[33]

1.2 Iridium-catalysed borylation

Catalytic borylation of C–H bonds was serendipitously discovered in 1995 by Hartwig and co-workers.[34] A solution of the simple metal-boryl complex [$CpFe(CO)_2Bcat$] was found to borylate a benzene solvent under photochemical conditions in a very good yield (**Scheme 1.3**). This activation process differed from typical C–H activation by metal-aryl complexes observed at the time as instead of alkyl groups being exchanged between the metal and the hydrocarbon, free functionalised products were formed.

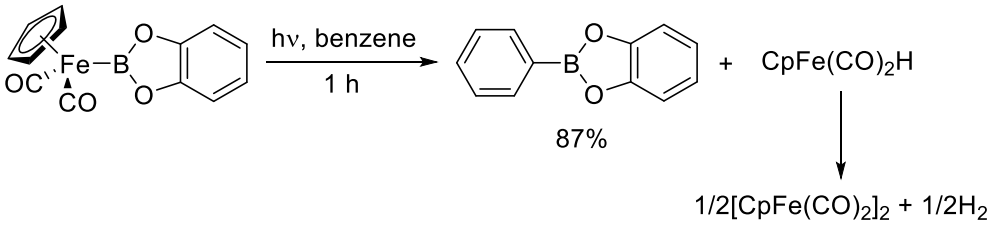

Scheme 1.3: Photochemical borylation of a benzene solvent.

Smith *et al.* carried out the first iridium-catalysed borylation of substituted arenes using the catalyst $Cp^*Ir(PMe_3)(H)(Bpin)$ ($Cp^* = \eta^5\text{-}C_5Me_5$). A vast excess of substrate was used, as well as high temperatures and high catalyst loading, but turnover numbers were low.[35] Electron-deficient substrates were found to be more reactive than electron-rich ones.

Hartwig later conducted studies in collaboration with Ishiyama, Miyaura and co-workers on catalyst systems based on the combination of an Ir^I precursor and a bipyridine ligand.[14] At the same time, Smith, Maleczka and co-workers worked on catalysts containing bisphosphine ligands, but these were found to be less active.[36] Hartwig's results showed that the Ir^I/bpy (bpy = 2,2'-bipyridine) system effected borylation of a series of different aromatic solvents in high yields under relatively mild conditions with low catalyst loading (**Scheme 1.4**).

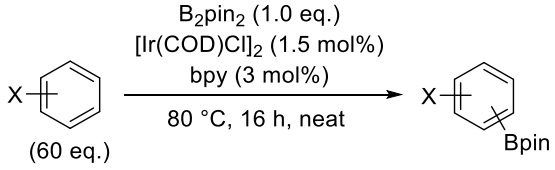

Scheme 1.4: Iridium-catalysed borylation of mono-, di- and polysubstituted benzene solvents.

These data also gave useful information on the regioselectivity of the borylation reaction which, for aromatic substrates, is almost completely governed by steric

effects. That is, a monosubstituted substrate would give a statistical ratio (2:1) of *meta* and *para* products, a 1,2-disubstituted arene will give exclusively the 1,2,4-trisubsubstituted product and a 1,3-disubstituted substrate will give solely the 1,3,5-trisubstituted product (**Figure 1.2**).

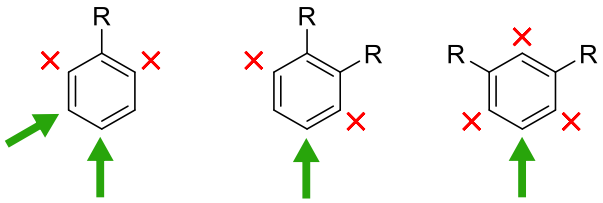

Figure 1.2: Preferred sites of borylation on substituted aromatic compounds.

1.2.1 Borylation of heteroarenes

Early work on the iridium-catalysed borylation of heteroarenes primarily involved the investigation of the selectivity of the reaction on five-membered heterocycles.[15–17] In 2002, Hartwig, Ishiyama and Miyaura reported the borylation of thiophene, furan and pyrrole catalysed by the combination of $[Ir(COD)Cl_2]_2$ (COD = 1,5-cyclooctadiene) and dtbpy (dtbpy = 4,4'-di-*tert*-butyl-2,2'-bipyridine) in octane at 80 – 100 °C.[15] In the preliminary reactions with thiophene and a bpy ligand, no product was detected when the reaction was carried out with 60 eq. substrate. This was thought to be due to the high coordinating ability of thiophene preventing the formation of the coordinatively unsaturated Ir^{III} tris-boryl species which is needed for C–H activation. The problem was solved by using 10 eq. of substrate diluted in 6 mL of octane (0.17 M). Borylation was observed exclusively at the 2-position with a 64% yield of monoborylated product which was later improved to 83% with dtbpy, thought to be due to enhanced solubility. The selectivity of monoborylation *vs.* diborylation was dependent on the stoichiometry of thiophene and B_2pin_2.

A representative set of heterocycles was then screened under optimised conditions to assess the scope and regioselectivity of the reaction (**Table 1.1**). Reactions with five-membered heterocycles other than thiophene (**Entry 1**) also provided 2-borylated products in high yields with some diborylated product (*ca.* 15%) (**Entries 2 and 3**). However, 2-methylthiophene gave exclusively the monoborylated product (**Entry 4**). Selective monoborylation of benzothiophene, benzofuran and indole was easily achieved as the activation barrier for reaction on the carbocycle is significantly higher than it is on the heterocycle (**Entries 5 – 7**). Reactions with

pyridine and quinoline required higher temperatures but the substrates were borylated in high yields at 100 °C. The products from the reaction with pyridine were a 2:1 mixture of 3-boryl and 4-boryl pyridine but quinoline was borylated exclusively at the 3-position (**Entries 8 and 9**).

Table 1.1: Iridium-catalysed borylation of heteroaromatic substrates.

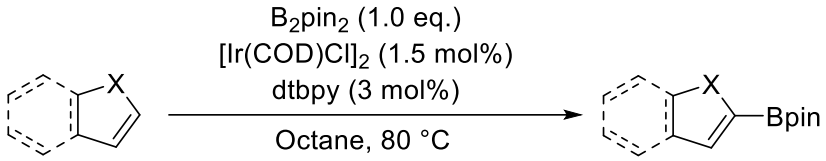

Entry	Product	% Yield	Entry	Product	% Yield	Entry	Product	% Yield
1	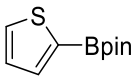	83[a]	**4**	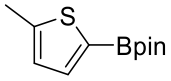	91	**7**	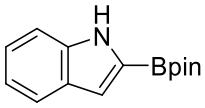	92
2	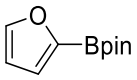	83[a]	**5**	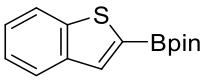	89	**8**	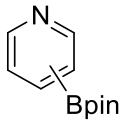	42[a,b]
3	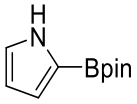	67[a]	**6**	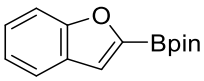	91	**9**	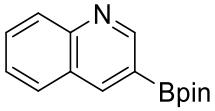	84[b]

[a]Diborylated products made in 12 – 17% yield. [b]Reaction carried out at 100 °C.

For five-membered heterocycles, the preference for borylation at the 2-position is due to the greater acidity of the α C–H bond over the β-position. With heteroarenes that contain a basic nitrogen such as pyridine, quinoline and other azines, borylation is observed β or γ to the basic nitrogen. Borylation is still thought to occur at the 2-position but the products undergo rapid protodeborylation.[20]

Protodeborylation is a well-known unwanted side reaction in organoboron chemistry and 2-pyridyl boronic acids are notorious for their susceptibility to it. It was initially put forward after a series of studies[37–40] by Kuivila and colleagues in the 1960s that protodeborylation of arene boronic acids proceeded *via* two mechanisms: an acid-catalysed process whereby H replaces B *via* an S_EAr process; or a base-catalysed route which was proposed to proceed *via* hydrolysis of the boronate anion ($[ArB(OH)_3]^-$) (**Scheme 1.5**).

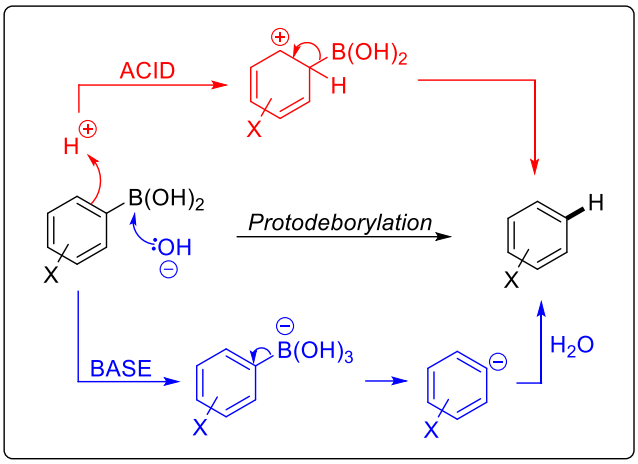

Scheme 1.5: Kuivila mechanisms for protodeborylation in aqueous acidic (red)[37] and basic (blue)[40] conditions.

A detailed kinetic study[41] was carried out by the group of Lloyd-Jones into the pH dependency on the rate of protodeborylation for a range of unstable boronic acids. 3- and 4-pyridyl boronic acids were found to undergo slow protodeborylation under heating and basic conditions ($t_{½}$ > 1 week, pH 12, 70 °C). Whereas 2-pyridyl boronic acids protodeborylate readily under heating and neutral conditions ($t_{½}$ = 25 – 50 s, pH 7, 70 °C). Interestingly, H^+/OH^- act as powerful inhibitors making the boronic acids unusually stable at extremes of pH. Between pH 4 and 8, a rapid equilibrium is established between the neutral species and an unstable zwitterionic boronate whose tendency to protodeborylate can be rationalised by the intramolecular stabilisation of the $B(OH)_3$ leaving group during C–B cleavage (**Scheme 1.6**). This hydrogen bonding from the pyridinium N–H effectively solvates the $B(OH)_3$. However, at higher pH, this interaction is attenuated and protodeborylation is slower.

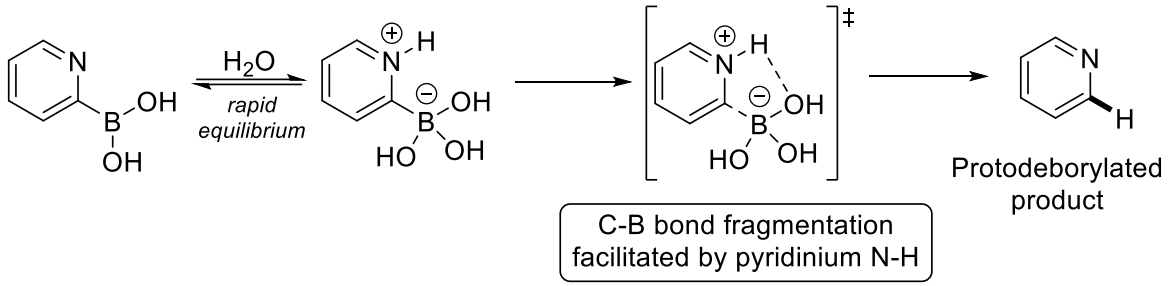

Scheme 1.6: Proposed mechanism for the protodeborylation of 2-pyridyl boronic acids.

1.2.2 Mechanism of the iridium-catalysed borylation reaction

Alongside their initial work investigating the reactivity and selectivity of the iridium-catalysed borylation of substituted arenes, Hartwig, Miyaura and Ishiyama focused on isolating potential Ir-boryl intermediates to help elucidate the

mechanism.[14] They synthesised the bis-boryl complex **8** from the dtbpy- and COD-ligated iridium complex **7** (**Scheme 1.7**). When **8** was stirred with B_2pin_2 and C_6D_6 at 80 °C for 5 h it generated C_6D_5–Bpin in 80% yield. However, when the same reaction was attempted without B_2pin_2, a reaction that would hypothetically complete the catalytic cycle, it simply regenerated B_2pin_2 and **7** without forming C_6D_5–Bpin.

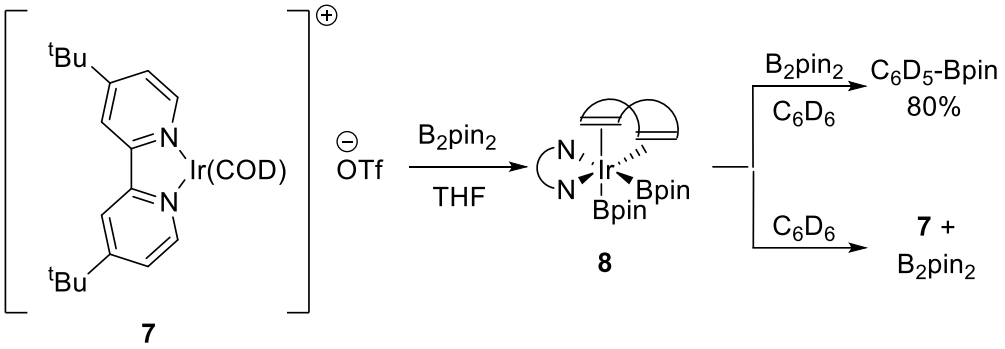

Scheme 1.7: Synthesis of bis-boryl **8** and subsequent regeneration of complex **7**.

In response to these data, iridium complexes were made that were ligated with COE (COE = cyclooctene) instead of COD. Reaction for 5 h at 50 °C between $[IrCl(COE)_2]_2$, 2 eq. of dtbpy, 10 eq. of B_2pin_2 in mesitylene solvent gave a complex in 15% yield. X-ray and spectroscopic data showed it to be the tris-boryl complex $[Ir(dtbpy)(COE)(Bpin)_3]$ **9** (**Figure 1.3**).

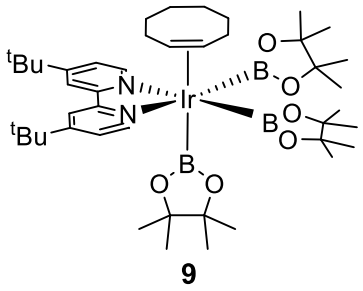

Figure 1.3: Tris-boryl complex **9**.

Dissolving complex **9** in C_6D_6 generated 3 eq. of Ph–Bpin in 80% yield within a few minutes at room temperature. As well as this, when reacted with a mixture of toluene and trifluoromethylbenzene, complex **9** demonstrated identical selectivity to that observed in the reactions when the precatalyst $[Ir(COD)Cl]_2$ was used in combination with bpy. Thus, there was strong evidence to suggest complex **9** was an intermediate in the catalytic cycle.

At the time there was no reliable method to synthesise **9** in high yields so mechanistic studies were very limited in their scope and depth. A DFT study[42] was carried out by Sakaki and colleagues on the mechanism of the reaction of arenes with the 16-electron species **10** that forms following the dissociation of COE from **9**. Their results suggested that the catalytic reaction occurred by a mechanism in which the arene reacts with complex **10** and the barriers calculated for the individual steps of the cycle implied that the turnover-limiting step was C–H bond cleavage of the arene.

Hartwig and colleagues later developed a procedure to prepare complex **9** in high yield (80 – 95%) (**Scheme 1.8**) and conducted a detailed mechanistic investigation into the reaction of arenes with this species.[43] Their results showed that **9** reacts with arenes following reversible dissociation of COE and corroborated the conclusion from Sakaki's study that C–H bond cleavage is turnover-limiting. However, the experimental value for this activation barrier (~8 – 12 kcal mol^{-1}) was found to be much less than the calculated value (20 kcal mol^{-1}), although it is crude to draw direct comparisons between the two sets of values as the experimental value accounts for the free energy changes involved in the dissociation of COE and association of C_6D_6. Electron-poor arenes were found to react faster than electron-rich arenes, as is the case with reactions when the catalyst is assembled *in situ*.

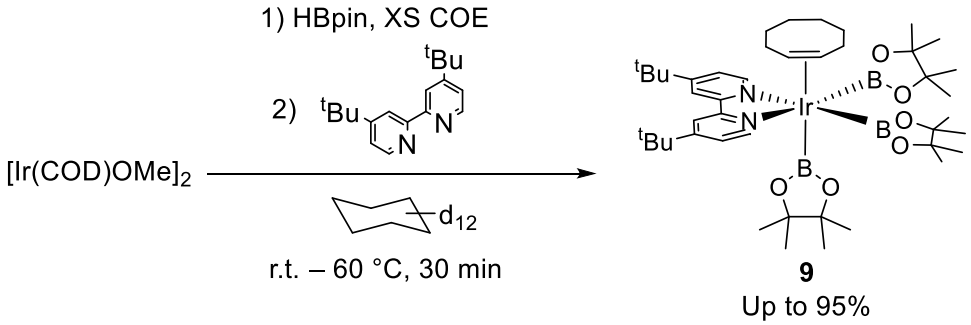

Scheme 1.8: Synthesis of complex **9** reported by Hartwig and colleagues.

A catalytic cycle consistent with the results of this study is shown below (**Scheme 1.9**). Oxidative addition of a (hetero)arene to complex **10** gives the seven-coordinate Ir^{V} species **11** which reductively eliminates (Het)Ar–Bpin to give a bis(boryl)Ir^{III} hydride complex **12**. Then, a molecule of B_2pin_2 oxidatively adds to the complex before reductively eliminating HBpin to regenerate **10**. HBpin also

participates in the catalytic cycle *via* a sequence of oxidative addition to **12**, followed by reductive elimination of H_2. This is thought to occur after consumption of B_2pin_2.

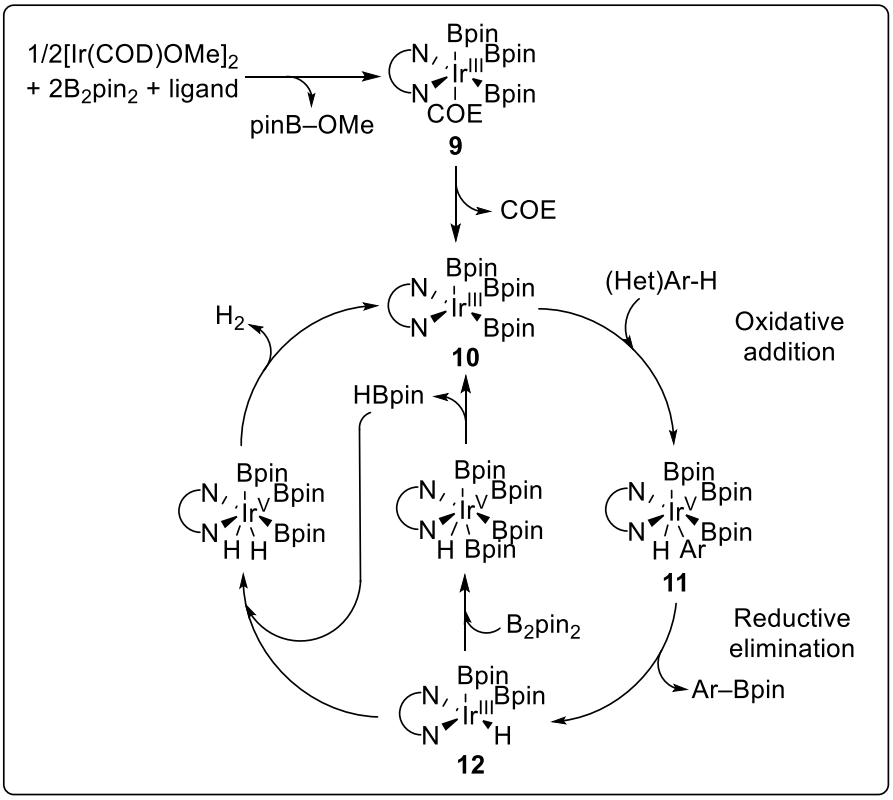

Scheme 1.9: Mechanism for the iridium-catalysed borylation of (hetero)arenes as proposed by Hartwig and colleagues.

It is worth mentioning that a borylation reaction proceeding *via* an $Ir^{I/III}$ cycle has been reported by Ozerov and colleagues.[44] The setup involves pincer-based iridium(I) complexes capable of activating C–H bonds, before reaction with HBpin to give an iridium dihydride. A stoichiometric quantity of sacrificial olefin is required to consume the equivalent of H_2 generated and return the iridium complex the 14-electron pincer complex (**Scheme 1.10**).

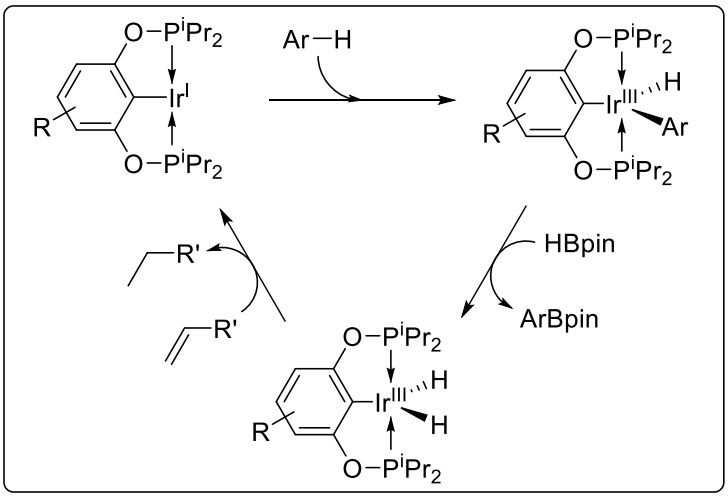

Scheme 1.10: Proposed catalytic cycle for C–H borylation catalysed by pincer complexes of iridium.

1.2.3 Iridium-catalysed borylation in late-stage functionalisation

As we have seen, the iridium-catalysed borylation reaction is tolerant of many simple heterocycles such as pyridine, furan, thiophene and indole. However, more complex 'drug-like' substrates which contain several heterocycles and more sensitive functionality present a much greater challenge. With more Lewis basic heteroatoms, the chance of the substrate coordinating to, and thus poisoning, the iridium catalyst is greater (**Scheme 1.11**). If the substrate concentration is high enough, the resting state of the catalyst can shift from the COE-ligated complex **9** to the heteroarene complex **13**. With the vacant site which is necessary for C–H activation occupied, the reaction can become sluggish or even halt completely.

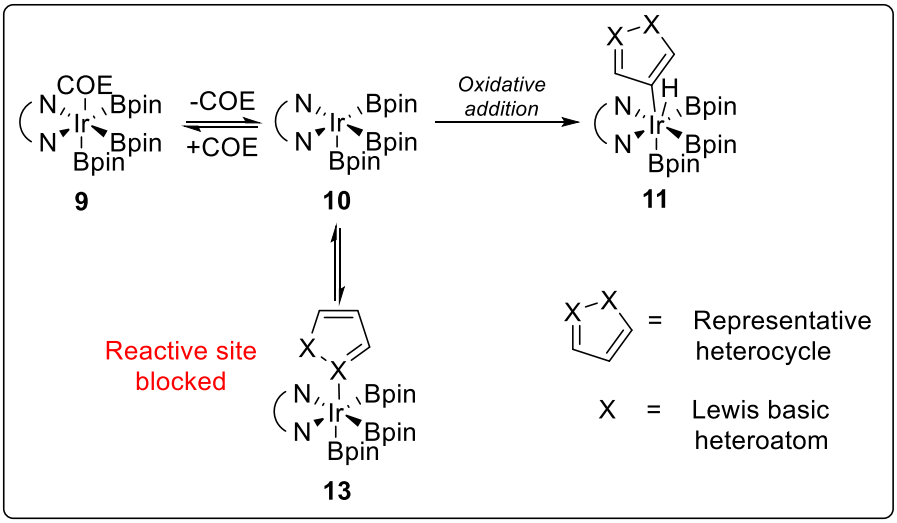

Scheme 1.11: Coordination of heteroarenes to the active catalyst **10**.

In a recent paper[20] on the scope and regioselectivity of iridium-catalysed borylation on a selection of heterocycles, Hartwig demonstrated the applicability of this methodology to late-stage functionalisation. In the first example given, pyrimidine **14** is borylated and oxidised *in situ* to give an excellent yield of the desired product **15**, an intermediate in the synthesis of the GPR119 agonist **16**,[45] a potential diabetes therapeutic (**Scheme 1.12**).

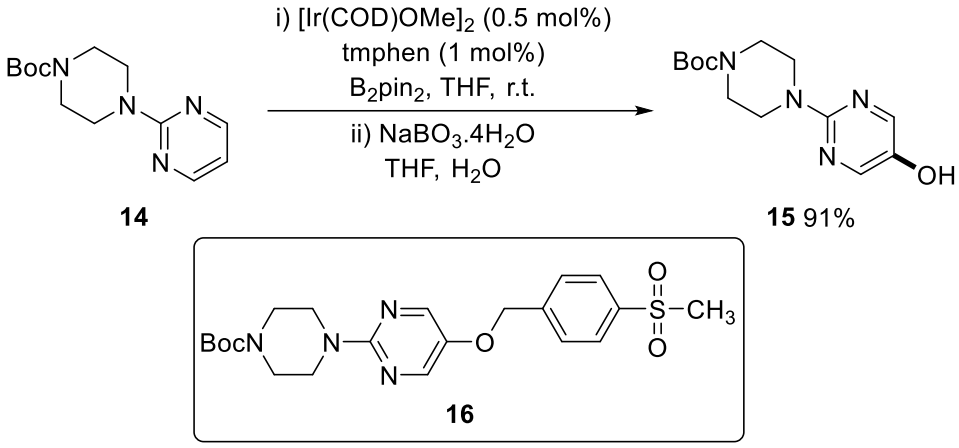

Scheme 1.12: A tandem C–H borylation and oxidation sequence as a route to a potential diabetes therapeutic.

Hartwig gives another example where the c-Met kinase inhibitor **18**, a potential cancer therapeutic,[46] is synthesised from **17**; the preceding intermediate in its established synthesis (**Scheme 1.13**).

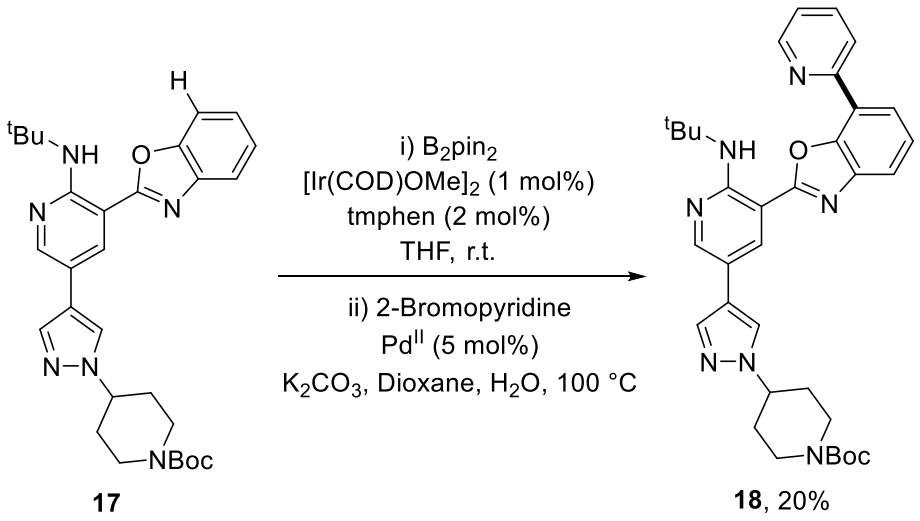

Scheme 1.13: Late-stage functionalisation of a c-Met kinase inhibitor.

In conclusion, the iridium-catalysed borylation reaction is very effective in functionalising simple, substituted (hetero)aromatic substrates under mild conditions with low catalyst loadings. However, more structurally complex substrates with basic

heterocycles and sensitive functional groups present a greater challenge and may require alternative methods.

1.3 Electrophilic borylation

A defining property of boron is the exceptional Lewis acidity it demonstrates with respect to electron donors. This can be ascribed to its electronic configuration ($1s^2 2s^2 2p^1$) which often gives rise to three-coordinate compounds where boron is sp^2 hybridised with six valence electrons and a vacant p orbital orthogonal to the plane of the molecule. This intrinsic electron deficiency has been harnessed in synthetically useful compounds such as $B(C_6F_5)_3$, $B(OCH_2CF_3)_3$ and BBr_3 which can act as activators, catalysts and stoichiometric reagents in processes including: Ziegler-Natta olefin polymerisation,[47,48] hydride abstraction,[49] catalytic amidation[50] and demethylation.[51] However, these boron species are still not electrophilic enough to react with unfunctionalised arenes *via* an intermolecular S_EAr mechanism.

In recent decades, however, progress, largely under the direction of Michael Ingleson, has been made in developing a borylation methodology that proceeds *via* S_EAr. Notably, this demonstrates complementary electronic and regioselectivity to that which is given by iridium-catalysed borylation.[20] That is, electron-rich arenes are preferred over electron-poor, and borylation occurs at the most nucleophilic site instead of the least hindered. In the wider context of late-stage functionalisation, this raises the tantalising possibility of functionalising along orthogonal vectors for a given substrate (**Scheme 1.14**).

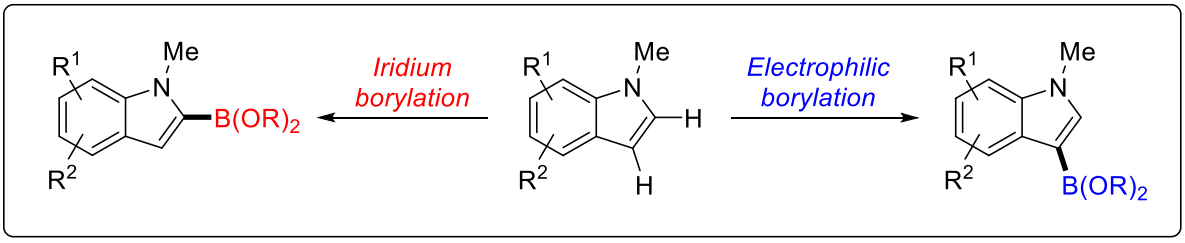

Scheme 1.14: Complementary regioselectivity demonstrated by iridium-catalysed and electrophilic borylation.

1.3.1 Cationic boron compounds

Boron cations (hereafter borocations) have emerged as promising reagents for their use as potent electrophiles, capable of aromatic C–H activation. Borocations have been categorised by Nöth[52] into three distinct structural classes based on the coordination number at boron.

Three-coordinate borocations are termed borenium cations and can be classed as 'superelectrophiles',[53] possessing a monocationic charge located formally on a

heteroatom adjacent to an unoccupied p orbital (**Scheme 1.15**). Akin to superacids, superelectrophilic borenium cations are counterbalanced with large, weakly coordinating anions. An in-depth review into their solution phase reactivity was recently published by Vedejs *et al.*[30]

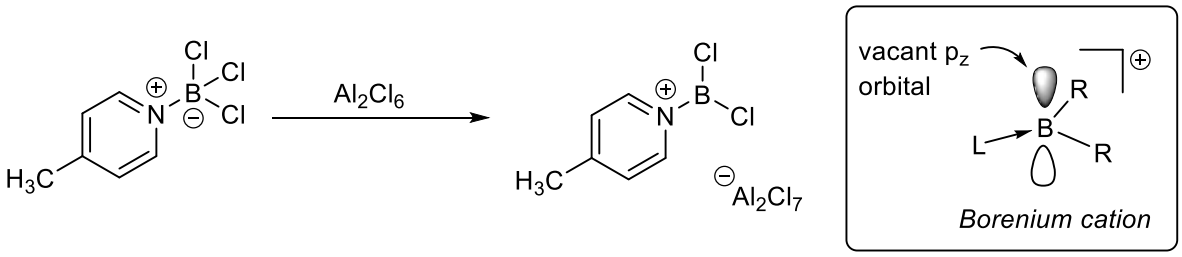

Scheme 1.15: Generation of exemplar borenium ion in solution.

Borenium cations comprise two σ-bound substituents (R) and one dative interaction with a ligand (L) that occupies a third coordination site and reduces some of the electron deficiency at the boron centre. It should be noted that, although the positive charge is drawn localised on the donor ligand, this is purely a formalism given that: 1) boron is more electropositive than most of the ligand donor elements; 2) computations indicate significant positive charge on boron; and 3) these compounds react as though they were boron cations.

Another class of borocations with the potential to be superelectrophiles are the two-coordinate borocations termed borinium cations.[52] Calculations,[54,55] as well as structurally characterised examples of borinium cations,[54,56] give a R–B–R angle at boron that is nearly linear and, thus, indicative of sp hybridisation. They are invariably ligated by bulky, π-donating substituents that effectively shield the boron from anion and solvent. Monodentate systems predominate due to the stabilisation brought about by linear geometry at the boron which allows for maximum orbital overlap from orthogonal π-donors, analogous to isoelectronic allenes (**Scheme 1.16**). Generally, boriniums that are stable enough to isolate and characterise will be undesirable from a reactivity perspective, as the π-bonding attenuates the electrophilicity of the boron.

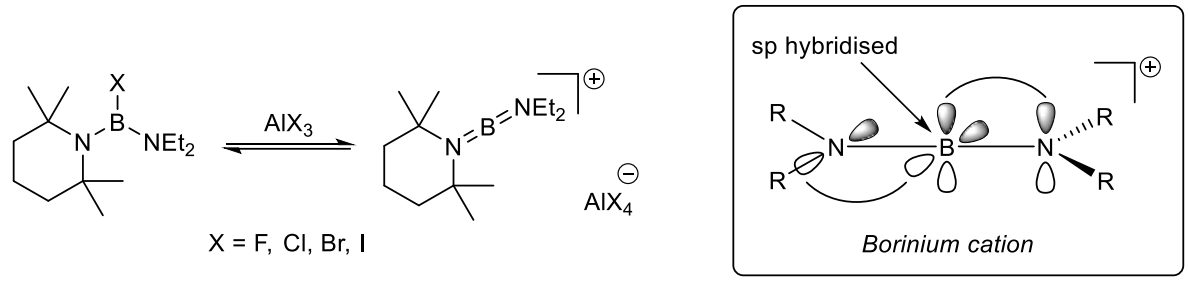

Scheme 1.16: Generation of an exemplar stable condensed-phase borinium cation, reported by Nöth and colleagues in 1982.[54] σ-Bonds excluded from atomic orbital diagram for simplicity.

A third class of cationic boron compounds is that of the tetrahedral, four-coordinate boronium cations, with two coordination sites occupied by σ-bonded substituents and the other two populated with neutral 2e⁻ donors (**Scheme 1.17**). Owing to their relative stability, which arises from a filled octet and a complete coordination sphere, these are the most thoroughly studied.[57,58] Interestingly, many catalytically relevant borenium ions may exist in equilibrium with the corresponding boronium ion. As long as a sufficiently high equilibrium concentration of the borenium is maintained, catalytic cycles can be established.[59,60]

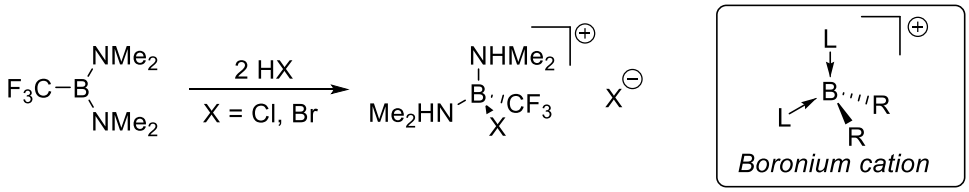

Scheme 1.17: Generation of exemplar boronium ion described by Brauer and colleagues.[61]

Although the innate reactivity of borocations makes characterisation challenging, their ^{11}B NMR chemical shifts are diagnostic (**Figure 1.4**). In general, more cationic charge density on the boron centre and a lower degree of electronic stabilisation results in a more downfield-shifted resonance signal. For example, bis(dialkylamino)borinium cations are typically in the range δ 30 – 38 ppm. Whereas, the corresponding signals for borinium ions ligated with alkyl substituents have been reported[54] around δ 60 ppm. Amine-ligated borenium cations of the form $R_3N{\rightarrow}B(OR_2)$ are slightly lower than the analogous boriniums (δ 25 – 30 ppm), while a larger range is observed for boronium cations (δ 0 – 15 ppm).

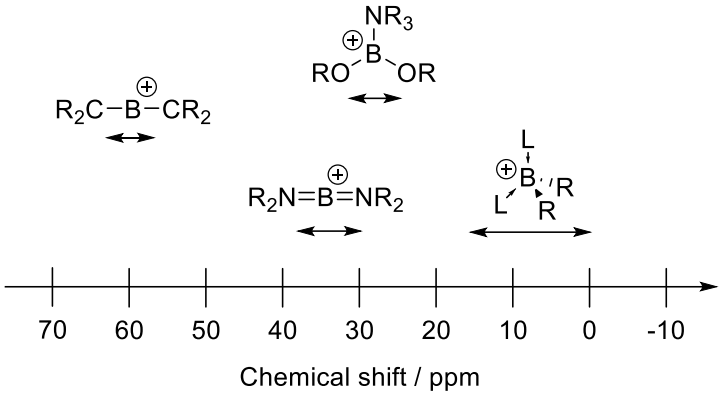

Figure 1.4: ^{11}B NMR Chemical shifts of borocations relative to $F_3B–OEt_2$ (positive charge drawn on the boron centre for simplicity).

In the 1970s/80s, reviews[52,57,58] on the topic of borocations focused largely on their synthesis and characterisation. However, their exceptional electrophilicity began to be harnessed for useful synthetic purposes. An elegant overview of the reactivity of borocations, in both the gas and solution phase, was provided by Piers *et al.* in 2005.[62]

Up until about a decade ago, intermolecular electrophilic borylation received very little attention.[63–65] However, progress was made by the groups of Vedejs[66–68] and Ingleson[69–71] who described the borylation of aromatic substrates by using stoichiometric, readily-synthesised borocations as electrophiles. The remainder of this section gives an overview of the work that has been carried out in this field to date.

1.3.2 Preceding work

The earliest accounts of electrophilic borylation date back to 1948, where Hurd reported the reactions of diborane with olefins, paraffins and benzene.[72] In 1959, Muetterties reported the borylation of simple, alkylated aromatics with BX_3 (X = Cl, Br, I) in the presence of AlX_3 (X = Cl, Br) or Al as activator (**Scheme 1.18**).[73] Mechanistic studies later confirmed that this proceeded *via* an S_EAr Friedel-Crafts-type mechanism.[74]

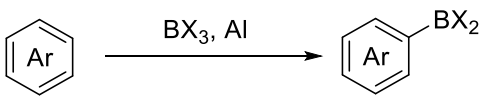

Scheme 1.18: Intermolecular electrophilic C–H borylation reported by Muetterties.

Progress in the area of electrophilic borylation stalled until the 1990s when the gas phase chemistry of the BH_2^+ ion was examined in detail.[75] It was found that BH_2^+ was capable of binding to and activating H_2 and other inert hydrocarbons. While, in the condensed phase, the BH_2^+ cation stabilised by R_3N coordination was shown by Vedejs to effect intramolecular arene borylation (**Scheme 1.19).**[66–68]

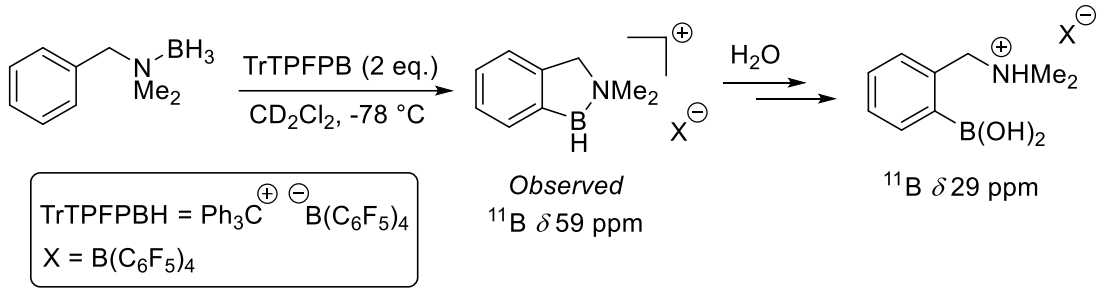

Scheme 1.19: Cyclisation of benzylic amine boranes proceeding *via* borenium ions generated *in situ* from hydrogen-bridged borocations.

1.3.3 Intermolecular electrophilic arene borylation

Despite great advances in C–H borylation throughout the 2000s *via* the use of iridium catalysis, the methodology was still subject to a number of limitations such as high cost and poor regioselectivity. The development of a direct arene borylation reaction proceeding *via* S_EAr was therefore highly desirable since it offers the potential for complementary regioselectivity to iridium catalysis. Analogous to Friedel-Crafts chemistry, the preferred site of borylation is determined by arene electronic effects rather than steric control.

1.3.3.1 Chelate restrained borinium cations

In 2010, Ingleson published a seminal paper that was the first to describe intermolecular arene borylation, proceeding *via* so-called 'chelate restrained' borocations.[69] We have seen in **Chapter 1.3.1** how borinium ions prefer to adopt a linear geometry to maximise π-donation into the boron's vacant p orbitals. Such a configuration is only possible with orthogonal monodentate ligands.

Ingleson's setup deviated from this model by instead generating borocations containing a chelating bidentate ligand. This conceptually generates a chelate restrained borinium ion in which the electrophilicity of the boron is enhanced by its nonlinear geometry. Such a species would have a vacant sp^2 orbital, unable to be stabilised by ligand π-donation (**Figure 1.5**). As well as this, chelation ensures a

significantly more accessible boron centre, which allows for more favourable reaction dynamics with respect to nucleophilic substrates.

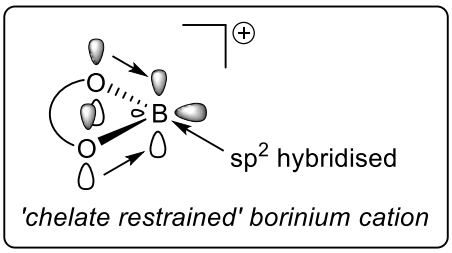

Figure 1.5: Chelate restrained borinium cation. σ-Bonds excluded for simplicity.

In solution, chelate restrained borinium cations are not feasible as any Lewis base that is present will readily interact with the Lewis acidic boron to give a borenium cation or anion-coordinated species. However, in weakly nucleophilic environments, chelate restrained boron species will be generated with electrophilicity approaching that of the superelectrophilic BX_2^+ gas phase cations (X = H, CH_3, OCH_3).[75]

Initial attempts to synthesise and isolate chelate restrained borocations were focused on the $[Bcat]^+$ subunit partnered with a range of weakly coordinating anions. Drawing inspiration from a previously reported diazaborole **19**,[76] Ingleson's group first synthesised the analogous compound, catBOTf **20** from catBCl *via* salt metathesis with AgOTf (**Scheme 1.20**).

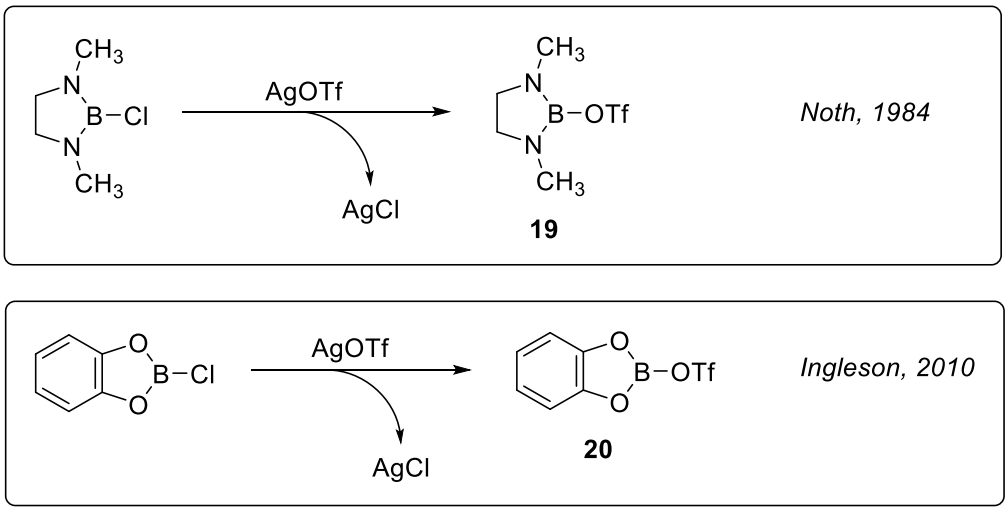

Scheme 1.20: Cationic chelate restrained boron systems reported by Nöth (top) and Ingleson (bottom).

When **20** was dissolved in benzene and stirred at reflux for 72 h, no PhBcat was detected and **20** was recovered unchanged (**Scheme 1.21**). This suggested that the triflate anion interacts too strongly with the boron centre, limiting its electrophilicity and preventing arene borylation.

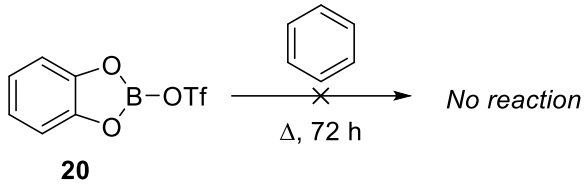

Scheme 1.21: Attempted reaction of **20** with benzene.

Seeking a more weakly coordinating anion to partner the $[catB]^+$ species, a different strategy was explored using halide abstraction *via* the use of $AlCl_3$. The use of strong MX_3 Lewis acids (M = B, Al, Ga; X = halide) is the prevalent route to linear borinium cations from $(R_2N)_2BCl$ (*vide supra*).[52]

When equimolar catBCl/$AlCl_3$ was stirred in arene solvents at room temperature, there was little discernible change (by ^{11}B and ^{27}Al NMR). But at 100 °C in toluene, a slow reaction took place giving largely BCl_3 (^{11}B δ 46.4 ppm) and trace amounts of tolylBCl$_2$ (^{11}B δ 55.0 ppm, generated by electrophilic borylation following activation of BCl_3 by $AlCl_3$), and tolylBcat (^{11}B δ 32.7 ppm) (**Scheme 1.22**). The lack of significant boronic ester formation from S_EAr with a $[catB][AlCl_4]$ species was attributed to a competing ligand redistribution reaction, giving rise to BCl_3.

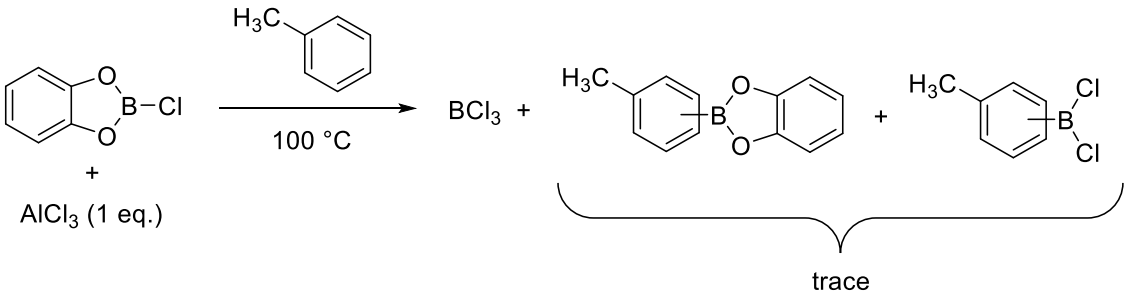

Scheme 1.22: Attempted Ar–H borylation *via* $AlCl_3$ activation.

In a similar reaction with catBBr and the stronger Lewis acid, BBr_3,[77] no arene borylation was detected at either 25 or 100 °C after prolonged periods, hinting that neutral MX_3 species are not sufficiently Lewis acidic to abstract a halide from catBX. This was believed to be due to the relative bond strength of M–Cl and catB–Cl as well as the lower stability of chelate restrained borocations compared to the linear borinium analogues.

An alternative route of investigation was instigated, based on reports of stable silyl cations partnered with extremely weakly coordinating carboranes [*closo*-1-H-$CB_{11}H_5Br_6$] (hereafter $[CbBr_6]^-$) (**Figure 1.6**), as well as $[B(C_6F_5)_4]^-$.[78,79]

Ingleson *et al.* hypothesised that a chelate restrained borocation partnered with one of these very weakly coordinating anions could react with arene solvents.

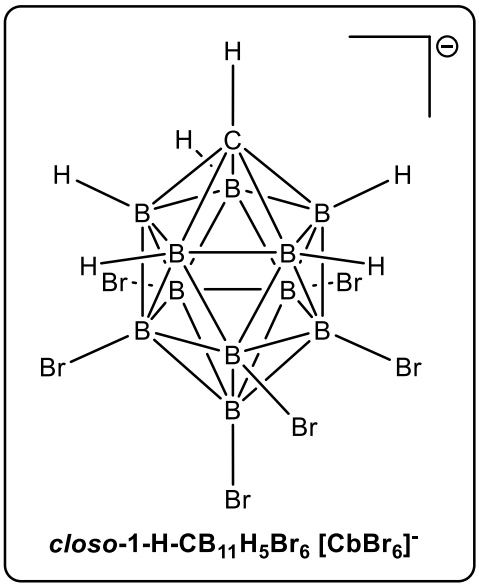

Figure 1.6: Carborane anion *closo*-1-H-$CB_{11}H_5Br_6$ ($[CbBr_6]^-$).

When $[Et_3Si][CbBr_6]$ was generated *in situ* from $[Ph_3C][CbBr_6]$ and Et_3SiH in benzene, it reacted rapidly with catBX (X = Cl, Br) to give PhBcat, with Et_3SiX observed as the expected byproduct (**Scheme 1.23**). HBcat was also observed following the abstraction of a hydride ion from Ph_3CH by $[catB]^+$, regenerating $[Ph_3C][CbBr_6]$. At higher temperatures, HBcat was found to react slowly in benzene following activation by an electrophile to give PhBcat, but attempts to eliminate the low temperature reverse reaction by removing Ph_3CH were unsuccessful due to the extreme sensitivity of the cationic silylium species.

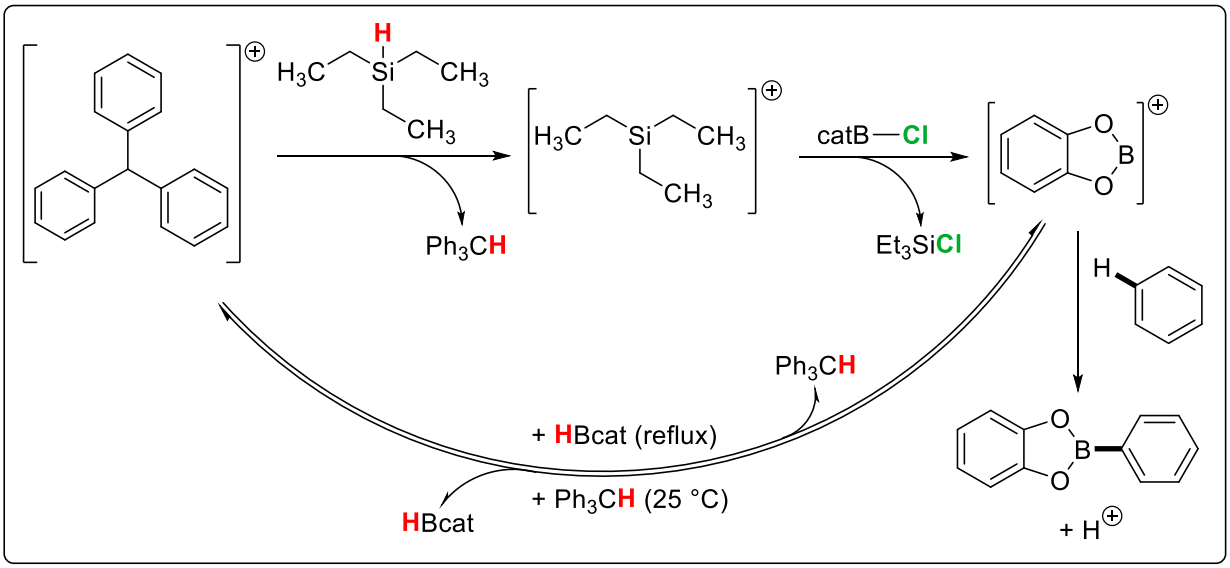

Scheme 1.23: Arene borylation through chelate restrained borocations. For clarity, the $[CbBr_6]^-$ anion is omitted. Formal net charges correspond to the molecule as a whole, as opposed to specific charges assigned to individual atoms.

Notably, borylation was found to occur with deactivated arenes such as 1,2-dichlorobenzene and fluorobenzene at 25 °C. This implied the presence of a highly reactive [catB][$CbBr_6$] species, but multiple attempts to detect any highly electrophilic boron species were unsuccessful, even at very low temperatures. Furthermore, arenium cations ($[C_6R_6(catB)]^+$), necessary for S_EAr reactions, were undetectable, along with any intermediates that might suggest a C–H insertion mechanism.

When the analogous reactions in **Scheme 1.23** were carried out with the perfluorinated tetraphenyl borate anion $[B(C_6F_5)_4]^-$ *in lieu* of $[CbBr_6]^-$, NMR data showed a closely comparable reaction outcome and no observable low-temperature intermediates. A notable difference between the two reactions was the observation of anion decomposition for $[B(C_6F_5)_4]^-$, but not $[CbBr_6]^-$. This severely impinges the usefulness of the $[B(C_6F_5)_4]^-$ anion in this system and gives extra weight to the theory that an exceptionally Lewis acidic $[catB]^+$ species is generated in a weakly nucleophilic environment.

1.3.3.2 Catalytic intermolecular electrophilic arene borylation

With an established procedure in hand to borylate arenes *via* the use of electrophilic boron, Ingleson's group then looked to develop a method that was catalytic (in Lewis acid). As shown in **Scheme 1.23**, the reaction of Ar–H with $[catB]^+$ generates H^+ and, thus, produces a strongly Brønsted acidic byproduct. Crucially, these have been

demonstrated[80] to react with B–H bonds in neutral boranes, liberating H_2 and generating a borocation electrophile. With these two reaction pathways combined in tandem, the possibility is raised of catalytic electrophilic arene borylation taking place (**Scheme 1.24**).

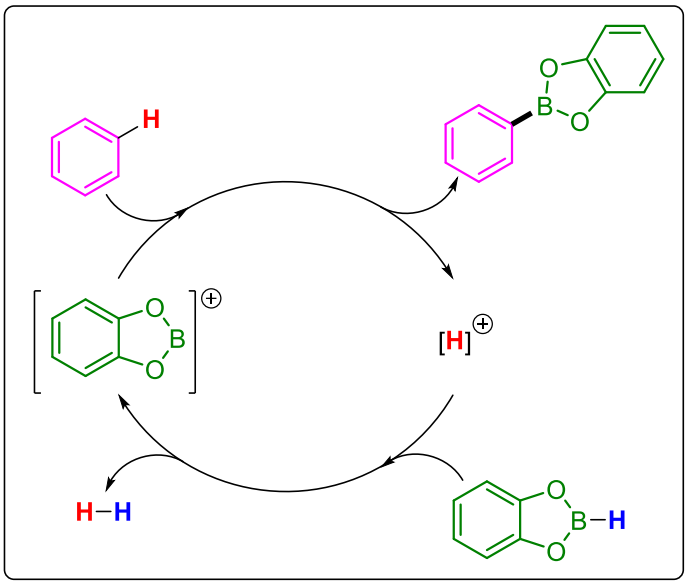

Scheme 1.24: Superelectrophile-catalysed production of aryl boronate esters from HBcat.

Turnover is only made possible due to the exceptionally poor nucleophilicity and high stability of the $[CbBr_6]^-$ anion as well as the Brønsted superacidity of its conjugate acid. These properties mean that any stabilising interactions with the $[catB]^+$ species that would frustrate the C–H activation step are avoided. It also helps give rise to a species acidic enough to protonate the strong B–H bond in catecholborane.

Highly efficient catalytic electrophilic borylation of a range of alkyl-substituted arenes with HBcat was then reported (**Scheme 1.25**). However, the methodology is severely limited by the superacidic byproducts and highly reactive boron electrophile. For example, long reaction times could be shortened by increasing the reaction temperature, but this incurred extensive isomerisation of alkyl arenes for substrates susceptible to 1,2-carbocation shifts. It also requires the use of a very expensive *closo*-carborane anion.

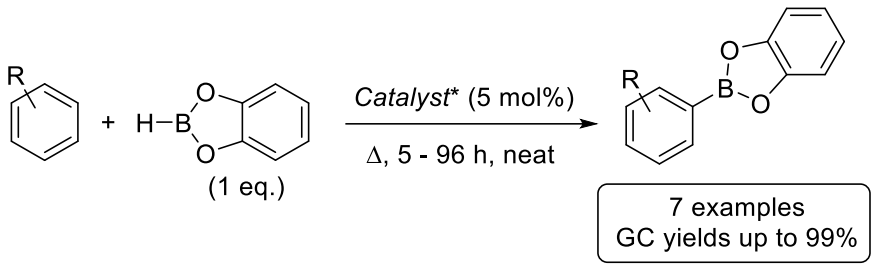

Scheme 1.25: Superacid-catalysed aromatic borylation. **Catalyst* = $Ph_3C[CbBr_6]/Et_3SiH/catBBr$.

The reaction was found to be unsuccessful when pinacolborane was used *in lieu* of catecholborane. This was due to the sensitivity of pinacolborane to cation-initiated ring-opening of its five-membered ring, analogous to Lewis acid-initiated ring-opening of THF.[81] Catalytic arene borylation *via* chelate restrained borocations therefore requires both anion and cation components to be stable to extremely Lewis acidic species.

1.3.3.3 Direct arene borylation with borenium cations

In recognition of the rigorous conditions required in their previous report,[69] Ingleson's group aimed to develop an electrophilic borylation procedure that was simple, inexpensive and scalable. The key challenge to overcome was maintaining a sufficiently electrophilic boron while sequestering H^+ ions to prevent competitive protodeborylation, product isomerisation (*e.g.* 1,2-alkyl shifts) and decomposition of acid-sensitive heterocycles. The key breakthrough came in switching the borocation from two-coordinate chelate restrained borinium ions to three-coordinate borenium ions.[70] Importantly, boreniums contain a Lewis base that would be liberated during arene borylation and able to quench the Brønsted acid byproduct.

We saw in **Chapter 1.3.3.1** how $AlCl_3$ is unable to abstract a Cl^- ion from catBCl at 20 °C. However, Ingleson found that addition of $AlCl_3$ to the amine adduct $catBCl(NR_3)$ resulted in the rapid formation of borenium ion $[catB{\leftarrow}NR_3]^+$ **21**, with $AlCl_4^-$ observed by ^{27}Al NMR (**Scheme 1.26**). Further addition of 1 eq. of NR_3 regenerated neutral species $catBCl(NR_3)$ along with $R_3N{\rightarrow}AlCl_3$. These equilibria are analogous to the reaction of (9-BBN)BCl (BBN = borabicyclo[3.3.1]nonane) and BCl_3 with pyridines and strong Lewis acids.[76,82] Borenium cations **21** are therefore highly electrophilic and were deemed good candidates for S_EAr.

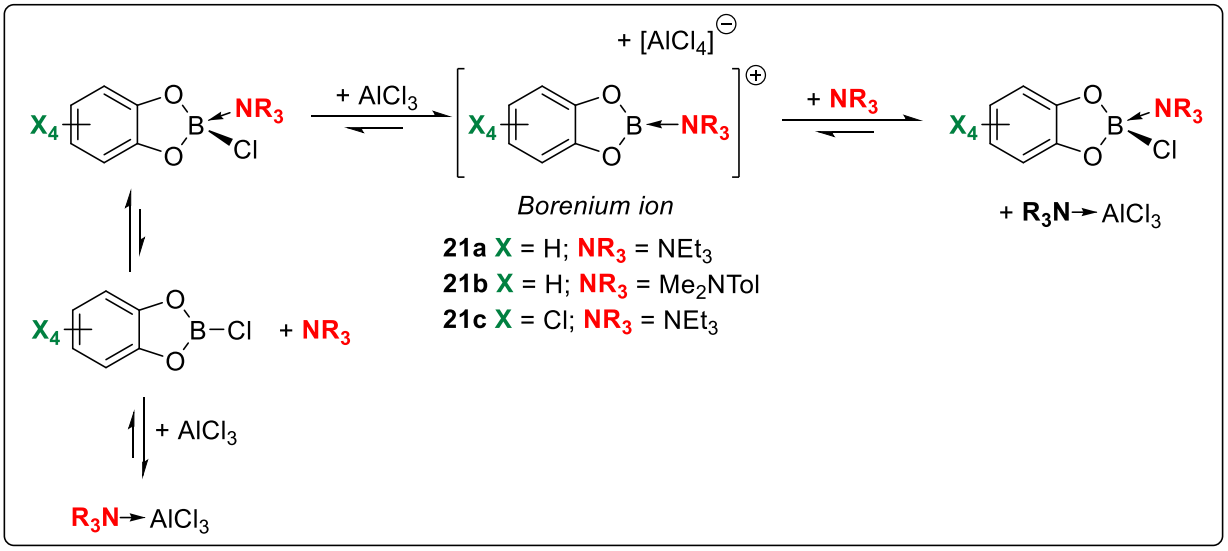

Scheme 1.26: Equilibria involved in the formation of borenium cations *via* halide abstraction with $AlCl_3$. Formal charges are attributed to the molecule as a whole and omitted altogether for species that are overall neutral.

Borenium ion **21a** generated *in situ* was found to react rapidly with 1 eq. of activated arene *N*,*N*-dimethylaniline in CD_2Cl_2 at 20 °C to give a near quantitative yield of *para*-substituted catechol boronate ester (by NMR spectroscopy). This regioselectivity contrasts with iridium-catalysed borylation, which for monosubstituted arenes gives a mixture of *meta*- and *para*-substituted isomers in a broadly statistical ratio (**Scheme 1.27**).[83]

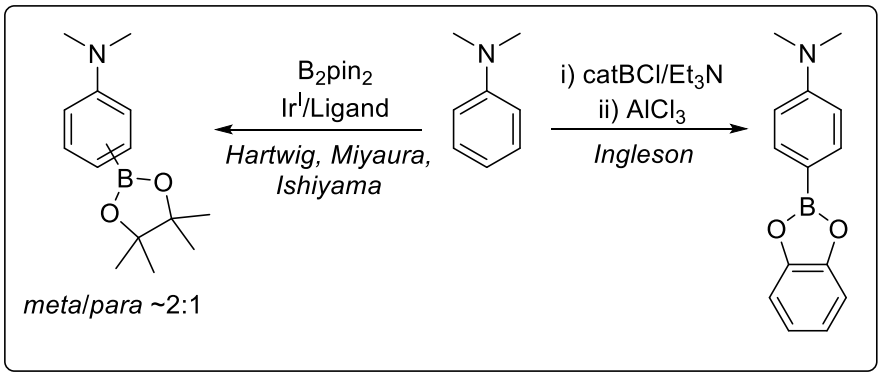

Scheme 1.27: Contrasting regioselectivity for iridium-catalysed and electrophilic borylation.

Attempts to isolate the catechol boronate ester products were challenging due to their susceptibility to protodeborylation. *In situ* transesterification of catechol for pinacol attenuated the electron deficiency of the boron atom and discouraged the coordination of protic species (*e.g.* H_2O), thus reducing the undesirable protodeborylation step. To avoid transesterifying altogether, pinacolato-ligated borenium cations ([pinB←(amine)]$^+$, amine = *N*,*N*-dimethylaniline or 2,6-lutidine) were explored as potential electrophilic species capable of undergoing S_EAr.

However, they failed to react with either *N*,*N*-dimethylaniline or *N*-methylpyrrole, due to their reduced electrophilicity.

Employing the borylation-transesterification two-step methodology, the scope of the reaction was examined with a range of anilines and N-heterocycles (*e.g.* indoles, carbazoles and pyrroles) (**Scheme 1.28**). Borylation was found to proceed in near quantitative yields (by NMR spectroscopy), with a facile one-pot transesterification enabling isolation of aryl pinacol boronate esters in good to excellent yields. Reaction times could be shortened by switching to borenium **21c**, with the weaker electron-donating ability of the polychlorinated catecholato moiety giving a more electrophilic boron centre.

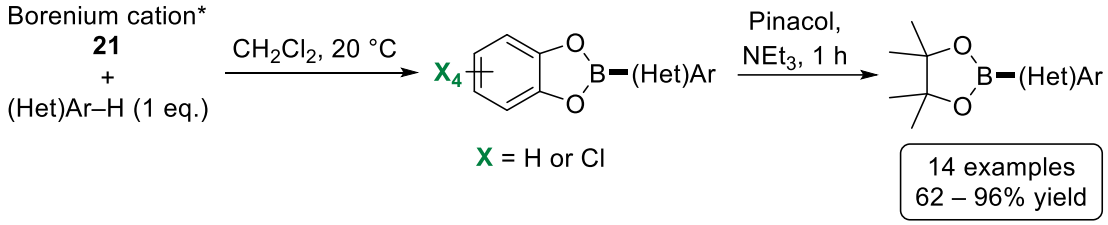

Scheme 1.28: One-pot direct arene borylation with borenium cations. $[AlCl_4]^-$ omitted for clarity. *Borenium cations made *in situ* in CH_2Cl_2 from 1 eq. catBCl (for **21a**) or Cl_4catBCl (for **21c**), 1.05 eq. NEt_3, and 1.1 eq. $AlCl_3$.

A follow-up report from the same group reported mechanistically very similar chemistry but with improved scalability and substrate scope.[71] This was achieved by eschewing catecholato-ligated boron electrophiles, for two primary reasons:

(i) For deactivated heterocycles such as *N*-TIPS-indole, large scale borylation using catBCl-derived boron electrophiles was extremely sluggish.
(ii) Also, the large-scale synthesis of catBCl is time-consuming and incurs high costs.

Inspired by a report from the group of Murakami on the intramolecular borylation of 2-arylpyridines,[84] Ingleson envisaged the generation of a stronger borenium electrophile based on $[X_2B(amine)]^+$ (X = halide). $[(2,6\text{-lutidine})BCl_2][AlCl_4]$ **22a** was readily prepared from stoichiometric combination of BCl_3 (1 M solution in CH_2Cl_2), $AlCl_3$ and 2,6-lutidine. NMR analysis of **22a** revealed a single ^{11}B NMR shift at δ 46.9 ppm which compares favourably to known $[(pyridyl)BCl_2]^+$ species.[52]

Electrophilic borylation with **22a** (or the active electrophile derived from **22a**) proceeded efficiently with the desired enhanced reactivity, borylating *N*-TIPS-pyrrole

completely in <14 h at 25 °C (*c.f.* with **21a**: 72 h at 20 °C). Moreover, compound **22a** was effective for the regioselective borylation of *N*-Me-carbazole and *N*,*N*-Ph_2-4-Me-aniline; substrates for which **21a** was not sufficiently electrophilic. As before, borylated substrates were amenable to transesterification to give isolable pinacolato boronate esters (**Scheme 1.29**).

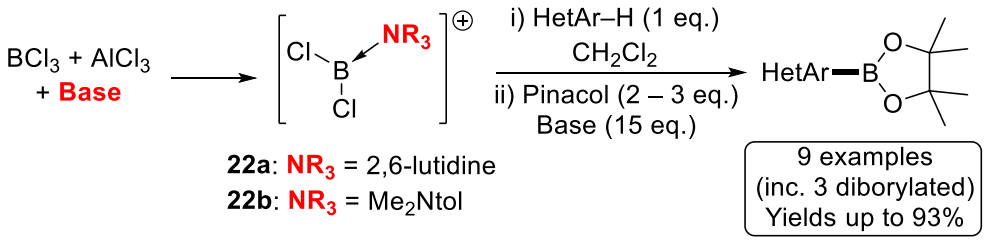

Scheme 1.29: Borylation of heterocycles using electrophiles derived from BCl_3 ($[AlCl_4]^-$ excluded).

The scope could be broadened further when the borenium cation **22** was appended with amines that were less basic. Replacing 2,6-lutidine for *N*,*N*-4-trimethylaniline (Me_2Ntol) (to give borenium **22b**) allowed access to more challenging substrates, such as thieno-[2,3,*b*]-thiophene, without compromising on functional group tolerance. A scaled-up reaction proved facile, furnishing borylated *N*-Me-carbazole in multi-gram quantities post esterification from simple, inexpensive reagents available from commercial suppliers.

The enhanced reactivity of **22b** also allowed for the diborylation of several substrates, despite the deactivating effect of having a $–BCl_2$ substituent installed. The authors were tentative to attribute the improved reactivity of **22b** compared to **22a** to a more Lewis acidic boron compound as the presence of multiple equilibria raises the prospect of a different electrophilic boron species acting as the borylating agent. Despite a limited number of examples reported, it is easy to envisage this methodology being applicable to a much wider scope of arenes. However, the authors acknowledged that a minimum degree of arene electrophilicity is required for the reaction to proceed. This was demonstrated by the borylation of *m*-xylene, in which reaction progress was not observed significantly below 140 °C.

Contemporaneously to Ingleson's work, Vedejs *et al.* reported a similar process based on a highly electrophilic boronium ion **23**.[85] The borocation **23** was generated efficiently by mixing Proton-sponge® (1,8-bis(dimethylamino)naphthalene) with [9-BBN][NTf_2] (**Figure 1.7**).

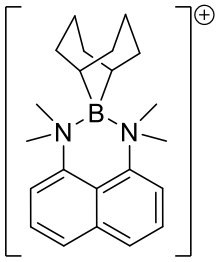

23

^{11}B δ 16.2 ppm

Figure 1.7: Boronium **23** ($[NTf_2]^-$ counterion excluded).

X-ray diffraction studies on a single crystal of **23** revealed remarkably long B–N bond distances (1.72 – 1.73 Å). This raises interesting questions over the classification of **23** under Nöth's rules,[52] *i.e.* the extent of its "boronium character". As discussed, boronium cations are coordinatively saturated and thought to be unreactive with nucleophiles. However, it was believed that the crowded steric environment around the boron centre leads to cleavage of a B–N bond, which generates a borenium ion in solution sufficiently electrophilic to react with electron-rich heterocycles. Indeed, a small selection of nitrogen heterocycles were shown to undergo borylation with **23** to give HetAr–BBN products in excellent yields (**Scheme 1.30**). However, the borylated products were found to be incredibly sensitive to protodeborylation and no subsequent steps to convert them to more stable pinacol esters were put forward by the authors.

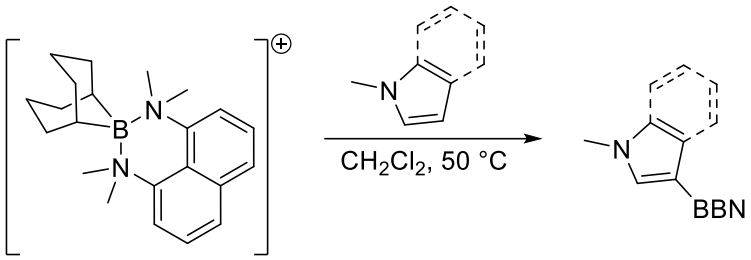

23

Scheme 1.30: 9-BBN-Based borylating system ($[NTf_2]^-$ excluded for simplicity).

1.3.3.4 Recent advances in aromatic electrophilic borylation

Over the last decade, the field of (hetero)aromatic electrophilic borylation has not seen significant progress. However, a method similar to that described by Ingleson was reported by Tanaka *et al.* recently that avoided use of $AlCl_3$ (**Scheme 1.31**).[86] As a trade-off, a more toxic and corrosive boron reagent (BBr_3) was used *in lieu* of BCl_3. The substrate scope focuses primarily on terminal alkenes but is shown to

effect fast, high-yielding borylation with two heteroarenes (*N*-methylindole and 2-methylthiophene).

Scheme 1.31: Electrophilic borylation of heteroarenes described by Tanaka and colleagues (base = 2,6-dichloropyridine or 2,6-lutidine).

With a similar aim of developing additive-free methods, Hatakeyama's group later reported the electrophilic borylation of arenes using just BI_3.[87] However, in contrast to other electrophilic borylation techniques, the regioselectivity of the reaction was found not to be governed by electronic effects. DFT calculations suggest the reaction takes place at the most sterically accessible carbon under kinetic control, where the HOMO is localised to a certain extent.

Very recently, Ingleson and colleagues made a further contribution to the field describing the zinc-catalysed electrophilic borylation of heteroarenes using HBpin or HBcat.[88] The most potent electrophile was generated from the combination of [(IPr)ZnEt][$B(C_6F_5)_4$] **24** (IPr = 1,3-bis(2,6-diisopropylphenyl)imidazol-2-ylidene) and DMT (DMT = *N*,*N*-dimethyl-*p*-toluidine) (**Scheme 1.32**).

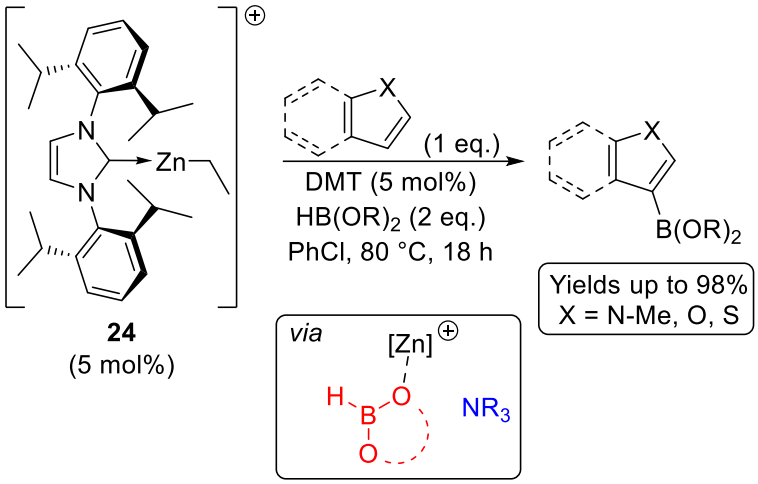

Scheme 1.32: Zinc-catalysed C–H borylation of heteroarenes ($[B(C_6F_5)_4]^-$ excluded for simplicity).

With HBpin, the substrate scope was limited to activated indoles with deactivated examples (*e.g.* 5-bromoindole) not reacting. Replacing HBpin with HBcat widened the scope to include deactivated indoles, *N*-methylpyrrole, 2-methylfuran and 2-methylthiophene. Interestingly, kinetic studies indicated that the (IPr)-zinc cation is

highly oxophilic and the borylation proceeds *via* activation of the hydroborane, not the heteroarene.

1.4 Free radical promoted borylation

The last few years have seen intense interest in borylation methodology that uses boryl radicals generated under mild, often metal-free conditions, to deliver the ever-desirable alkyl, vinyl and aryl boronate esters.[31] As discussed, catalytic borylation using transition metals such as palladium,[89] rhodium[90] and iridium[91] is well-established, but the usefulness of these methods hinges on their ability to tolerate certain functionality in the substrate and the ease of separation of metal impurities from the product. Furthermore, the strict rules governing the regioselectivity of these reactions can prohibit access to potentially valuable substitution patterns. An efficient, metal-free process to deliver boron onto organic frameworks with complementary selectivity is therefore very desirable.

Recent reports of free radical initiated borylation have been demonstrated on substrates such as aryl halides,[92,93] alkyl halides,[94] aryl amines,[95] aryl triflates[96] and aryl diazonium salts[97] (**Scheme 1.33**).

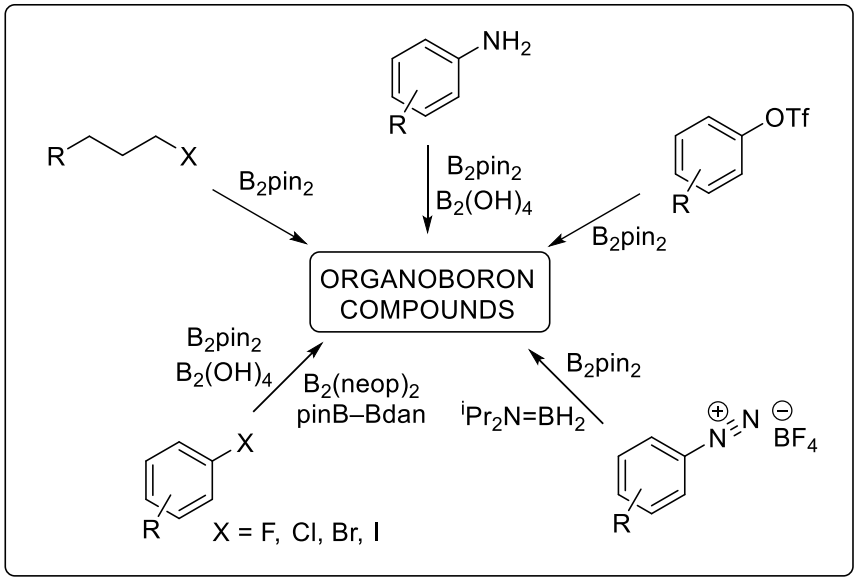

Scheme 1.33: C–B bond formation *via* a free radical pathway.

The last section of this introduction will focus on the different techniques that have been used to date to promote the generation of radicals in borylation reactions. These include the addition of a Lewis base or irradiation by UV light.

1.4.1 Generation of boryl radicals *via* an anionic adduct

A number of groups have shown in recent years that aryl radicals can be generated from aryl halides in the presence of a base and an organic additive *via* a

single-electron transfer/carbon-halogen bond cleavage sequence.[98–101] More recently, the groups of Li and Zhu have demonstrated the generation of boryl radicals *via* the cooperative coordination of two Lewis bases to one diboron molecule (**Scheme 1.34**).[102] Here, the 4-cyanopyridine molecules were proposed to both induce homolytic cleavage of the B–B bond and stabilise the boryl radical once formed through the captodative effect.[103]

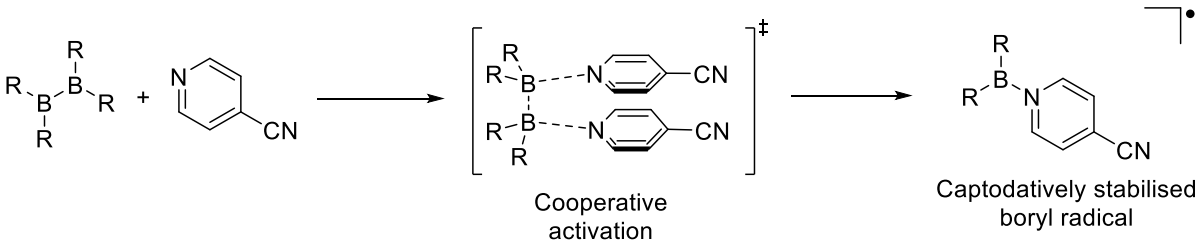

Scheme 1.34: Homolytic B–B cleavage using 4-cyanopyridine.

In 2016, Jiao *et al.* hypothesised that if transient aryl radicals and persistent boryl radicals were generated in the same reaction system, the two could be coupled together to give aryl boronate esters selectively (**Scheme 1.35**).[92] Zhang's group had already demonstrated the ability of caesium carbonate to mediate the borylation of aryl iodides in 2013 but at the time ruled out a radical mechanism.[104]

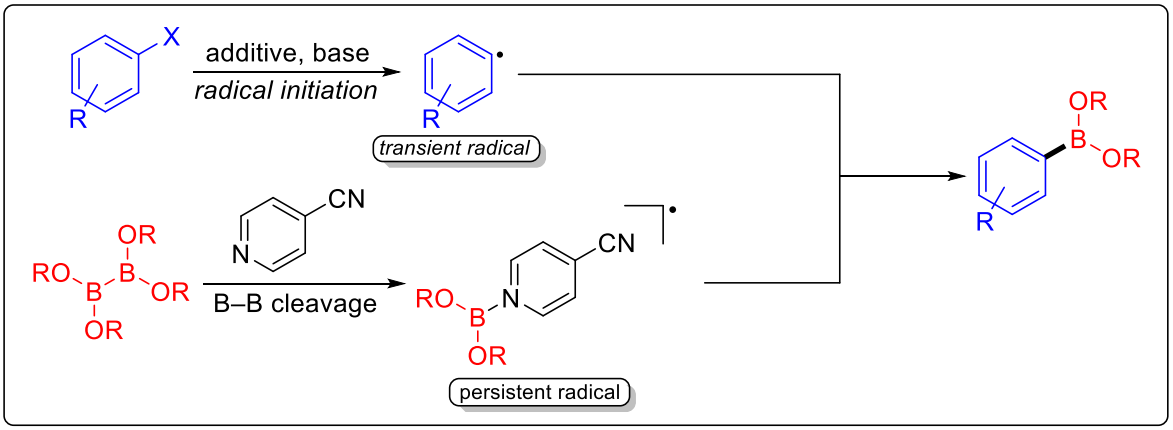

Scheme 1.35: Borylation *via* a radical coupling pathway.

When first attempted, only trace amounts of the desired product were generated with 4-cyanopyridine as the organic additive. However, optimisation afforded an idealised set of conditions with which a scope of aryl halides were tested (**Scheme 1.36**).

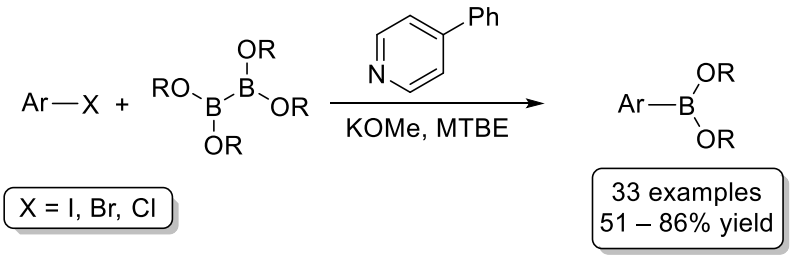

Scheme 1.36: Pyridine-catalysed borylation of aryl halides. Reaction conditions: Ar–X (0.5 mmol, 1 eq.), 4-phenylpyridine (20 mol%), KOMe (2 eq.), diboron reagent (2 eq.), MTBE (0.4 mL), 85 °C, 12 h.

The diboron reagent used primarily was B_2pin_2 but others were found to give good yields. Heteroaryl halides were found to be compatible substrates with this methodology except for 3-bromofuran and 3-iodopyridine which gave poor yields. The reactivity followed a series whereby Ar–I > Ar–Br > Ar–Cl. This allowed for selective mono- or diborylation on substrates such as 1-bromo-4-iodobenzene by adjusting the reaction stoichiometry accordingly.

In their mechanistic studies, aryl radical formation was confirmed by trapping experiments. Further to this, a series of competition experiments confirmed the involvement of an aryl radical and a pyridine-related boryl species in carbon-boron bond formation. Interestingly, EPR studies showed that a radical species could be generated from reaction of 4-phenylpyridine with the preformed 'ate' complex [B_2pin_2•MeOK] but not with the diboron itself. This meant that homolytic fission of the B–B bond could only occur once the ate complex had formed. With all this experimental data, a plausible mechanism was put forward (**Scheme 1.37**).

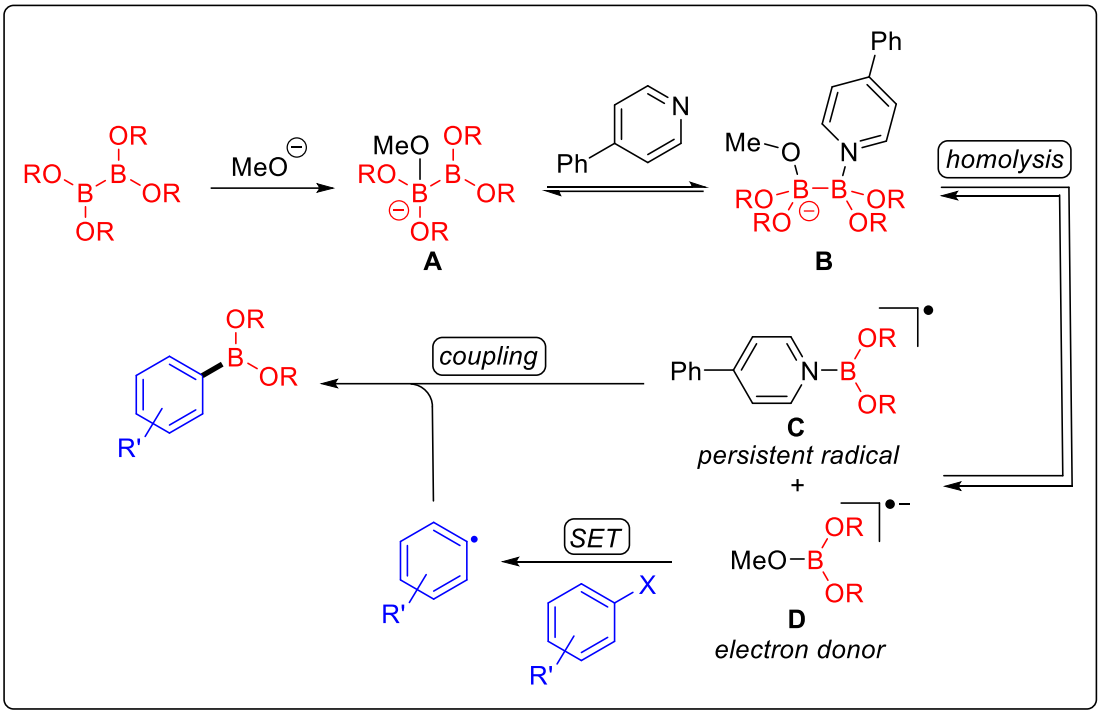

Scheme 1.37: Plausible reaction mechanism for pyridine catalysed radical borylation of aryl halides.

A methoxide anion reacts with B_2pin_2 to form the ate complex **A**, which can further react with pyridine to give the adduct **B**. Homolytic cleavage of **B** generates the pyridine-stabilised boryl radical **C** and the methoxyboronate radical anion **D**. The latter acts as a strong electron donor to undergo single electron transfer (SET) to an aryl halide leading to carbon-halogen bond cleavage. Finally, the aryl radical combines with the boryl radical **C** to give the borylated product.

Contemporaneously to this work by Jiao, Pucheault and colleagues reported similar findings on metal free radical borylation of aryl iodides.[93] A more exhaustive optimisation process led them to conclude that a CsF base in DMSO was a more effective system than an alkoxide in an ether solvent. A substrate scope showed largely comparable or slightly improved yields to the results of Jiao and colleagues.

Interestingly, Pucheault's group put forward a slightly different mechanism to Jiao (**Scheme 1.38**). Pucheault proposed that it is the Lewis base adduct **A** that is the electron donor which reduces the aryl iodide *via* an SET process to generate the radical anion. Simultaneously, boryl radical pyridine adduct **B** is formed as well as the fluoroboronate ester **C**. The starting diboron can be regenerated by reaction of intermediate **C** with adduct **A** which in turn gives **D**. The presence of species **A**, **C** and **D** was confirmed by ^{11}B and ^{19}F NMR spectroscopy.

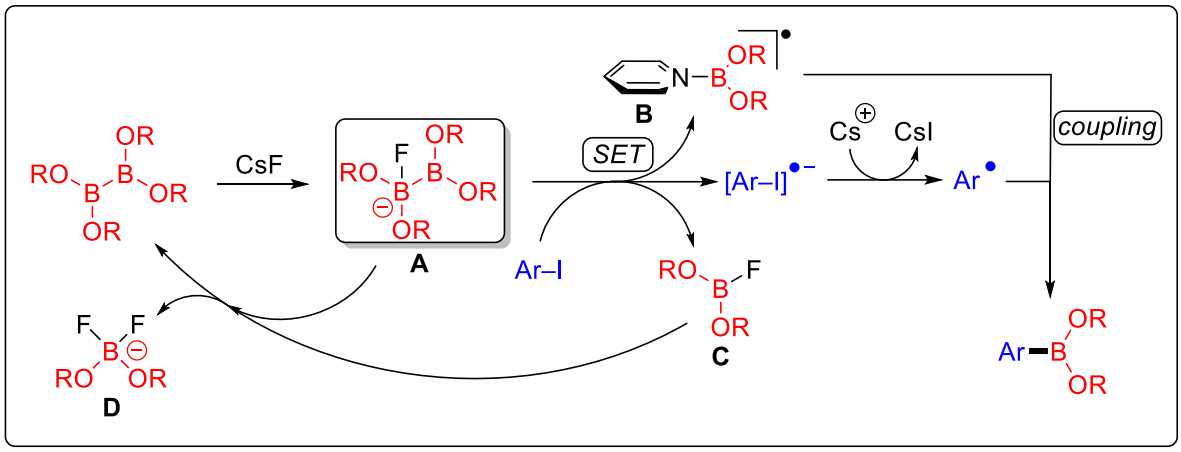

Scheme 1.38: Proposed reaction mechanism suggested by Pucheault and colleagues.

Pucheault commented on the discord between the two proposed mechanisms but argued that, since the reaction is possible in the absence of pyridine, the species undergoing the SET process is the ate complex **A**.

Employing similar chemistry to the work on the borylation of aryl halides, Cook *et al.* reported in 2016 the manganese-catalysed borylation of unactivated alkyl chlorides with the scope widened to encompass alkyl bromides and iodides (**Scheme 1.39**).[94] The authors did not propose a mechanism but trapping and competition experiments confirmed a free radical pathway.

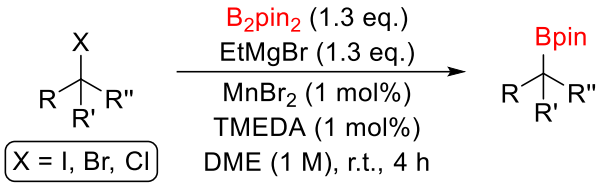

Scheme 1.39: Manganese-catalysed borylation of alkyl halides.

Predating much of the aforementioned work, Marder reported in 2015 the zinc-catalysed dual C–X and C–H borylation of aryl halides (**Scheme 1.40**).[105] It was postulated that a $[B_2pin_2{\bullet}OMe]^-$ anion reduces a $(dtbpy)_nZn^{II}XY$ complex (n = 1 or 2; X, Y = OMe, Bpin or both) to produce a Zn^{II}-stabilised $[dtbpy]^{\bullet-}$ radical. This species can transfer an electron to Ar–X to generate $[Ar–X]^{\bullet-}$, which reacts with $K^+[B_2pin_2{\bullet}OMe]^-$ (in a step-wise or concerted fashion) to give 1,2-diborylated arene and regenerate the $[Zn\text{-}dtbpy]^{\bullet-}$ radical anion.

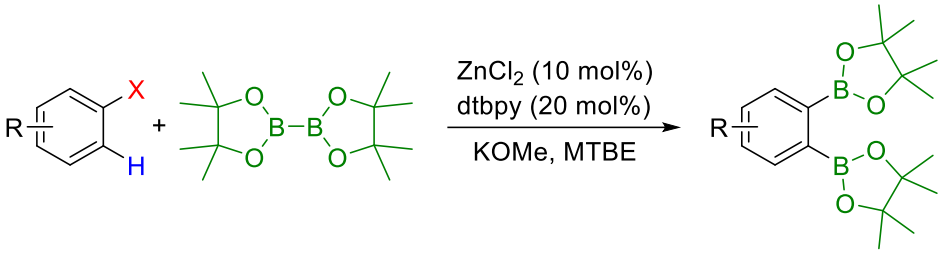

Scheme 1.40: Zinc-catalysed C–X and C–H activation to yield 1,2-diborylarenes.

Although radicals were not detected directly, product yields were reduced when 1 eq. of radical inhibitor 9,10-dihydroanthracene was added, and the reaction shut down when 7 eq were used.

1.4.2 Photoinduced borylation

Photochemical activation of organic compounds allows for the generation of highly reactive intermediates that may not be possible *via* thermal activation. In recent years, photoinduced synthetic approaches to organoboron compounds have received a vast amount of research interest.[106] Many of the previous reports on photochemically activated reactions such as alkylation,[107] arylation[108] and photocyclisation[109] involve as a key step the homolytic cleavage of an Ar–X bond under irradiation with visible light. *Via* the same process, photoinduced borylation has been shown to be a valuable strategy for generating aryl organoboron compounds from aryl halides with simple equipment, mild conditions and wide substrate scope.

In 2016, Larionov and colleagues reported the photoinduced borylation of aryl halides including electron-rich fluoroarenes as well as arylammonium salts to give borylated products directly.[110] The methodology worked with a range of diboron reagents to give aryl boronic acids and esters under ultraviolet light in the absence of catalysts and additives in a simple and scalable manner (**Scheme 1.41**).

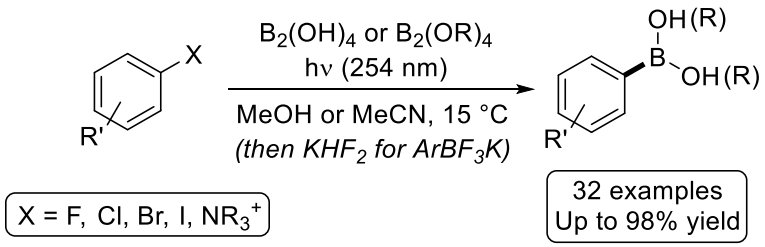

Scheme 1.41: Photoinduced borylation of aryl halides.

Exploration of the reaction's scope showed good functional group tolerance with both electron-donating and electron-withdrawing substituents accommodated. Heterocyclic substrates also did not pose a problem. The relative reactivity of the aryl halides was in accordance with the Ph–X bond dissociation energies (C–I 272, C–Br 336, C–Cl 400 kJ mol^{-1})[111] with Ar–I > Ar–Br > Ar–Cl. This differential reactivity was exploited for the chemoselective synthesis of substrates bearing more than one different halogen. Performing the reaction in the dark did not lead to product formation.

Fluorobenzene proved resistant to borylation, consistent with the high bond dissociation energy of the Ph–F bond (526 kJ mol^{-1})[111] that exceeds the energy of UV light at 254 nm (469 kJ mol^{-1}). Interestingly though, fluoroarenes bearing electron-donating substituents such as fluorophenols and fluoroanilines were found to be competent substrates.

The authors did not put forward a mechanism but suggested in their closing statement that a homolytic substitution could be involved. Homolytic substitution is a general type of reaction for organoboron compounds which, when taking place at a diboron reagent produces unstable radicals (**Scheme 1.42**, **Path A**).[112] This can be made vastly more thermodynamically favourable by the prior formation of an sp^2-sp^3 adduct, as we saw in **Chapter 1.4.1** (**Scheme 1.42**, **Path B**). Indeed, Larionov's group proposed the formation of Lewis base-diboron adducts in their report.

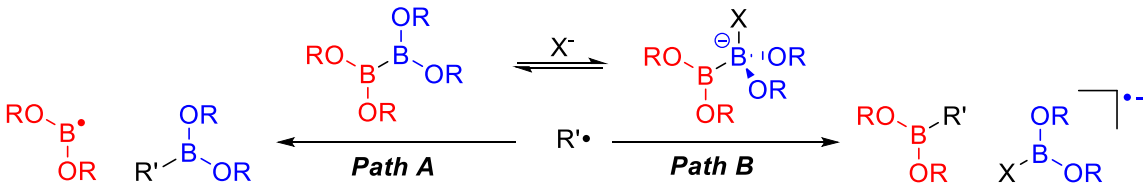

Scheme 1.42: Homolytic substitution at diboron reagents.

Shortly after this work, Li *et al.* reported a novel photolytic borylation of aryl halides under batch and continuous-flow conditions (**Scheme 1.43**).[113] The reaction setup lacked the simplicity of Larionov's reaction with quartz test tubes and a 300 W high pressure mercury lamp being a necessity. Regardless, this had many of the same advantages detailed in Larionov's report such as excellent functional group tolerance; broad substrate scope; high yields and mild conditions. However, its major advantage to Larionov's reaction is its very short reaction times which were made

possible once they switched from a batch process to a continuous-flow photochemical reactor which they designed and assembled themselves. This allowed reactions to be performed in 15 min with comparable or improved yields to those which were recorded in 4 h batch processes.

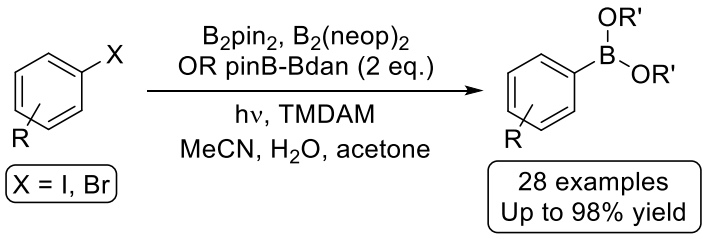

Scheme 1.43: Photoinduced borylation reported by Li and colleagues (TMDAM = *N*,*N*,*N*',*N*'-Tetramethyldiaminomethane).

A series of control experiments provided insight into the reaction mechanism leading the authors to propose two pathways, both involving an aryl radical intermediate (**Scheme 1.44**).

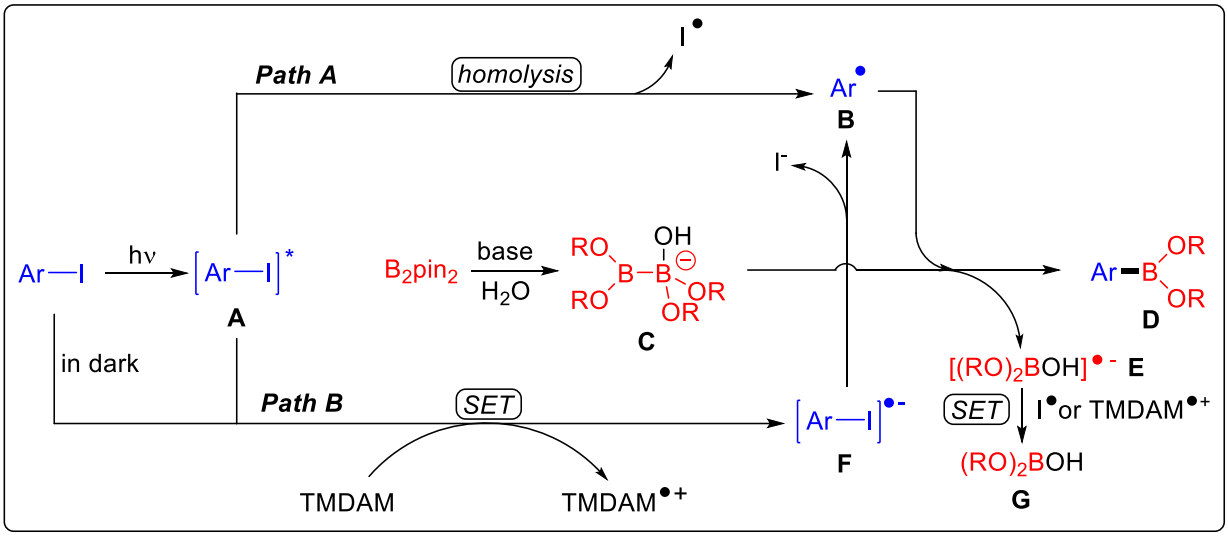

Scheme 1.44: Proposed reaction mechanism for the photoinduced borylation of aryl halides.

The excited state **A** is generated by ultraviolet irradiation of the starting aryl iodide. In **Path A**, the C–I bond of **A** undergoes homolytic fission to give aryl radical **B** and an iodine atom. Under aqueous conditions, TMDAM activates a water molecule, combining with B_2pin_2 to form the sp^2-sp^3 adduct **C**. Aryl radical **B** then reacts with **C** to give aryl boronate **D** and boryl radical anion **E**. Alternatively, **Path B** starts with the excited state **A** (or non-excited aryl halide if in the dark, with lower efficiency) being reduced by TMDAM *via* an SET process to give radical anion **F** and a TMDAM-derived radical cation. The C–I bond of **F** then undergoes heterolytic

cleavage to provide aryl radical **B** and an iodide anion. In the final step, **E** is oxidised by the iodine atom (if **Path A**) or the TMDAM-derived radical cation (**if Path B**) to form borate **G** as a byproduct.

2 Project aims

The primary aim of this project was to find novel methods to convert C–H bonds to C–B bonds in aromatic and heteroaromatic compounds. We were particularly interested in an emerging field of drug discovery based on Protac (Proteolysis Targeting Chimera) technology.[114–116] Protacs operate *via* a conceptually different method to typical antagonist (*i.e.* inhibitory) drug compounds on the market. Instead of maximising drug receptor occupancy to inhibit the target protein, Protacs commandeer the cell's natural waste disposal system that destroys unwanted proteins. One end of the Protac is designed to bind to the target, while the other recruits an E3 ligase which leads to the 'tagging' of the desired intracellular protein with one or more units of ubiquitin, thereby marking it for degradation by the proteasome (**Scheme 2.1**).

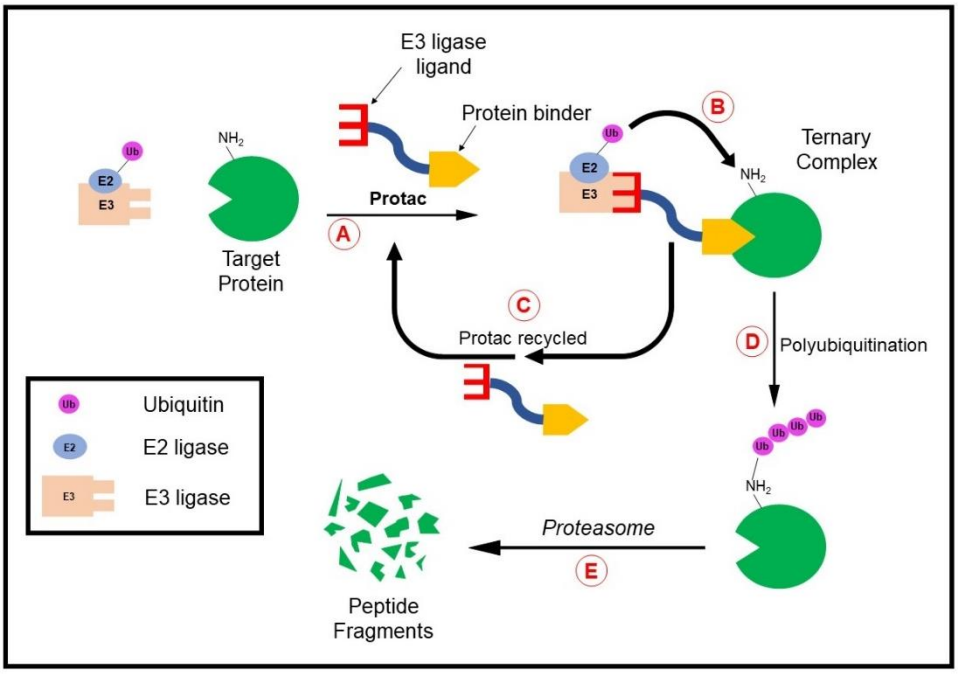

Scheme 2.1: Schematic of Protac action. **A**: A Protac binds selectively to both the target protein and an E3 ligase to form a ternary complex. **B**: This induced proximity causes ubiquitin to be transferred from the E2 ligase to a lysine residue on the target protein. **C**: Following ubiquitination, the ternary complex dissociates and the Protac molecule is recycled. **D**: Multiple cycles of ubiquitination lead to a polyubiquitin chain being formed. **E**: The polyubiquitinated protein is recognised and destroyed by the proteasome.

As long as the ubiquitinylation machinery is correctly orientated, it is not important where exactly on the target protein the Protac binds. This opens the possibility of targeting proteins previously thought to be 'undruggable' due to an inaccessible active site. Also, since one Protac molecule can bring about the degradation of many

proteins, a lower dose of the drug may be sufficient to produce a pharmacological effect, saving money and reducing the likelihood of off-target effects.

At present, the synthesis of Protacs often requires revision of the existing synthesis of the protein binder such that a functional group can be incorporated into the molecule for linker attachment. However, in this project we aim to demonstrate that linkers can be attached directly *via* late-stage functionalisation, thereby shortening synthetic routes. With orthogonal techniques providing complementary regioselectivity, it raises the prospect of more than one different Protac being made for a given protein binder. To this end, we will explore various aromatic C–H borylation techniques (**Scheme 2.2**).

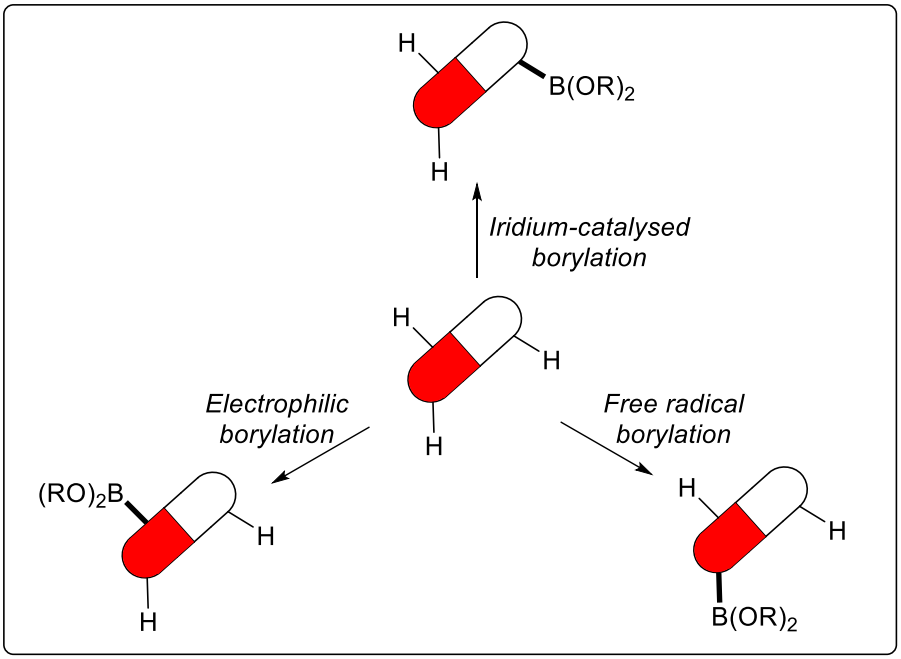

Scheme 2.2: Possibilities for the regiodivergent C–H borylation of pharmaceutically relevant compounds.

Iridium-catalysed borylation is well-established and a highly efficient technique for simple (hetero)arenes. However, the catalyst is sensitive to basic heterocycles and its functional group tolerance is not fully understood. Electrophilic borylation is selective for very electron-rich substrates but has the potential to offer complementary regioselectivity to iridium-catalysed borylation (electronic, not steric control). Also, upon the outset of this project (November 2017), numerous reports were emerging of free radical aromatic C–X borylation (X = F, Cl, Br, I, OTf, N_2^+). However, aromatic C–H borylation proceeding *via* a free radical pathway was still to be explored.

The aims of this project were:

- To probe, where unknown, the scope, regioselectivity and limitations of iridium-catalysed borylation by applying the methodology to a representative set of ‘drug-like’ heterocyclic compounds.
- To develop a novel C–H borylation protocol that proceeds *via* a free radical, Minisci-type mechanism.
- To develop a novel electrophilic C–H borylation methodology mediated catalytically, or otherwise, by a late transition metal (Cu, Au).

3 Results and discussion

3.1 Free radical borylation

3.1.1 Introduction and project aims

Several reports leading up to the start of this project (November 2017) detailed the generation of boron radicals in the presence of a diboron reagent and a base (see **Chapter 1.4.1**). We proposed an alternative, base-free setup, inspired by Santos' reports of the unsymmetrical diboron compound PDIPA diboron **25** (PDIPA = pinacolato diisopropylaminato).[117,118]

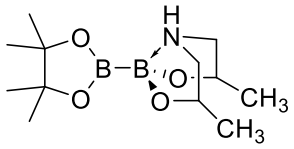

25

Figure 3.1: PDIPA diboron **25**. Formal charges excluded for simplicity.

Diboron **25** is said to be "internally pre-activated" on account of its sp^2-sp^3 hybridisation and, therefore, elongated B–B bond with respect to B_2pin_2. We hope to harness this enhanced reactivity, potentially with the aid of transition metal catalysts (Mn, Fe, Cu) and other additives, to deliver the Bpin moiety of **25** onto heterocyclic scaffolds *via* a Minisci-type free radical addition mechanism.

Minisci showed[119–121] in the 1970s that an alkyl radical will readily add to a heteroaromatic base (**Scheme 3.1**) and a recent review[122] by Duncton *et al.* demonstrated the applicability of the Minisci reaction to medicinal chemistry.

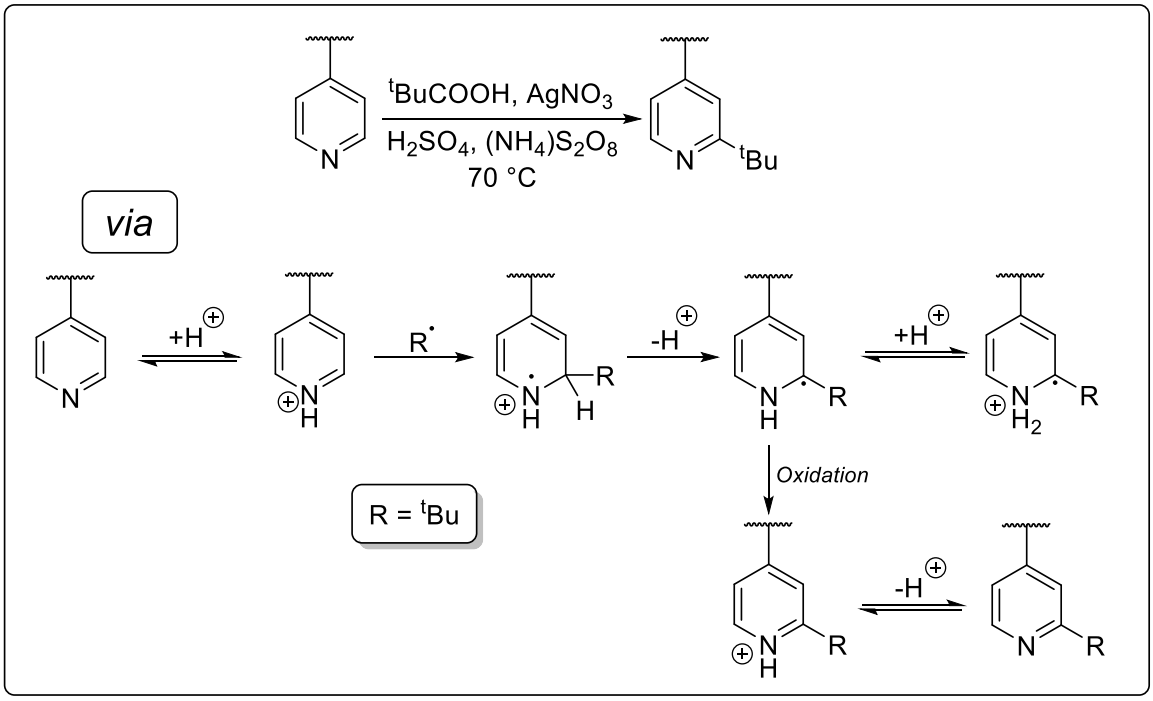

Scheme 3.1: Minisci reaction with accompanying mechanism. A 4-substituted pyridine has been used as a representative substrate.

Before looking at heterocyclic substrates, we first hoped to demonstrate that aryl halides can be borylated *via* a free radical mechanism with unsymmetrical diboron **25**, instead of B_2pin_2 and a base. It was envisaged that an analogous reaction mechanism could be established to that which Jiao proposed in 2016 (**Scheme 3.2**).[92]

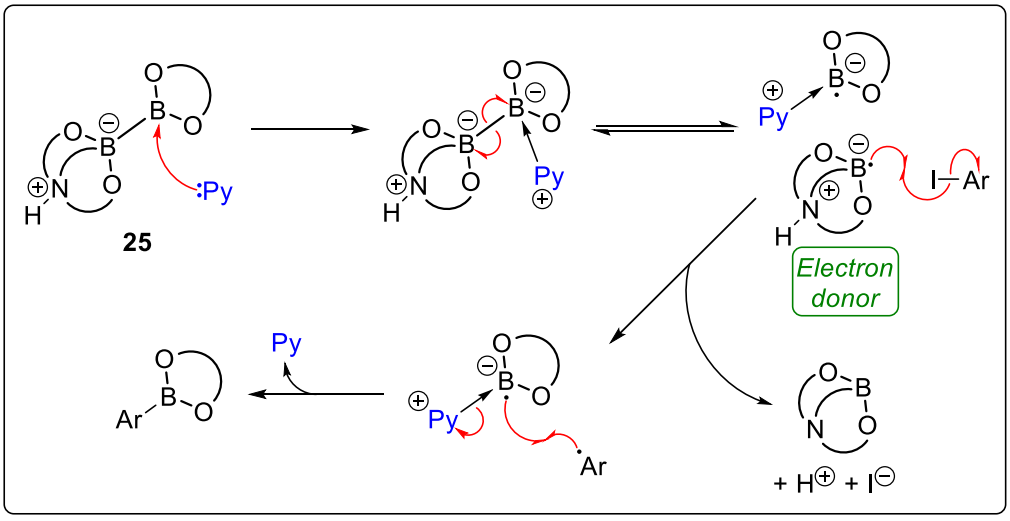

Scheme 3.2: Plausible mechanism for the base-free reaction of diboron **25** with Ar–I in the presence of a catalytic amount of pyridine (Py = pyridine).

3.1.2 Results and discussion

To confirm the quality of our reagents and become familiar with the relevant techniques, the borylation of 4-iodotoluene was attempted according to a procedure carried out by Pucheault and colleagues.[93] A moderate yield of the desired aryl boronate ester **26** was obtained after work-up and purification (**Scheme 3.3**).

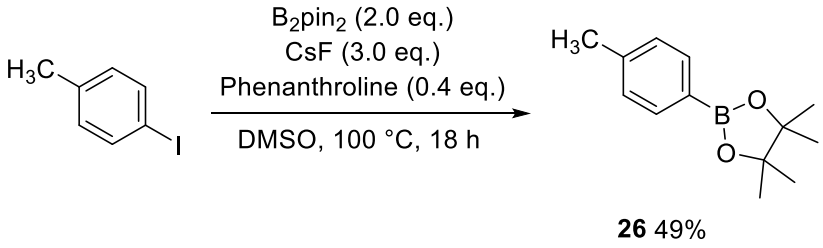

Scheme 3.3: Free radical borylation of 4-iodotoluene to give **26**.

In order to test the hypothesis that B_2pin_2 and the CsF Lewis base could be replaced by an unsymmetrical sp^2-sp^3 hybridised diboron compound, PDIPA diboron **25** was prepared on a gram scale according to a literature procedure (**Scheme 3.4**).[117]

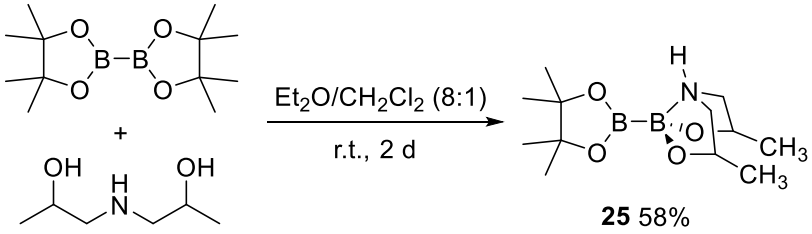

Scheme 3.4: Preparation of PDIPA diboron **25**.

The ^{11}B NMR spectrum of diboron **25** showed two distinct peaks at δ 34.9 ppm and 8.3 ppm, consistent with the presence of a tri- and tetra-coordinate boron centre, respectively. It also showed the disappearance of the signal corresponding to B_2pin_2 (δ 31.1 ppm) (**Figure 3.2**). Since our amine diol starting material was a statistical mixture of all four diastereoisomers, diboron **25** was formed as a 50:50 mixture of the *cis* and *trans* isomers. Although, the stereochemical information of the DIPA moiety is inconsequential since it comprises the sacrificial half of the diboron compound.

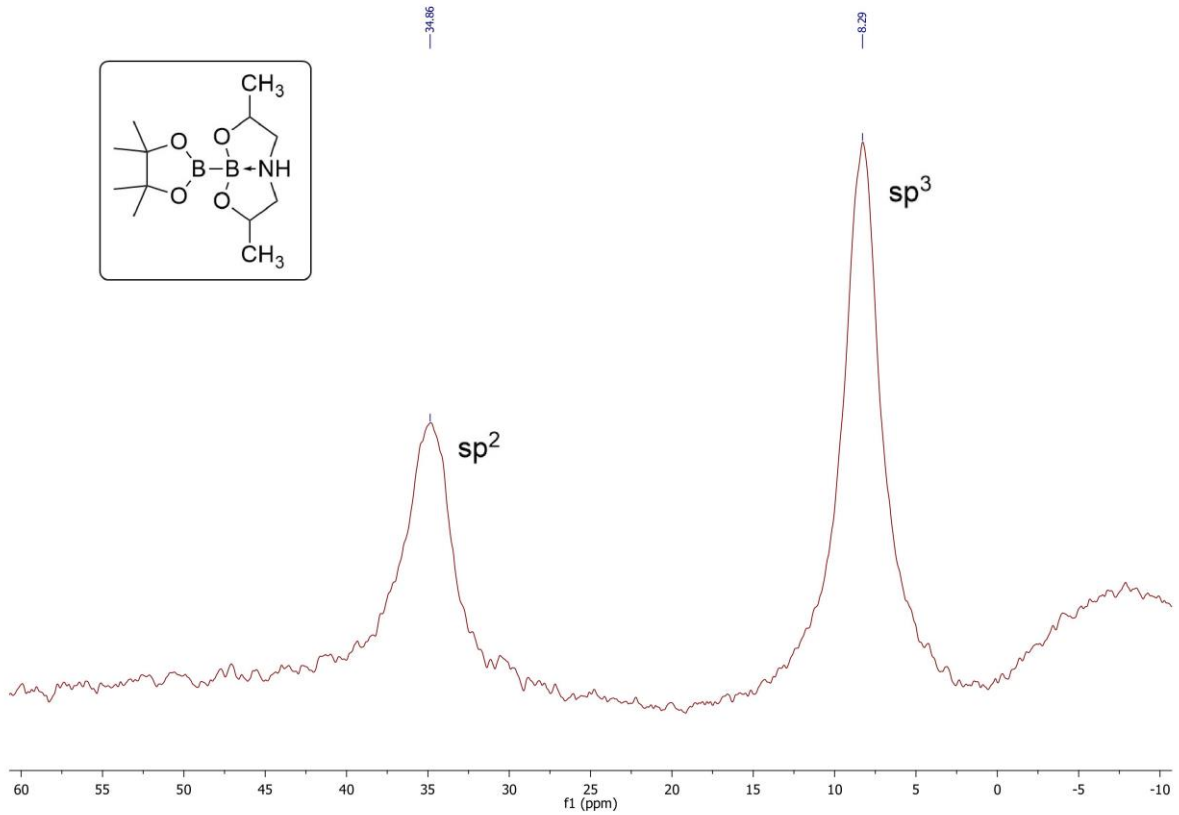

Figure 3.2: ^{11}B NMR of diboron **25** (225 MHz) in CD_3CN at room temperature.

With diboron **25** successfully synthesised and characterised, a repeat of the reaction detailed in **Scheme 3.3** was set up with diboron **25** *in lieu* of B_2pin_2 and CsF, as well as a stoichiometric amount of phenanthroline (**Scheme 3.5**).

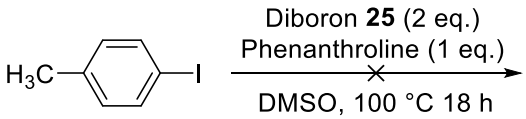

Scheme 3.5: Attempted borylation of 4-iodotoluene with diboron **25** *via* Pucheault's conditions.

To our disappointment, no conversion of starting material was observed. This was also the case when we switched from Pucheault's conditions to Jiao's (**Scheme 3.6**).[92]

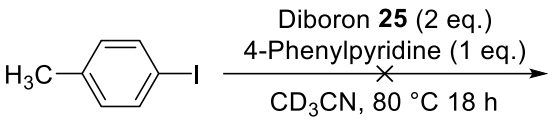

Scheme 3.6: Attempted borylation of 4-iodotoluene with diboron **25** *via* Jiao's conditions.

Despite no turnover of aryl iodide, there was clear conversion of the starting diboron **25** by ^{11}B NMR. An NMR experiment was set up to examine how 4-phenylpyridine interacts with diboron **25** (**Scheme 3.7**).

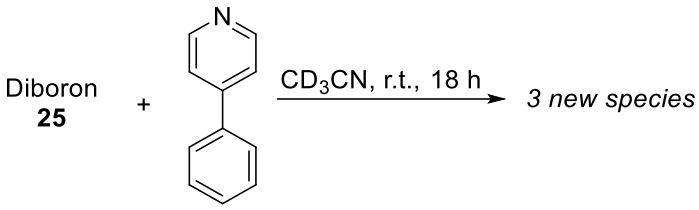

Scheme 3.7: Reaction of diboron **25** with 4-phenylpyridine.

After 30 min at room temperature, six new signals in the ^{11}B NMR had formed (**Figure 3.3**). This most likely indicated the generation of three new boron-containing species, although diastereoisomerism may account for additional boron environments. As expected, several new peaks were observed in the ^{1}H NMR spectrum (δ 1 – 5 ppm) but it was too convoluted to draw any meaningful conclusions from this. The aromatic peaks corresponding to 4-phenylpyridine did not shift to a notable extent. When the reaction was warmed to 80 °C and left overnight, the reaction developed an orange colour but there was little discernible change by ^{11}B NMR spectroscopy.

These data show that pyridines can readily interact with diboron **25** to form new compounds. Significantly, the appearance of signals around δ 21 – 24 ppm suggest that the B–B bond has been successfully broken, as this is where B(XR)$_3$ (X = N, O) species appear. However, it was impossible to know whether cleavage of the B–B bond was homolytic, as desired.

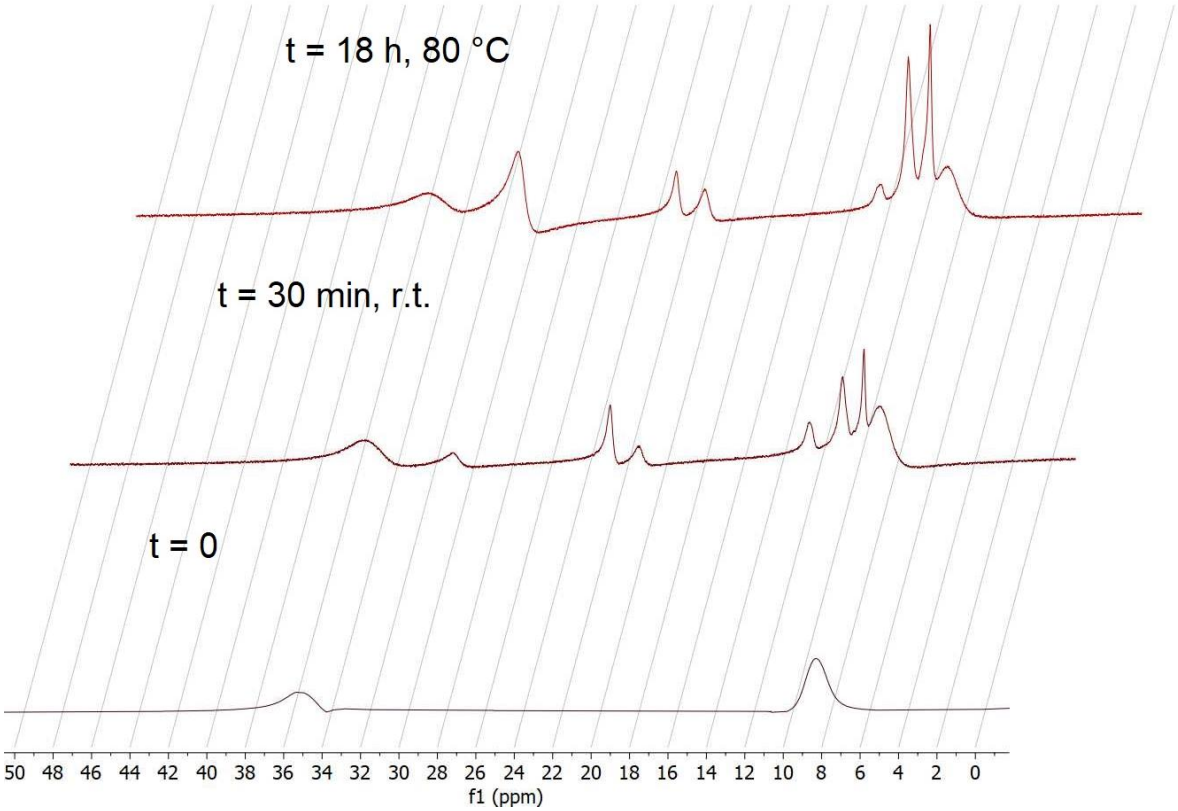

Figure 3.3: ^{11}B NMR (225 MHz) monitoring the reaction of diboron **25** and 4-phenylpyridine in CD_3CN at t = 0 (bottom), t = 30 min (middle) and t = 18 h (top).

Changing strategy, the reaction detailed in **Scheme 3.5** was repeated but in the presence of a catalytic amount of $FeCl_3$. First-row d-block elements are known for their tendency to take part in single electron redox processes, including reactions forming C–B bonds.[123] If our proposed mechanism outlined in **Scheme 3.2** is valid, we will be generating a stoichiometric amount of I^-. Thus, a single electron oxidant may help propagate the reaction by generating a highly reactive iodine radical capable of reacting with diboron **25**.

When carried out, formation of aryl boronate **26** was detected by ^{1}H NMR such that the Ar–I/**26** ratio was 11:1 after 2 h and 5.2:1 after 18 h (**Scheme 3.8**). Since the ^{1}H NMR spectrum of the crude material showed no arene-derived side products, it is reasonable to normalise to 100 and quote this as a 16% NMR yield.

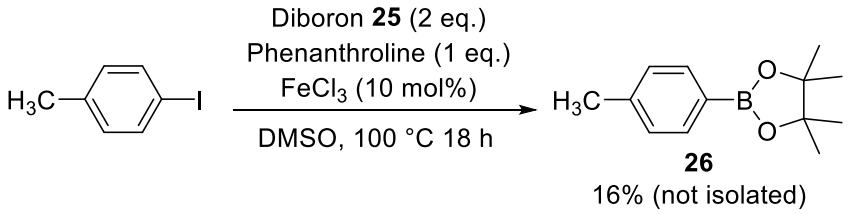

Scheme 3.8: Borylation of 4-iodotoluene in the presence of a catalytic amount of $FeCl_3$.

This result was of great interest as it suggested that a single electron oxidant may help promote borylation *via* a free radical pathway. In pursuit of higher conversion, the same reaction under identical conditions was then screened against a set of single electron oxidants to see if they gave an improved degree of conversion (**Table 3.1**).

Table 3.1: Screen of single electron oxidants in the reaction of 4-iodotoluene with diboron **25**.

Entry	Single e^- oxidant	% Yield*
1	$FeCl_3$	16
2	$Mn(acac)_3$	9
3	$Mn(OAc)_3.2H_2O$	10
4	$Cu(NO_3)_2.3H_2O$	n.r.
5	$Cu(OAc)_2$	n.r.
6	$Cu(OTf)_2$	n.r.
7	$(NH_4)Ce(NO_3)_6$	0

*% Yields estimated by measuring the ratio of Ar–I/**26** and normalising to 100. n.r. = No reaction.

Mn^{III} salts were found to give comparable conversions to that which was seen with $FeCl_3$ (**Entries 2 and 3**). By contrast, experiments with Cu^{II} reagents did not reveal any turnover of starting material (**Entries 4 – 6**). Reaction with the most powerful oxidant $(NH_4)_2Ce(NO_3)_6$, returned a complex looking outcome with neither the starting aryl iodide nor the aryl boronate **26** detectable (**Entry 7**).

Encouraged by the results with Fe and Mn additives, we returned to these reagents and performed further iterations of the experiment with modifications to the reaction parameters. Elevated temperatures did not bring higher turnover, nor did degassing the DMSO solvent or using a re-purified batch of our diboron **25** (recrystallised from CH_2Cl_2/EtOAc 1:2). Stoichiometric quantities of metal salt also did not help.

To confirm that the desired product **26** was not degrading under acid work up conditions *via* protodeborylation, an authentic sample of boronate **26** was acquired from a commercial supplier and subjected to each of the work up steps. This gave a reasonable mass recovery of 84%. When we tried again with neutral water *in lieu* of acid, it returned 81%. These results do not suggest that our work up was

problematic, rather, that the reaction was thermodynamically or kinetically unfeasible.

3.1.3 Significant literature developments

During the course of this work, Jiao's group published a follow-up paper to their work on pyridine-catalysed free radical borylation.[124] The report details the structure of the organic electron donor species (classed a "super electron donor" [SED][125]) involved in their reaction system and the mechanism by which it forms. Their findings upended their prior assumptions made on the nature of the electron donor (**Scheme 3.9**),[92] discussed in depth in **Chapter 1.4.1**.

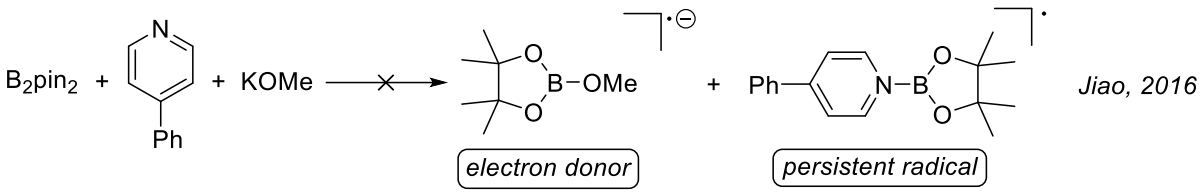

Scheme 3.9: Reactive intermediates proposed by Jiao in 2016.

Previously, full characterisation of reactive intermediates had not been possible due to the poor solubility of potassium methoxide in DMSO which limited the concentration of the electron donor, thus hampering structural characterisation. However, when they prepared a reaction in THF with 18-crown-6 (18-C-6) as an additive, a homogenous solution formed with clearly resolved signals in NMR and EPR spectra (**Scheme 3.10**).

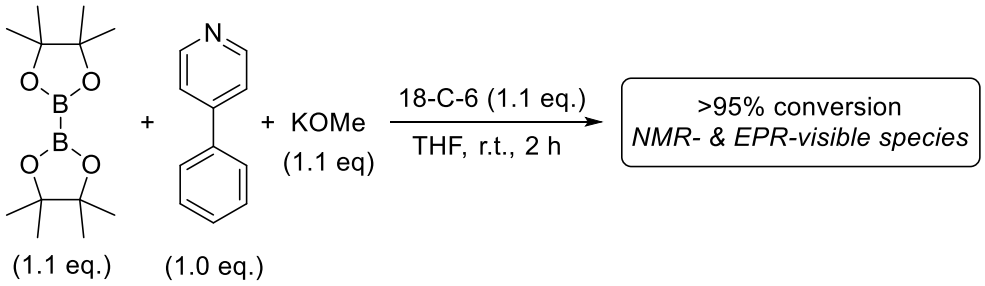

Scheme 3.10: Reaction conditions for the model study carried out by Jiao's group.

The ^{1}H NMR revealed clean conversion of the 4-phenylpyridine to another major product **27** (*ca.* 77% yield). The phenyl signals were not significantly altered, but the pyridine C–H peaks (two doublets, 2H each), shifted drastically upfield to four distinct signals (1H each). This indicated a disruption both to the aromaticity of the heterocyclic ring, and its C_{2v} symmetry. Further 1D NOESY data implied that the

pyridine had two new chemical bonds at the 1- and 2-positions (**Figure 3.4**) and ^{11}B NMR indicated the formation of a four-coordinate boron (singlet at δ 6.2 ppm).

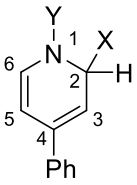

27

Figure 3.4: NMR-visible species formed from the reaction of 4-phenylpyridine, B_2pin_2 and KOMe.

Despite these useful NMR data, more information was required to fully elucidate the structure of the new species **27**. Attempts to crystallise it directly from the reaction mixture were unsuccessful, but an alternative setup yielded a yellow crystalline solid (**Scheme 3.11**). After treatment with 18-C-6, it produced identical ^{1}H, ^{11}B and ^{13}C NMR data to that which were observed previously. Single crystal XRD analysis performed on the yellow crystalline intermediate revealed it to be the ate complex **27** DME, which suggested the NMR-visible species was a complex with the composition **27** 18-C-6.

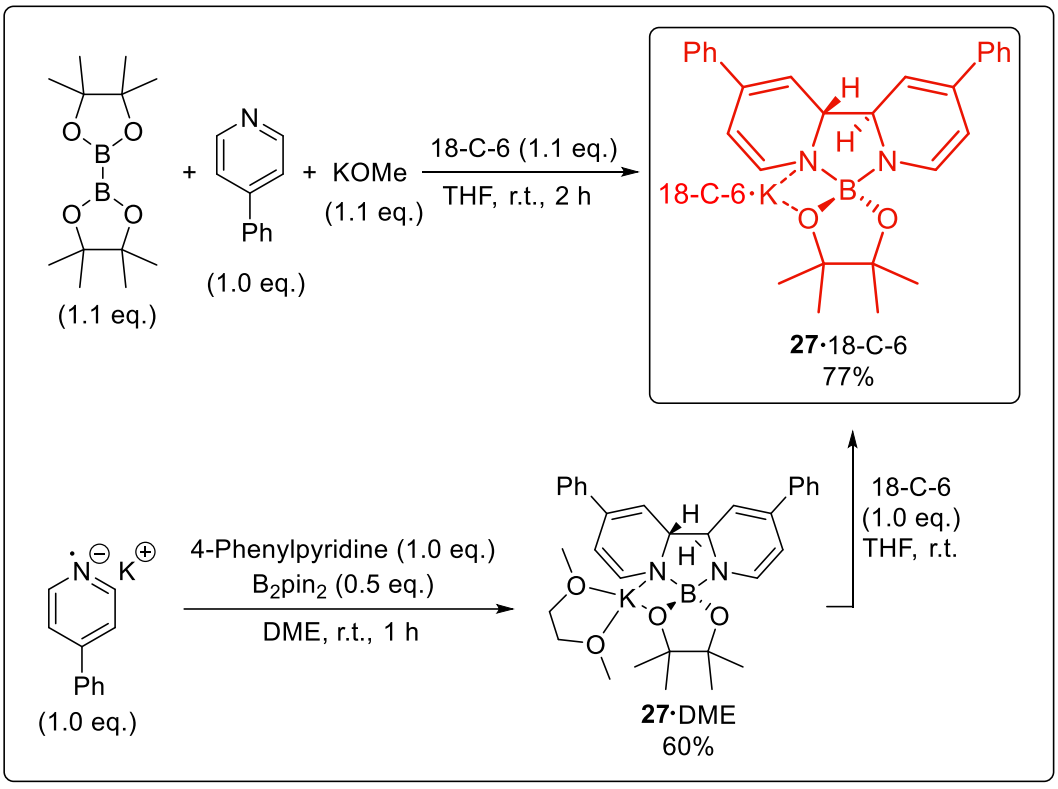

Scheme 3.11: Independent preparation of the NMR-visible species **27**•18-C-6.

Cyclic voltammetry and differential pulse voltammetry experiments were carried out on **27**•DME to assess its redox properties. They found the complex to have a similar oxidation potential to that of other reported SEDs,[125] implying it is capable of SET to organic substrates. This was exemplified when **27** DME was reacted with excess 4-iodoanisole, forming reduction product anisole in good yield after 30 min, along with 4-phenylpyridine and complex **28** (**Scheme 3.12**). Interestingly, no arylboronate was detected, indicating that **27** serves as an electron donor, but not a borylation reagent.

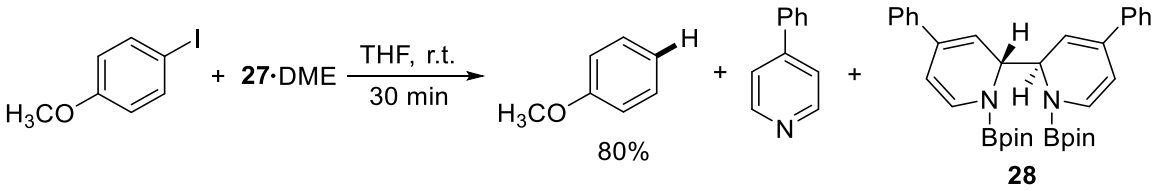

Scheme 3.12: Electron donor character of complex **27**.

As well as ate complex **27**, it was clear from the EPR spectrum of the B_2pin_2/4-phenylpyridine/KOMe/18-C-6 mixture that radical species were produced. Moreover, the EPR spectrum matched that of the original borylation mixture, confirming that the same radical species were being generated in both setups. However, the original proposal that the reaction generated methoxyboronate radical anion (MeO–Bpin$^{\bullet-}$) and pyridine-stabilised boryl radical (4-PhPy•Bpin$^{\bullet}$) was ruled out after DFT calculations revealed this to be thermodynamically unfavourable.

A useful observation was made when a 4-phenylpyridine radical anion, partnered with a Na^+ counterion, was found to give a deep purple crystal when reacted with B_2pin_2 in THF (**Scheme 3.13**). Analysis *via* XRD showed the crystal to be Lewis adduct **29** which, notably, when redissolved in THF with 18-C-6, gave a similar EPR spectrum to that observed with the reductive mixture (see **Scheme 3.10**).

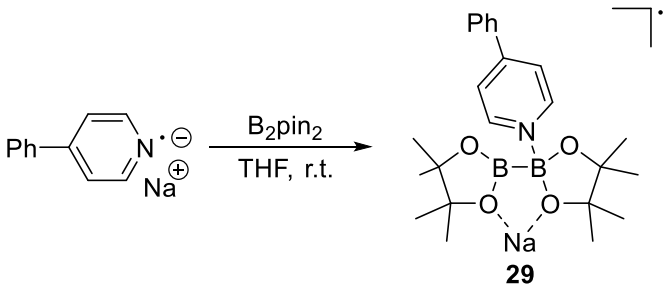

Scheme 3.13: Preparation of complex **29**. Formal charges have been omitted for clarity.

Jiao's group could therefore assume that their unknown EPR-visible species was also a complex of the 4-phenyl pyridine radical anion and a boron Lewis acid. This hypothesis was confirmed when an analogous solution of the pyridine radical was reacted with MeOBpin (**Scheme 3.14**). The resulting solution gave EPR spectral data that correlated favourably with the B_2pin_2/4-phenylpyridine/KOMe/18-C-6 mixture. Thus, the EPR-visible radical species was understood to be a complex between the 4-phenylpyridine radical anion and MeOBpin, denoted as 4-PhPy$^{\bullet-}$•B(OMe)pin **30**.

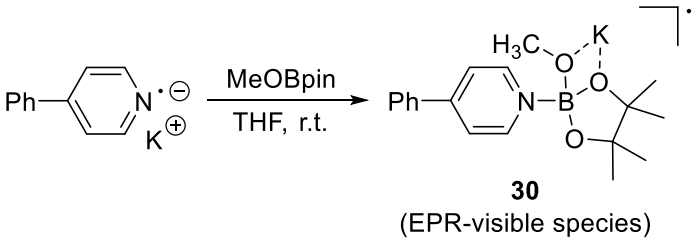

Scheme 3.14: Preparation of complex **30**. Formal charges have been omitted for clarity.

Further analysis from UV-vis data supported this structural assignment and demonstrated the electron donating ability of complex **30**. Thus, the findings made by Jiao's group suggest that the reaction of diboron, methoxide and 4-phenylpyridine proceeds smoothly to give two boryl-pyridine complexes: ate complex **27** as the major species (NMR-visible) and radical anion complex **30** as the minor species (invisible in the NMR spectrum but detectable by EPR). Both diboron-derived species act as SEDs, capable of reducing haloarenes *via* SET (**Scheme 3.15**).

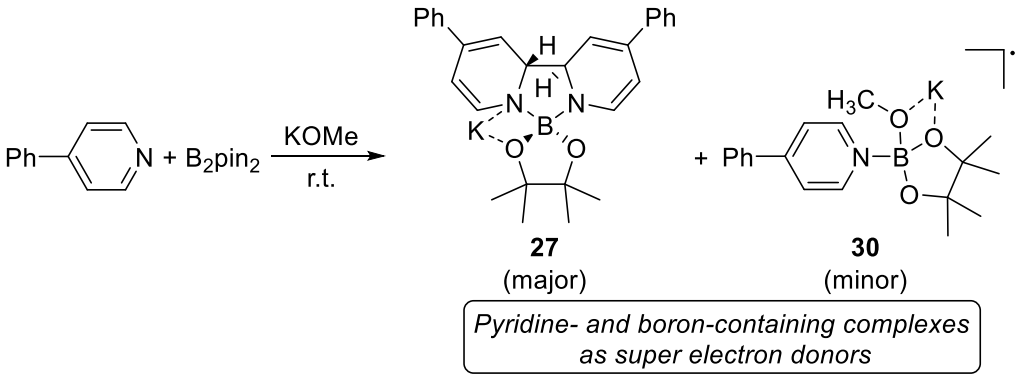

Scheme 3.15: Super electron donors present in the reaction system.

With the SED species confidently assigned, the authors proceeded to report the findings of a comprehensive DFT study to determine the mechanism by which they form. Their first aim was to establish the mode of B–B cleavage (**Figure 3.5**).

Homolytic fission of the B–B bond to give radical anion **IN3** and stabilised boryl radical **IN4** was ruled out after calculations revealed this pathway to be highly endergonic (+17.5 kcal mol^{-1} relative to adduct **IN2**). By contrast, an alternative route involving heterolytic scission to give MeOBpin and pyridine stabilised boryl anion **IN5** was found to be exergonic (−27.6 kcal mol^{-1}) with an activation barrier of $G^{\ddagger}$ = 12.7 kcal mol^{-1}. Thus, the heterolytic cleavage pathway was deemed to be both kinetically and thermodynamically feasible.

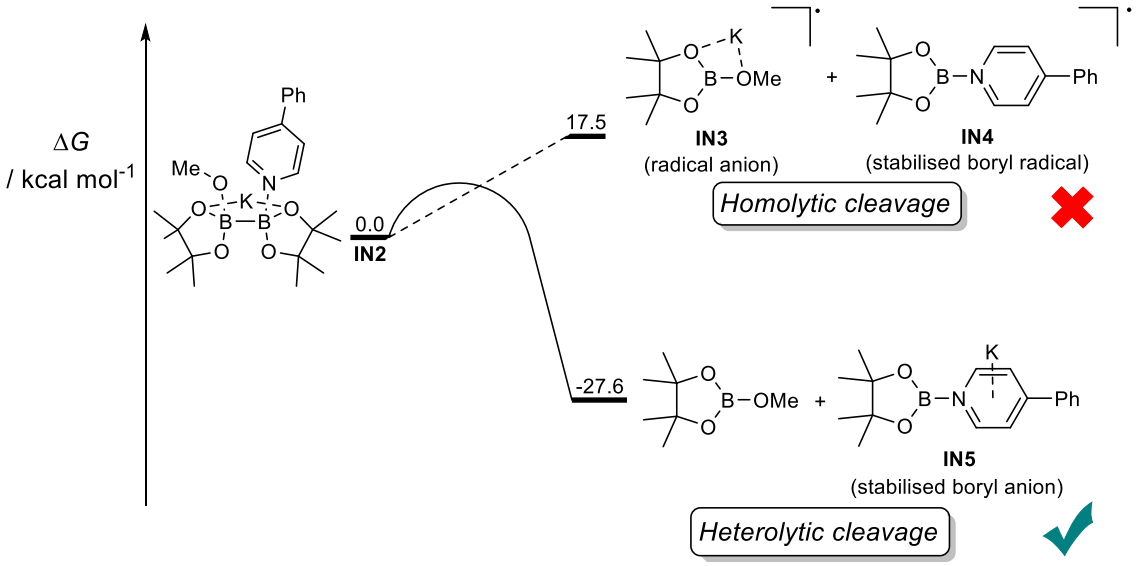

Figure 3.5: Gibbs free energy ($\Delta G_{solv\ 298\ K}$) profile for the homolytic and heterolytic cleavage pathways of diboron. Calculations based on DMSO as reaction solvent. Not to scale.

It was proposed that **IN5** is then transformed further to NMR-visible ate complex **27**, with the addition of an extra equivalent of 4-phenylpyridine (**Scheme 3.16**). The overall conversion was calculated to be exergonic by −2.1 kcal mol^{-1} with a reasonable free energy barrier ($G^{\ddagger}$ = 23.1 kcal mol^{-1}).

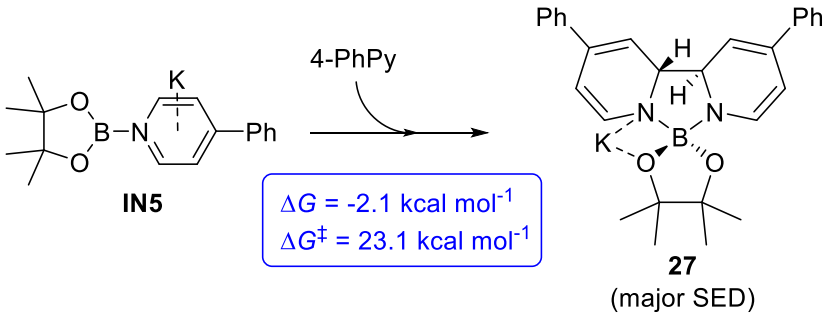

Scheme 3.16: Formation of ate complex **27** from pyridine-stabilised boryl anion **IN5**.

Experimental studies suggested that the other SED (radical anion complex **30**) was formed upon addition of MeOBpin to boryl anion **27**, with subsequent loss of

4-PhPy•Bpin$^{\bullet}$ (**IN4**). Independently synthesised **27**•DME reacted with 1 eq. MeOBpin in *ca*. 20% conversion to give radical anion **30**, verified with UV-vis and EPR analysis (**Scheme 3.17**). The low conversion was explained by a calculated overall Gibbs free energy change of 0.1 kcal mol^{-1}.

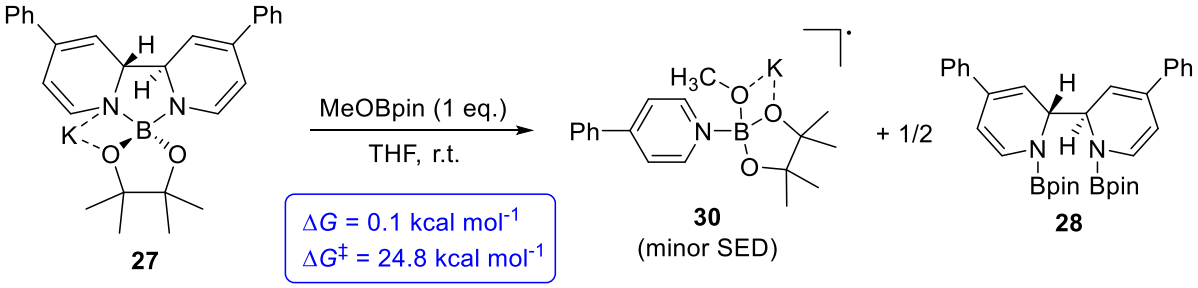

Scheme 3.17: Formation of radical anion **30** from complex **27**.

The sensational findings from this in-depth study are at odds with the prior assumptions made by the same group originally.[92] Previously, diboron cleavage promoted by methoxide and pyridine was believed to be homolytic, giving a methyl borate radical **IN3** (the SED) and stabilised boryl radical **IN4**. Once **IN3** had generated an aryl radical *via* SET, **IN4** could then react with the aryl radical to give the desired aryl boronate. However, not only was a homolytic pathway found to be energetically unfavourable *via* DFT, but calculations also reveal **IN4** to be unstable with respect to dimerisation to **28**. Moreover, kinetic competition experiments found that the relative borylation rate was affected by [B_2pin_2] but not [4-PhPy]. This indicated that the aryl radical reacts with B_2pin_2 rather than a pyridine-containing boryl species in the crucial C–B bond formation step.

Very recently, Leonori *et al.* published a landmark report that realises the goal of developing a Minisci-type borylation reaction that proceeds *via* boron-centred radicals (**Scheme 3.18**).[126] The procedure relies on the catalytic presence of a photoredox catalyst (PC) under irradiation of blue light. Its long-lived excited state (PC*) is capable of SET to a persulphate anion to generate a radical anion ($S_2O_8^{2-}$ + PC* → SO_4^{2-} + $SO_4^{\bullet-}$ + PC^{+}). Radical anion $SO_4^{\bullet-}$ then abstracts a hydrogen atom from a simple and inexpensive amine borane complex to generate a boron-centered radical ($SO_4^{\bullet-}$ + H_3B–NMe_3 → HSO_4^{-} + H_2B–$NMe_3^{\bullet}$). The boryl radical is highly nucleophilic and was shown to be capable of site-selective addition to protonated nitrogen-based heterocycles (pyridines, quinolines, isoquinolines, pyrimidines, pyridazines, azaindoles *etc.*).

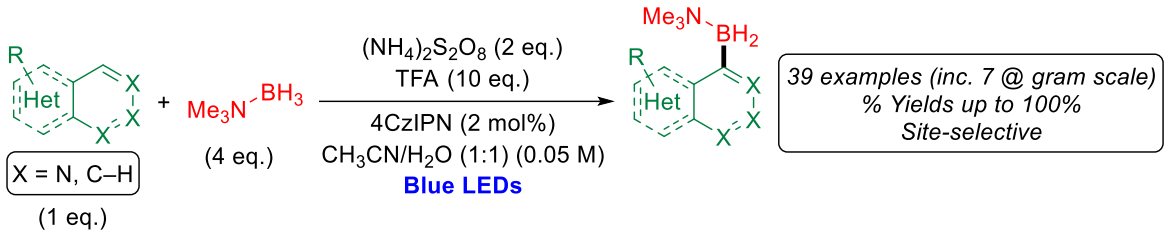

Scheme 3.18: Radical C–H borylation of azines. 4-CzIPN = 1,2,3,5-Tetrakis(carbazol-9-yl)-4,6-dicyanobenzene.

Impressively, the authors go on to demonstrate that the azine amine-boranes are capable of further elaboration *via* techniques such as oxidation, Suzuki cross-coupling, Chan-Lam amination and Chan-Lam etherification.

3.1.4 Conclusion

This project aimed to develop a novel method to generate boryl radicals *via* a base-free setup with an internally preactivated mixed diboron compound **25**. However, the hypothesis for our work was underpinned by the available literature in 2017. Thus, we believed base-promoted diboron cleavage would generate boryl radicals capable of reacting with aryl halides or, preferably, heteroaromatic bases *via* a Minisci-type reaction. Leonori's work validates this original hypothesis, provided a suitable method for boron radical generation can be found.

In our work, turnover of diboron **25** was observed but we failed to achieve significant yields of aryl boronate. Although, Fe^{III} and Mn^{III} salts may offer some assistance. Besides, the emergence of Jiao's detailed study into the nature of the SEDs involved in pyridine-catalysed borylation undermined the hypothesis on which we had designed this project. In the light of this report, we retired our work on free radical borylation to explore other experimental methods to form C–B bonds.

3.2 Iridium-catalysed borylation of heteroarenes

3.2.1 Scope, limitations and functional group tolerance

Upon the outset of this project, the scope and regioselectivity of iridium-catalysed C–H borylation on heteroarenes had been explored to an appreciable extent.[17,20,127] However, an exhaustive robustness screen to probe the tolerance of the methodology to a wide range of heterocycles and functionality has not yet been published. We therefore aimed to further assess the limitations of iridium-catalysed borylation reaction, particularly with respect to structurally complex 'drug-like' molecules.

The first compound selected for investigation was amide **31a**. Examining the functionality and structural motifs, we did not envisage any major difficulties. Alkoxy groups, thiophenes and amide bonds have all been demonstrated to be amenable to iridium-catalysed borylation. As expected, amide **31a** reacted smoothly under standard iridium borylation methodology to furnish both the mono- and diborylated products **31b** and **31c**, respectively (**Scheme 3.19**).

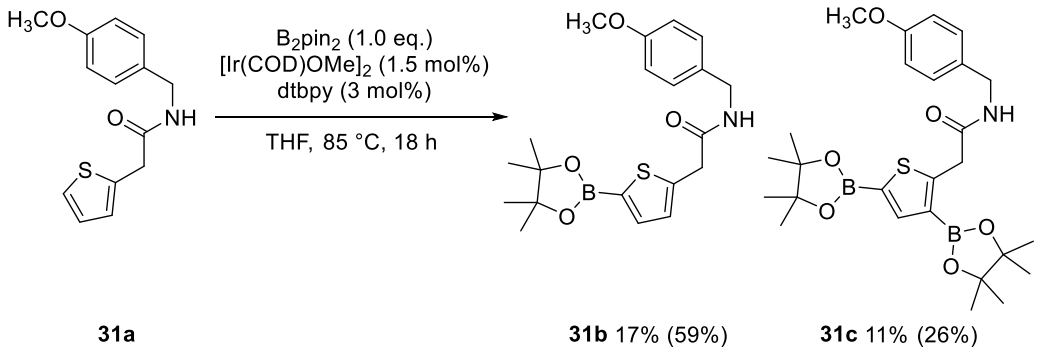

Scheme 3.19: Iridium-catalysed borylation of amide **31a**. NMR yields given in parentheses.

The reactivity of **31a** followed an expected pattern with the first borylation occurring on the thiophene ring at the more reactive 5-position, α to the S atom. The second borylation was found to occur at the more hindered and less reactive 3-position, β to the S atom. This was verified by comparing the NOE correlations associated with the methylene group connected to C-2 in each of the products (**Scheme 3.20**).

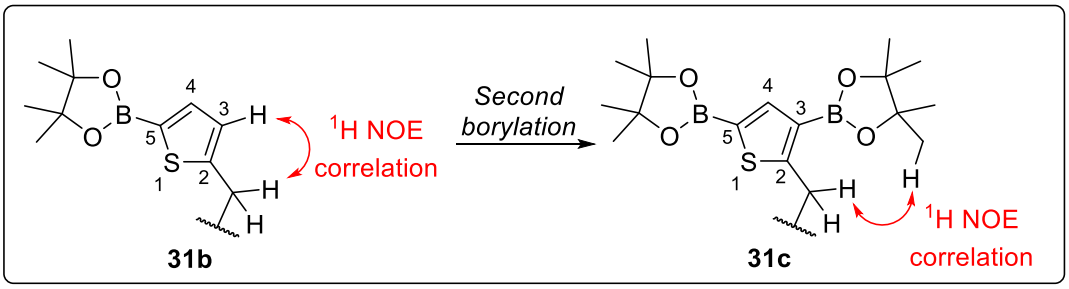

Scheme 3.20: NOE relationships associated with the –CH_2– group attached to C-2 in **31b** and **31c**.

With unsymmetrical 2,5-disubstituted thiophenes, borylation regioselectivity is often poor.[128] However, in the case of **31b**, a significantly greater steric constraint is provided by the −Bpin on C-5 than that which is given by the −CH_2R connected to C-2. Thus, there is no viable pathway to borylation at the 4-position. Also, it is possible that C-3 activation is encouraged by the carbonyl oxygen coordinating to the iridium centre and inducing proximity between the C-3 C−H and the metal centre (**Scheme 3.21**). Such a phenomenon has been observed before and exploited to give directed *ortho*-borylation in benzoate esters.[129]

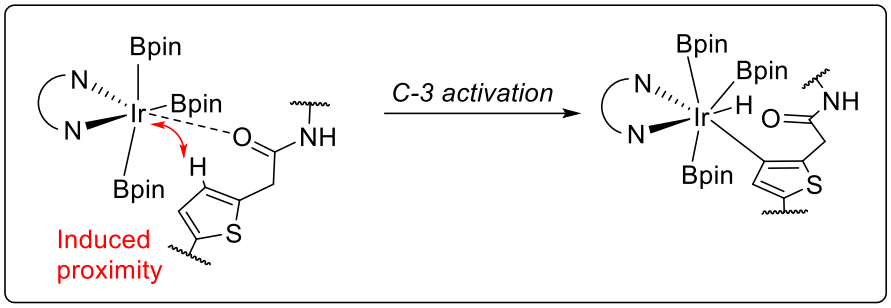

Scheme 3.21: Suggested rationale for the borylation of monoborylated amide **31b** at the hindered C-3 position. Bond lengths and bond angles have been distorted for clarity.

No borylation was found to occur on the anisole ring. This will primarily be due to high steric demands but the electron-rich nature of the ring further disfavours C−H insertion. A repeat of the reaction with tmphen (tmphen = 3,4,7,8-tetramethyl-1,10-phenanthroline) *in lieu* of dtbpy did not deliver higher NMR yields (**31b** 48%, **31c** 31%).

In terms of synthetic usefulness, a mixture of mono- and diborylated products is undesirable. Changing the reaction parameters allowed for outcomes that favoured one product over the other. For example, carrying out the reaction at a lower temperature and higher dilution (**Conditions A**) gave the same yield of **31b** (by ^{1}H NMR) as observed previously, but with only a trace quantity of **31c** detected.

More forcing conditions (**Conditions B**) delivered exclusively **31c**, although there was clear evidence by ^{1}H NMR spectroscopy of product degradation *in situ* (**Scheme 3.22**).

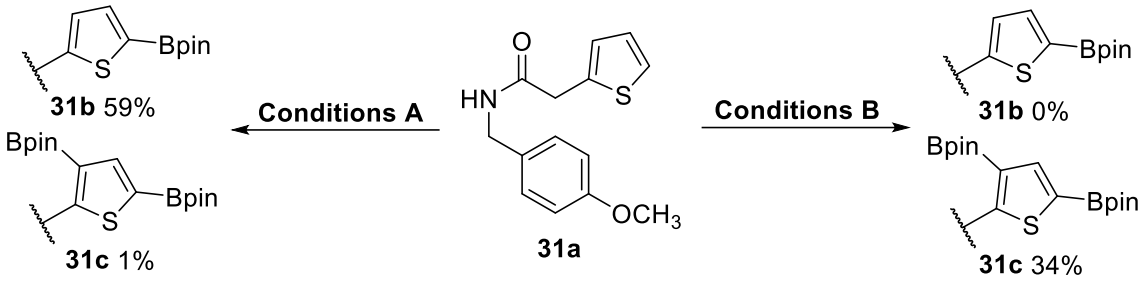

Scheme 3.22: Reaction conditions to favour mono- *vs.* diborylation. **Conditions A**: B_2pin_2 (1.0 eq.), $[Ir(COD)OMe]_2$ (1.5 mol%), dtbpy (3 mol%), THF (0.2 M), 50 °C,18 h. **Conditions B**: B_2pin_2 (2.0 eq.), $[Ir(COD)OMe]_2$ (3 mol%), dtbpy (6 mol%), dioxane (1 M), 100 °C, 48 h.

Although NMR yields were good, isolated yields were poor. This was largely due to repeated silica gel column chromatography, which was necessary to remove residual $B(OR)_3$ species. However, we pondered if this issue could be circumvented with *in situ* modification of the Ar−$B(OR)_2$ functional group. We repeated the reaction of amide **31a** under **Conditions A**, followed by typical Suzuki-Miyaura cross-coupling conditions (**Scheme 3.23**). Our hope was to generate the monoarylated product **31d** selectively in a one-pot tandem sequence.

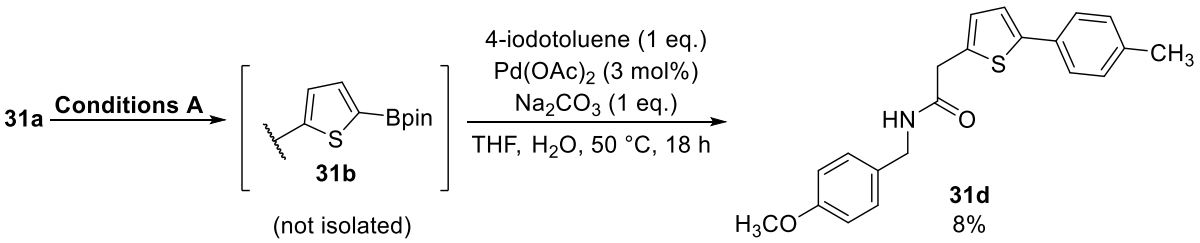

Scheme 3.23: One-pot tandem iridium-catalysed borylation–Suzuki-Miyaura cross-coupling sequence.

To our disappointment, analysis of the crude reaction mixture revealed a complex mixture of products with only 8% of monoarylated **31d** separable by column chromatography. The appearance of diarylated product **31e** and monoborylated, monoarylated **31f** hinted that perhaps the borylation had continued to progress in the interval between the two steps (**Figure 3.6**). However, yields of these compounds were very low too, suggesting that perhaps our Suzuki conditions were not forcing enough. It is also possible that our cross-coupling reaction was being outcompeted by a base-catalysed protodeborylation process, given the presence of aqueous

Na_2CO_3. Although, reported one-pot iridium borylation–Suzuki coupling procedures employ similarly basic conditions for the second step.[130]

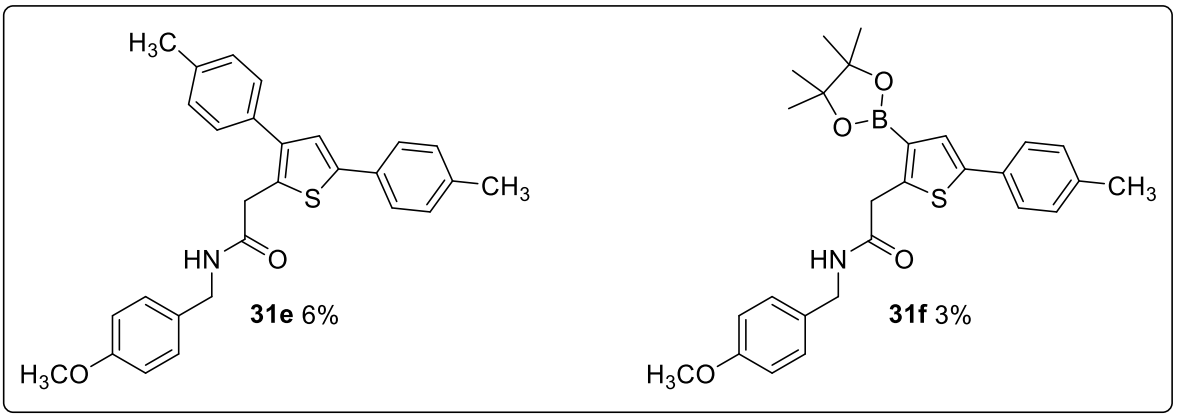

Figure 3.6: Further elaborated products of diborylated amide **31c**.

Our data highlight the challenges of controlling the reactivity in substrates with multiple unhindered sites. Future attempts at *in situ* modification of Ar–Bpin compounds should involve regular monitoring and be immediately followed by the sequential step if the substrate is prone to diborylation. Alternatively, difunctionalised amide **31f** could be viewed as a highly desirable intermediate due to its potential for diversification. It is possible to envisage a method whereby forcing borylation conditions are employed to deliver diborylated **31c**, followed by a mild sequential step to functionalise selectively at one site, while leaving another –Bpin handle installed elsewhere.

Broadening the scope of our investigation, we then sought to better understand how the reactivity of the amide substrate would change if the S on the thiophene was replaced with a different heteroatom. Two analogues of **31a** were selected for investigation; one with furan *in lieu* of thiophene (**32a**) and one with *N*-methylpyrrole (**33a**). Unprotected pyrrole was avoided due to its tendency to undergo self-polymerisation.[131] However, C–H activation at the C-2 position may be discouraged somewhat by a steric influence from the *N*-methyl group.

Synthesis of amide **32a** was facile as the corresponding carboxylic acid is readily available. The desired product was isolated in excellent yield following an amidation protocol developed in our group (**Scheme 3.24**).[50]

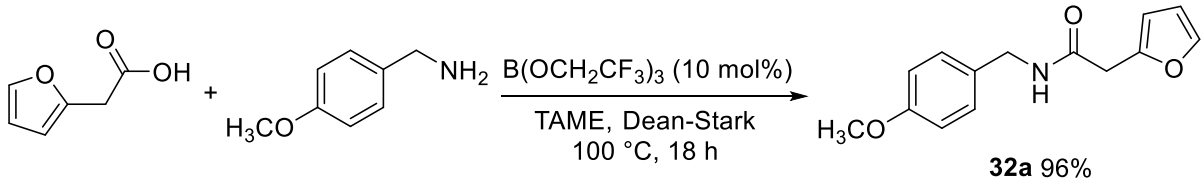

Scheme 3.24: Synthesis of amide **32a**.

For amide **33a**, the corresponding carboxylic acid was prohibitively expensive, so it was synthesised in-house according to published methods.[132] The formation of the desired product **35** was confirmed *via* ^{1}H NMR spectroscopy, but to avoid complications in purification, crude material was used directly in the final amidation step (**Scheme 3.25**).

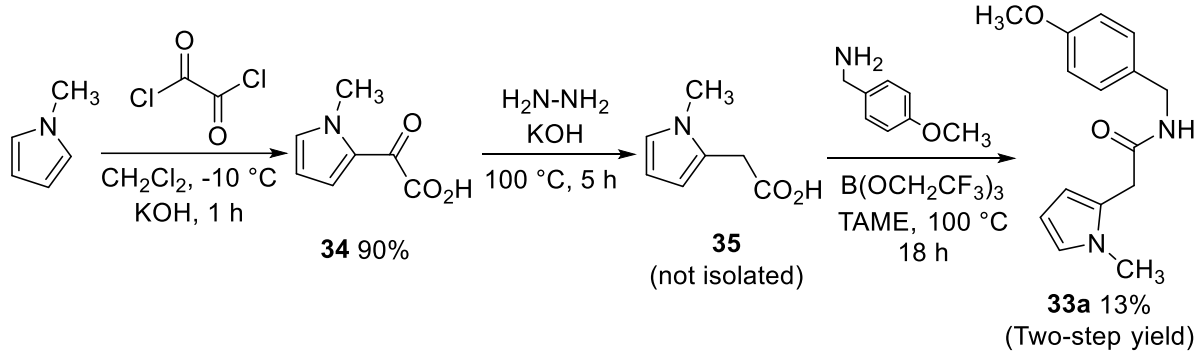

Scheme 3.25: Synthesis of amide **33a** from *N*-methylpyrrole.

With two novel amides successfully synthesised, **32a** and **33a** were subjected to the same reaction conditions as described in **Scheme 3.19** (**Table 3.2**). Since we had plentiful stocks of amide **32a**, an additional reaction was set up in parallel with tmphen as the ligand *in lieu* of dtbpy. Interestingly, the Ir-tmphen catalytic system proved to be more active than Ir-dtbpy. Hartwig's group have demonstrated that tmphen can outperform dtbpy in a number of cases, particularly for electron-rich substrates.[20] They credit this to tmphen's "greater electron-donating ability" and "backbone rigidity". However, as we have seen, it is not consistently superior to dtbpy. A definitive set of guidelines to predict which catalytic system would be more active for a given substrate has not yet been put forward.

A third reaction with amide **32a** was carried out at 75 °C instead of 85 °C. Remarkably, the ^{1}H NMR of the crude mixture revealed a mono-/diborylated product ratio of 3:1 (*c.f.* at 85 °C: **32b**/**32c** 1:2). This indicates that the second borylation β to the heteroatom has a lower kinetic barrier in the furan-containing amide **32a** compared to the thiophene analogue **31a**.

Amide **33a** reacted to give roughly equal proportions of **33b** and **33c** but yields were low. This was assumed to be due to a high kinetic barrier for C–H activation adjacent to the N–Me group, as anticipated. However, analysis of the reaction *via* ^{1}H NMR revealed other unwanted side products, suggesting that pyrroles may be too unstable at elevated temperatures.

Table 3.2: Iridium-catalysed borylation of amides **31 – 33a**.[a]

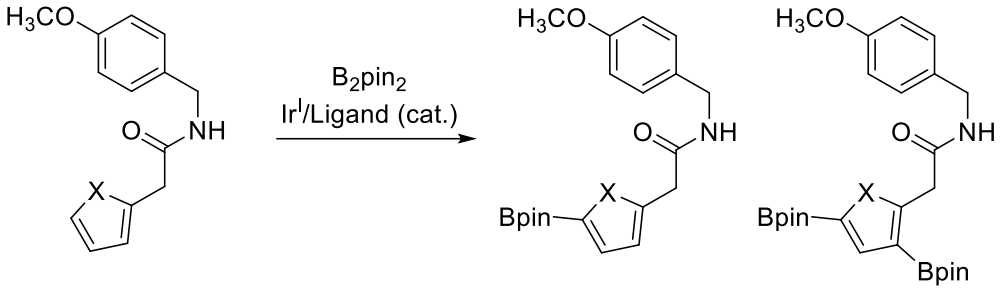

31a: X = S
32a: X = O
33a: X = N-CH_3

31 – 33b **31 – 33c**

Amide	X	% Yield[b]	
		Monoborylated	**Diborylated**
31a	S	17 (59)	11 (26)
32a[c]	O	8 (19)	18 (37)
33a	N–CH_3	15 (15)	11 (13)

[a]Reaction conditions: **Amide** (1 mmol), B_2pin_2 (1 mmol), $[Ir(COD)OMe]_2$ (1.5 mol%), dtbpy (3 mol%), THF (1.0 mL), 85 °C, 18 h, sealed tube, Ar atmosphere. [b]Crude yields are determined from ^{1}H NMR analysis with 1,3,5-trimethoxybenzene as the internal standard and given in parentheses. [c]Data shown is for when tmphen was used as the ligand *in lieu* of dtbpy (*cf.* crude yields with dtbpy: **32b** 13%, **32c** 30%).

Seeking to further explore the compatibility of iridium-catalysed borylation, other compounds were selected from in-house stocks (**Figure 3.7**). Amide **36** did not react under standard conditions despite possessing suitable structural motifs. It is possible that the free –NH_2 is basic enough to coordinate to the iridium catalyst and block C–H activation. Conveniently, we were able to test this supposition by screening amide **37**, the drug molecule sitagliptin with its primary amine Boc-protected. It was envisaged that borylation on the polysubstituted phenyl ring would be possible due to fluorine's very low Van der Waals radius. However, amide **37** did not borylate under

the reaction conditions either. In this case, the fused triazole heterocycle may be too basic, despite the deactivating presence of the $–CF_3$ group.

As a sterner test, the diuretic drug furosemide **38** was subjected to the same procedure as before. The Ar–H bonds on the benzene ring are too sterically crowded to react with the iridium catalyst, but the 2-substituted furan is accessible and amenable to this methodology, as we have seen. Also, the amine was assumed to be too bulky to coordinate to the iridium and its basicity would be attenuated due to overlap with the delocalised π-system of the benzene ring. However, no conversion of starting material was observed by TLC at 85 °C, or in dioxane at 100 °C. It is conceivable that the sulphonamide or carboxylic acid deactivated the catalyst, since these functional groups do not feature in published reports of iridium-catalysed borylation on substituted aromatics.

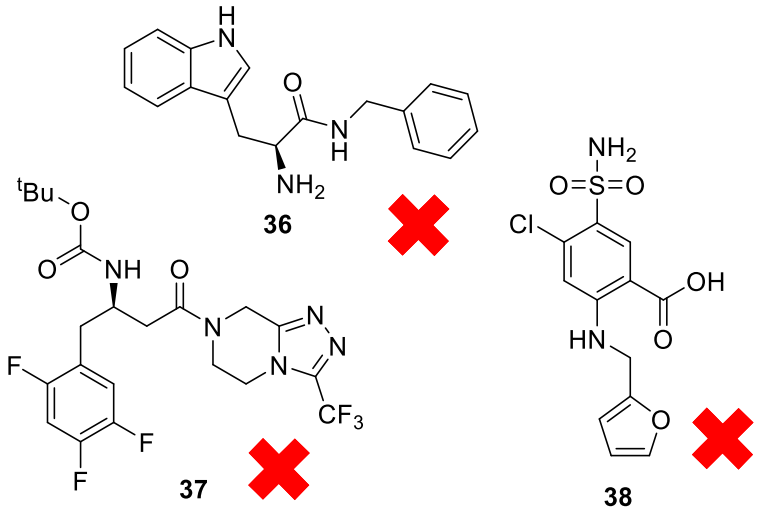

Figure 3.7: Amides **36** and **37** and furosemide **38**. Unless stated otherwise, substrates subjected to the following reaction conditions: Substrate (1 eq.), B_2pin_2 (1 eq.), $[Ir(COD)OMe]_2$ (1.5 mol%), dtbpy (3 mol%), THF (1 M), 85 °C, 18 h, Ar atmosphere.

When antiemetic drug ondansetron **39** was screened, substantial conversion of starting material was observed. However, TLC analysis revealed a complex mixture of at least seven different components. Purification by column chromatography provided **40** in a very low yield and a trace amount of impure carbazole **41** (**Scheme 3.26**). Notably, the formation of compound **40** reveals the existence of a reductant in the reaction mixture. This is consistent with the established reaction mechanism for iridium-catalysed borylation (described in **Chapter 1.2.2**), which suggests the presence of reductive species (Ir–H, H–Bpin and H_2). Since no

borylated material formed in our reaction, efforts were not made to resolve the mixture further.

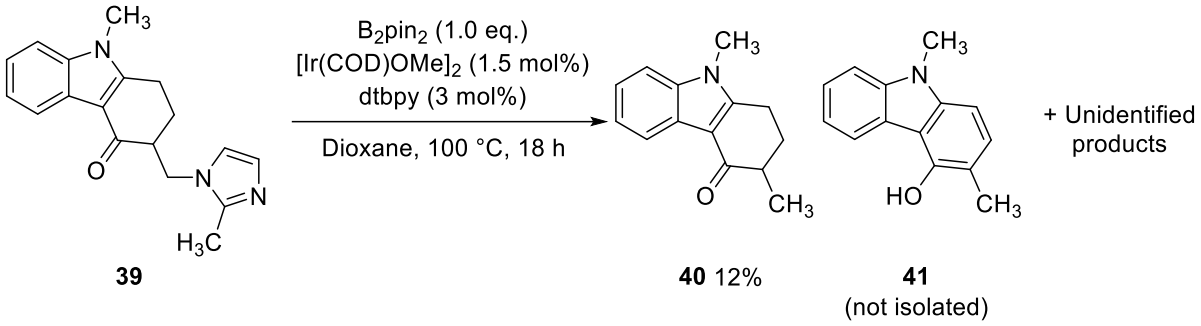

Scheme 3.26: Reaction of ondansetron **39** under standard iridium borylation conditions.

In the hope of cleaner reactions, we simplified our substrate scope to include substituted heterocyclic scaffolds with lower molecular weights. Indazole **42** was deemed a good candidate. The iridium-catalysed borylation of *N*-protected indazoles has been studied with an array of mono-substitutions on the carbocyclic ring.[133] Borylation has been shown to occur first at C-3 for 5-, 6- and 7-substituted indazoles, but at C-6 when 4-substituted. To the best of our knowledge, 3-substituted indazoles have not been investigated.

Consistent with our earlier attempts to react substrates with an unencumbered basic nitrogen, indazole **42** did not react. To mitigate this, we converted the substrate into the tosyl-protected indazole **43**, to block any interactions with the catalyst. However, this compound did not react either (**Scheme 3.27**).

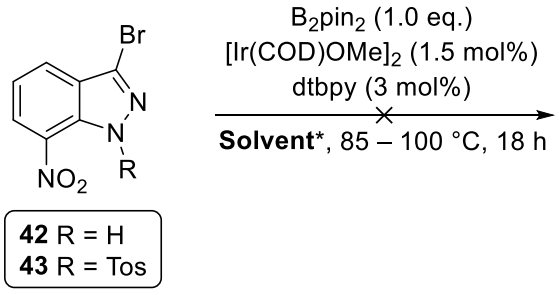

Scheme 3.27: Unsuccessful borylation attempts of indazoles **42** and **43**. *Attempted in both THF (at 85 °C) and dioxane (at 100 °C).

We suspected that the –NO_2 group may be incompatible with the catalyst, since this functional group is absent from published reports of iridium borylation. To test this, we set up the reactions of *m*-xylene **44a** and 1,3-dinitrobenzene **45a** in parallel. Confirming our assumption, 1,3-dinitrobenzene did not react. By contrast, *m*-xylene

borylated readily, delivering aryl boronate ester **44b** in good yield, with evidence of dimerisation and diborylation taking place at the benzylic position on account of overly forcing conditions (**Scheme 3.28**).

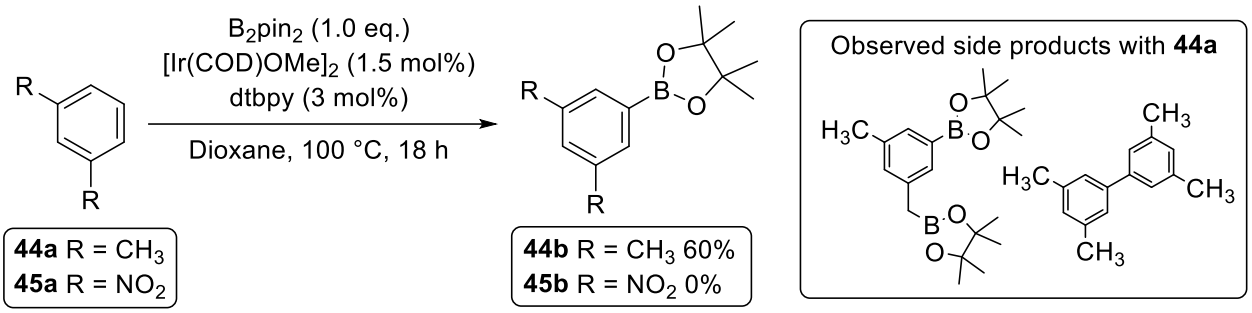

Scheme 3.28: Borylation of 1,3-disubstituted arenes.

Returning to the indazole scaffold, we acquired nitro-free indazole **46a**, which failed to react when unprotected. However, the tosyl-protected indazole **47a**, did undergo borylation to give a mixture of products **47b**, albeit in a very low combined yield of 14% (**Scheme 3.29**). We were unable to separate borylated regioisomers *via* column chromatography. Although, NMR analysis revealed that our product mixture was dominated by the 5- and 6-borylated isomers in a 1.7:1 ratio.

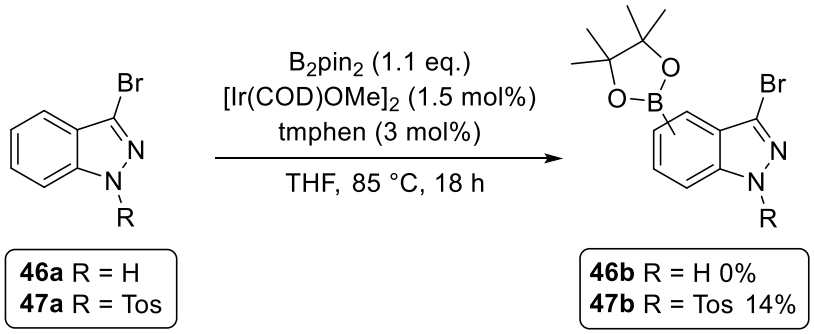

Scheme 3.29: Attempted borylations of indazoles **46a** and **47a**.

The low conversion of **47a** was unlikely to be due to the sulphonyl group, since mesyl-protected indazoles have been shown to be amenable to iridium-catalysed borylation.[133] To investigate whether steric factors were at play, the Boc-protected indazole **48a** was synthesised and screened against standard conditions (**Scheme 3.30**). Although, to our dismay, we did not observe any turnover of starting material. It is possible that we underestimated the steric influence of a Boc group, and that its three-dimensional nature impedes close approach to the iridium catalyst.

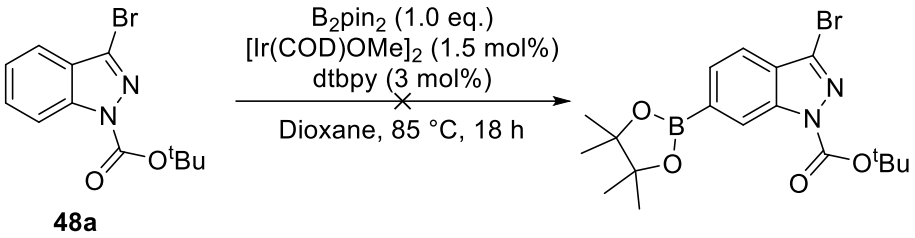

Scheme 3.30: Iridium-catalysed borylation of indazole **48a**.

The next substrate to be investigated was quinoline **49a**. Quinoline is a very common moiety in pharmaceuticals[2] and natural products,[134] so its direct functionalisation is of relevance to medicinal chemistry. The reaction of quinolines with various substitution patterns under iridium borylation conditions has been explored.[135–137] However, 4-substituted quinolines have not yet been investigated.

Quinoline **49a** reacted under standard iridium borylation conditions to give a mixture of 6- and 7-borylated products in a 1.3:1 ratio, respectively. Purification *via* silica gel column chromatography afforded an inseparable mixture of **49b** and **49c** in 33% yield (**Scheme 3.31**).

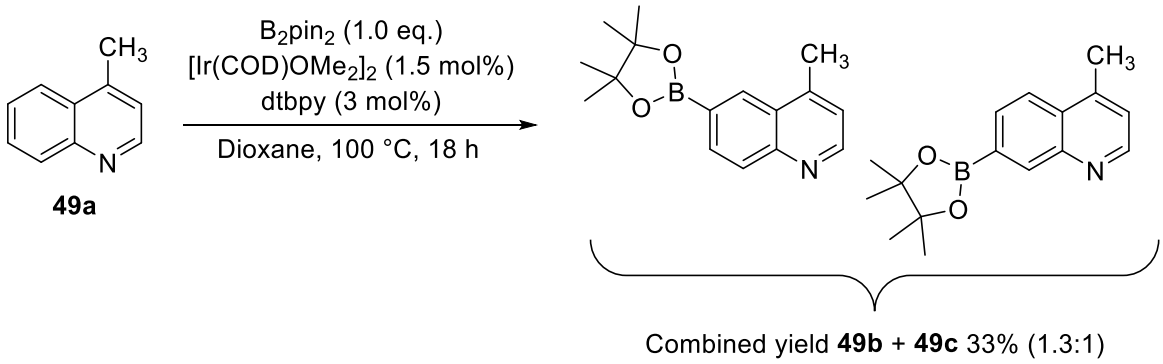

Scheme 3.31: Iridium-catalysed borylation of quinoline **49a**.

It was interesting to note the influence of the methyl group giving a slight preference for borylation at the 6-position over the 7-position. Under the same reaction conditions, unsubstituted quinoline has been shown[138] to borylate first in the 3-position, and then with equal probability at the 6- or 7-position. Since steric effects are unlikely to be a factor in the borylation of **49a**, it must be the electronic effect of the methyl group which causes one site to become more reactive than the other. Intrigued by this observation, a project was designed to investigate how altering the electronic nature of the substituent at the 4-position influences the regioselectivity of the iridium-catalysed borylation reaction.

3.2.2 Investigation into the borylation of 4-substituted quinolines

In selecting a set of substrates to be investigated, the aim was to choose compounds whose 4-substituents varied greatly in their electronic nature to help identify any trends in our results (**Figure 3.8**). Ether **50a** as well as the initial compound **49a** were to comprise the electron-rich quinolines and ester **51a** and amide **52a** were the electron-poor structures. Quinolines **53 – 55a** were also included since these would be available as precursors or intermediates during the synthetic approach to our chosen substrates.

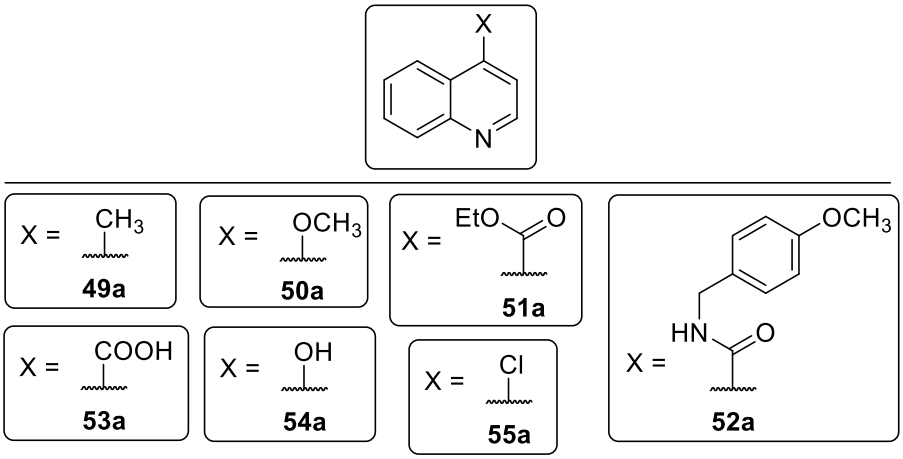

Figure 3.8: 4-Substituted quinolines selected for investigation.

3.2.2.1 Synthesis of substrates

To synthesise ester **51a**, carboxylic acid **53a** was reacted with ethanol *via* standard Fischer esterification methodology[139] to give a fair yield of the desired product after work up and purification (**Scheme 3.32**).

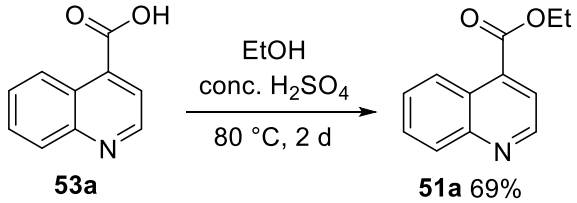

53a **51a** 69%

Scheme 3.32: Synthesis of **51a** from **53a**.

Next, the synthesis of amide **52a** was attempted *via* Sheppard amidation methodology (**Scheme 3.33**).[50] Since carboxylic acid **53a** didn't appear to dissolve in the solvent at reflux, the reaction was left for an extended period in the hope that trace amounts of dissolved **53a** would react to form **52a**. To our delight, the reaction

mixture eventually became homogenous and the desired product could be filtered out of the reaction once cooled to give the desired amide **52a** in excellent yield.

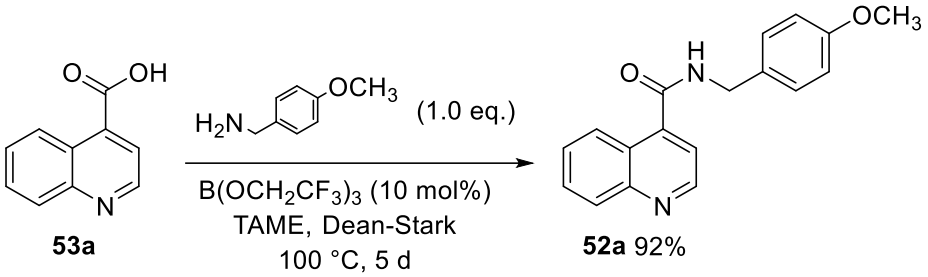

Scheme 3.33: Synthesis of **52a** from **53a**.

With the two electron-withdrawing compounds successfully synthesised, we turned our attention to the synthesis of ether **50a**. A two-step synthesis reported by García-Mancheño and colleagues[140] was employed (**Scheme 3.34**). Quinolinol **54a** was chlorinated to provide intermediate **55a** in good yield, before being stirred in a mixture of sodium in methanol at reflux for 2 d to give a fair yield of the desired product **50a** (overall yield = 37%).

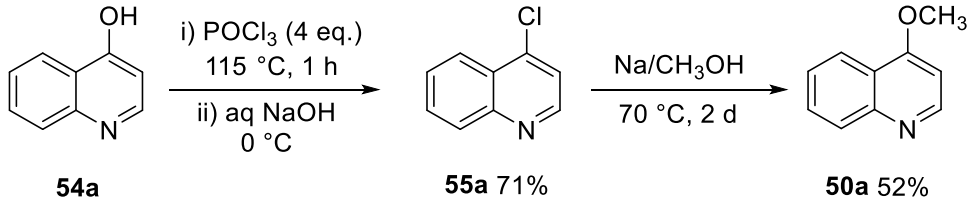

Scheme 3.34: Two-step synthesis of **50a** from **54a**.

3.2.2.2 Optimisation

Before undertaking the investigation, it was important to ensure that the reaction conditions were optimised (**Table 3.3**). Since the efficiency of the iridium catalyst varies somewhat unpredictably when dtbpy and tmphen ligands were exchanged and reacted with different substrates, both were used in the investigation. A range of solvents known to be compatible with iridium borylation were also screened which confirmed dioxane to be the most suited to this reaction (**Entries 4 – 6**).

Table 3.3: Optimisation of the iridium-catalysed borylation of **49a***.

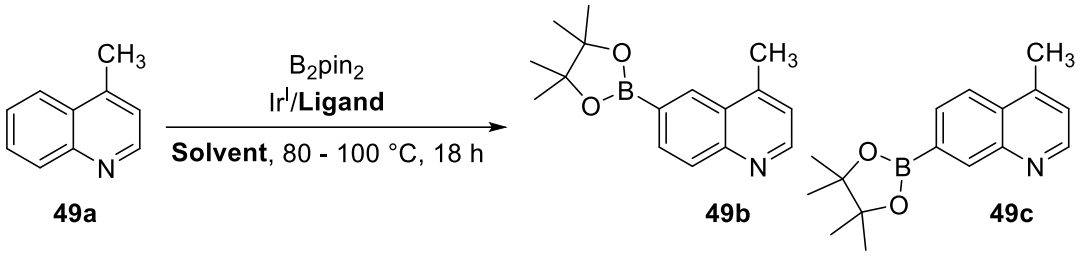

Entry	Ligand	Solvent	Temp / °C	% 49a	% 49b	% 49c
1	dtbpy	Dioxane	80	24	23	19
2‡	**dtbpy**	**Dioxane**	**100**	**26**	**25**	**19**
3§	**tmphen**	**Dioxane**	**100**	**11**	**28**	**21**
4	dtbpy	THF	80	20	23	16
5	dtbpy	Hexane	80	43	6	5
6	dtbpy	CPME	80	37	16	10

*Reaction conditions: **49a** (1 mmol, 1.0 eq.), B_2pin_2 (1.0 eq.), $[Ir(COD)OMe]_2$ (1.5 mol%), ligand (3 mol%), solvent (1 mL), 80 – 100 °C, 18 h, sealed tube, Ar atmosphere. % Yields determined by ^{1}H NMR spectroscopy with 1,3,5-trimethoxybenzene as an internal standard. SM was 95% pure. ‡2% diborylated product detected. §12% diborylated product detected.

While useful, these results raised some concern over whether material was being lost in the work up as the total % yield of SM and reaction products (**49a** + **49b** + **49c**) was considerably less than 100%. Weighing the reaction after filtration through a silica plug confirmed a near full retention of material hinting at the formation of unwanted side products. A similar observation has been made before by Hartwig and co-workers in an experiment designed to investigate the mass balance of the reaction of 4-picoline with B_2pin_2 (**Scheme 3.35**).[20] Without sterically accessible C–H bonds, 4-picoline was thought to undergo slow borylation at the 2-position followed by rapid decomposition.

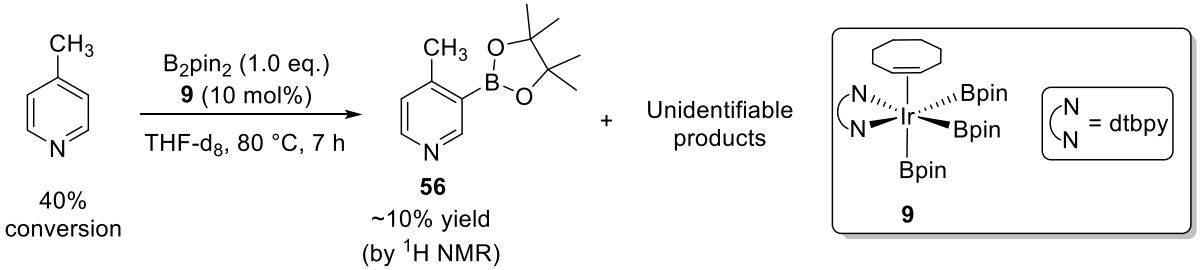

Scheme 3.35: Decomposition of 4-methylpyridine under standard iridium borylation conditions.

Indeed, when 4-picoline was heated with B_2pin_2 at 80 °C in the presence of 10 mol% complex **9**, several unidentifiable aromatic compounds were formed along with a small amount of pyridyl boronate ester **56**. Since, after 7 h the conversion of 4-picoline was 40% but the yield of **56** was ~10%, this strongly implied that a significant amount of starting material was converted into side products resulting from decomposition of the 2-boryl pyridine product.

Given that 4-picoline is a substructure of 4-methylquinoline, it is easy to draw comparisons between Hartwig's findings and the discrepancies listed in the data in **Table 3.3** and assume that we were observing a similar phenomenon. To confirm this, we set up the reaction of the regioisomer 2-methylquinoline under identical conditions to those used in **Table 3.3, Entry 1** (**Scheme 3.36**). The substrate underwent borylation efficiently and reacted along several vectors to give a mixture of mono- and diborylated regioisomers, in accordance with literature reports.[137]

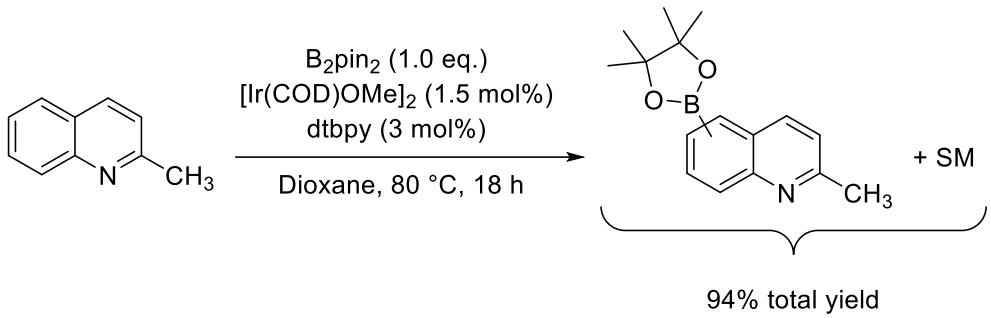

Scheme 3.36: Reaction of 2-methylquinoline with B_2pin_2.

As before, the reaction was analysed *via* ^{1}H NMR spectroscopy with the use of an internal standard. For simplicity, all CH_3 peaks visible were integrated collectively to measure the total yield of borylated products and unreacted starting material. This revealed that 94% of quinoline-derived material had been retained, compared to 71% in the analogous reaction with 4-methylquinoline. Moreover, qualitative analysis of the ^{1}H NMR spectrum for the reaction with 2-methylquinoline was visibly cleaner compared to the corresponding spectrum with 4-methylquinoline. This suggests that having the C-2 position accessible leads to side reactions.

For the avoidance of doubt, the side reactions we encountered were more complex and pernicious than the well-known tendency of 2-boryl pyridines to undergo rapid protodeborylation (discussed in **Chapter 1.2.1**, *vide supra*). This process cannot

explain our data as protodeborylation should, in theory, return Ar–H starting material, not consistent with the high conversions we were seeing in **Table 3.3**.

Steel's group suggested[137] in a 2012 publication that the absence of borylation at the 2- and 8-position of quinolines is due to the influence of the nitrogen lone pair. However, the origin of this effect, whether steric or electronic in nature, is not investigated.

A few years later, Hartwig's group conducted an in-depth study into the lack of borylation at the *ortho*-position relative to a basic nitrogen. DFT calculations showed a higher energy barrier in the reaction profile for the borylation of pyridine at the 2-position compared to the 3- and 4-position.[20] However, the highest energy along the reaction pathway for 2-borylation is only ~1 kcal mol^{-1} higher than it is for 3- or 4-borylation, so this alone cannot account for the difference in selectivity.

In the same study, Hartwig and colleagues examined this phenomenon by conducting the borylation of pyridine-d_5 in the presence of 5 mol% unlabelled 2-borylpyridine **57** and monitoring the fate of **57** (**Scheme 3.37**).

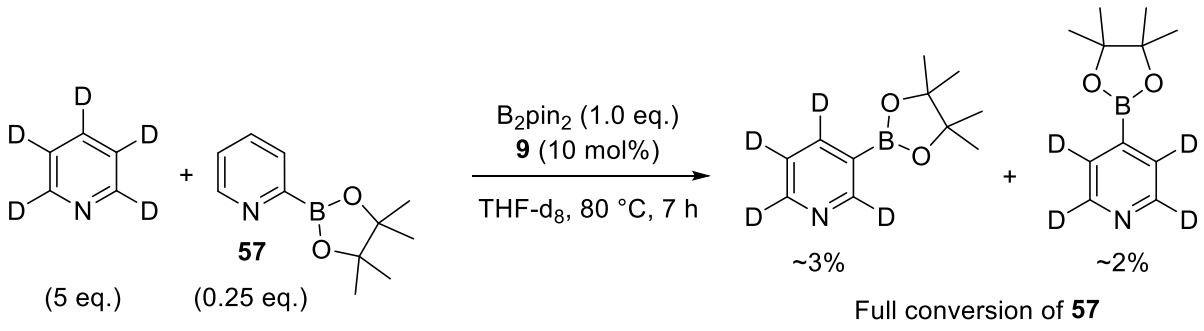

Scheme 3.37: Decomposition of 2-borylpyridine **57** during the borylation of pyridine-d_5.

Since only ~5% yield of borylated product was observed by the time the degradation of **57** was complete, it was clear that this decomposition was faster than the borylation of pyridine-d_5. Thus, the lack of observation of 2-boryl products during the borylation of pyridines is accounted for.

Without pre-functionalising our substrates with a group that sterically blocks the 2-position, we were allowing for this deleterious reaction pathway to occur in our investigation.

3.2.2.3 Borylation of quinoline substrates

All substrates were subjected to the two optimised reaction conditions, A and B (**Table 3.3**, **Entries 2** and **3, respectively**), with the highest yielding reactions listed in **Table 3.4**. The reaction of ether **50a** showed a surprisingly low degree of conversion but did afford **50b** and **50c** with opposite selectivity to **49a**. Out of the electron-poor quinolines, ester **51a** reacted smoothly and was also found to exhibit a preference for 7-borylation, while amide **52a** showed good conversion of starting material but no indication of borylated product. Similarly, carboxylic acid **53a** did react to a small extent but it was unclear from the ^{1}H NMR spectrum of the crude material whether any borylated product was generated. Quinolinol **54a** gave the most selective borylation with its 6-position reacting by far the most favourably. Lastly, to our surprise, aryl chloride **55a** reacted to give several unwanted products despite chloropyridines being known to undergo iridium borylation very efficiently.[141]

Table 3.4: Iridium-catalysed borylation of 4-substituted quinolines.

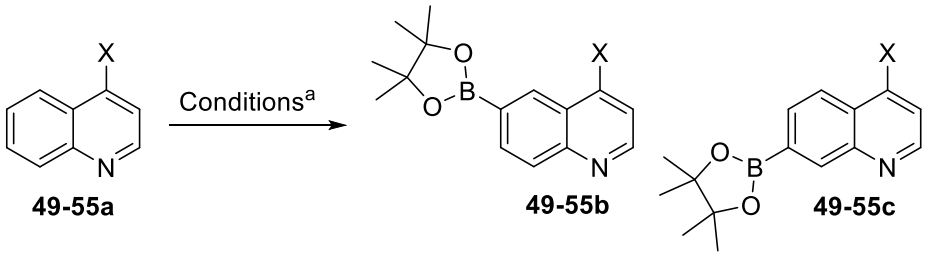

Quinoline	X	Conditions	% Conv[b]	% Yield[b]	6-/7-
49a[‡]	CH_3	B	89	49	1.3:1
50a	OCH_3	A	76	46	1:1.3
51a	COOEt	B	78	21	1:1.1
52a	$CONHCH_2Ar$	A	66	0	n.d.
53a	COOH	-	-	0	n.d.
54a	OH	A	77	30	2.3:1
55a	Cl	A	86	14	1:1

[a]Reaction conditions A: **Table 3.3**, **Entry 2** (using dtbpy) and Reaction conditions B: **Table 3.3**, **Entry 3** (using tmphen). [b]% Yields, conversions and isomer ratios were determined from ^{1}H NMR yields with 1,3,5-trimethoxybenzene as an internal standard. [‡]12% diborylated product detected. n.d. = Not determined.

We began to notice a trend in our data which mirrored a similar, more holistic observation made previously in a recent publication by Steel and Marder.[137] They showed that the site of reactivity in the iridium borylation of (hetero)arenes is typically the aryl hydrogen with the furthest downfield chemical shift. However, in pyridines and quinolines, the most shifted proton will be at the C-2 position, adjacent to the pyridyl nitrogen (**Figure 3.9**); a site at which borylation is seldom observed (*vide supra*).[141]

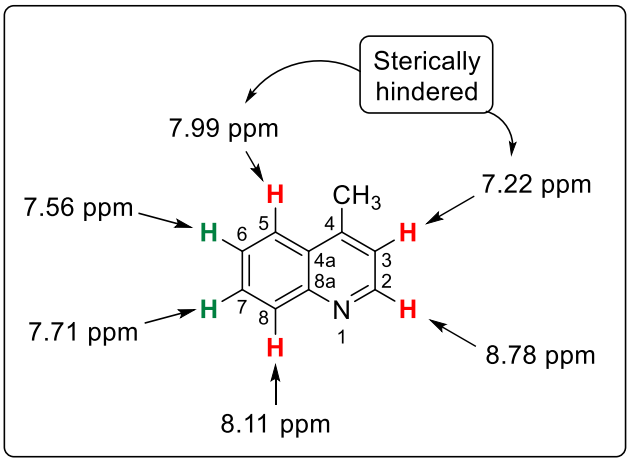

Figure 3.9: Chemical shifts for the aryl hydrogens of quinoline **49a**. NMR experiment run in $CDCl_3$ at 700 MHz.

Although pyridines and quinolines deviate from Steel's guidelines for reactivity, this premise still serves as a somewhat useful predictive tool in determining whether the 6- or 7-position will show preference for borylation when screening 4-substituted quinolines. Our data showed that in all but the case of **49a**, the preferred site of borylation was the highest shifted aryl hydrogen out of the 6- and 7-positions (**Table 3.5**). It may be significant that quinoline **49a** is the only substrate whose 4-substituent is not capable of interacting with the core scaffold mesomerically. Aryl chloride **55a** did not show significant preference for reaction at its higher-shifted C-7 position, although, this reaction was low yielding. Crucially, it seems that the electronic nature of the 4-substituent, *i.e.* whether it is electron-donating or electron-withdrawing, does not appear to flip the selectivity from one site to the other.

Table 3.5: Predicting the regiochemistry in the borylation of 4-substituted quinolines.

Quinoline	X	6-/7-	^{1}H NMR Shifts*		Consistent with Steel?
			$\delta_{H\text{-}6}$ / ppm	$\delta_{H\text{-}7}$ / ppm	
49a	CH_3	1.3:1	7.56	7.70	No
50a	OCH_3	1:1.3	7.49	7.68	Yes
51a	COOEt	1:1.1	7.61	7.72	Yes
54a	OH	2.3:1	7.62	7.37	Yes
55a	Cl	1:1	7.62	7.75	n.a.

*NMR experiments run in $CDCl_3$ at 700 MHz. n.a. = Not applicable.

Attempts to purify the crude reaction mixtures *via* silica gel column chromatography proved to be exceptionally challenging for several reasons. Primarily, this was due to residual Bpin-derived species which would often 'drag' on the silica column and coelute with the desired products. As well as this, these impurities could not be visualised on a TLC plate so it was difficult to make informed choices when selecting an eluent system. Obviously, they couldn't be removed in an oxidative work up or *via* the use of boron scavengers as it would destroy our desired products.

Trituration of the crude reaction of **54a** with petroleum ether did, however, work well for removing *ca.* 50% of the residual Bpin material from the sample in washings that contained almost entirely $B(OR)_3$ compounds (by ^1H NMR spectroscopy). Unfortunately, when attempted with the much less polar substrate **49a**, the petrol washings removed both Bpin material and desired compounds with equal preference.

An added difficulty with purification was the presence of tetrahydroquinoline (THQ) side products **Xd**, **Xe** and **Xf** (**X** = **49 – 55**) (**Figure 3.10**) which revealed the existence of a competing reduction mechanism.

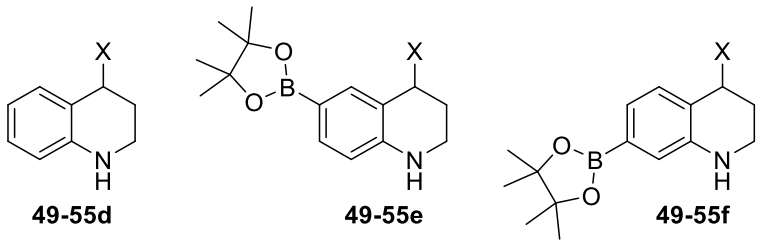

49-55d **49-55e** **49-55f**

Figure 3.10: THQ-derived side products observed in the iridium-catalysed borylation of quinolines **49-55a**.

Successive attempts to purify these reactions *via* column chromatography drew vast amounts of time and resources which ultimately gave isolated yields that were clearly not representative of their true value (**Table 3.6**).

Table 3.6: % Yields from the iridium-catalysed borylations of **49a** and **51a**.

Quinoline	X	% Yield*				
		b	**c**	**d**	**e**	**f**
49a	CH_3	16 (49)		5 (9)	1	1
51a	COOEt	8 (21)		5 (7)	3	

*NMR yields shown in parentheses. Combined yields are shown for **Xb** + **Xc** and for **51e** + **51f**.

To generate more reliable data that we could use to make valid comparisons between different substrates, not influenced by deleterious separation techniques, the decision was made to just measure crude % yields by ^{1}H NMR spectroscopy. In the context of iridium-catalysed borylation, this was deemed acceptable as aryl boronate esters are commonly elaborated further *in situ* without isolating borylated intermediates (*vide supra*).

3.2.2.4 Mechanistic study

To better understand the origin of the THQ side products being formed, we conducted a short study to determine whether the borylated THQ products are formed *via* borylation of reduced starting material (**Scheme 3.38**, **Path A**), by the reduction of our desired product (**Scheme 3.38**, **Path B**), or a combination of both.

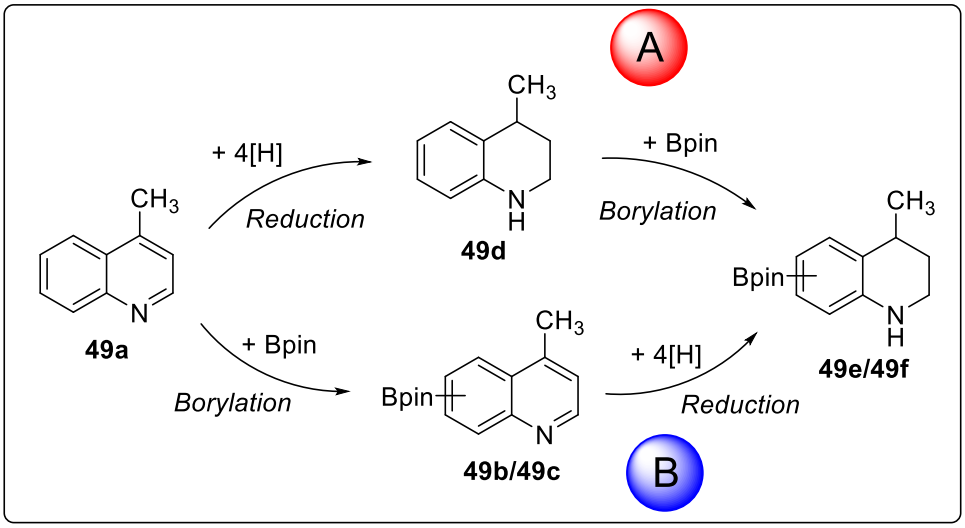

Scheme 3.38: Two possible routes to form the undesired borylated THQs.

Firstly, the propensity of THQ **49d** to undergo iridium borylation was explored (**Scheme 3.39**). If THQs were found to be highly unreactive with respect to iridium

borylation, this would point towards a borylation-reduction sequence, *i.e.* **Path B**. However, good yields would not necessarily rule out either pathway.

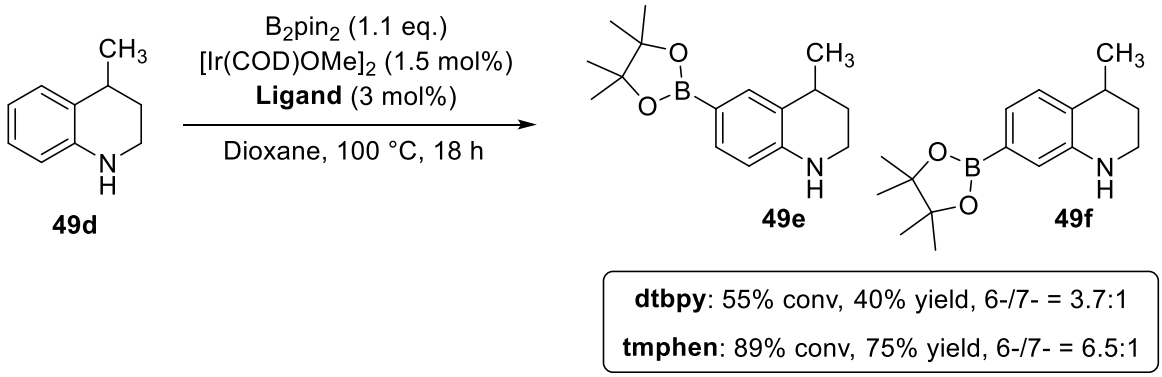

Scheme 3.39: Borylation of THQ **49d** under optimised conditions with both a dtbpy- and tmphen-ligated iridium catalyst.

Given that THQ **49d** was found to react to an appreciable extent under both iridium borylation conditions, it was not possible to reject **Path A** at this stage. As a further test, a competition experiment was designed whereby quinoline **49a** and THQ **49d** were subjected to the same two sets of iridium borylation conditions as before (**Table 3.3**, **Entries 2** and **3**). The fate of the two starting materials, as well as any borylated material that formed, was monitored after 18 h (**Table 3.7**).

Table 3.7: Competition experiment to determine whether THQ **49d** or quinoline **49a** is more reactive under iridium-catalysed borylation conditions*.

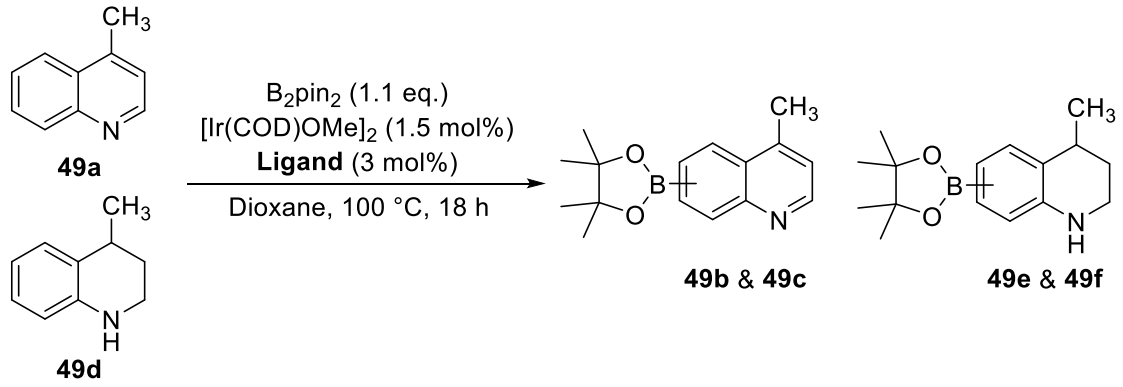

Ligand	% Remaining		% Yield	
	Quinoline **49a**	THQ **49d**	**49b** & **49c**	**49e** & **49f**
dtbpy	67	88	6 & 4	0 & 0
tmphen	59	90	14 & 11	3 & 0

*% Yields and conversions were determined from crude ^{1}H NMR data with 1,3,5-trimethoxybenzene as an internal standard.

The results showed clearly that, under iridium borylation conditions, quinolines are more reactive than THQs based on their higher rate of consumption and the low quantities of borylated THQ products **49e** and **49f** observed. However, an important caveat of these results is that some of quinoline **49a** will have been converted to THQ **49d** as we observed previously (**Table 3.6**). Our data show that, after 18 h, for every 10 moles of quinoline **49a** consumed, *ca.* 6 moles of monoborylated product are formed along with *ca.* 1 mole diborylated and *ca.* 1 mole is reduced to THQ **49d**. If we account for this in this experiment and assume that the reduction pathway competes with borylation to the same extent, quinoline is still found to be considerably more reactive than THQ. We conclude, therefore, that the borylated THQ side products we have observed during this investigation, **Xe** and **Xf**, form primarily due to a borylation-reduction sequence, *i.e.*, **Path B** (**Scheme 3.38**).

3.2.3 Reduction of quinolines to 1,2,3,4-tetrahydroquinolines

The relatively high proportion of THQ product generated in these borylation reactions led us to consider whether we could improve the selectivity for this product and develop a method for reducing quinolines to THQs under mild conditions. To the best of our knowledge, this has not yet been reported with an iridium catalyst and a borane reagent, though reactions with an iridium catalyst and H_2 are well-precedented.[142–146] An optimisation process was carried out to see the extent to which we could encourage reduction over borylation (**Table 3.8**).

Table 3.8: Iridium-catalysed reduction of 4-methylquinoline **49a** to 1,2,3,4-tetrahydroquinoline **49d**[a].

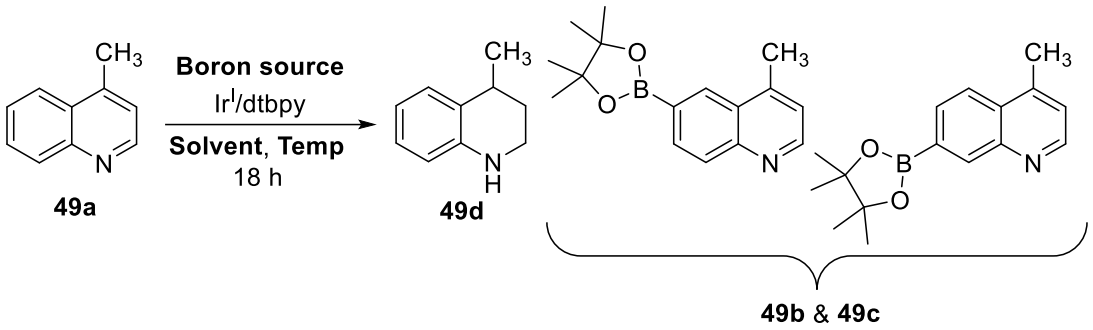

Entry	Boron source	eq.	Temp / °C	Solvent	% Yield		
					49a	49d	49b/49c
1	B_2pin_2	1.1	r.t.	THF	71	14	2
2	B_2pin_2	1.0	80	Hexane	42	14	20
3	B_2pin_2	1.0	80	CPME	38	9	26
4	HBpin	2.4	85	Dioxane	n.d.[d]	13[e]	n.d.
5	HBpin	5.0	50	Dioxane	30	15	10
6	HBpin	5.0	50	Hexane	74	9	11
7	HBpin	5.0	50	THF	66	8	18
8	HBpin	5.0	50	CH_3CN	54	10	7
9	HBpin	5.0	75	Hexane	43	9	17
10	HBpin	5.0	75	THF	21	7	26
11	HBpin	5.0	100	Dioxane[f]	55	7	13
12	HBpin	5.0	r.t.	None	45	7	27
13	None	-	100	Dioxane	90	2	0
14	HBcat	5.0	100	Dioxane	0	0	0

[a]Reaction conditions: **49a** (2.0 mmol, 1.0 eq.), Boron source (1.0 – 5.0 eq.), $[Ir(COD)OMe]_2$ (1.5 mol%), dtbpy (3 mol%), solvent (2.0 mL), r.t. – 100 °C, 18 h, sealed tube, Ar atmosphere. [b]Unless stated otherwise, yields were determined by ^{1}H NMR spectroscopy based on **49a** with 1,3,5-trimethoxybenzene as the internal standard. [c]SM was 95% pure; contains 4% (w/w) **49d**. [d]n.d. = not determined. [e]Isolated yield. [f]10 mL solvent.

Initial reactions with B_2pin_2 in different solvents showed relatively high levels of THQ formation (**Entries 1 – 3**) but, despite this, we explored reactions with HBpin as this is known to be considerably less reactive for iridium borylation with the

precatalyst/ligand combination used in these experiments,[19] but should still generate Ir–H bonds readily. When reacted first at 85 °C, these conditions afforded THQ **49d** as the major product, but the isolated yield was poor (**Entry 4**). To reduce unwanted borylation, the temperature was lowered to 50 °C and the borane equivalents increased to 5.0 (**Entries 5 – 8**). The crude yield of **49d** dipped from **Entry 4** but the results were beginning to show dioxane to be the most effective solvent. This was confirmed by repeats with THF and hexane at slightly elevated temperature that showed no improvement in the yield of **49d** (**Entries 9 – 10**). Carrying out the reaction at five-fold dilution reduced the efficiency of both borylation and reduction (**Entry 11**). Control experiments showed that performing the reaction neat at room temperature appears to promote borylation much more effectively than reduction and that borane is essential for reduction to take place (**Entries 12** and **13**).

HBcat is not used in iridium borylation which led us to consider whether it may be a good alternative to HBpin by avoiding the borylation pathway whilst still providing Ir–H bonds, that we assumed would be necessary for reduction. When the reaction was attempted, it brought about a very different outcome to the reactions with HBpin (**Entry 14**). It was difficult at first to glean any information from the ^{1}H NMR of the crude reaction mixture as residual Bcat material dominated the region of the spectrum where the diagnostic peaks of **49d** are found. However, we were greatly encouraged by the absence of any peaks corresponding to **49a**, **49b** or **49c**.

Column chromatography provided a cleaner sample and confirmed the presence of reduced starting material, but the R_f value according to silica TLC did not match that of **49d**. ^{1}H NMR data revealed a mixture of products of which the major component only had three signals from the saturated heterocyclic ring instead of five. We tentatively assigned our mixture as an equilibrium of imine **49g** with hemiaminal **49h (Scheme 3.40**).

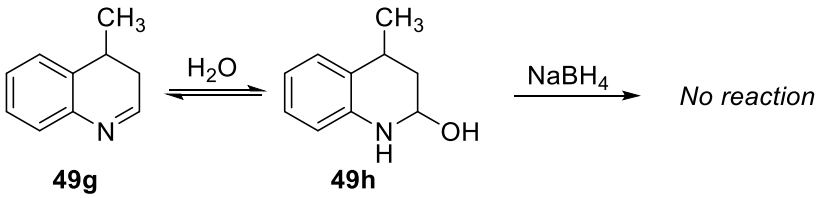

Scheme 3.40: Proposed mixture of products generated in the reaction of **49a** with HBcat. No reaction was observed when the sample was stirred with $NaBH_4$.

After washing the mixture with aqueous Na_2CO_3 to remove residual catechol, we stirred the resulting sample with 1 eq. $NaBH_4$ at r.t. for 2 h, assuming this would reduce **49g** and **49h** to deliver the desired THQ **49d**. However, to our surprise, the ^1H NMR remained largely unchanged and column chromatography gave the two unknown compounds in a combined yield of 12% in a 1:5 ratio, respectively. Further analysis of 2-dimensional NMR data revealed that our sample was not a mixture of **49g** and **49h** but instead 4-methyl-1,2,3,4-tetrahydroquinolin-3-ol **49i**, with unique sets of NMR shifts depending on whether the $–CH_3$ and –OH groups had a *syn* or *anti* relationship (**Figure 3.11**).

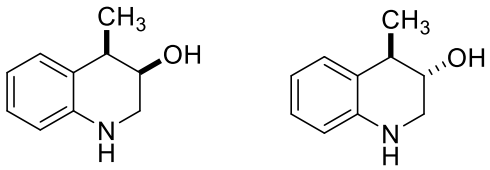

***syn*-49i** ***anti*-49i**

Figure 3.11: Diastereoisomers of **49i**.

The transformation of quinolines to β-hydroxytetrahydroquinolines *via* a hydroboration-oxidation one-pot sequence is well-known.[147,148] On that basis, as well as the fact that we hadn't discovered a high-yielding route to THQs from quinolines, we retired this side project.

3.2.4 Conclusions and future work

At first, we aimed to probe, where unknown, the scope and limitations of iridium-catalysed borylation, particularly with respect to more challenging heterocyclic scaffolds. Our data suggest that the methodology is intolerant of $–NO_2$, –COOH and $–SO_2NH_2$ functional groups, as well as certain heterocycles (triazoles, imidazoles and various 3-substituted indazoles). Amide substrates with differing 2-substituted five-membered heterocycle were readily borylated at the vacant 5-position in the case of thiophene and furan, but low yields were seen with *N*-methylpyrrole. The tendency of these substrates to undergo a second borylation at the more hindered 3-position appeared to be highly sensitive to temperature, reflecting a higher kinetic barrier.

A spin-off project set out to determine how the nature of the substituent in the 4-position of quinoline influenced the regioselectivity of the iridium-catalysed borylation reaction. Our results show that 4-substituted quinolines react first at the

6- or 7-position and, in some cases, again at the sterically encumbered 3-position. No discernible trend was observed between the electronic nature of the 4-substituent (*i.e.*, electron-withdrawing or electron-donating) and the reaction's preference for reacting at the 6- or 7-position. A better guideline came from correlating the most reactive site with the Ar–H signal that had a greater chemical shift out of the 6- and 7-position, although this pattern did not extend to substrates whose 4-substituent could not overlap with the quinoline's π-system. Besides, most substrates reacted with a roughly equal preference along each vector, with all but one example giving similar amounts of each isomer.

Moreover, this project reveals 4-substituted quinolines to be poor candidates for iridium borylation for three primary reasons:

1. It is difficult to tune the selectivity towards a preferred regioisomer.
2. Having the C-2 hydrogen accessible allows for deleterious reaction pathways to take place. In many cases, these side reactions occur more rapidly than borylation at the 6- or 7-position. Furthermore, a quinoline unsubstituted at C-2 possesses an unencumbered basic nitrogen that may be capable of catalyst poisoning.
3. A reduction mechanism competes with borylation, consuming both starting material and borylated product to give THQ derivatives. A mechanistic study revealed that this most likely occurs after borylation. This is consistent with the fact that reductive species such as HBpin, H_2 and Ir–H bonds would gradually accumulate over the course of an iridium borylation reaction.

A side project designed to encourage this reduction pathway with the hydroboranes HBpin and HBcat in the presence of the same iridium catalyst gave a maximum yield of 15%.

Future work borylating 4-substituted quinolines should avoid direct functionalisation without protecting group strategies that block the C-2 hydrogen. As we have shown by carrying out high yielding borylation reactions with THQs and 2-methylquinoline, having the C-2 site accessible is a major factor that limits the reaction's success.

A mysterious phenomenon that featured repeatedly in our work on iridium-catalysed borylation was the unpredictability of which catalyst-ligand combination would be the

best performing system for a given reaction. Although Hartwig's group have identified some trends,[20] an exhaustive screen exploring a range of substrates, solvents and perhaps sequences of addition is required to fully understand the factors at play.

A high throughput screening study of the iridium borylation reaction concluded that Ir-tmphen is more active than Ir-dtbpy.[19] The authors comment that this is consistent with tmphen being more electron-rich. However, if electron-donating ability were the main contributing factor, then 4,4'-bis(dimethylamino)-2,2'-bipyridine (dmabpy) would outperform both tmphen and dtbpy since it is more electron-rich. Yet, in a test reaction with 2,6-dimethylanisole, the conversions measured follow the order: dtbpy < dmabpy < tmphen, indicating that tmphen outperforms a ligand that is more electron-rich (**Figure 3.12**). Another suggestion is that tmphen's constrained dihedral angle along the chelate backbone prevents dissociation of a nitrogen atom. However, in many cases, dtbpy will outperform tmphen, despite its unconstrained C2–C2' axis.

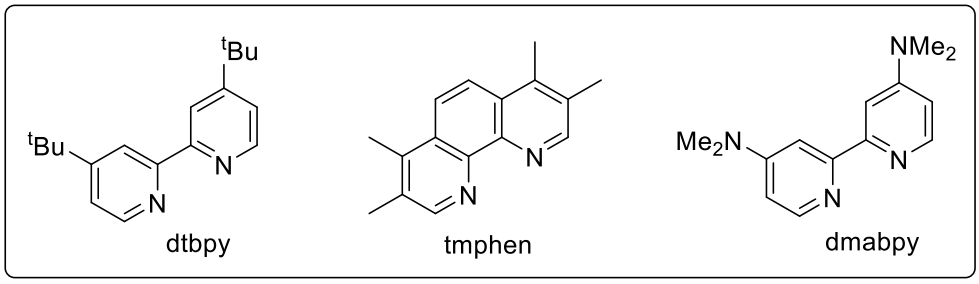

Figure 3.12: Chelating, nitrogen-based ligands for iridium-catalysed borylation.

Another major theme to our work in this area concerned the instability of 2-pyridyl boronic acid derivatives. This is a well-known problem,[149] but work by Yoshida *et al.* has shown that "2-pyridyl-Bdan" (**Figure 3.13**) is stable enough to be isolated by silica gel column chromatography.

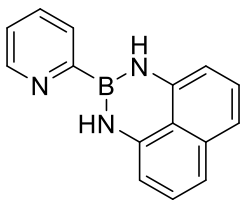

Figure 3.13: "2-Pyridyl-Bdan".

In Yoshida's work, C–X bonds of alkyl, alkenyl and (hetero)aryl halides are converted to C–Bdan, either *via* copper catalysis with pinB–Bdan,[150] or *via* the Grignard reagent and HBdan.[151] However, direct C–H borylation of a pyridine α to the nitrogen to deliver 2-pyridyl-Bdan has not been reported.

Elsewhere, Suginome has shown that it is possible to adapt typical iridium borylation conditions to transfer Bdan instead of Bpin onto a range of simple, substituted aromatic substrates.[152] However, the reactivity of the system was found to be significantly lower than for the counterpart borane HBpin, so a vast excess of arene is required (30 – 120 eq.). Also, the reported scope encompasses just one heterocycle (thiophene).

We believe there is merit in attempting to synthesise and isolate 2-pyridyl-Bdan under Suginome's reported conditions. Use of a 4-substituted quinoline or 2,4-disubstitued pyridine scaffold may help block other reactive sites. Shortly before the preparation of this thesis, HBdan **58** was synthesised (**Scheme 3.41**) and some borylation reactions were attempted on toluene and *m*-xylene, although yields were very low. Due to time constraints, we were not able to investigate this further.

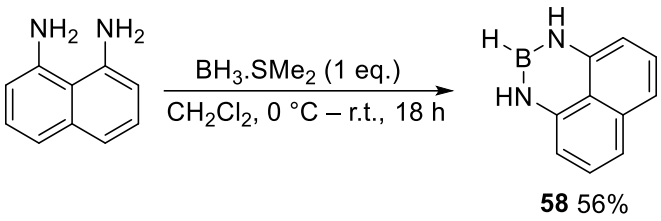

58 56%

Scheme 3.41: Synthesis of HBdan **58** *via* Suginome's reported conditions.

3.3 Electrophilic aromatic C–H borylation mediated with copper and gold

3.3.1 Copper-mediated C–H borylation

3.3.1.1 Introduction and project aims

To date, (hetero)aromatic borylation methods that proceed *via* an S_EAr mechanism are much less studied than techniques catalysed by mid-to-late transition metals such as iridium, rhodium, and ruthenium (*vide supra*). However, they have the potential to offer complementary electronic and site-selectivity which raises the prospect of orthogonal C–H functionalisation for a given compound.

We hypothesised a novel electrophilic borylation procedure that brought together two different facets of copper catalysis:

- Firstly, Santos' report on the β-boration of α,β-unsaturated carbonyl compounds *via* a copper(I) boryl intermediate (**Scheme 3.42**).[117]

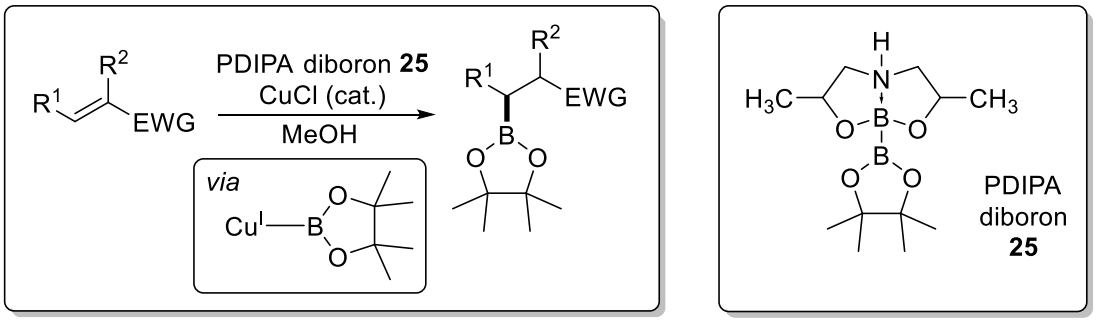

Scheme 3.42: Copper-catalysed β-boration of α,β-unsaturated conjugated compounds.

- Secondly, the contemporaneous work on the *meta*-selective arylation of acetanilide derivatives proceeding *via* a $Cu^{I/III}$ cycle, recently reported by Gaunt (**Scheme 3.43**).[153]

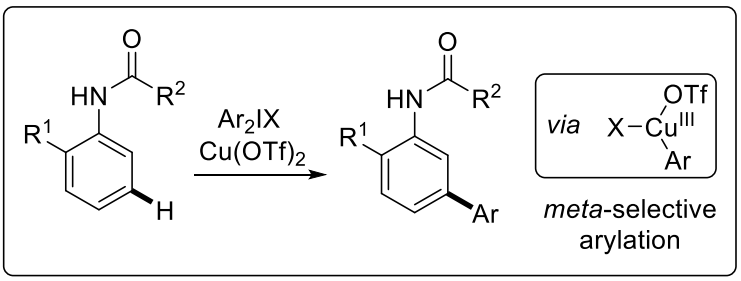

Scheme 3.43: *meta*-Selective copper-catalysed C–H bond arylation.

Combining these processes, we envisaged a borylation protocol whereby a copper(I) salt is mixed with diboron **25** to generate a copper(I) boryl species as in Santos' report (**Scheme 3.44**, **I**). Subsequent addition of a hypervalent iodine compound

would then oxidise the copper to form a highly electrophilic d^8 copper(III) boryl complex **II**. We would expect such a species to react readily with an electron-rich (hetero)arene *via* a Friedel-Crafts-type mechanism to give intermediate **III**. Reductive elimination would then form the desired (hetero)aryl boronate ester, and a copper(I) salt, which could regenerate **I** in the presence of diboron **25**.

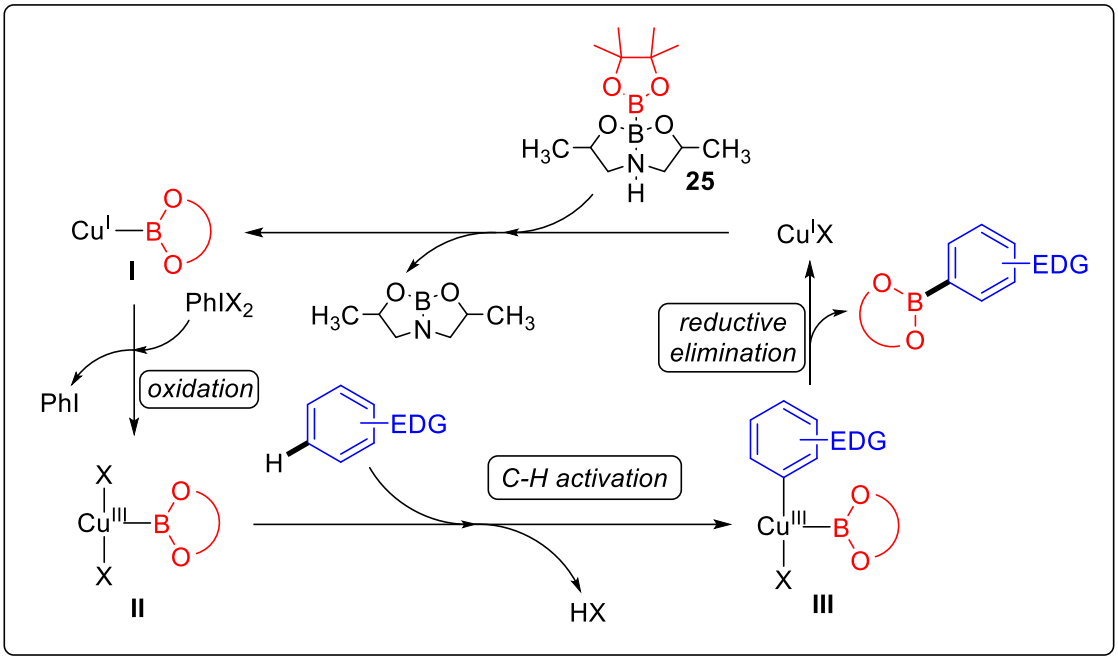

Scheme 3.44: Hypothetical catalytic cycle for the $Cu^{I/III}$-mediated borylation of electron-rich (hetero)arenes.

If successful, this would pave the way for a new catalytic borylation method that demonstrates unique regioselectivity with a cheap and highly abundant transition metal. However, it is worth noting that this setup relies on our diboron reagent **25** resisting oxidation in the presence of a hypervalent iodine reagent. It also hinges on reductive elimination of our desired (Het)Ar–Bpin being more favoured than elimination of Ar–X or pinB–X.

3.3.1.2 Results and discussion

Before attempting our hypothesised protocol, we aimed to verify the quality of our reagents. Since generation of a Cu^{I}–Bpin complex is fundamental to our proposed reaction, we replicated a procedure from Santos' β-boration paper (**Scheme 3.45**).[117] Pleasingly, the desired β-borated product **59** was isolated following work up and purification.

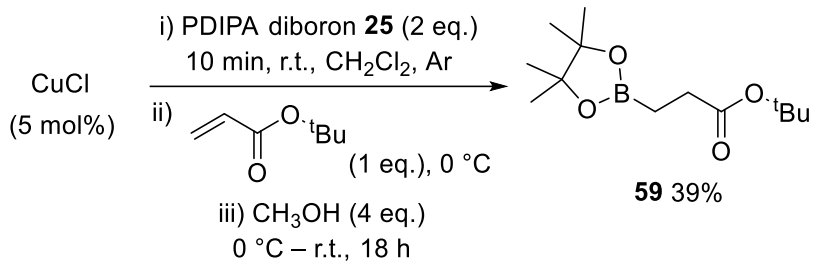

Scheme 3.45: Copper-catalysed β-boration of *tert*-butyl acrylate, as described by Santos.

Satisfied that we could transfer boron onto copper, we then focused on the oxidative step. We synthesised aniline **60** and used it to replicate Gaunt's *meta*-selective arylation protocol (**Scheme 3.46**). This successfully delivered biaryl **61** after work up and purification.

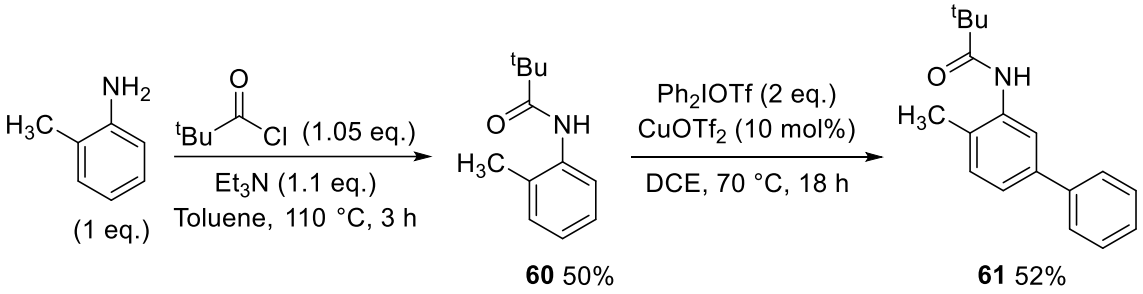

Scheme 3.46: Generation of aniline **60** and subsequent arylation, as described by Gaunt.

To test our hypothesised reaction, we employed *N*-methylindole as the substrate as it has been demonstrated to be amenable to electrophilic borylation in literature reports,[70,71] delivering boron β to the N atom. To gain experience handling and purifying the desired heteroaryl boronate **62**, as well as a full suite of characterisation data, a sample was prepared *via* a literature method (**Scheme 3.47**).[86]

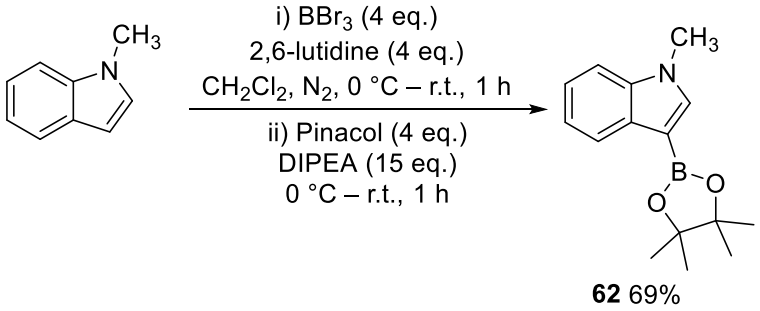

Scheme 3.47: Synthesis of heteroaryl boronate **62**.

In the first attempt at our novel method, we mimicked the initial step described by Santos, mixing 10 mol% CuCl with 2 eq. diboron **25** and waited for the indicative brown solution to develop (*ca*. 10 min). We then cooled to 0 °C to add the indole

substrate, followed by the hypervalent iodine oxidant (**Scheme 3.48**). A series of colour changes were observed over the ensuing 15 min (green → yellow → pale orange → rose → crimson), suggesting that the copper catalyst had successfully undergone oxidation.

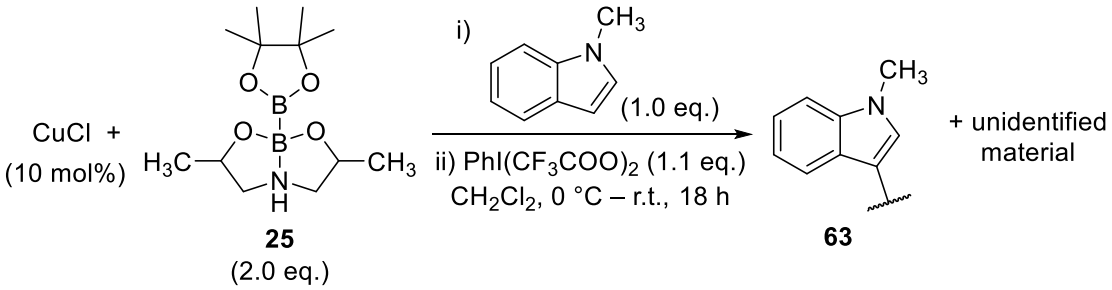

Scheme 3.48: Attempted borylation of indole *via* a Cu^{III}–boryl species.

A TLC after 15 min revealed new material but not full consumption of starting material. Extended reaction times did not help achieve full conversion, so we attempted to purify our reaction *via* silica gel column chromatography. We managed to isolate a mixture of our SM and another indole-derived compound **63** in *ca.* 5:1 ratio, respectively. Interestingly, compound **63** had a singlet in its ^{1}H NMR at *δ* 7.04 ppm, hinting at C-3 functionalisation. However, this was significantly upfield to where we would expect the corresponding H-2 shift in our desired product **62** (*ca. δ* 7.52 ppm). We researched literature NMR data for any plausible compounds and concluded that indole **63** was most likely 3-chloro-*N*-methyl-1*H*-indole **63**, although we did not attempt to isolate it from our crude sample. Instead, we prepared a small batch *via* a literature method[154] and correlated the peaks from ^{1}H and ^{13}C NMR data (**Scheme 3.49**).

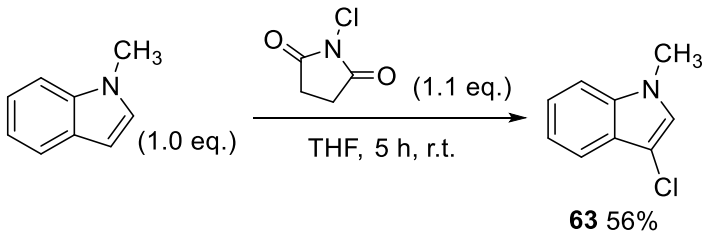

Scheme 3.49: Chlorination of *N*-methylindole to give indole **63**.

To avoid formation of chlorinated indole **63**, a repeat of the reaction described in **Scheme 3.48** was repeated but with $Cu(OTf)_2$ *in lieu* of CuCl. Interestingly, analysis *via* NMR the following day revealed the formation of a different 3-substituted indole in a 1:3 ratio with SM, although, it was still not the desired borylated product. A

search of the literature was conducted, as before, to find a plausible structure for the by-product, and it was identified as 3-iodo-*N*-methyl-1*H*-indole **64**, which we failed to isolate from the crude mixture *via* column chromatography.

An attempt to prepare an authentic sample of indole **64** efficiently delivered the desired product, but it was only stable when stored under high dilution, which explained our previous difficulty isolating it (**Scheme 3.50**).

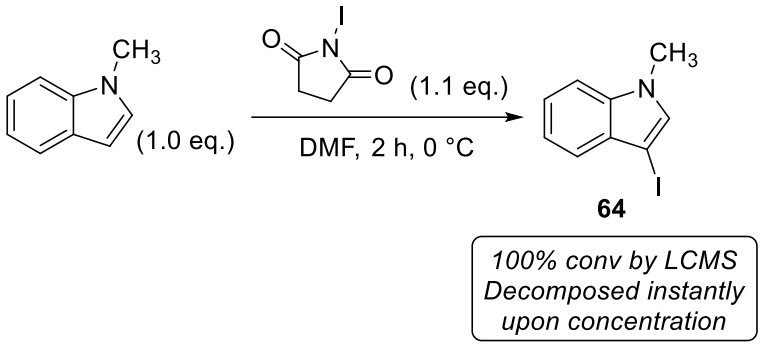

Scheme 3.50: Reaction of *N*-methylindole with *N*-iodosuccinimide to give indole **64**.

To probe the influence that different reagents were having in our setup, two control experiments were run in parallel: one in the absence of diboron **25** (**Scheme 3.51**, **right**), another without diboron **25** or CuCl (**Scheme 3.51**, **left**).

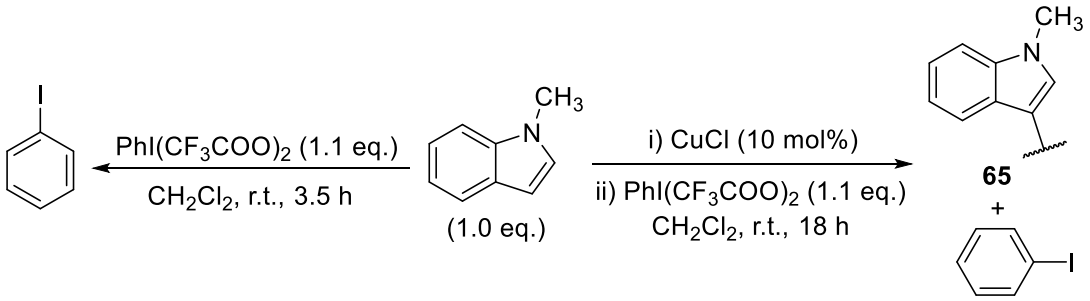

Scheme 3.51: Control experiments in the absence of: diboron **25** and CuCl (left); and diboron **25** (right).

The experiment with just SM and oxidant was analysed by GCMS after 3.5 hours and found to contain 52% iodobenzene and 40% SM. Since the starting indole is the only oxidisable species present, we must assume it has been oxidatively oligomerised to insoluble polyindole that we cannot analyse spectroscopically.

In the other control experiment, with just diboron **25** excluded, a TLC after 15 min was closely comparable to that which was observed in the initial reaction (**Scheme 3.48**). However, the ^{1}H NMR of the crude material after 18 h revealed full consumption of our indole SM, leaving a *ca.* 3:1 mixture of iodobenzene and another

3-substituted indole **65**, along with a complex mixture of aromatic compounds. These unidentifiable compounds could plausibly form following decomposition of iodinated indole **64**. However, generation of indole **64** should give equimolar quantities of phenyl trifluoroacetate, which we did not detect (**Scheme 3.52**). Likewise, chlorinated indole **63** was not observed.

Unknown indole species **65** was tentatively assigned as *N*-methyl-1*H*-indol-3-yl 2,2,2-trifluoroacetate, as this could form *via* an oxidation–reductive elimination sequence from a HetAr–I^{III}(Ph)(CF_3COO) (red) or HetAr–Cu^{III}(X)(CF_3COO) (blue) intermediate (**Scheme 3.52**). Although, indole **65** is not a known compound in the literature so we could not compare NMR data to verify this. In any case, a reaction pathway proceeding *via* an electrophilic copper(III) species was a more reassuring proof of concept than direct reaction with the external oxidant.

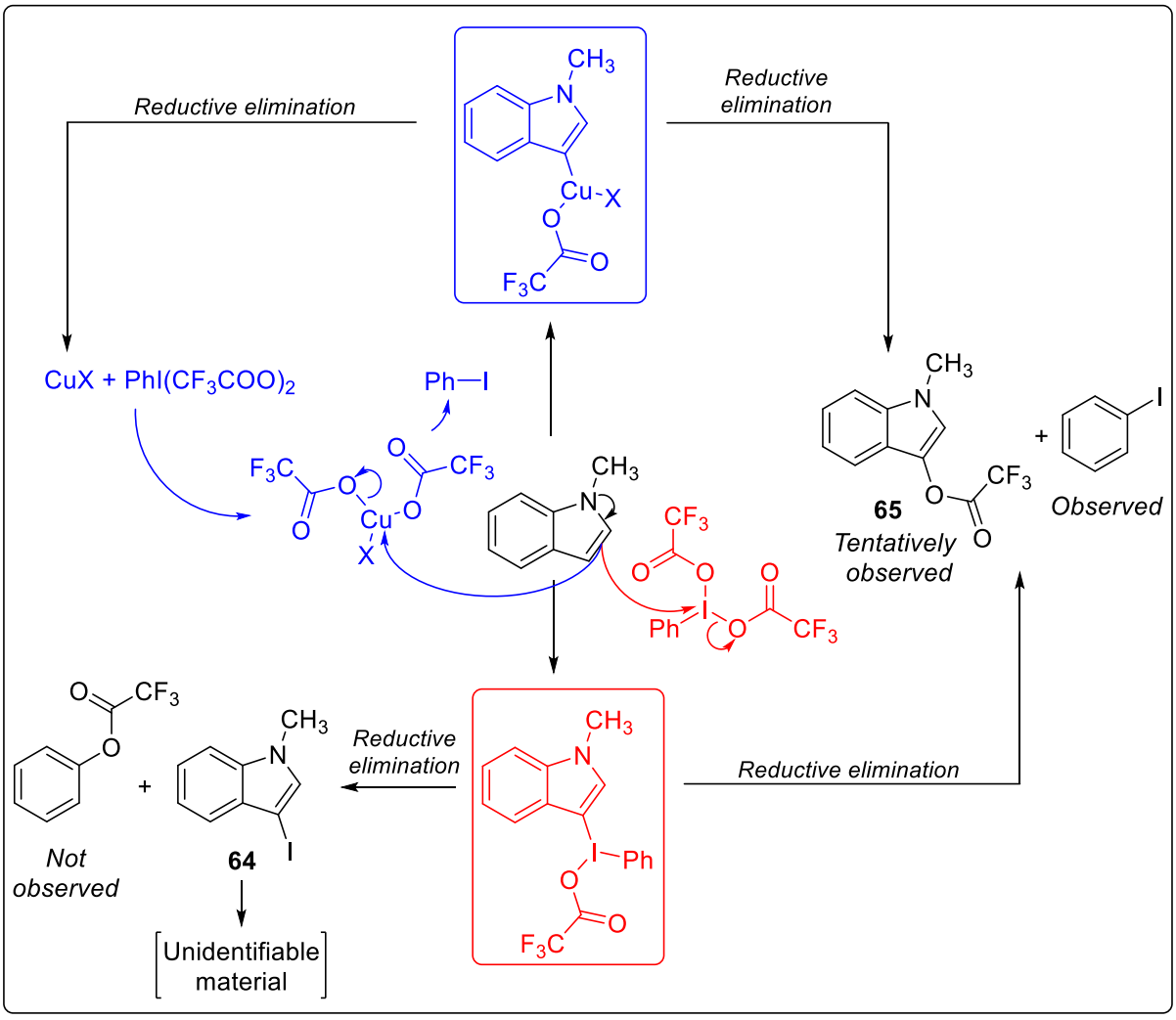

Scheme 3.52: Plausible schematic representation of possible side reactions ensuing from direct reaction of starting indole with hypervalent iodine oxidant (red) or an electrophilic copper(III) species.

Concerned by the possibility that the SM and oxidant were interacting with one another, we switched to weaker oxidant $PhI(OAc)_2$ and screened a few substrates that we expected to be less reactive (**Scheme 3.53**). As an added measure to avoid side reactions, we used stoichiometric quantities of copper. This was to ensure that all diboron **25** was consumed before being exposed to the oxidant. We also altered the sequence of addition such that the oxidant was added to the Cu–Bpin solution before the substrate to avoid iodination of the SM, as discussed above. After exploring a few substrates, we screened some other copper salts against the original *N*-methylindole substrate.

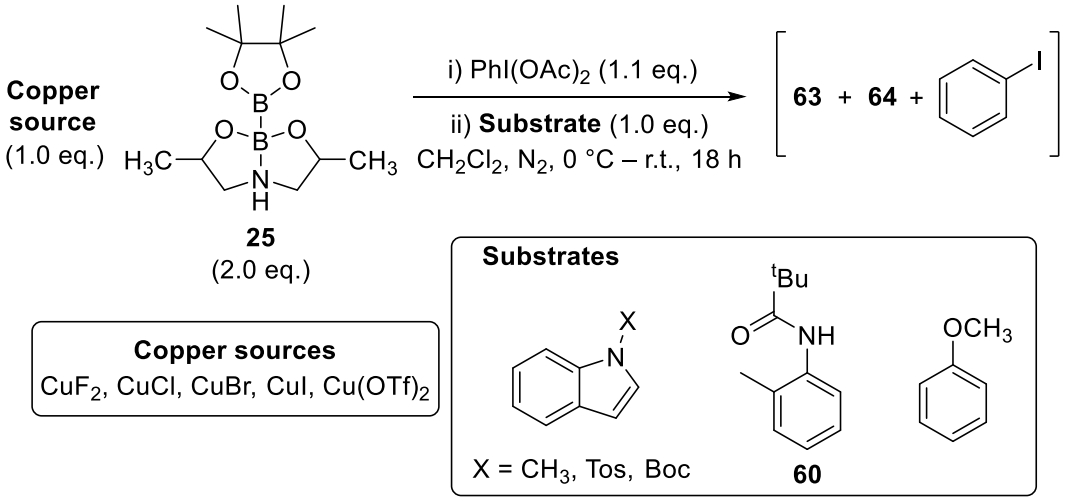

Scheme 3.53: Screen of substrates and copper salts in attempted electrophilic borylation reactions.

To our disappointment, none of the conditions we trialled generated detectable levels of the desired borylated indole **62**. In all cases, large quantities of iodobenzene and unreacted SM were observed, occasionally along with small amounts of chlorinated and iodinated indoles **63** and **64**, respectively.

3.3.1.3 DIPA–dan diboron

Deviating from our core aim of borylating electron-rich (hetero)arenes *via* a Friedel-Crafts-type mechanism, we refocused on Santos' report on borylating electron-deficient substrates *via* Cu^{I}–boryl species.[117] We considered that a novel sp^2-sp^3 hybridised diboron compound, DIPA–dan diboron **66** (DIPA–dan = diisopropanolaminato-1,8-naphthalenediaminato), may hold the potential to transfer Bdan onto copper *via* the same means as PDIPA diboron **25** and CuCl (**Figure 3.14**).

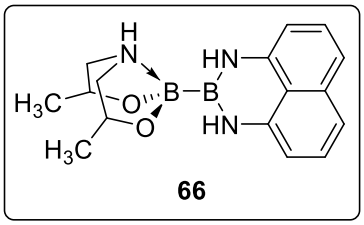

Figure 3.14: DIPA–dan diboron **66**. Formal charges excluded for simplicity.

Successful generation of Cu–Bdan *in situ* raises the prospect of borylating electron-deficient alkenes in a similarly regioselective fashion to that which is described in Santos' report. The alkyl–Bdan products generated should possess a higher degree of robustness compared to their pinacolato boronate cousins. This is because the dan moiety acts as a masking group on the boron atom, attenuating its Lewis acidity and preventing further interactions.[152,155]

A similar reaction has been reported before by Fernández *et al.* in 2014 (**Scheme 3.54**).[156] In their work, pinB–Bdan is selectively activated by an alkoxide at the more Lewis acidic Bpin moiety, allowing Bdan to transfer to the β-position of α,β-unsaturated carbonyl compounds. However, this reaction proceeds *via* a different mechanism to Santos', with no transition metal necessary. Alternatively, a catalytic amount of phosphine is used to interact with the substrate and form a zwitterionic phosphonium enolate, capable of deprotonating MeOH. The role of phosphines in the organocatalytic β-boration reaction is described in depth in a separate publication.[157]

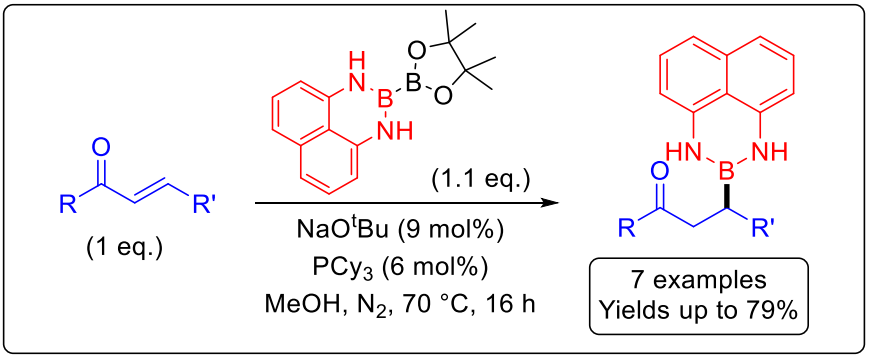

Scheme 3.54: Selective β-boration of α,β-unsaturated carbonyl compounds described by Fernández.

Our first attempt at synthesising DIPA–dan diboron **66** mimicked Suginome's reported preparation of pinB–Bdan **67**.[158] Instead of pinacol, 1 eq. of diastereomerically mixed bis(2-hydroxypropyl)amine was stirred with tetrakis(dimethylamino)diborane and 1,8-diaminonaphthalene (dan-H_2)

(**Scheme 3.56**, **Path A**). Unfortunately, we were only able to detect unreacted starting material and trace amounts of B_2dan_2 in our crude reaction mixture.

These data suggested that the B(DIPA) moiety may be more challenging to assemble *in situ* than the Bdan subunit. Changing strategy, we stirred PDIPA diboron **25** with 1 eq. of dan-H_2 with the hope of exchanging the pinacolato-ligated boron for dan, leaving the B(DIPA) half intact (**Scheme 3.56**, **Path B**). However, analysis of the crude reaction mixture by ^{1}H NMR revealed considerable disruption to the B(DIPA) framework. Interestingly, the aromatic region of the spectrum revealed the presence of pinB–Bdan **67** in a 1:4 ratio with unreacted dan-H_2. ^{11}B NMR confirmed full consumption of diboron **25** but there was insufficient evidence of product formation to investigate further.

In our third attempt, we decided to start with pinB–Bdan **67** and exchange the pinacolato for DIPA. A batch of pinB–Bdan **67** was prepared according to Suginome's aforementioned conditions (**Scheme 3.55**).[158]

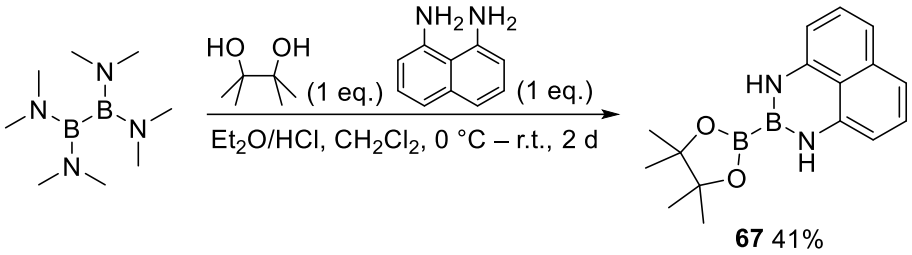

Scheme 3.55: Synthesis of pinB–Bdan **67** *via* Suginome's reported conditions.

Diboron **67** was then stirred at room temperature with 1 eq. of bis(2-hydroxypropyl)amine for 4 d (**Scheme 3.56**, **Path C**). After the reaction solvent was removed and the residue washed with Et_2O, the remaining material was analysed by ^{1}H NMR. Much to our excitement, integrations of chemical shifts that corresponded to dan agreed favourably with ones that corresponded to DIPA, pointing to successful formation of our desired diboron **66**.

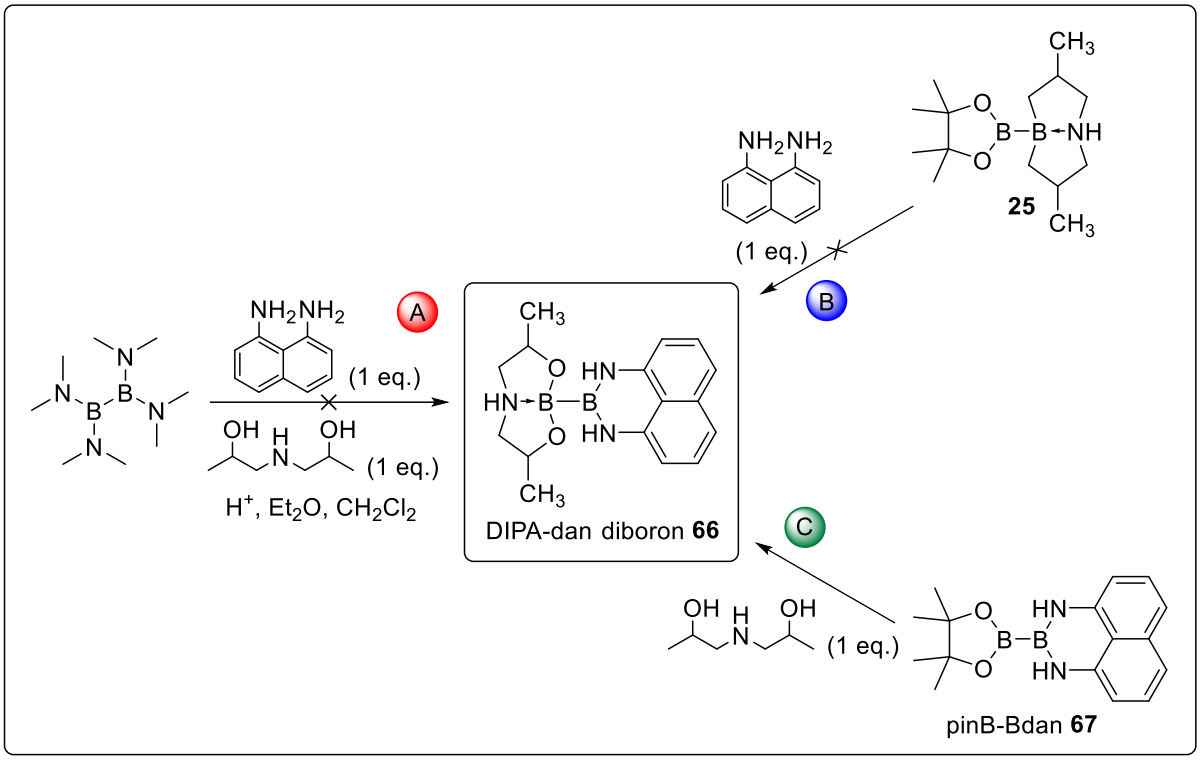

Scheme 3.56: Three routes to DIPA–dan diboron **66** explored.

^{11}B NMR shifts observed at *δ* 10.5 and 9.6 ppm indicated successful quaternisation of boron and offered plausible values for the B(DIPA) subunit. However, since the amine diol reagent was a 1:1:1:1 mixture of diastereoisomers, characterisation *via* ^{1}H NMR was complicated by the stereochemical complexity of diboron **66**. An attempt to recrystallise our crude sample by redissolving it in hot toluene caused immediate decomposition to a black, insoluble tar-like substance.

To simplify the analysis *via* ^{1}H NMR, we decided to repeat the reaction with a simpler, achiral amine diol starting material. However, when we swapped in diethanolamine for bis(2-hydroxypropyl)amine and stirred it with **67** as described above, the two species did not react (**Scheme 3.57**). It is possible that the two methyl groups in bis(2-hydroxypropyl)amine facilitate cyclisation to B(DIPA) *via* the Thorpe-Ingold effect.

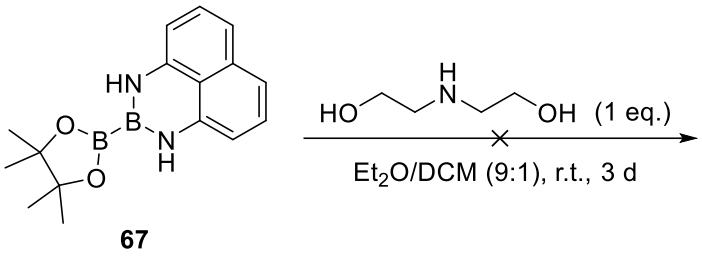

Scheme 3.57: Attempted exchange of the pinacolato-ligated boron of **67** with diethanolamine.

As an alternative way of simplifying NMR analysis, we considered synthesising diboron **66** diastereoselectively, thereby generating one set of NMR shifts. Santos' group have undertaken a similar approach to give a diastereomerically enriched (*R*,*R*)-**25** and we decided to adopt this synthesis (**Scheme 3.58**).[118] First, benzylamine was stirred with 2 eq. of (*R*)-propylene oxide in MeOH at 60 °C to generate amine diol (*R*,*R*)-**68** in excellent yield. The benzyl protecting group was then cleaved *via* heterogeneous catalytic hydrogenation to deliver (*R*,*R*)-**69** in quantitative yield.

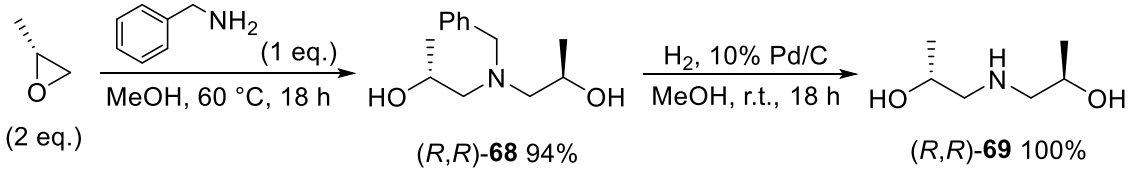

Scheme 3.58: Two-step synthesis to generate amine diol (*R*,*R*)-**69**.

Amine diol (*R*,*R*)-**69** was stirred with diboron **67** at room temperature for an extended period of time (**Scheme 3.59**). The reaction was then filtered and washed with copious amounts of Et_2O to leave a grey powdery solid. When analysed by ^1H NMR, it appeared we had successfully formed (*R*,*R*)-**66** in a 1:1.25 ratio with unreacted (*R*,*R*)-**69**. However, this only amounted to an 8% yield of our desired compound.

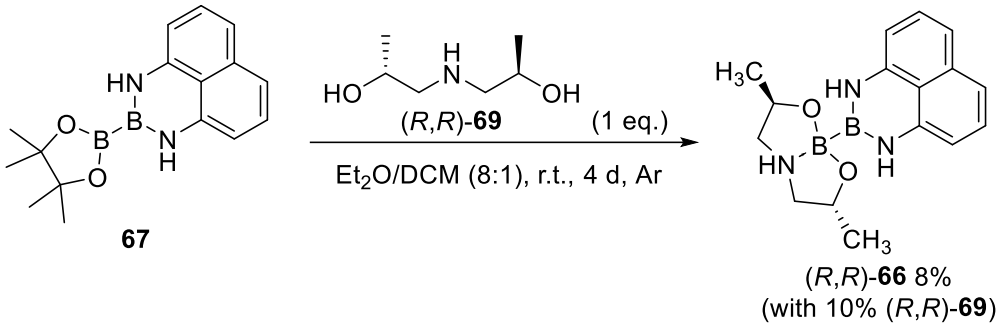

Scheme 3.59: Synthesis of (*R*,*R*)-DIPA–dan diboron (*R*,*R*)-**66**.

The aromatic region of the ^1H NMR spectrum showed little change with all Bdan peaks shifting slightly upfield with respect to pinB–Bdan **67** (**Figure 3.15**).

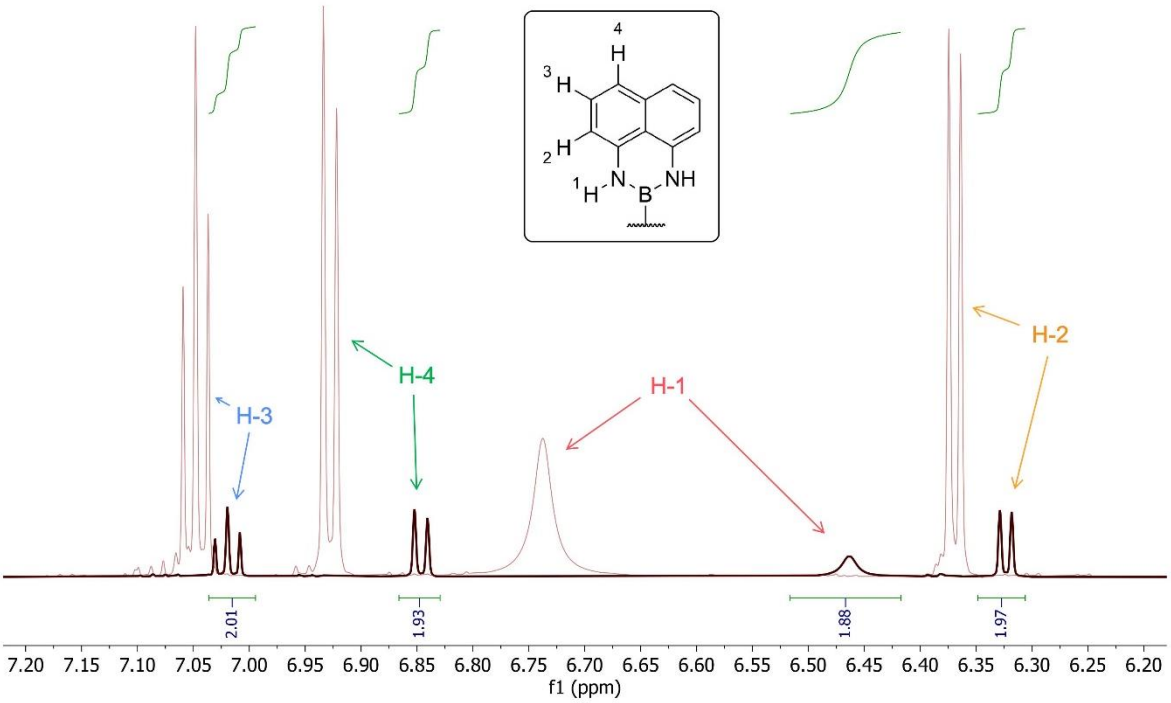

Figure 3.15: ^{1}H NMR of crude sample of (*R*,*R*)-**66** (bold) overlaid with pinB–Bdan **67** (faint) in the range *δ* 6.20 – 7.20 ppm. NMR experiments run in CD_3CN at 700 MHz.

In the aliphatic region, three chemical shifts (each ∫ = 2H) that corresponded to unreacted (*R*,*R*)-**69** were detectable (excluding –CH_3) (**Figure 3.16**). However, six unique chemical shifts (each ∫ = 1H) were observed in the range 1.94 – 4.14 ppm, which appeared to relate to the B(DIPA) backbone. This is consistent with a loss of C_2 symmetry upon complexation of boron. The ^{1}H – ^{1}H COSY spectrum allowed us to determine which of the six ^{1}H shifts were α to the amine nitrogen and which were β, but we were unable to refine this assignment further with the data available. A broad singlet at 5.36 ppm (∫ = 1H) was a plausible shift for the quaternised amine N–H.

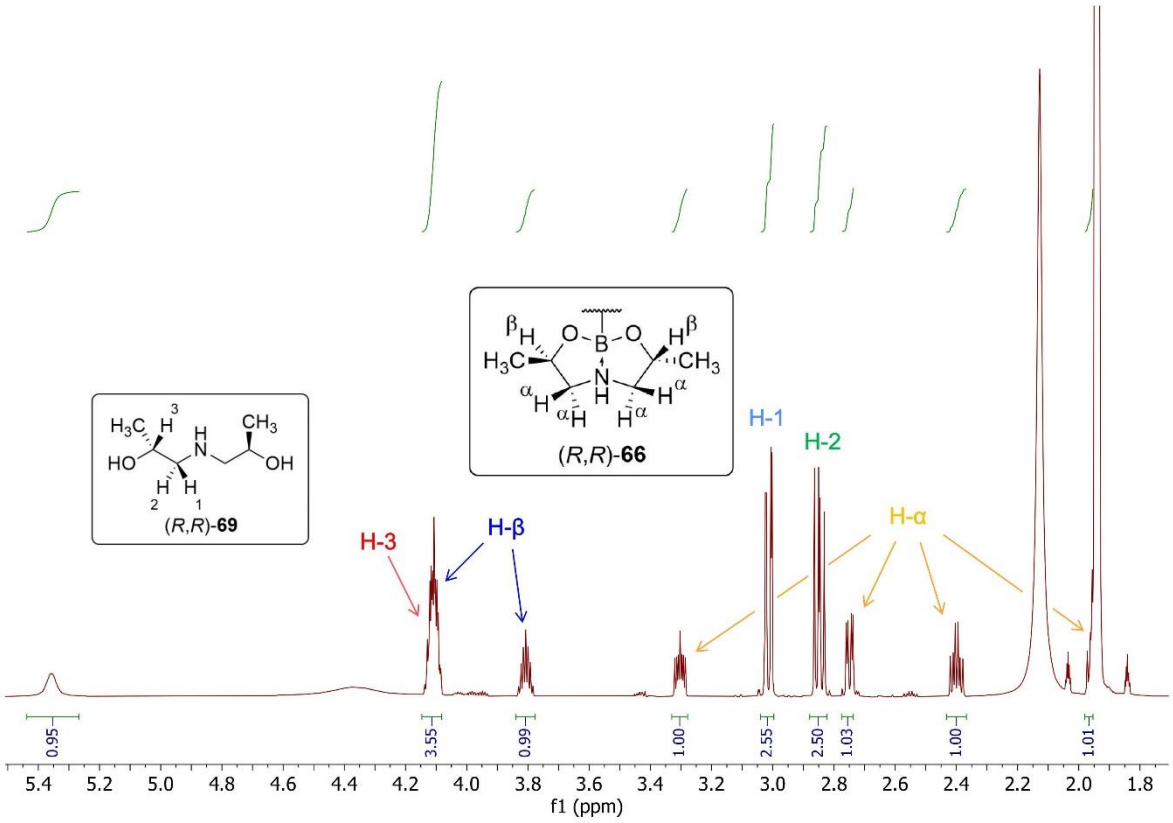

Figure 3.16: ^{1}H NMR of crude sample of (*R*,*R*)-**66** in the range 1.80 – 5.40 ppm. NMR experiment run in CD_3CN at 700 MHz.

To rule out the possibility that we had a 1:1 mixture of a DIPA- and a dan-containing species whose ^{1}H shift integrals serendipitously agreed, the ^{1}H NOESY spectrum was inspected (**Figure 3.17**). Pleasingly, we were able to detect a dan N–H — DIPA N–H (blue) and a dan N–H — DIPA H-β (red) correlation. This unambiguously confirms that we had formed a diboron compound ligated with both DIPA and dan.

From our flat representation of (*R*,*R*)-**66** (**Figure 3.17**, **inset**), it is perhaps harder to visualise how the dan N–H and DIPA N–H could be brought close in space. However, when we drew the structure using molecular modelling software and crudely optimised the geometry (UFF), we can see how both this interaction and the dan N–H — DIPA H-β are plausible (**Figure 3.18**).

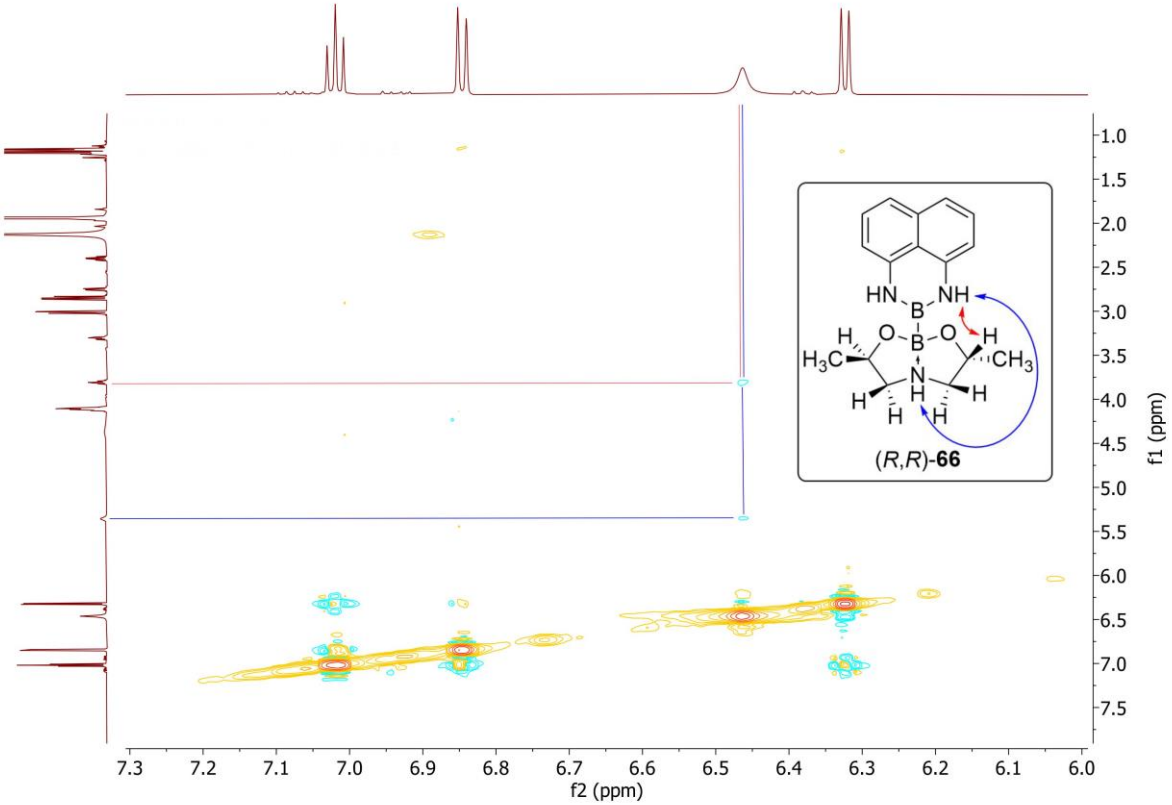

Figure 3.17: ^{1}H – ^{1}H NOESY NMR of crude sample of (*R*,*R*)-**66**.

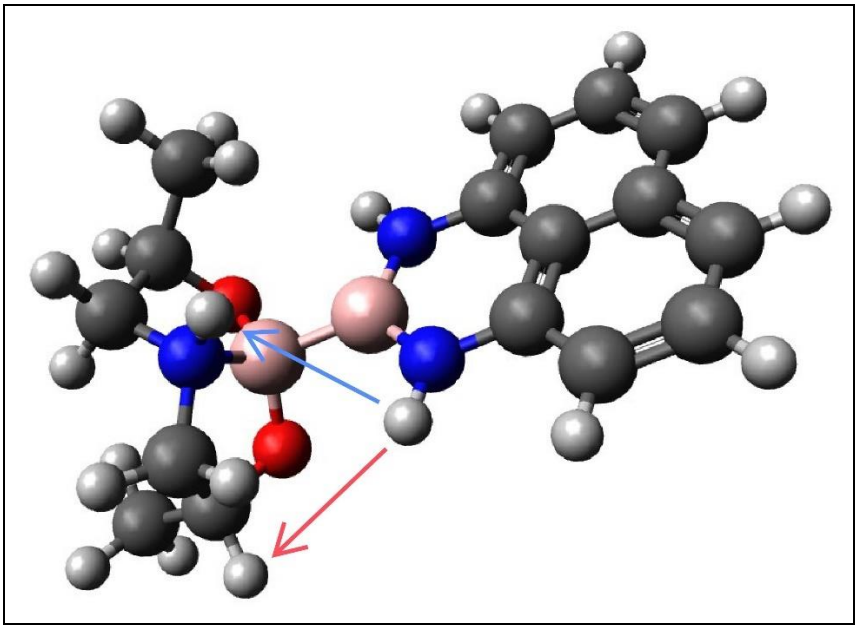

Figure 3.18: (*R*,*R*)-**66** drawn using Avogadro and optimised *via* UFF. NOE correlations indicated with arrows.

In the ^{11}B NMR spectrum, the same peaks observed previously in our reaction with diasteroeomerically mixed **69** reappeared (9.6 ppm (major) and 10.4 ppm (minor)). It is interesting that two distinct signals are observed for the quaternised boron, unlike in PDIPA diboron **25** (**Figure 3.19**). This suggests that there may be some rotational

isomerism due to the more sterically imposing Bdan moiety compared to Bpin. It may also be that the B(DIPA) moiety undergoes conformational inversions that are slow on the NMR timescale. Further downfield, a shift at 35.6 ppm can be ascribed to the Bdan boron. This is a considerable downfield shift (+ 7.7 ppm) relative to diboron **67**, indicating a significant lengthening of the B–B bond upon exchange of pin for DIPA. A similar increase is observed during the synthesis of diboron **25** from B_2pin_2, although not to the same extent (+ 4.8 ppm).

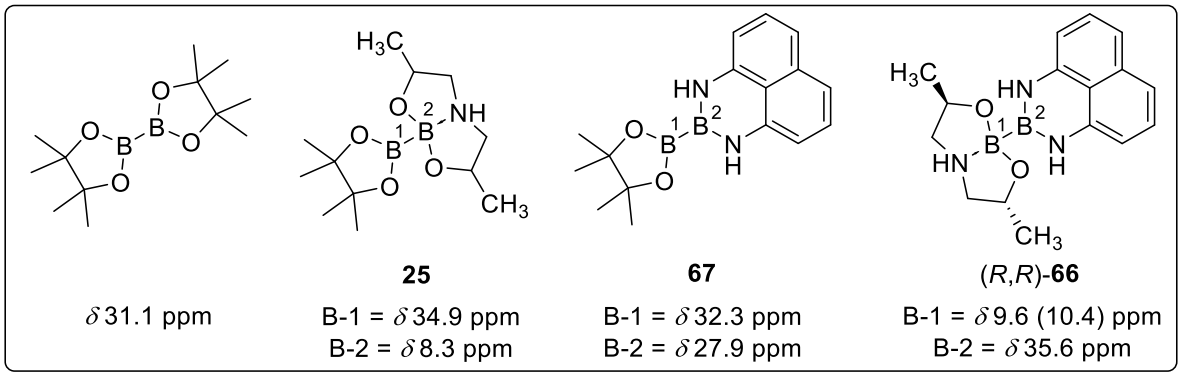

Figure 3.19: ^{11}B NMR chemical shifts of selected diboron reagents in CD_3CN. Shift quoted for B_2pin_2 is a literature value.[117]

When we examined the ether washings, the ^{1}H NMR revealed a 7:1 ratio of pinB–Bdan **67** and (*R*,*R*)-**69**. This was an encouraging endorsement for washing our crude material with Et_2O in future attempts, although the separation of unreacted (*R*,*R*)-**69** remained a pernicious issue.

With the aim of improving conversion of starting material, we designed a repeat experiment of our reaction to form diboron (*R*,*R*)-**66**. However, we were concerned to notice that our batch of (*R*,*R*)-**69** had darkened in colour significantly (pale yellow → brown). Reanalysing our material by ^{1}H NMR revealed several new peaks and a downfield shift of our original set of signals. Similarly, our pure sample of diboron (*R*,*R*)-**66** had decomposed within days at room temperature. A ^{11}B NMR shift at 23.4 ppm was indicative of oxidised material.

We repeated the two-step synthesis to generate another batch of (*R*,*R*)-**69** and stored it in a refrigerator under dry argon. We were able to attempt another ligand exchange reaction with pinB–Bdan **67** using DCM as the solvent instead of the Et_2O/DCM (8:1) mix. Unfortunately, consumption of pinB–Bdan **67** remained very low and new material that did form was an intractable mix of compounds. To add to

our frustration, we later noticed our second batch of (*R*,*R*)-**69** had decomposed in a similar fashion to before, in spite of its careful storage. Curiously, we noticed EtOH in the ^{1}H NMR spectrum of the decomposed sample, suggesting that the $(CH_3)(OH)HC—CH_2(NH)$ bond had been cleaved.

We decided to return to using the commercially available diastereomeric mixture of amine diol **69**, on account of its improved stability. With a set of NMR shifts in hand for (*R*,*R*)-**66**, we should be able to overlay these spectra with those of diastereomerically mixed **66** to verify product formation. We screened two further reaction solvents (DCE and pentane/DCM (4:1)) but we failed to observe an appreciable degree of product formation. Although, ^{11}B NMR did show some evidence of pin — DIPA exchange. It is noteworthy how much more easily these ligands exchange in B_2pin_2 compared to pinB–Bdan **67**. This will most likely be due to the increased steric influence of Bdan compared to the smaller Bpin. Due to a lack of progress, we retired this project.

3.3.2 Gold-mediated C–H borylation

3.3.2.1 Introduction and project aims

With our attempts at developing a copper-mediated borylation protocol unsuccessful, we changed strategy to see if we could devise a borylation procedure with a different Group 11 metal; gold. There are very few documented examples of gold boryl species in the literature.[159,160] However, several reports of cross-coupling reactions proceeding *via* a $Au^{I/III}$ cycle have emerged over the last two decades.[161,162] This allowed us to envisage a similar electrophilic borylation procedure to that which we aimed for with copper (*vide supra*). That is:

1) A redox-neutral ligand exchange of $(L)Au^{I}–X \rightarrow (L)Au^{I}–B(OR)_2$ **I**.
2) Oxidation to $(L)X_2Au^{III}–B(OR)_2$ **II**.
3) Reaction with an electron-rich (Het)Ar–H *via* a Friedel-Crafts-type process to give (Het)Ar–$B(OR)_2$ and regenerate $(L)Au^{I}–X$ **I** (**Scheme 3.60**).

As with copper, this hypothetical reaction is fraught with the same risk of other reductive elimination pathways from intermediate **III**, or perhaps elimination of X–Bpin from complex **II**. If successful, this would represent the first gold-mediated C–H borylation reaction, catalytic or otherwise.

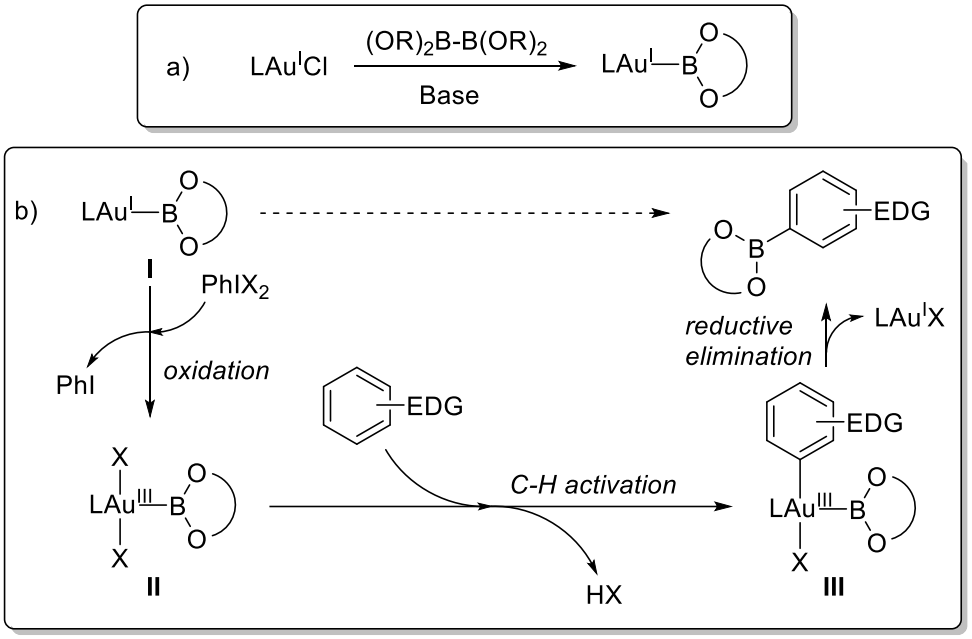

Scheme 3.60: a) Transmetallation of a diboron compound onto a gold(I) complex. b) Hypothetical pathway for the Au$^{I/III}$-mediated borylation of electron-rich arenes.

Our first objective was to prove that we can transmetallate boron onto gold in a simple and efficient manner. A new class of gold-boryl complexes ligated with *N*-heterocyclic carbenes (NHC) recently reported by Nolan and colleagues drew our interest.[160] However, the reaction conditions reported to form the (NHC)AuBpin complexes employ carcinogenic solvents and the use of a glovebox (**Scheme 3.61**).

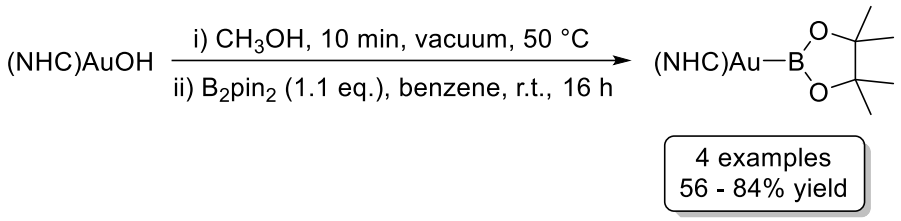

Scheme 3.61: Synthesis of (NHC)AuBpin complexes.

The (NHC)AuBpin complexes were found to be stable to air and possessed unique reactivity. Computational and experimental studies revealed interesting differences between (IPr)AuBpin and the copper analogue, (IPr)CuBpin. As we have discussed, Cu^{I}–Bpin complexes can exhibit nucleophilic behaviour and react with electron-deficient alkenes (*vide supra*). However, when electron-poor organic molecules such as styrene, phenylacetylene, and benzaldehyde were separately mixed with (IPr)AuBpin in a 1:1 ratio, no reaction was observed. This was backed up by a computational study which predicted a very strong and highly polarised Au–B bond (838 kJ mol^{-1}).

Once satisfied we could transfer boron onto gold, we needed to explore its redox properties. A number of recent papers have demonstrated the ability of gold to act as a catalyst in biaryl synthesis.[163–169] Typically, these processes are catalysed almost exclusively by palladium but they are tempered somewhat by the lack of selectivity shown by the alternating Pd^{II} and Pd^{IV} species towards each of the coupling partners.[170,171] This leads to unwanted homocoupling and often requires a directing group to be incorporated into one coupling partner and for the other to be in vast excess to ensure cross-coupling is achieved. However, an interesting property of gold allows it to show a uniquely high degree of selectivity towards aromatic substrates of opposite electron density depending on its oxidation state. For example, Larrosa and Nolan have shown that gold(I) compounds can mediate the C–H activation of electron-poor arenes (**Scheme 3.62**).[172–174]

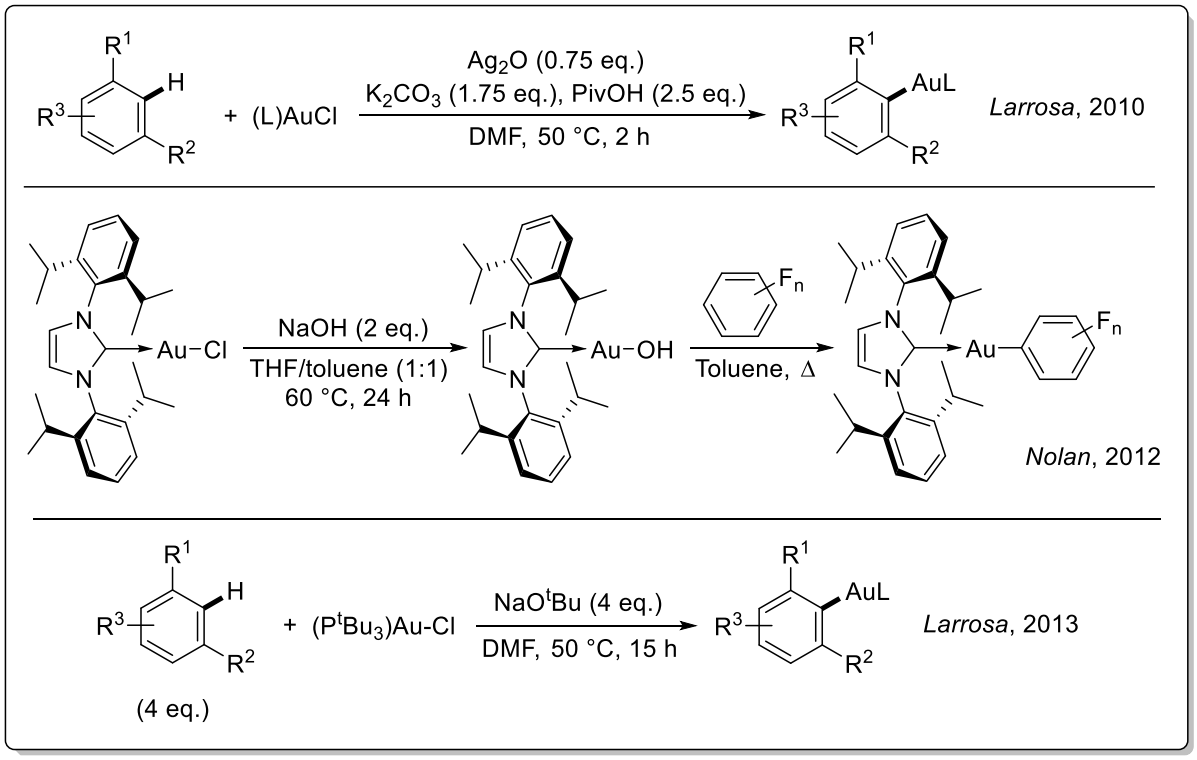

Scheme 3.62: C–H Auration techniques reported by the groups of Larrosa and Nolan.

Yet, gold(III) salts possess the contrasting ability to perform C–H activation on electron-rich arenes (**Scheme 3.63**).[175,176]

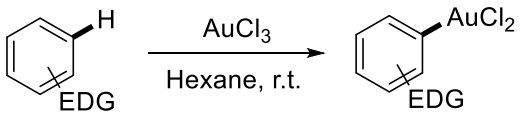

Scheme 3.63: Au^{III}-catalysed C–H activation.

This orthogonal selectivity has been exploited to develop cross-coupling methodology based on a completely selective double C–H activation. This was first hypothesised by Larrosa in 2013 when he reported the $Au^{I/III}$-mediated oxidative cross-coupling of electron-poor aryl gold(I) species with electron-rich aromatic substrates (**Scheme 3.64**).[164]

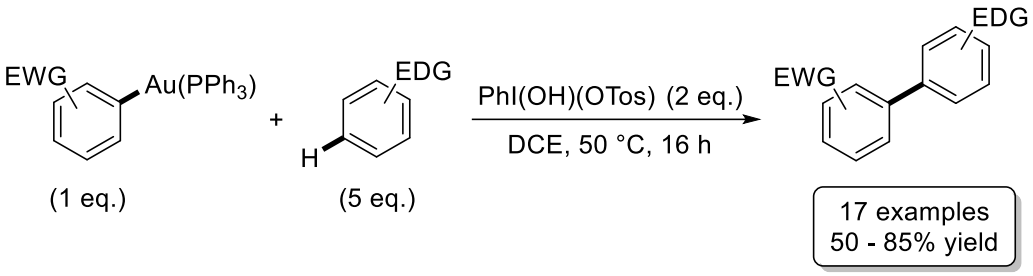

Scheme 3.64: $Au^{I/III}$-mediated oxidative cross-coupling (EWG = electron-withdrawing group).

The same group later developed this into a catalytic process compatible with a broad scope of electron-deficient arenes and electron-rich (hetero)arenes (**Scheme 3.65**).[166] The reaction tolerated several sensitive functional groups, including ones that are often problematic with established transition metal catalysis (–NO_2, –CN). As well as this, carbon-halogen bonds were left intact due to gold(I)'s reluctance to react with aryl halides by oxidative addition, thus allowing for further derivatisation *via* orthogonal palladium-catalysed transformations. However, the reaction required the presence of a silver salt in a substoichiometric quantity to ensure catalytic turnover.

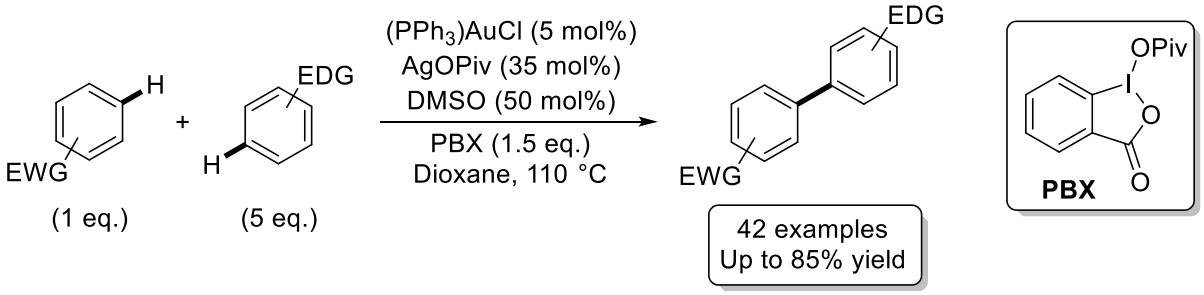

Scheme 3.65: Gold-catalysed oxidative cross-coupling described by Larrosa and colleagues.

3.3.2.2 Results and discussion

Our first aim was to establish a simple and reliable method to generate Au–B bonds *in situ*. Eager to steer away from Nolan's convoluted procedure to generate (IPr)AuBpin, we sought inspiration from literature accounts of gold-catalysed arylation with boron coupling partners. A 2006 publication from Gray *et al.* described the transmetallation of aryl boronic acids onto gold(I) complexes (**Scheme 3.66**).[177]

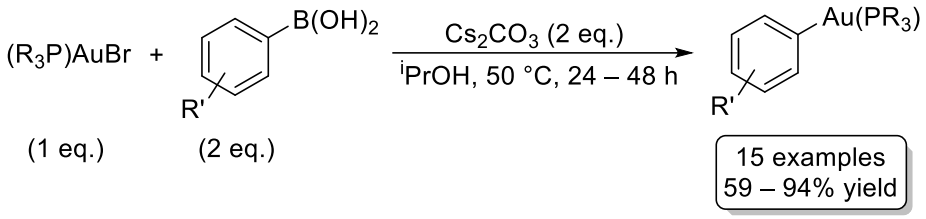

Scheme 3.66: Ar–Au bond formation by selective transmetallation of boronic acids.

The rationale behind the reaction setup evolved from the well-known Suzuki-Miyaura palladium-catalysed cross-coupling reaction where, it is thought that the auxiliary base is required to quarternerise boron and facilitate transmetallation of the Ar–B(OR)$_2$ species.[178] Consistent with this theory, Gray reported that control experiments in the absence of base found no reaction. With this in mind, we postulated that, if the boronic acid was swapped for a diboron reagent, this would lead to transmetallation given the similarity between Ar–B(OH)$_2$ and (RO)$_2$B–B(OR)$_2$.

To familiarise ourselves with the reaction, we replicated a procedure from Gray's paper and successfully isolated a pure sample of aryl gold(I) complex **70** (**Scheme 3.67**). Although, it was clear that we had sacrificed significant quantities of material during the numerous purification steps as we recorded a very poor yield. Wary of this, we considered analysing our attempts at generating gold(I) boryl species prior to any washes, extractions or crystallisations.

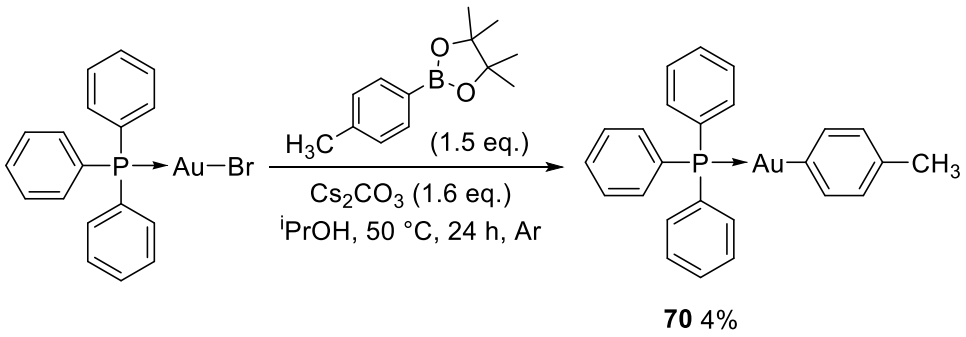

Scheme 3.67: Synthesis of aryl gold(I) complex **70**.

It was noteworthy how downfield the ^{13}C NMR shift was for the carbon bound directly to the gold (δ 170.1 ppm). Remarkably, this reveals the *ipso* carbon to be more deshielded than the corresponding carbon in 4-methylbenzoic acid,[179] *p*-nitrotoluene[180] and *p*-fluorotoluene[181] (**Figure 3.20**). This observation is consistent with the very high ^{11}B chemical shift reported for (IPr)AuBpin **71** of δ 49.5 ppm (*c.f.* BCl_3 δ 46.4 ppm[69]).

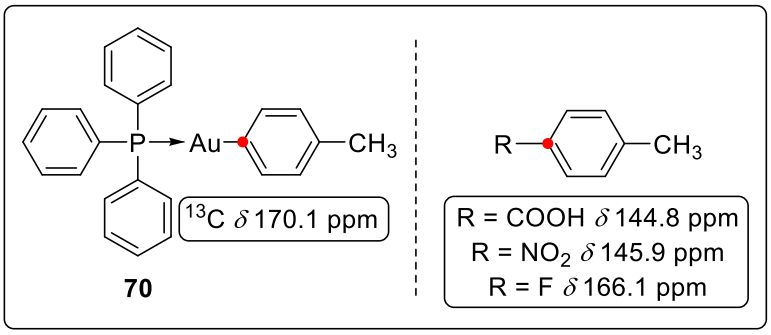

Figure 3.20: ^{13}C NMR shifts for the *ipso* carbon in aryl gold(I) complex **70** and a selection of *p*-tolyl arenes.

We adapted Gray's procedure in an attempt to synthesise (IPr)AuBpin **71**. B_2pin_2 was employed instead of an aryl boronic acid and (IPr)AuCl replaced $(PPh_3)AuBr$ (**Scheme 3.68**).

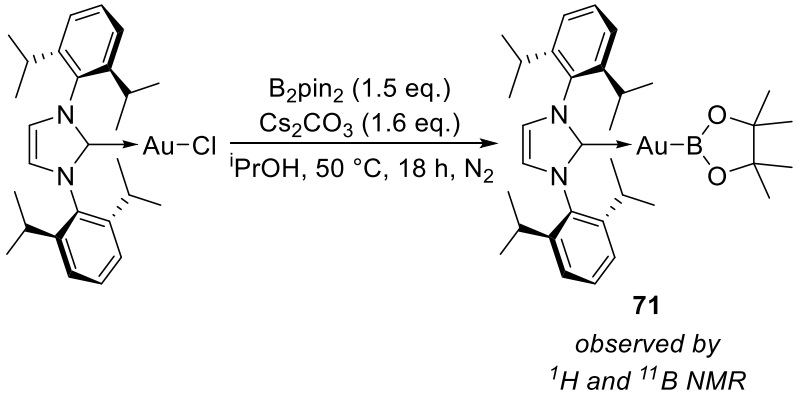

Scheme 3.68: Synthesis of (IPr)AuBpin **71** *via* Gray's conditions.

After 18 h, an aliquot was removed, concentrated and redissolved in CD_2Cl_2. Analysis *via* ^{11}B NMR revealed a shift at *δ* 48.7 ppm, hinting at successful formation of a Au–B bond. The other two ^{11}B shifts detected could be ascribed to plausible side products. For example, a shift at *δ* 21.9 ppm is an excellent match for ^{i}PrO–Bpin, and a signal at *δ* 8.4 ppm is likely the quaternised boron species $[(^{i}PrO)_2Bpin]^-$. As an additional reassuring proof of concept, no free B_2pin_2 was detected in the reaction mixture (*δ* ~30 ppm). This tells us that $^{i}PrO^-$ ions are effective at coordinating to B_2pin_2 and facilitating B–B scission and transmetallation of boron onto gold. But despite these encouraging signs, the ^1H NMR spectrum revealed unreacted (IPr)AuCl as well as a third IPr-derived species that we were unable to identify.

We considered that this reaction may be kinetically very feasible and that Gray's conditions may be more forcing than necessary. To investigate this, a repeat reaction was set up at room temperature and monitored directly by ^{11}B NMR

spectroscopy in the reaction solvent at 1 h, 4 h and 18 h. We also examined the B_2pin_2/Cs_2CO_3 mixture after 30 min stirring in ^{i}PrOH, moments before (IPr)AuCl was added. This revealed a more complex picture than expected with ^{11}B shifts at δ 28.7, 19.9, 15.6, 6.2 and 3.4 ppm.

Pleasingly, NMR analysis 1 h after adding the gold complex featured the diagnostic ^{11}B shift at δ 48.9 ppm, as well as δ 20.5, 16.1, 6.8 and 3.3 ppm. These lower four chemical shifts can be correlated to those observed in the B_2pin_2/Cs_2CO_3 mixture, but it is interesting that addition of gold should drive the consumption of B_2pin_2 to completion. Subsequent analysis at 4 h and 18 h revealed identical spectra, indicating that our reaction plateaus within 1 h. When we removed ^{i}PrOH solvent from what was remaining of our reaction at 18 h and resubmitted a ^{11}B NMR in CD_2Cl_2, it was an identical match to our previous reaction (**Scheme 3.68**).

We set up repeat reactions with the aim of isolating a pure sample of complex **71** (**Scheme 3.69**). When we stopped the reaction after 1 h and filtered the mixture, we were often deceived into thinking we had a pure sample, once concentrated down. This was due to the presence of NMR-invisible inorganic species which were not effectively removed *via* filtration. However, these would precipitate out of solution once redissolved in DCM, allowing for extra filtration(s) to bring the % yield <100.

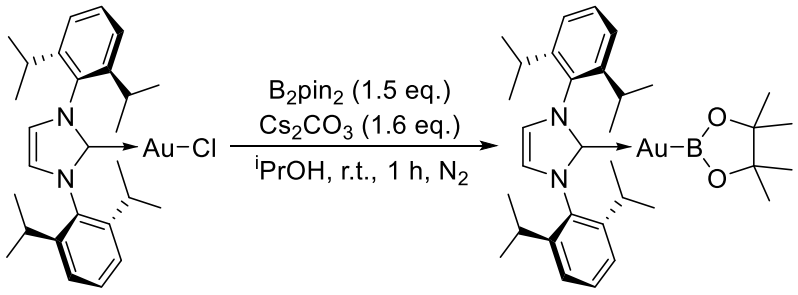

Scheme 3.69: Synthesis of (IPr)AuBpin **71**.

On some runs of the reaction, residual $B(OR)_3$ species that failed to quaternise and precipitate out (*e.g.*, pinB–O–Bpin, pinB–O^{i}Pr) were detectable by ^{11}B NMR spectroscopy (^{11}B δ 21 – 23 ppm). We tried to selectively wash out these impurities with pentane, petroleum ether and diethyl ether, but these all dissolved considerable amounts of our desired complex **71**.

Concerned by the inconsistent outcomes we were getting from this reaction, we considered that a different base may help drive conversion of (IPr)AuCl, as well as offer improved precipitation of boron adducts. A short screen of CsOPiv, CsOAc, K_2CO_3 and potassium 2-ethyl hexanoate was run under the same conditions described in **Scheme 3.69**, but no improvement was observed.

To get around the issue of inseparable inorganic material altogether, we contemplated a simpler, base-free reaction analogous to the transfer of boron onto copper described by Santos in **Scheme 3.42**.[117] A series of (IPr)Au–X compounds were readily synthesised *via* silver salt metathesis reactions (**Scheme 3.70**).

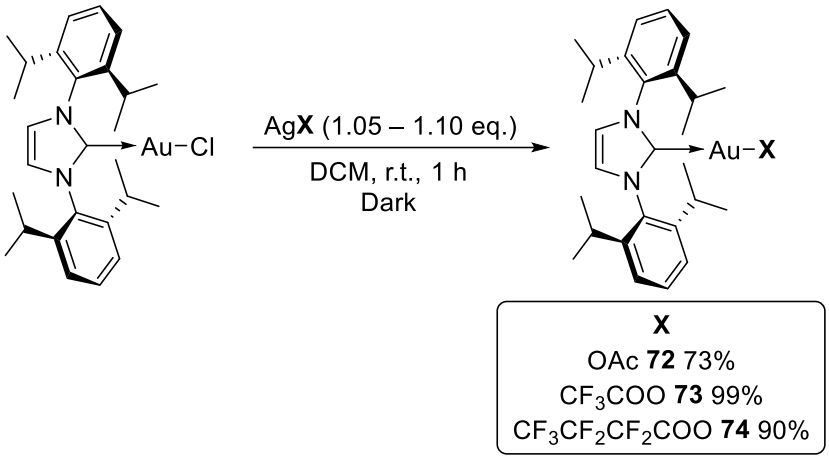

Scheme 3.70: Synthesis of (IPr)Au–X compounds *via* silver salt metathesis.

With a series of gold(I) compounds in hand, a set of reactions were run in parallel with each (IPr)Au–X complex stirred for 1 h with 1.5 eq. of diboron **25** on a 0.05 mmol scale (**Scheme 3.71**). Each reaction was run in $CDCl_3$, DCM, CH_3CN and THF and analysed directly *via* ^{11}B NMR to look for (IPr)Au–Bpin **71** formation (δ 45 – 50 ppm).

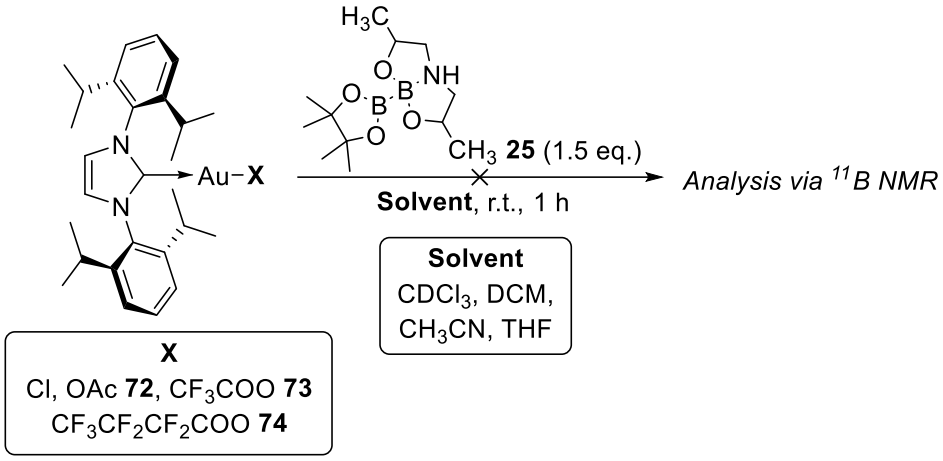

Scheme 3.71: Screen of attempted base-free transmetallations of Bpin onto an (IPr)Au^{I} scaffold.

To our disappointment, no reaction screened revealed any evidence of complex **71**. This indicates a clear divergence from the reactivity of copper analogues, in which this reaction is facile. Given the high bond enthalpy of Au–B, thermodynamics should favour this reaction, provided the right conditions can be found.

We tried a similar reaction under the same conditions with (PPh_3)Au–OAc and B_2pin_2 in DCM. This gave a clean outcome *via* ^{31}P NMR with one new shift appearing (δ 57.0 ppm). However, the ^{11}B NMR spectrum revealed two shifts at δ 30.5 and 22.5 ppm, that will most likely correspond to unreacted B_2pin_2 and pinB–OAc or pinB–O–Bpin, respectively (*c.f.* Au–Bpin ^{11}B δ ~50 ppm).

Despite our issues with reproducibility, we had enough material to explore the potential of complex **71** as a C–H borylation reagent. Complex **71** was stirred with 2 eq. oxidant and an excess of 1,3-dimethoxybenzene (5 eq.) at 80 °C and analysed by ^{1}H NMR (**Scheme 3.72**).

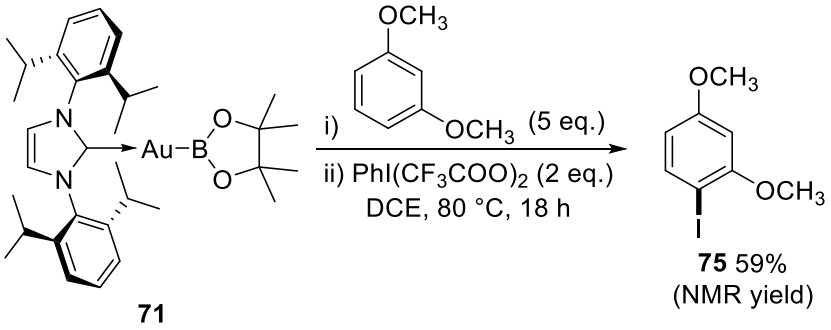

Scheme 3.72: Attempted oxidative borylation of 1,3-dimethoxybenzene.

To our excitement, analysis *via* ^{1}H NMR revealed another set of signals for our substrate with a substituent added at the 4-position, as intended. Although, when we

tried to correlate NMR shifts from the unidentified compound with reported data for 2,4-dimethoxyphenyl boronic acid pinacol ester, we could not convincingly align the two sets of signals. The same was true of the corresponding boronic acid and boroxine. It later became clear that the tri-substituted compound we had made in appreciable quantities was 1-iodo-2,4-dimethoxybenzene **75**.

This indicated that our choice of oxidant was inappropriate, so we set about synthesising the less potent 1-pivaloyloxy-1,2-benziodoxol-3(1*H*)-one (PBX) **77** *via* a two-step synthesis described by Larrosa (**Scheme 3.73**).[166]

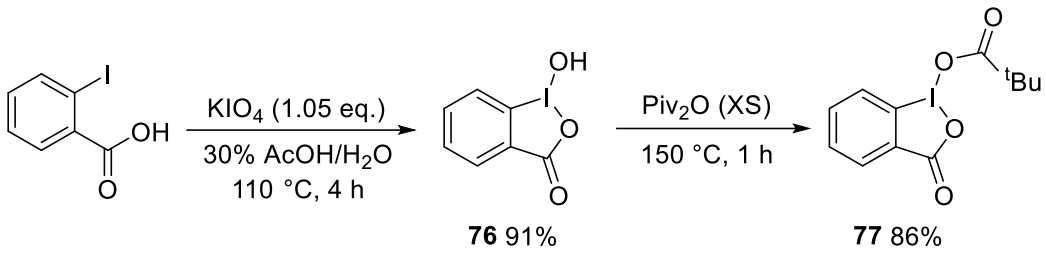

Scheme 3.73: Synthesis of PBX **77** *via* HBX **76**.

Next, we set up control experiments to assess the degree to which PBX **77** interacts with our substrate, compared to $PhI(CF_3COO)_2$, the oxidant employed in **Scheme 3.72**. We replicated the conditions and stoichiometry used previously, only with no gold present. Each oxidant was tested at 80 °C and room temperature and the % yield of **75** was measured *via* the use of an internal standard (**Scheme 3.74**). The results clearly showed that PBX **77** was considerably less oxidising than $PhI(CF_3COO)_2$, as it did not appear to interact with the substrate at all, even at 80 °C.

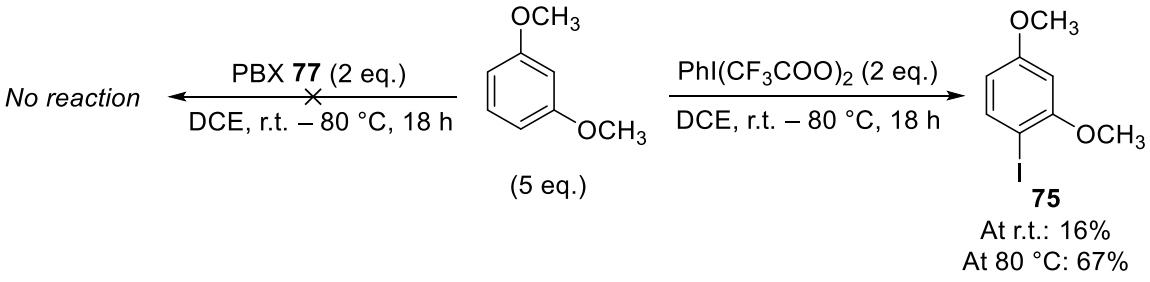

Scheme 3.74: Control experiment to determine the deleterious effect of $PhI(CF_3COO)_2$ and PBX **77** on 1,3-dimethoxybenzene at r.t and 80 °C.

The obvious next step was to repeat the attempt at an oxidative borylation, with PBX **77** as the oxidant (**Scheme 3.75**). This successfully consumed all complex **71** present, but no borylated material was detected.

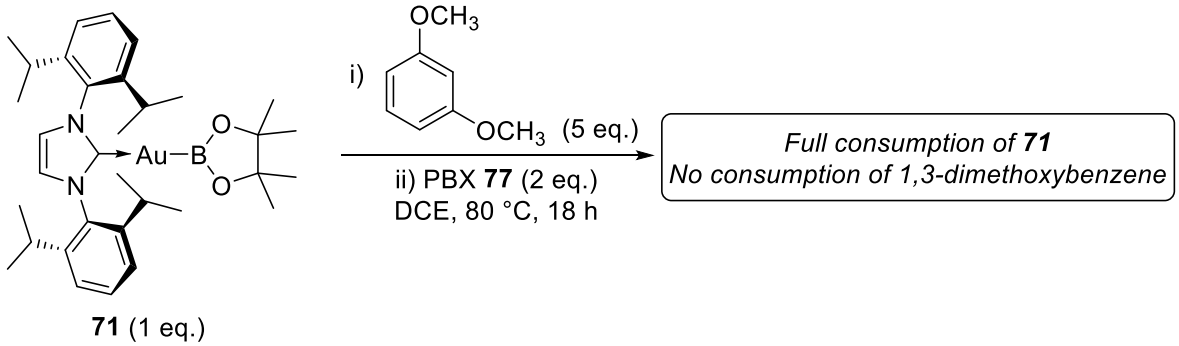

Scheme 3.75: Re-attempt at borylating an electron-rich aromatic compound *via* a gold(III) boryl intermediate.

To examine whether the conditions were too forcing, complex **71** was stirred with 2 eq. PBX **77** in CD_2Cl_2 at room temperature for 1 h and analysed directly *via* NMR. The ^{11}B NMR spectrum revealed full conversion of **71** with shifts at *δ* 22.5 and 21.9 ppm dominating. These can be plausibly correlated with pinB–O–Bpin and pinB–OPiv, respectively.

A clear problem presented itself, in which either: (1) the boron of **71** was being oxidised preferentially to the gold centre; or (2) complex **71** was successfully oxidised to a (IPr)Au^{III}(X)(OPiv)Bpin complex, but reductively eliminated pinB–OPiv before reaction with an arene could take place. To mitigate against the first scenario, we hypothesised that a less oxophilic boron subunit may be more robust to oxidation. We targeted a novel structural analogue, (IPr)AuBdan **78**, employing the same methodology as we did to synthesise complex **71** but with pinB–Bdan **67** instead of B_2pin_2 (**Scheme 3.76**).

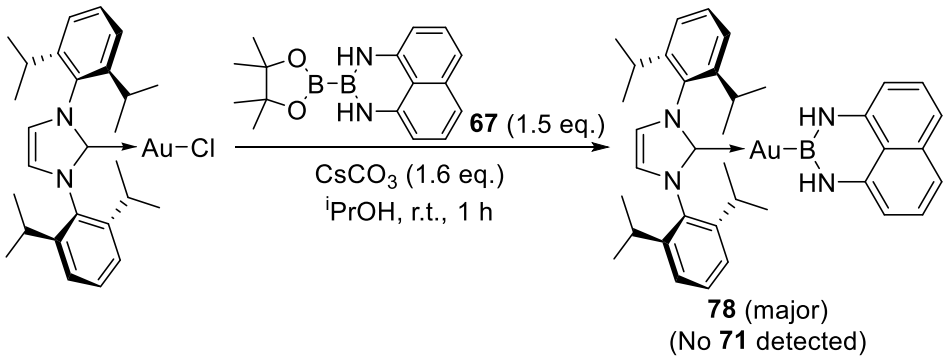

Scheme 3.76: Reaction of (IPr)AuCl with diboron **67** in the presence of an auxiliary base to give novel gold complex **78**.

As mentioned in **Chapter 3.3.1.3**, pinB–Bdan **67** is selectively activated by electron pair donors at its more Lewis acidic Bpin. This conceptually guarantees transfer of Bdan onto gold in preference to Bpin. Pleasingly, this is exactly what we observed when we carried out the reaction and analysed the reaction after filtration. Interestingly, the ^{11}B NMR shift of complex **78** was δ ~40 ppm (*c.f.* complex **71** δ ~48 ppm). This is consistent with a more shielded boron environment.

Although encouraged that our reaction generated healthy quantities of our desired product, we ran into the same problems as we did with complex **71** when it came to isolation. That is, incomplete conversion of (IPr)AuCl and difficulty separating boron material and inorganic by-products. When the stoichiometry was adjusted to minimise leftover material (SM/**67**/$CsCO_3$ 1:1.1:1.2), the outcome was considerably less clean. Also, diboron **67** was proving harder to separate out of solution compared with B_2pin_2, which seemed to be quaternised by $CsCO_3$ more readily. We tried a third run at SM/**67**/$CsCO_3$ 1:1.1:1.6, which was better but still not as good as the original setup.

As before, purification steps such as washes (pentane, benzene, Et_2O) and filtrations (Celite, gravity) failed to give pure material. Although, curiously, when we collected material off filter paper after one reaction where we did not rinse with DCM, we were astonished to discover that this sample was extraordinarily clean by ^{1}H NMR (**Figure 3.21**).

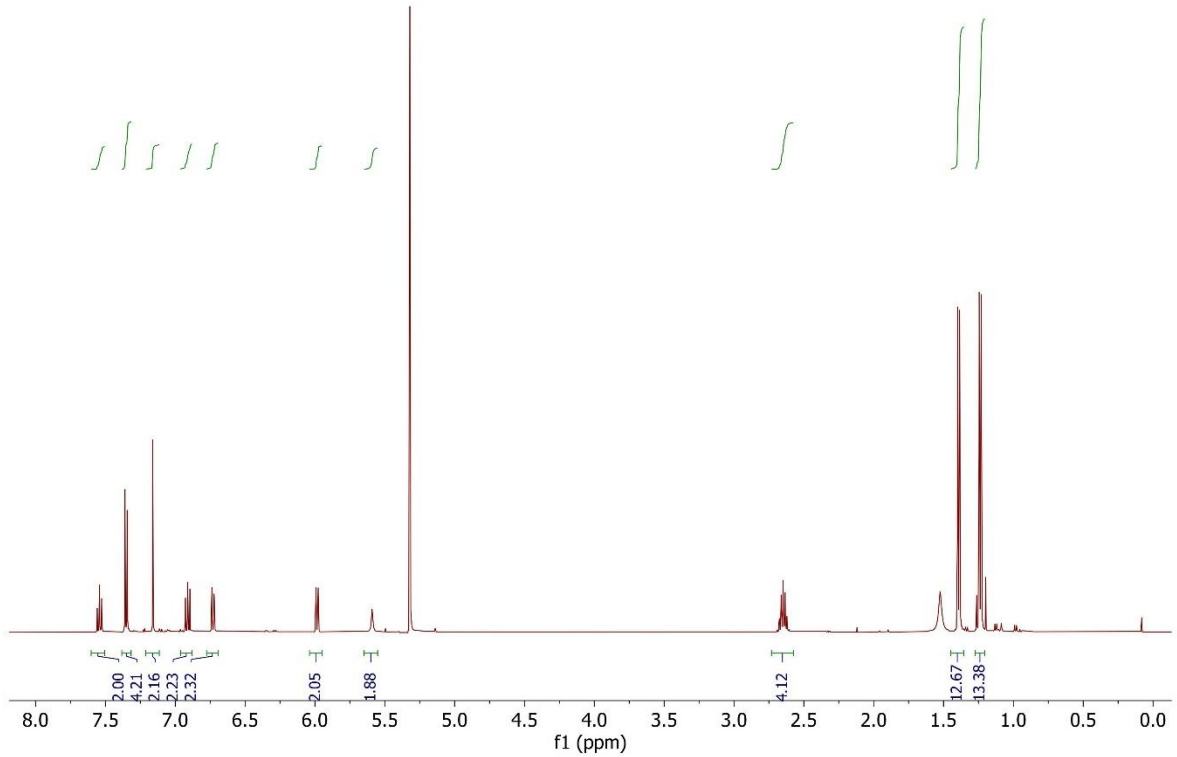

Figure 3.21: Sample of (IPr)AuBdan **67**. NMR experiment run in CD_2Cl_2 at 500 MHz.

To unambiguously confirm the structure, we attempted to crystallise complex **78** and submit it for XRD analysis. Pentane vapour was diffused into a concentrated solution of our sample in DCM and left for 1 week. To our disappointment, though, no material crystallised out of solution. Instead, the mother liquor turned blue and an insoluble grey solid lined the inside wall of the container. Interestingly, NMR analysis revealed that most of our sample had returned to the starting (IPr)AuCl. This indicates that complex **78** was not stable under the crystallisation conditions. Also, given the high ligand cone angles of IPr and Bdan, it is plausible that these two moieties interact with one another when ligated to the same gold atom, favouring decomposition to a simpler complex.

A positive to take from this reaction was that our desired complex **78** possesses some degree of insolubility and may be separable from other reaction components *via* crystallisation with the right combination of solvents. Subsequent repeats of the method described above did not cause sufficient quantities of material to be intercepted by the filter paper. Changing plan, we made sure to wash with copious amounts of DCM after filtering the reaction. Then, we removed the solvent under a current of air and redissolved in the minimum amount of an aromatic solvent such as

benzene and toluene and left it in on the benchtop for several days. On one occasion, we observed needle-like off-white crystals forming, but XRD analysis revealed this to be (IPr)Au–H.

Despite laborious and determined efforts to optimise this reaction and crystallise complex **78**, it remained unreliable and so we decided not to pursue this work any further.

3.3.3 Conclusions and future work

Initially, this project aimed to develop a Friedel-Crafts-type electrophilic borylation reaction proceeding *via* a hypothetical copper(III)–boryl intermediate. By analogy, the same was also attempted with gold *in lieu* of copper. In both cases, we had good evidence of successful $(L)M^{I}–BX_2$ formation, but there was no indication that we were able to generate $(L)X_2M^{III}–BX_2$ species. In many instances, metal(I)-boryl complexes were exposed to oxidants in the presence of highly electron-rich (hetero)aromatics, only to yield oxidised boron (and occasionally oxidised starting material), with no sign of borylated material.

Regardless of the issues we encountered with reactivity, there was merit in attempting to isolate (IPr)Au–Bdan **78** as an interesting, novel gold–boryl complex. But, despite tireless efforts, we failed to optimise the reaction and isolate the compound in significant quantities. It may be advantageous to handle this complex in a glove box, which we did not have access to.

One avenue left to explore in this work would be a setup ensuring boron reagents are not exposed to any oxidants. This would involve reversing the sequence of addition and thereby flipping the electronic selectivity, *i.e.* reacting an electron-deficient gold(III)–aryl species with a nucleophilic source of boron, *e.g.* diboron **25** (**Scheme 3.77**).

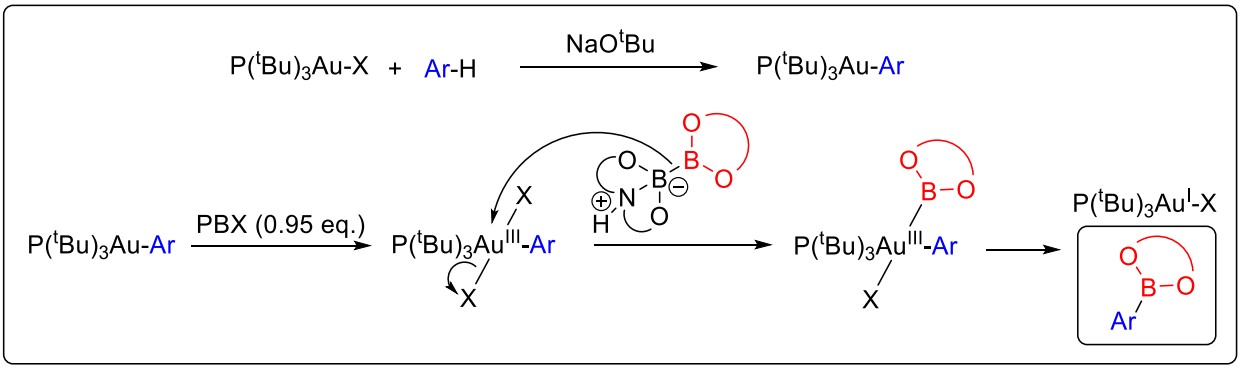

Scheme 3.77: Proposed reaction to generate Ar–Bpin compounds *via* gold(III)–aryl complexes.

Since gold(I)–aryl complexes are unusually stable (including with respect to silica),[172,173] we were able to easily replicate a procedure described by Larrosa to make a small range of compounds (**Scheme 3.78**).[174]

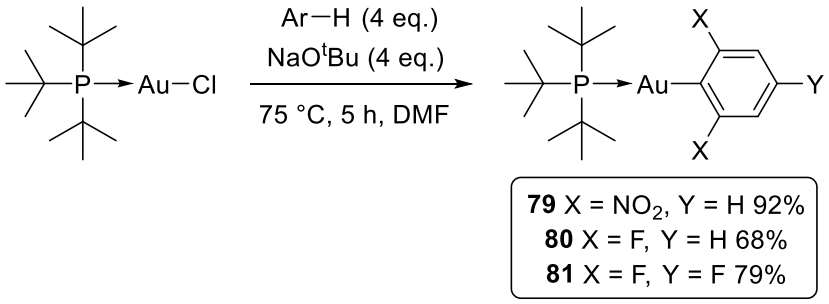

Scheme 3.78: Synthesis of tri-*tert*-butylphosphinegold(I) aryl complexes **79 – 81**.

A blank NMR spectrum of complex **79** mixed with just diboron **25** in CD_2Cl_2 revealed no interaction between the two species at room temperature, as expected. Although, we were surprised that a different control experiment in which complex **79** was mixed with 1 eq. PBX **77** at room temperature for 8 h in CD_2Cl_2 also revealed no change spectroscopically. It may be that higher temperatures, stronger oxidants, or complexes **80** and **81** will offer improved reactivity. This work is ripe for exploration but, due to time constraints, it was not pursued further.

We also attempted to isolate a structurally-intriguing, novel diboron compound DIPA–dan diboron **66**, with the hope that Bdan could be transferred onto copper and reacted with electron-deficient alkenes. We were successful in making the desired compound but only at very low yield and we could not isolate it before it decomposed. It is possible that the size of the two subunits ligating the diboron core is so large they interact with one another. Higher powered computational simulations should be run to determine if diboron **66** is synthetically feasible.

3.4 Mono-*N*-alkylation of primary amines and activation of nitriles *via* halomethyl boronates

Amines are a fundamental class of compounds in organic chemistry due to their prevalence as synthetic intermediates,[182] agrochemicals (*e.g.* **82**),[183] dyes (*e.g.* **83**)[184] and pharmaceuticals (*e.g.* **84**)[185] (**Figure 3.22**).

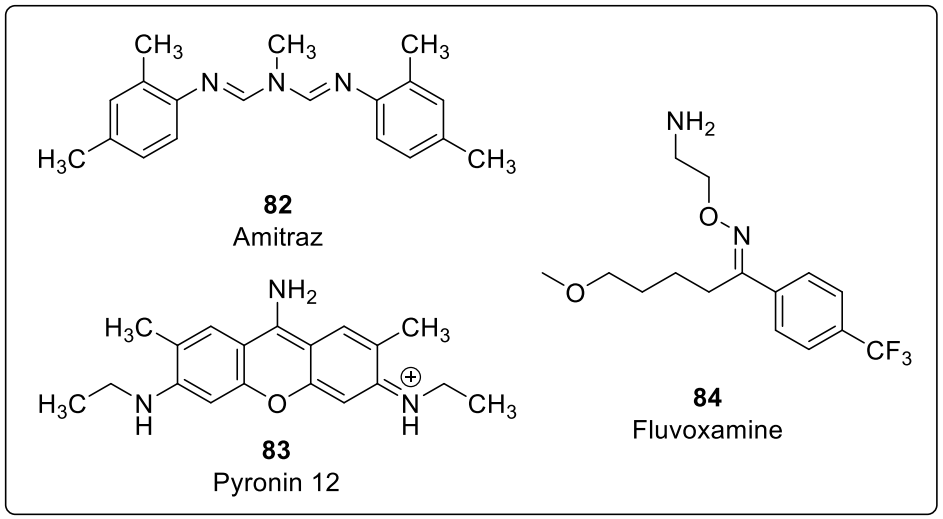

Figure 3.22: Commercially available amines.

N-Alkylation of amines can drastically alter their chemical and pharmacodynamic properties. For example, amphetamine is available *via* prescription in the US and Canada to treat attention-deficit disorders and narcolepsy.[186] However, its mono-*N*-methylated cousin, methamphetamine, is a potent stimulant of the central nervous system and strictly prohibited under many jurisdictions (**Scheme 3.79**).

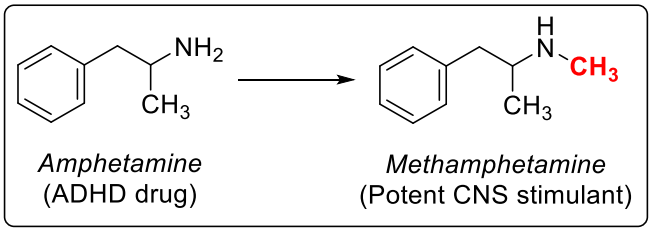

Scheme 3.79: Mono-*N*-methylation of amphetamine to give methamphetamine.

N-Alkylating amines is commonly performed with alkyl halides or their equivalents (*e.g.* dialkyl sulphates or sulphonates) *via* a simple S_N2 reaction.[187] However, this method is not feasible for the selective monoalkylation of primary amines due to the ease of over-alkylation, giving mixtures of primary, secondary and tertiary amines, as well as quaternary ammonium salts. Reductive amination is another common

method but can also be difficult to control, particularly for monomethylation of primary amines. It is also somewhat inefficient due to often needing to synthesise the reagents from the corresponding alcohol.[188] Monoalkylation techniques have therefore been the focus of research for several decades.[189–194]

Unpublished work in our group has demonstrated that halomethyl boronates are incredibly efficient at delivering a –CH_2Bpin moiety onto cysteine (**Scheme 3.80**).[195] Our results showed reaction completion in 5 minutes in either CD_3OD or D_2O with no discernible difference between the chloro-, bromo- or iodomethyl boronate reagents.

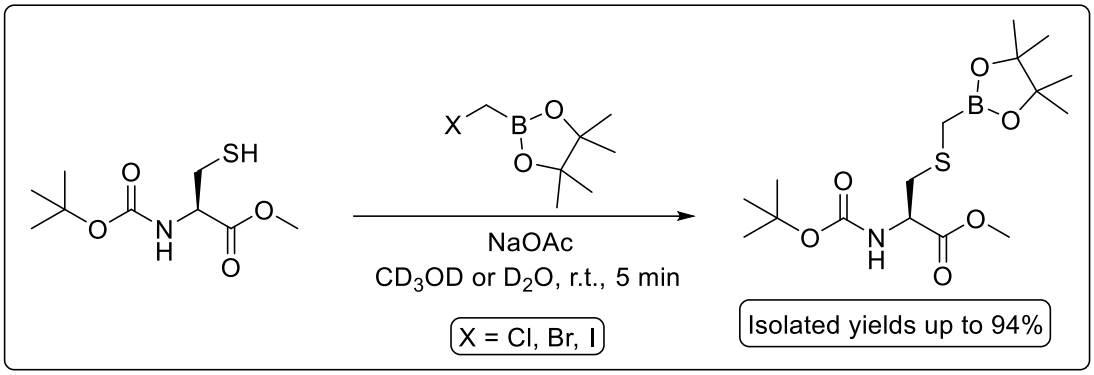

Scheme 3.80: Modification of cysteine with halomethyl boronate esters.

In the light of these data, we considered that halomethyl boronates may be useful for monomethylation of primary amines. In an analogous fashion to cysteine, we would expect a primary amine **I** to coordinate to the boron reagent, then rearrange to displace the chloride (**Scheme 3.81**). The resulting α-aminoboronate **III** should be unstable with respect to rearrangement to the N–Bpin species **IV**, where the reaction should stop, thus preventing overalkylation. An aqueous work up should readily hydrolyse the N–Bpin species **IV** to give the *N*-methylated amine **V** and quench any unreacted $ClCH_2$Bpin in the process. To sequester the HCl by-product, an extra equivalent of amine starting material would be needed or a non-nucleophilic external base.

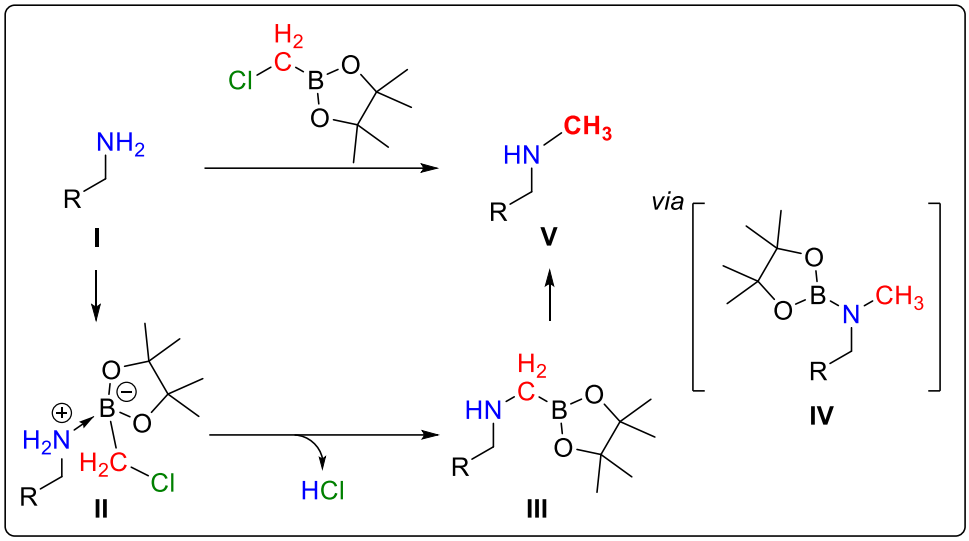

Scheme 3.81: Proposed mechanism for the selective mono-*N*-methylation of primary amines with halomethyl boronate esters.

This proposed reaction bears a striking similarity to one recently reported by Dong *et al.*[196] In their study, a series of tertiary α-aminoboronates is synthesised *via* the so-called aza-Matteson reaction (**Scheme 3.82**). This involves the formation of R_2N–Bpin species *in situ*, followed by reaction with $LiCH_2Cl$ to give an amine-borate complex. This rearranges in the same manner we propose (**Scheme 3.81**, **II** → **III**), to displace the chloride and give α-aminoboronates, stable enough for further derivatisation. Overall, this represents the insertion of methylene into N–B bonds.

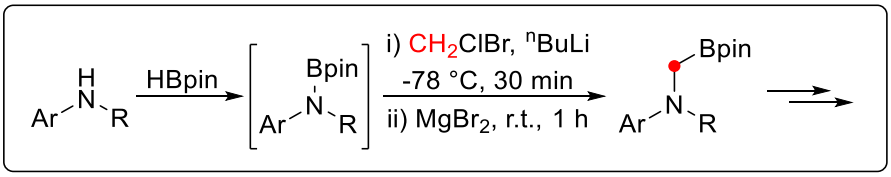

Scheme 3.82: Aza-Matteson reaction reported by Dong *et al.*

3.4.1 *N*-Methylation of primary amines

We employed 4-methoxybenzylamine **85** as our substrate in test reactions due to the simplicity of its ^{1}H NMR spectrum. In the first attempt at a reaction, we included an extra equivalent of starting material to neutralise the HCl formed and performed the reaction in CD_3CN to monitor directly *via* NMR spectroscopy (**Scheme 3.83**).

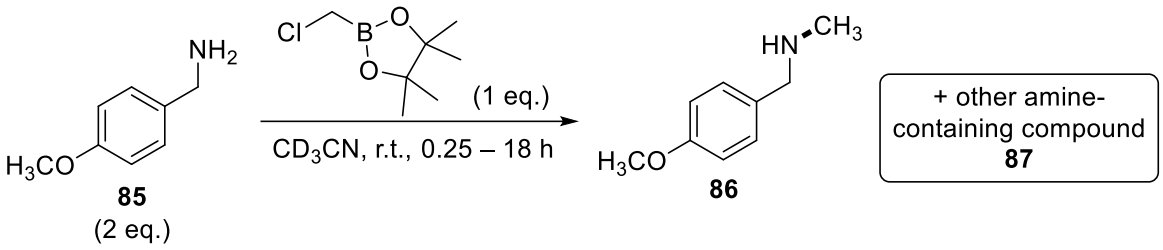

Scheme 3.83: *N*-methylation of 4-methoxybenzylamine **85**.

A white precipitate developed after a few minutes of stirring which we assumed to be the amine-borate complex **II**, although over time we would expect the amine hydrochloride salt to comprise this too. To our delight, we were able to observe the formation of the desired *N*-methylated product **86** after just 15 min by ^{1}H NMR. At the same time point, almost all $ClCH_2Bpin$ appeared to have been consumed (by ^{11}B NMR).

The reaction showed signs of further progression when monitored at 2 h and plateaued before the 18 h time point, to leave three major amine-derived species: starting amine **85**, *N*-methylated amine **86** and an unidentified compound **87**. A basic work up was carried out, designed to wash out residual boron but mass recovery was low (30%) and, curiously, a boron-containing species remained in our sample (^{11}B δ 7.6 ppm). Further treatment of this residue with boron scavengers also failed to remove unwanted boron material.

Intrigued by this side product, we repeated the reaction but with protio acetonitrile and gathered 2D NMR data to elucidate its structure. Our assignment led us to diazaborole **87** (**Figure 3.23**). This was easily observable by TLC, allowing for facile separation *via* column chromatography to give a pure sample of **87** in 8% yield. High-resolution mass spectrometry agreed with our NMR assignment.

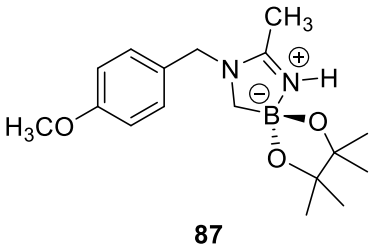

87

Figure 3.23: Diazaborole **87**.

The formation of diazaborole **87** revealed the existence of a competing mechanism, whereby the α-aminoboronate **III** activates a molecule of MeCN, rather than rearranging to the N–Bpin species **IV** (**Scheme 3.84**). This behaviour is characteristic of a frustrated Lewis Pair which nitriles appear capable of "quenching".

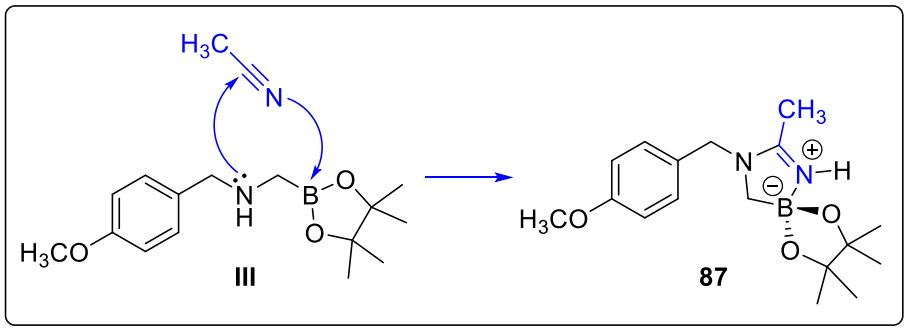

Scheme 3.84: Activation of nitrile solvent with intermediate **III** to give diazaborole **87**.

To avoid formation of **87**, it was clear we needed to switch solvent. When the reaction was repeated in THF, we observed a cleaner reaction with higher conversion and significantly improved mass recovery.

Since, in practical syntheses, it is often not feasible to have an extra equivalent of starting material, we carried out a screen of non-nucleophilic organic bases (**Table 3.9**).

Table 3.9: Base screen for the mono-*N*-methylation of 4-methoxybenzylamine **85**.*

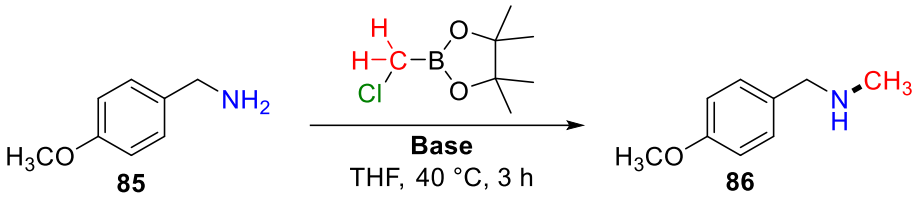

Entry	Base	% Yield[a]
1	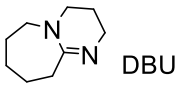 DBU	25
2	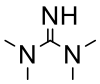 TMG	45
3	 DBN	33
4	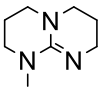 mTBD	30

*Reaction conditions: **85** (0.5 mmol, 1.0 eq.), $ClCH_2Bpin$ (1.5 eq.), base (1.5 eq.), THF (2 ml), 40 °C, 3 h, scintillation vial. [a]% Yields determined by ^1H NMR spectroscopy with 1,3,5-trimethoxybenzene used as an internal standard.

Modest yields of methylated amine **86** were achieved with all bases, with *N*,*N*,*N'*,*N'*-tetramethylguanidine (TMG) offering the most promising activity (**Entry 2**). Given the structural similarity of amine **85** and desired product **86**, it is not feasible to separate these two components from a crude mixture to obtain a pure sample of **86**. Further optimisation of this *N*-methylation reaction should therefore focus on achieving full conversion of starting amine. At the time of writing, this is an active area of research in our lab.

3.4.2 Synthesis of diazaboroles

We retained a curious interest in the earlier appearance of spiro compound diazaborole **87** and began to consider if other structural analogues could form. Since these compounds bring together amine, boron reagent and nitrile solvent, they have far-reaching potential for diversification (**Scheme 3.85**).

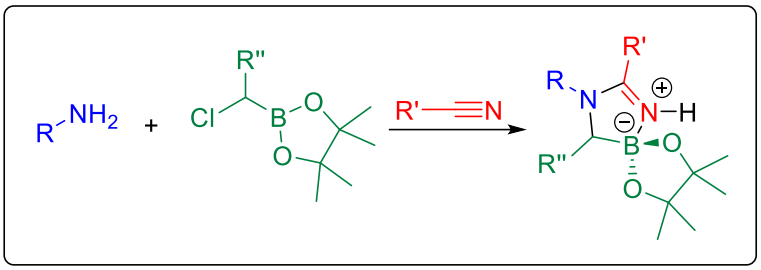

Scheme 3.85: Three-component reaction of primary amines, chloromethyl boronate esters and nitriles to form diazaboroles.

The heterocycle that assembles *in situ* is known as 3,4-dihydro-1,4,2-diazaborole. Although uncommon, literature reports of other boron-centred spiro compounds containing this molecular architecture exist. For example, in 1991, Biedrzycki and colleagues reported a series of aliphatic and benzylic bifunctional boronate esters as potential ligands for affinity chromatography (**Scheme 3.86**).[197]

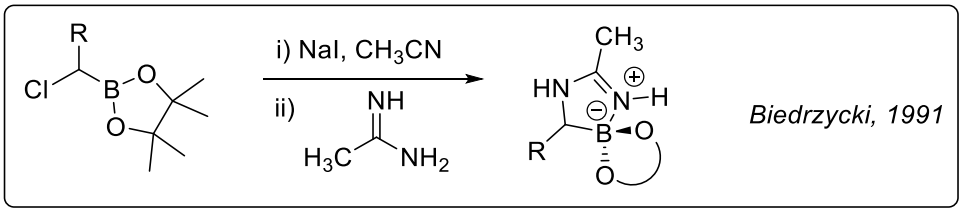

Scheme 3.86: Diazaborole synthesis described by Biedrzycki and colleagues.

More recently, Nizioł *et al*. modified the nucleoside deoxycytidine to give a boron-containing derivative under similar conditions to our setup (**Scheme 3.87**).[198] However, the diazaborole forms differently, as N→B coordination from the pyrimidinone to boron is intramolecular and occurs after formation of the α-aminoboronate.

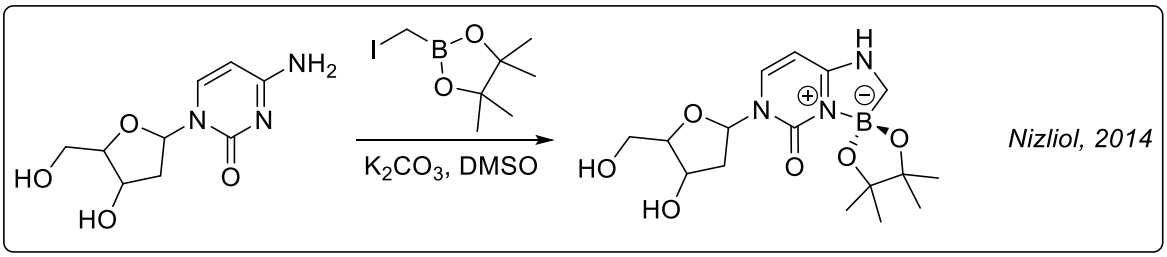

Scheme 3.87: Modification of deoxycytidine to incorporate the diazaborole heterocycle under study.

Further examples of these unique spiro compounds can be found in works by Miura and Hirano,[199] as well as Marder,[200] but, as in the other examples, neither involve the activation of nitrile solvent.

Herein, we report a short series of boron-centred diazaborole spiro compounds with interchanging amine and nitrile components (**Scheme 3.88**). To simplify purification, 2 eq. of starting amine were used instead of adding 1 eq. of base.

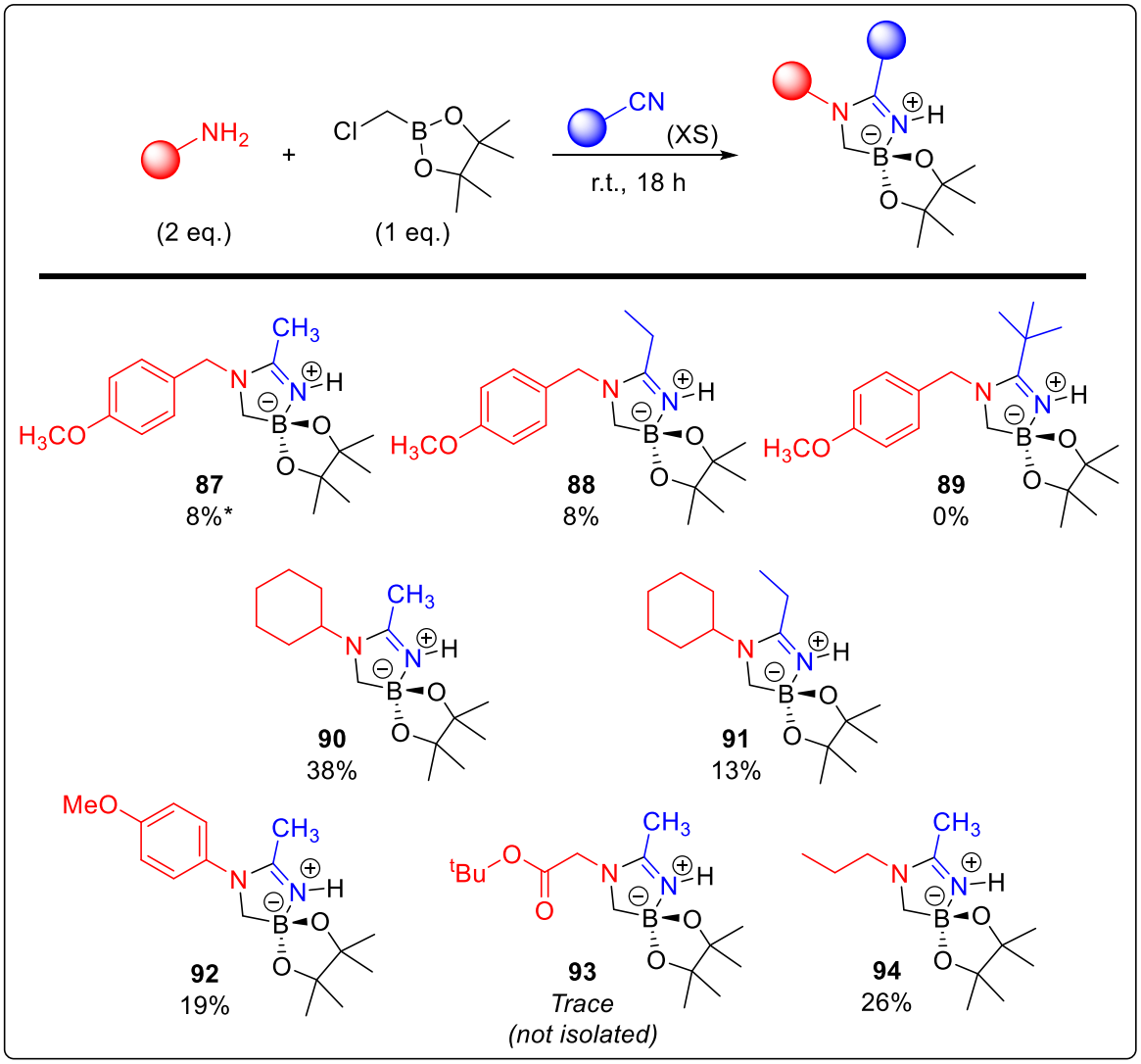

Scheme 3.88: Scope of diazaboroles. Reaction conditions: primary amine (2 mmol, 2 eq.), $ClCH_2Bpin$ (1 eq.), nitrile (2 mL), r.t., 18 h, scintillation vial. % Yields shown are of isolated products. *% Yield shown is from the reaction described in **Scheme 3.83**.

Reaction of amine **85** with the halomethyl boronate reagent in propionitrile gave diazaborole **88** in comparable yield to the analogous acetonitrile-derived compound **87**. When the same reaction was attempted in pivalonitrile, formation of diazaborole **89** was not detected after work up. This is consistent with pivalonitrile's exceptionally sterically crowded nitrile carbon, blocking nucleophilic attack of the C–N π* orbital and preventing activation of the nitrile. In this reaction we observed a mixture of starting amine **85**, *N*-methyl amine **86** and imine **95** (**Figure 3.24**).

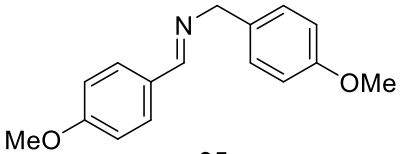

95
(not isolated)

Figure 3.24: By-product imine **95**.

We suspect that amine **85** is sensitive to self-condensation when concentrated under a current of air. As, although only trivial amounts of imine **95** were seen in the ^{1}H NMR spectrum of the crude material, large quantities eluted when column chromatography was later carried out. *N*-Methylated amine **86** was isolated in 39% yield as an inseparable mixture of **86**/**85** in a 55:45 ratio. Imine **95** was not collected.

Cyclohexylamine proved amenable to diazaborole formation in both MeCN and propionitrile, delivering **90** and **91** in 38% and 13% yield, respectively. Interestingly, *p*-anisidine was sufficiently nucleophilic to activate MeCN and give **92**. Glycine *tert*-butyl ester did show some formation of diazaborole **93**, but only in trace quantities. Propylamine formed diazaborole **94**, which crystallised on standing as the monohydrate, allowing us to perform single-crystal XRD analysis, verifying our proposed structure (**Figure 3.25**).

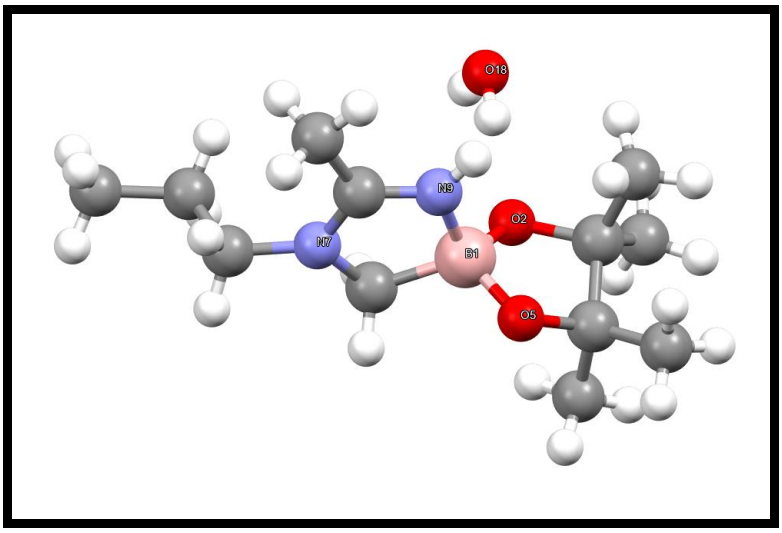

Figure 3.25: XRD crystal structure of diazaborole **94**. Experimental details can be found in the Appendix.

The molecule of water that co-crystallises with diazaborole **94** is situated such that each of its H atoms interact with an O-2 atom on an adjacent molecule of **94** (**Figure 3.26**). Additionally, a lone pair of electrons on the water's oxygen (O-18) form a hydrogen bond with the N–H at N-9.

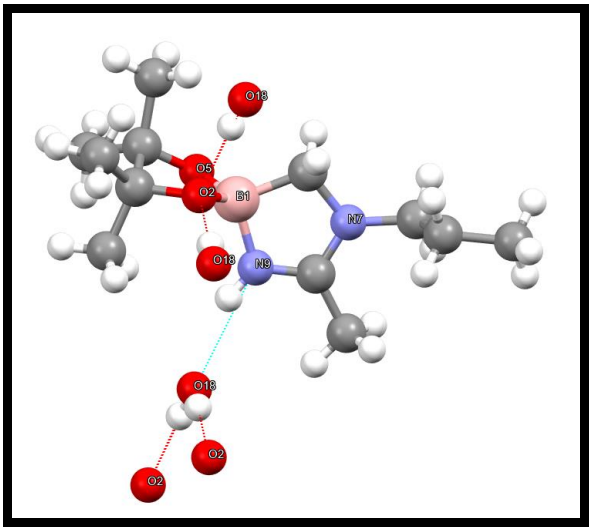

Figure 3.26: Diazaborole **94** with H-bonds included.

3.4.3 Conclusions and future work

The aim of this work was to develop a novel method to selectively mono-*N*-methylate primary amines *via* the use of a halomethyl boronate reagent. We were successful in realising this goal with a simple reaction setup at low temperature. However, we are yet to find an optimised set of conditions which will consistently take the reaction to completion. This is crucial if this method is to be applied in synthesis, as primary amines are invariably too similar to their corresponding *N*-methylated analogue to be easily separable *via* purification.

Our data suggest that THF and hindered nitrile solvents give clean and efficient reactions, although a comprehensive solvent screen has not yet been carried out. Guanidine-derived bases such as TMG appear to deliver higher yields than other organic bases, although there is room for exploration.

The appearance of novel diazaborole **87** in our initial exploratory work caught our attention as a structurally interesting side product. When we tried to synthesise a series of structural analogues, we had success with straight-chain amines, cyclic amines and anilines. Acetonitrile and propionitrile were successfully activated but pivalonitrile proved to be too hindered.

We plan to optimise this reaction further and broaden the scope significantly in the near future to test the limits of the required amine nucleophilicity as well as nitrile steric hindrance. Amino acid-derived substrates such as glycine ethyl ester **96** and the more structurally complex amide **97** will provide examples on bioactive drug-like

molecules. (*S*)-α-Methylbenzylamine **98** is a potentially interesting substrate as, together with amide **97**, it features a chiral centre adjacent to the amine nitrogen. Deactivated aniline **99** and 2-aminopyridine **100** will provide a formidable test for this reaction system on account of their reduced nucleophilicity, and nitriles **101** and **102** offer a degree of steric pressure that may reduce reactivity. It is possible to envisage compounds analogous to nitriles (*e.g.* thiocyanates, CO, CO_2) being activated *via* similar means to give novel heterocycles.

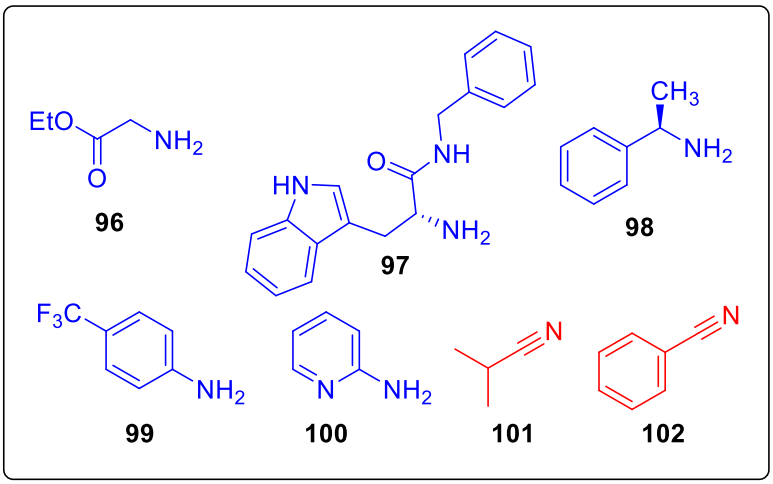

Figure 3.27: Possible starting feedstocks to expand the diazaborole scope.

In this work, the boron reagent was fixed as chloromethyl boronic acid pinacol ester, but we have recently generated alternatives *via* the Matteson reaction[201] in order to explore a third vector (**Scheme 3.89**). This will install a chiral centre on the diazaborole ring, adjacent to the boron.

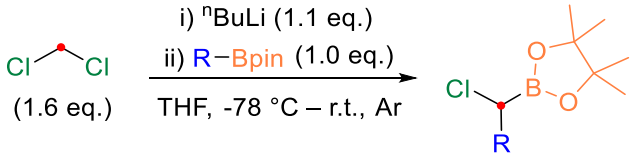

Scheme 3.89: Formation of halomethyl boronate reagents *via* the Matteson reaction.

4 Experimental

4.1 General Methods

General considerations

All reagents and solvents were purchased and used as supplied unless otherwise stated. All reactions were stirred and carried out at atmospheric pressure under air atmosphere unless otherwise indicated. A “reaction tube” refers to a Radleys® Quick-Thread Glass Reaction Tube. All reactions were monitored by TLC, ^{1}H NMR spectroscopy or ^{11}B NMR spectroscopy.

Thin-layer chromatography

TLC plates used were pre-coated with silica gel 60 F254 on aluminium (Merck KGaA). The spotted TLC plates were visualised by UV light at 254 nm or 365 nm.

Flash column chromatography

Flash column chromatography refers to purification performed using a Biotage Isolera flash purification system with either Büchi FlashPure, Biotage SNAP or GraceResolv flash cartridges prepacked with silica gel (40 – 60 μm).

NMR spectroscopy

Chemical shifts are quoted in parts per million (ppm) and assigned using the following abbreviations: singlet (s), doublet (d), triplet (t), quartet (q), quintet (qn), sextet (sext), septet (sept), multiplet (m), broad (br), or a combination of these. Reported shifts are relative to tetramethylsilane (^{1}H and ^{13}C) and $F_3B{\bullet}OEt$ (^{11}B). Coupling constants (*J*) are quoted in Hertz (Hz) to one decimal place. NMR experiments were recorded at ambient temperature.

^{1}H NMR spectra were recorded at 500 MHz on a Bruker Avance 500 spectrometer, at 600 MHz on a Bruker Avance 600 spectrometer, or at 700 MHz on a Bruker Avance 700 spectrometer. Chemical shifts are reported to the nearest 0.01 ppm and compared against residual solvent signals: $CDCl_3$ (δ = 7.26 ppm, s), CD_2Cl_2 (δ = 5.32 ppm, s), CD_3CN (δ = 1.94 ppm, qn), DMSO-d_6 (δ = 2.50 ppm, qn), C_6D_6 (δ = 7.16 ppm, s), D_2O (δ = 4.79 ppm, s) or CD_3OD (δ = 3.31 ppm, qn).

^{13}C NMR spectra are proton-decoupled and were recorded at 126 MHz on a Bruker Avance 500 spectrometer, at 150 MHz on a Bruker Avance 600 spectrometer, or at 176 MHz on a Bruker Avance 700 spectrometer. Shifts are reported to the nearest

0.1 ppm and compared against residual solvent signals: $CDCl_3$ (δ = 77.2 ppm, t), CD_2Cl_2 (δ = 53.8 ppm, qn), CD_3CN (δ = 118.3 ppm, s; 1.3 ppm, sept), DMSO-d_6 (δ = 39.5 ppm, sept), C_6D_6 (δ = 128.1 ppm, t).

^{11}B NMR spectra were recorded at 160 MHz on a Bruker Avance 500 spectrometer or at 225 MHz on a Bruker Avance 700 spectrometer. Reported shifts are given to the nearest 0.1 ppm.

Mass spectrometry

Mass spectrometry was performed on VG70 SE (ES+, CI, ES− modes).

IR spectroscopy

Infra-red (IR) spectra were recorded using a Perkin-Elmer Spectrum 100 FTIR Spectrometer operating in ATR mode as thin films. All frequencies are given in reciprocal centimetres (cm^{-1}).

Melting point analysis

Melting points were measured with a Gallenkamp heating block and are uncorrected.

4.2 General Procedures

General Procedure A – Amidation

This method is based on a procedure described by Sheppard and colleagues.[50] A round-bottomed flask was loaded with the carboxylic acid (5.0 mmol, 1.0 eq.), the amine (5.5 mmol, 1.1 eq.) and TAME (5 mL). The suspension was then heated to reflux in Dean-Stark apparatus (side-arm filled with TAME) and $B(OCH_2CF_3)_3$ (500 µmol; 5 mL of a 0.1 M solution in TAME) was added into the reaction through the Dean-Stark apparatus *via* a syringe. Afterwards, the reaction was stirred for 1 – 5 d.

General Procedure B – Iridium-catalysed borylation of 4-substituted quinolines

The quinoline (2.0 mmol, 1.0 eq.), B_2pin_2 (609 mg, 2.4 mmol, 1.2 eq.), 1,5-cyclooctadiene(methoxy)iridium(I) dimer (20 mg, 30 µmol, 0.015 eq.) and the ligand (60 µmol, 0.03 eq.) were weighed into a reaction tube and sealed with a Teflon-lined screw cap. The tube was then evacuated and refilled with argon (three cycles) before dry dioxane (2 mL) was added *via* a syringe and the mixture stirred at 85 °C for 18 h. The reaction mixture was then concentrated under reduced pressure to give the crude product which was purified by silica gel column chromatography.

General Procedure C – Synthesis of aryl (tri-*tert*-butylphosphine)gold(I) complexes

This method is based on a procedure described by Larrosa and colleagues.[174] ($^tBu_3P$)AuCl (1 eq.), arene (4 eq.) and NaO^tBu (4 eq.) were dissolved in DMF (0.2 M). The reaction mixture was stirred at the temperature and for the time indicated. The mixture was allowed to cool to room temperature, and the suspension was filtered through a plug of Celite. Evaporation of the solvent under a current of air left an impure residue that was purified by flash column chromatography to afford the corresponding aryl gold(I) complexes.

General Procedure D – Synthesis of diazaboroles

The amine (2.0 mmol, 2.0 eq.) was added to the nitrile (2 mL) in a scintillation vial followed by $ClCH_2Bpin$ (1.0 mmol, 1.0 eq.). The reaction was then stirred at room temperature for 18 h. The resulting suspension was added to 20 mL sat aq $NaHCO_3$

and extracted with CH_2Cl_2 (3 × 20 mL), washed with brine (20 mL), dried ($MgSO_4$) and filtered. Concentration of the filtrate under reduced pressure left an impure residue that was purified by silica gel column chromatography.

4.3 Characterisation data

4.3.1 Free radical borylation

4,8-Dimethyl-2-(4,4,5,5-tetramethyl-1,3,2-dioxaborolan-2-yl)-1,3,6,2-dioxazaborocane (PDIPA diboron) 25

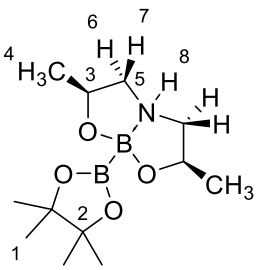

cis

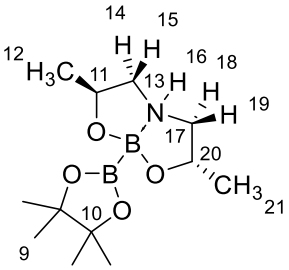

trans

This method is based on a procedure described by Santos and colleagues.[117] A solution of bis(2-hydroxypropyl)amine (5.25 g, 39.4 mmol, 1.0 eq.) in CH_2Cl_2 (20 mL) was added to a solution of bis(pinacolato)diboron (10.00 g, 39.4 mmol, 1.0 eq.) in Et_2O (160 mL) and the resulting mixture was stirred at room temperature for 72 h. The white precipitate formed was filtered and washed with copious amounts of Et_2O to provide **25** (6.16 g, 58%, *cis*:*trans* 1:1) which required no further purification;

m.p. 202 – 203 °C;

δ_H (700 MHz, CD_3CN) 5.39 (1H, br s, H-8, *cis*), 5.14 (1H, br s, H-16, *trans*), 4.04 – 4.12 (3H, m, *cis* H-3; *trans* H-11), 3.64 – 3.69 (1H, m, *trans* H-20), 3.26 – 3.31 (1H, m, *trans* H-15), 2.83 (2H, dd, *J* 11.7 Hz, 4.6 Hz, *cis* H-7), 2.69 (1H, dd, *J* 11.4 Hz, 3.8 Hz, *trans* H-19), 2.45 – 2.50 (2H, m, *cis* H-6), 2.22 – 2.28 (1H, m, *trans* H-18), 1.86 – 1.91 (1H, m, *trans* H-14), 1.16 (12H, s, *cis* H-1), 1.15 (12H, s, *trans* H-9), 1.12 (3H, d, *J* 6.0 Hz, *trans* H-12), 1.11 (3H, d, *J* 6.0 Hz, *trans* H-21), 1.07 (6H, d, *J* 6.0 Hz, *cis* H-4);

δ_C (176 MHz, CD_3CN) 82.3 (s, *cis* C-2), 82.2 (s, *trans* C-2), 71.6 (s, *cis* C-3), 68.4 (s, *trans* C-11), 67.7 (s, *trans* C-20), 58.9 (s, *trans* C-17), 58.8 (s, *cis* C-5), 57.4 (s, *trans* C-13), 25.6 (s, *trans* C-9), 25.6 (s, *trans* C-9), 25.6 (s, *cis* C-9), 21.3 (s, *cis* C-3), 20.0 (s, *trans* C-21), 19.2 (s, *trans* C-12);

δ_B (225 MHz, CD_3CN) 34.9 (sp^2-B), 8.3 (sp^3-B);

LRMS (CI) 412 (20), 403 (20), 287 (20), 272 (100), 271 (50), 134 (25);

Data consistent with the literature.[117]

_p_-Tolylboronic acid pinacol ester 26

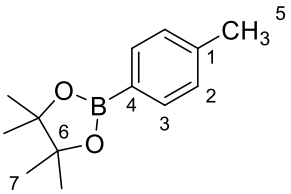

This method is based on a procedure described by Pucheault and colleagues.[93] A reaction tube was loaded with 4-iodotoluene (236 mg, 1.08 mmol, 1.0 eq.), B_2pin_2 (528 mg, 2.08 mmol, 1.9 eq.), phenanthroline (87 mg, 480 µmol, 0.5 eq.) and CsF (471 mg, 3.10 mmol, 2.9 eq.) and sealed with a Teflon-lined screwcap. The tube was then evacuated and refilled with argon (three cycles) before dry DMSO was added *via* a syringe (500 µL). The mixture was then stirred at 100 °C for 18 h. Once complete, the reaction was diluted in 0.1 M HCl (10 mL) and Et_2O (100 mL). The aqueous layer was extracted with Et_2O (3 × 20 mL) and the combined organic extracts were dried ($MgSO_4$), filtered and concentrated under reduced pressure. Flash column chromatography eluted with petroleum ether/EtOAc (100:0 – 70:30) provided **26** as a pale yellow oil (116 mg, 49%);

R_f 0.3 (petroleum ether/EtOAc 95:5);

δ_H (700 MHz, $CDCl_3$) 7.71 (2H, d, *J* 7.6 Hz, H-3), 7.19 (2H, d, *J* 7.6 Hz, H-2), 2.37 (3H, s, H-5), 1.34 (12H, s, H-7);

δ_C (176 MHz, $CDCl_3$, C–B not visible) 141.5 (s, C-1), 135.0 (s, C-3), 128.7 (s, C-2), 83.8 (s, C-6), 25.0 (s, C-7), 21.9 (s, C-5);

δ_B (225 MHz, $CDCl_3$) 30.9;

LRMS (EI) 218 ($[M]^+$, 100), 203 ($[M-CH_3]^+$, 95), 161 (10), 132 (65), 119 (75), 91 ($[M-Bpin]^+$, 10).

Data consistent with the literature.[93]

4.3.2 Iridium-catalysed borylation of heteroarenes

4.3.2.1 Initial exploratory work

***N*-(4-Methoxybenzyl)-2-(5-(4,4,5,5-tetramethyl-1,3,2-dioxaborolan-2-yl)-thiophen-2-yl)acetamide 31b & *N*-(4-methoxybenzyl)-2-(bis-3,5-(4,4,5,5-tetramethyl-1,3,2-dioxaborolan-2-yl)-thiophen-2-yl)acetamide 31c**

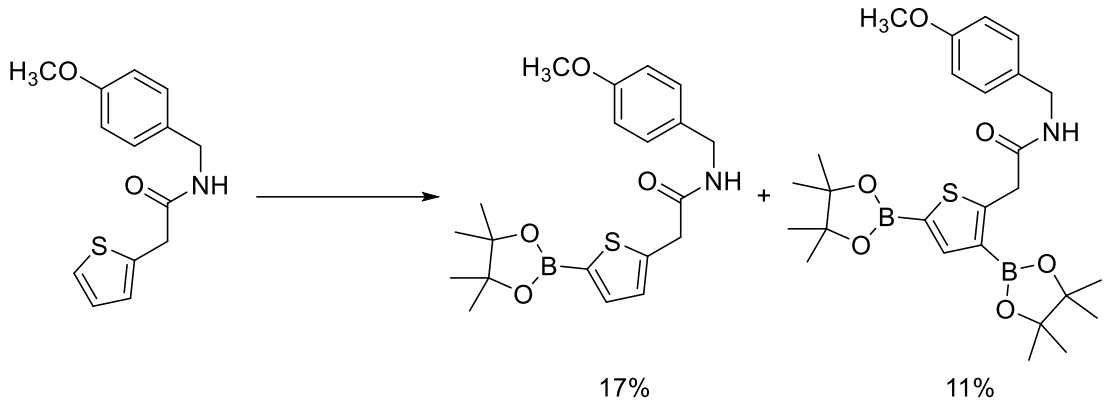

N-(4-Methoxybenzyl)-2-(thiophen-2-yl)acetamide **31a** (523 mg, 2.0 mmol, 1.0 eq.), B_2pin_2 (520 mg, 2.05 mmol, 1.0 eq.), $[Ir(COD)OMe]_2$ (20 mg, 30 µmol, 0.015 eq.) and dtbpy (16 mg, 60 µmol, 0.03 eq.) were weighed into an oven-dried reaction tube and sealed with a Teflon-lined screw cap. The tube was then evacuated and refilled with argon (three cycles) before dry THF (2 mL) was added via a syringe. The resulting mixture was stirred at 85 °C for 18 h to yield a mixture of products which were separated by flash column chromatography eluted with petroleum ether/EtOAc (100:0 – 40:60).

***N*-(4-Methoxybenzyl)-2-(5-(4,4,5,5-tetramethyl-1,3,2-dioxaborolan-2-yl)-thiophen-2-yl)acetamide 31b**

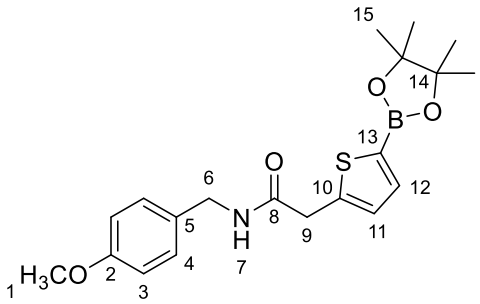

Orange oil (66 mg, 17%);

R_f 0.5 (petroleum ether/EtOAc 1:1);

δ_H (700 MHz, $CDCl_3$) 7.50 (1H, d, *J* 3.4 Hz, H-12), 7.13 (2H, d, *J* 8.6 Hz, H-3), 7.00 (1H, d, *J* 3.4 Hz, H-11), 6.83 (2H, d, *J* 8.6 Hz, H-4), 5.81 (1H, br s, H-7), 4.35 (2H, d, *J* 5.8 Hz H-6), 3.85 (2H, s, H-9), 3.78 (3H, s, H-1), 1.33 (12H, s, H-15);

δ_C (176 MHz, $CDCl_3$, C–B not visible) 169.5 (s, C-8), 159.1 (s, C-2), 143.4 (s, C-10), 137.9 (s, C-12), 130.1 (s, C-5), 129.1 (s, C-3), 129.1 (s, C-11), 114.2 (s, C-4), 84.3 (s, C-14), 55.4 (s, C-1), 43.3 (s, C-6), 37.9 (s, C-9), 24.9 (s, C-15);

δ_B (225 MHz, $CDCl_3$) 28.3;

ν_{max} (film/cm^{-1}) 3292 (N–H), 2977 (C–H), 2931 (C–H), 1647 (C=O), 1613 (Ar), 1585 (Ar), 1536 (Ar), 1512 (Ar), 1462 (Ar);

LRMS (EI) 387.2 ($[M]^{+\bullet}$, 10), 223.1 ($[M-ArCH_2NHCO]^{+\bullet}$, 10), 177.1 ($[M-ArBpin]^{+\bullet}$, 15), 146.1 (10), 121.0 ($[M-NHCOCH_2ArBpin]^{+\bullet}$, 100);

HRMS Found (EI): $[M]^{+\bullet}$ 386.1707 $[C_{20}H_{26}O_4NSB]^+$ requires 386.1706.

_N_-(4-Methoxybenzyl)-2-(bis-3,5-(4,4,5,5-tetramethyl-1,3,2-dioxaborolan-2-yl)-thiophen-2-yl)acetamide 31c

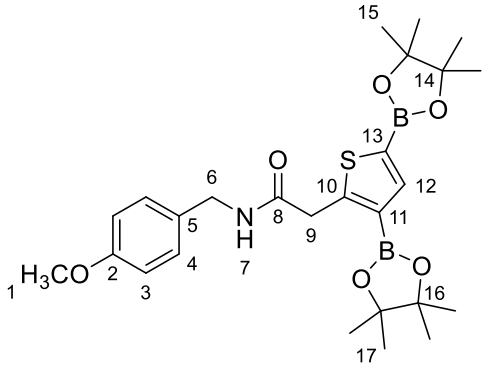

Yellow oil (56 mg, 11%);

R_f 0.7 (petroleum ether/EtOAc 1:1);

δ_H (700 MHz, $CDCl_3$) 7.86 (1H, s, H-12), 7.09 (2H, d, *J* 8.6 Hz, H-3), 6.80 (2H, d, *J* 8.6 Hz, H-4), 6.63 (1H, br s, H-7), 4.28 (2H, d, *J* 5.5 Hz, H-6), 4.03 (2H, s, H-9), 3.77 (3H, s, H-1), 1.31 (12H, s, H-15), 1.17 (12H, s, H-17);

δ_C (176 MHz, $CDCl_3$, C–B not visible) 169.7 (s, C-8), 159.1 (s, C-2), 155.7 (s, C-10), 144.7 (s, C-6), 130.4 (s, C-5), 129.2 (s, C-3), 114.4 (s, C-4), 84.2 (s, C-14), 84.0 (s, C-16), 55.5 (s, C-1), 43.3 (s, C-6), 38.7 (s, C-9), 24.9 (s, C-15), 24.8 (s, C-17);

δ_B (225 MHz, $CDCl_3$) 28.4;

ν_{max} (film/cm^{-1}) 3344 (N–H), 2977 (C–H), 2932 (C–H), 1660 (C=O), 1536 (Ar), 1513 (Ar), 1462 (Ar);

LRMS (EI) 513.3 ([M]$^{+\bullet}$, 30), 349.2 ([M−ArCH_2NHCO]$^{+\bullet}$, 15), 329.1 (15), 177.1 ([M−Ar(Bpin)$_2$]$^{+\bullet}$, 10), 136.0 ([M−COCH_2Ar(Bpin)$_2$]$^{+\bullet}$, 15), 121.0 ([M−NHCOCH_2Ar(Bpin)$_2$]$^{+\bullet}$, 100), 83.0 (20);

HRMS Found (EI): [M]$^{+\bullet}$ 511.2596 [$C_{26}H_{37}O_6NB_2S$]$^+$ requires 511.2595.

***N*-(4-Methoxybenzyl)-2-(5-(*p*-tolyl)thiophen-2-yl)acetamide 31d**, **2-(3,5-di-*p*-tolylthiophen-2-yl)-*N*-(4-methoxybenzyl)acetamide 31e** & ***N*-(4-methoxybenzyl)-2-(3-(4,4,5,5-tetramethyl-1,3,2-dioxaborolan-2-yl)-5-(*p*-tolyl)thiophen-2-yl)acetamide 31f**

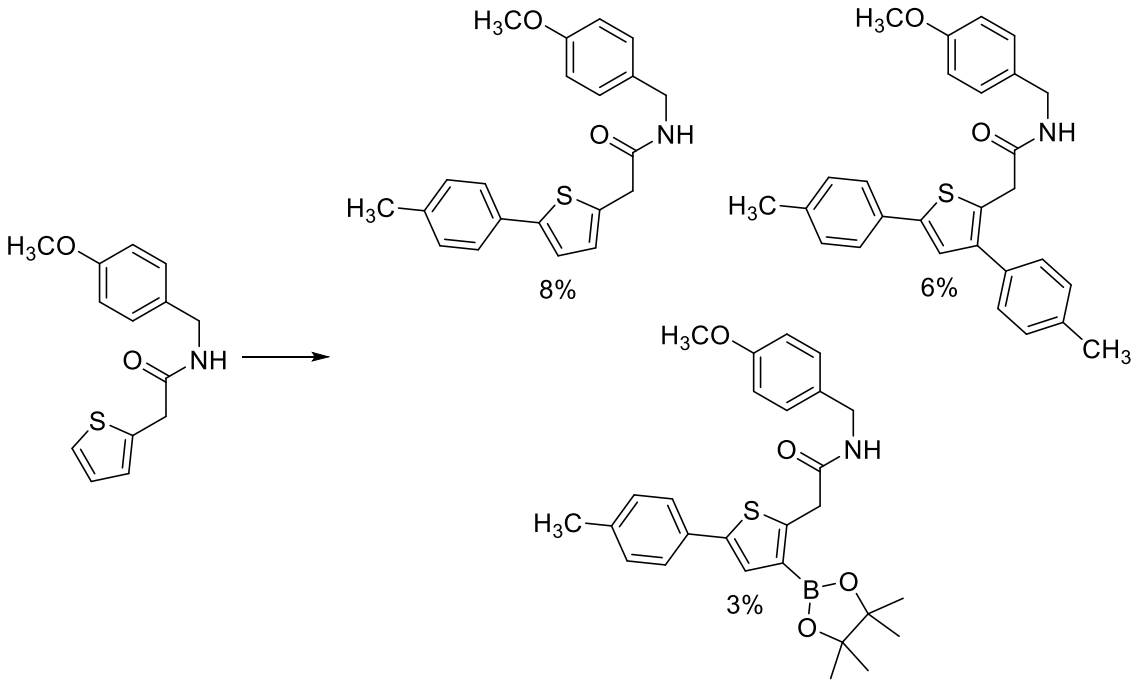

N-(4-Methoxybenzyl)-2-(thiophen-2-yl)acetamide **31a** (523 mg, 2.0 mmol, 1.0 eq.), B_2pin_2 (530 mg, 2.1 mmol, 1.05 eq.), [Ir(COD)OMe]$_2$ (20 mg, 30 µmol, 0.015 eq.) and dtbpy (16 mg, 60 µmol, 0.03 eq.) were weighed into an oven-dried reaction tube and sealed with a Teflon-lined screw cap. The tube was then evacuated and refilled with argon (three cycles) before dry THF (10 mL) was added via a syringe. The resulting mixture was stirred at 50 °C for 18 h. Then, the reaction tube was charged with 4-iodotoluene (436 mg, 2.0 mmol, 1.0 eq.), $Pd(OAc)_2$ (13 mg, 60 µmol, 0.03 eq.) and

2 M aq Na_2CO_3 (1 mL). The reaction tube was then purged with argon and resealed before being stirred at 50 °C for a further 18 h. Afterwards, the reaction was cooled and concentrated down to leave an orange residue. The crude material was purified by silica gel column chromatography eluted with cyclohexane/EtOAc (90:10 – 50:50) to give a mixture of products.

_N_-(4-Methoxybenzyl)-2-(5-(_p_-tolyl)thiophen-2-yl)acetamide 31d

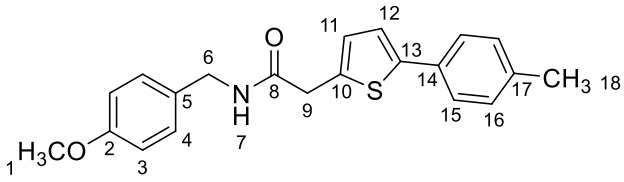

White solid (58 mg, 8%);

R_f 0.5 (cyclohexane/EtOAc 1:1);

m.p. 161 – 162 °C;

δ_H (700 MHz, $CDCl_3$) 7.44 (2H, d, *J* 8.3 Hz, H-15), 7.17 (2H, d, *J* 8.3 Hz, H-16), 7.15 (2H, d, *J* 8.6 Hz, H-4), 7.11 (1H, d, *J* 3.6 Hz, H-12), 6.87 (1H, d, *J* 3.6 Hz, H-11), 6.83 (2H, d, *J* 8.6 Hz, H-3), 5.91 (1H, br s, H-7), 4.38 (2H, d, *J* 5.8 Hz, H-6), 3.80 (2H, s, H-9), 3.78 (3H, s, H-1), 2.36 (3H, s, H-18);

δ_C (176 MHz, $CDCl_3$) 169.6 (s, C-8), 159.2 (s, C-2), 145.0 (s, C-13), 137.7 (s, C-17), 135.0 (s, C-10), 131.4 (s, C-14), 130.2 (s, C-5), 129.7 (s, C-16), 129.1 (s, C-4), 128.5 (s, C-11), 125.7 (s, C-15), 122.8 (s, C-12), 114.2 (s, C-3), 55.4 (s, C-1), 43.4 (s, C-6), 38.1 (s, C-9), 21.3 (s, C-18);

ν_{max} (film/cm^{-1}) 3287 (N–H), 2923 (C–H), 2854 (C–H), 1639vs (C=O), 1612 (Ar), 1548 (Ar), 1513 (Ar), 1467 (Ar), 1252 (H_2C–H), 802 (Ar–H);

LRMS (ES+) 352.1 ($[M+H]^+$, 100), 262.1 ($[M-tol+2H]^+$, 20), 244.1 ($[M-(4\text{-}(MeO)Ph)^-]^+$, 15), 167.1 (5), 149.1 (15), 135.1 (35), 121.1 ($[4\text{-}(MeO)PhCH_2]^+$, 75), 107.0 ($[4\text{-}(OMe)Ph]^+$, 35);

HRMS Found (ES+): $[M+H]^+$ 352.1366 $[C_{21}H_{21}O_2NS+H]^+$, requires 352.1366.

2-(3,5-Di-*p*-tolylthiophen-2-yl)-*N*-(4-methoxybenzyl)acetamide 31e

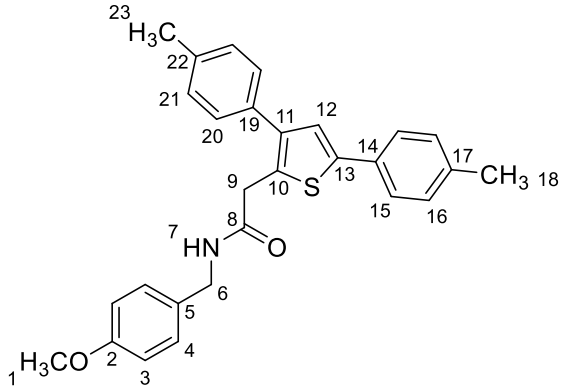

Yellow/brown solid (19 mg, 6%);

R_f 0.2 (cyclohexane/EtOAc 9:1);

m.p. 152 – 154 °C;

δ_H (700 MHz, $CDCl_3$) 7.47 (2H, d, *J* 7.9 Hz, H-15), 7.23 (2H, d, *J* 7.8 Hz, H-20), 7.21 (1H, s, H-12), 7.16 – 7.20 (4H, m, H-16 & H-21), 7.09 (2H, d, *J* 8.5 Hz, H-4), 6.81 (2H, d, *J* 8.5 Hz, H-3), 5.90 (1H, br s, H-7), 4.35 (2H, d, *J* 5.8 Hz, H-6), 3.81 (2H, s, H-9), 3.78 (3H, s, H-1), 2.38 (3H, s, H-23), 2.36 (3H, s, H-18);

δ_C (176 MHz, $CDCl_3$) 169.8 (s, C-8), 159.1 (s, C-2), 143.1 (s, C-13), 142.4 (s, C-11), 137.8 (s, C-17), 137.5 (s, C-22), 133.0 (s, C-19), 131.2 (s, C-14), 130.1 (s, C-5) 129.8 (s, C-21), 129.6 (s, C-16), 129.1 (s, C-4), 128.9 (s, C-10), 128.4 (s, C-20), 125.7 (s, C-15), 125.1 (s, C-12), 114.2 (s, C-3), 55.4 (s, C-1), 43.3 (s, C-6), 36.5 (s, C-9), 21.3 (s, C-18 & C-23);

ν_{max} (film/cm^{-1}) 3284 (N–H), 2919 (C–H), 2851 (C–H), 1646 (C=O), 1544 (Ar), 1512 (Ar), 1247 (H_2C–H), 809 (Ar–H);

LRMS (ES+) 442.2 ($[M+H]^+$, 100), 269.2 (10), 199.2 (10), 158.2 (10), 131.1 (55);

HRMS Found (ES+): $[M+H]^+$ 442.1832 $[C_{28}H_{27}NO_2S+H]^+$ requires 442.1835.

_N_-(4-Methoxybenzyl)-2-(3-(4,4,5,5-tetramethyl-1,3,2-dioxaborolan-2-yl)-5-(_p_-tolyl)thiophen-2-yl)acetamide 31f

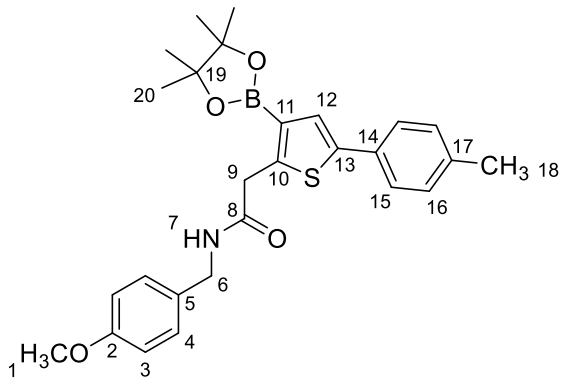

Red/brown oil (27 mg, 3%);

R_f 0.4 (cyclohexane/EtOAc 7:3);

δ_H (700 MHz, $CDCl_3$) 7.47 (2H, d, *J* 8.1 Hz, H-15), 7.41 (1H, s, H-12), 7.15 (2H, d, *J* 8.0 Hz, H-16), 7.12 (2H, d, *J* 8.6 Hz, H-4), 6.81 (2H, d, *J* 8.6 Hz, H-3), 6.73 (1H, br s, H-7), 4.32 (2H, d, *J* 5.5 Hz, H-6), 3.99 (2H, s, H-9), 3.76 (3H, s, H-1), 2.35 (3H, s, H-18), 1.20 (12H, s, H-20);

δ_C (176 MHz, $CDCl_3$, C–B not visible) 170.1 (s, C-8), 159.2 (s, C-2), 148.0 (s, C-10), 143.8 (s, C-13), 137.4 (s, C-17), 131.3 (s, C-14), 130.5 (s, C-5), 129.6 (s, C-16), 129.3 (s, C-4), 128.4 (s, C-12), 125.9 (s, C-15), 114.2 (s, C-3), 84.1 (s, C-19), 55.4 (s, C-1), 43.4 (s, C-6), 38.7 (s, C-9), 24.8 (s, C-20), 21.3 (s, C-18);

δ_B (225 MHz, $CDCl_3$) 28.9;

ν_{max} (film/cm^{-1}) 3338 (N–H), 2977 (C–H), 2929 (C–H), 1658 (C=O), 1613 (Ar), 1546 (Ar), 1513vs (Ar), 1464 (Ar), 1387 (Ar), 1249 (ArO–CH_3);

LRMS (ES+) 478.2 ($[M+H]^+$, 100), 388.2 ($[M-tol+2H]^+$, 25), 352.1 ($[M-Bpin+2H]^+$, 35), 269.2 (15), 232.1 (25), 137.1 ($[CH_3OC_6H_4CH_2NH_2]^+$, 5), 121.1 ($[CH_3OC_6H_4CH_2]^+$, 30);

HRMS Found (ES+): $[M+H]^+$ 477.2254 $[C_{27}H_{32}BNO_4S+H]^+$ requires 477.2254.

***N*-(4-Methoxybenzyl)-2-(furan-2-yl)acetamide 32a**

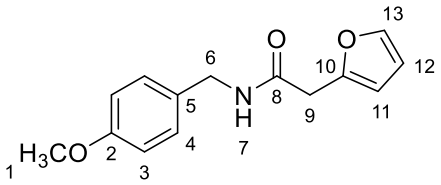

Prepared according to **General Procedure A** from furan-2-acetic acid (631 mg, 5.0 mmol, 1.0 eq.) and 4-methoxybenzylamine (650 µL, 5.0 mmol, 1.0 eq.) for 18 h. After heating, the reaction was diluted two-fold by transferring solvent from the Dean-Stark side-arm trap before being allowed to cool. Amide **32a** then spontaneously crystallised out as a pale yellow solid (1.18 g, 96%);

m.p. 109 – 110 °C;

δ_H (600 MHz, $CDCl_3$) 7.36 (1H, dd, *J* 1.9 Hz, 0.8 Hz, H-13), 7.15 (2H, d, *J* 8.8 Hz, H-3), 6.84 (2H, d, *J* 8.8 Hz, H-4), 6.34 (1H, dd, *J* 3.2 Hz, 1.9 Hz, H-12), 6.22 (1H, dd, *J* 3.2 Hz, 0.8 Hz, H-11), 5.90 (1H, br s, H-7), 4.36 (2H, d, *J* 5.7 Hz, H-6), 3.78 (3H, s, H-1), 3.65 (2H, s, H-9);

δ_C (150 MHz, $CDCl_3$) 168.5 (s, C-8), 159.1 (s, C-2), 148.8 (s, C-10), 142.7 (s, C-13), 130.2 (s, C-6), 129.1 (s, C-3), 114.2 (s, C-4), 111.0 (s, C-12), 108.8 (s, C-11), 55.4 (s, C-1), 43.3 (s, C-6), 36.5 (s, C-9);

ν_{max} (film/cm^{-1}) 3286 (N–H), 2933 (C−H), 2836 (C–H), 1641 (C=O), 1612 (Ar–H), 1586 (Ar–H), 1547 (Ar–H), 1512 (Ar–H);

LRMS (ES+) 491.2 ($[2M+H]^+$, 40), 383.2 (100), 268.1 ($[M+Na]^+$, 25), 246.1 ($[M+H]^+$, 20);

HRMS Found (ES+): $[M+H]^+$ 246.1134 $[C_{14}H_{15}O_2N+H]^+$ requires 246.1130.

_N_-Methylpyrrol-2-oxo-2-yl acetic acid 34

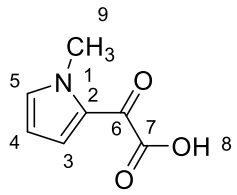

This method is based on a procedure described by Bandichhor and colleagues.[132] A solution of oxalyl chloride (7.84 g, 62 mmol, 1.0 eq.) in CH_2Cl_2 (25 mL) was cooled to −10 °C in a brine/ice bath before a solution of *N*-methylpyrrole (5.00 g, 62 mmol, 1.0 eq.) in CH_2Cl_2 (50 mL) was slowly added as the temperature of the mixture was raised to 0 °C. After stirring for 1 h at 0 °C, the pH was adjusted to 10 with the dropwise addition of 25% aq KOH solution at −10 to 0 °C. The reaction mixture was then stirred for a further 30 min and the layers were separated. The aqueous layer was then washed with CH_2Cl_2 (25 mL) before dil H_2SO_4 was added until the pH had been adjusted to *ca*. 1 – 2. After stirring for a further 30 min, the solid was filtered, washed with chilled water and dried under reduced pressure to give **34** (8.50 g, 90%) as a black solid which required no further purification;

m.p. Accurate melting point analysis was not possible due to product decomposition.

δ_H (700 MHz, $CDCl_3$, COOH not visible) 8.05 (1H, dd, *J* 4.4 Hz, 1.6 Hz, H-5), 7.10 (1H, t, *J* 1.6 Hz, H-4), 6.28 (1H, dd, *J* 4.4 Hz, 2.3 Hz, H-3), 3.99 (3H, s, H-9);

δ_C (176 MHz, $CDCl_3$) 170.5, (s, C-7), 160.3 (s, C-6) 136.7 (s, C-5), 129.0 (s, C-3), 126.7 (s, C-2), 111.2 (s, C-4), 38.3 (s, C-9);

LRMS (ESI) 198.0 ($[M+2Na-H]^+$, 5), 192.0 ($[M+K]^+$, 10), 190.1 (35), 176.0 ($[M+Na]^+$, 100), 168.1 (40), 154.1 ($[M+H]^+$, 55), 140.1 (10), 108.1 ($[M-COOH]^+$, 50);

Data consistent with the literature.[132]

_N_-Methylpyrrole-2-yl acetic acid 35

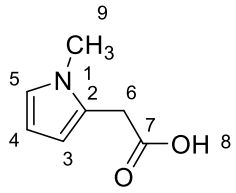

This method is based on a procedure by Bandichhor and colleagues.[132] A round-bottomed flask was loaded with *N*-methylpyrrole-2-oxo-2-yl acetic acid (8.00 g, 52.2 mmol, 1.0 eq.) and hydrazine hydrate (4.19 mL, 86.2 mmol, 1.7 eq.) before 20% aq KOH solution (90 mL) was added slowly and the mixture heated to reflux. After refluxing for 5 h, the mixture was cooled to room temperature and 36% HCl was added dropwise until the reaction mass was pH 2. The reaction mixture was then extracted with CH_2Cl_2 (4 × 100 mL) and the combined organic fractions were washed with water (50 mL), dried ($MgSO_4$), filtered and then concentrated under reduced pressure to give crude **35** as a black viscous liquid. The compound was not purified but confirmatory analysis *via* ^{1}H NMR indicated that it was appropriate to proceed to the next step;

δ_H (700 MHz, $CDCl_3$) 6.61 (1H, m, H-5), 6.07 – 6.09 (2H, m, H-3 & H-4), 3.67 (2H, s, H-6), 3.58 (3H, s, H-9);

Data consistent with the literature.[132]

_N_-(4-Methoxybenzyl)-2-(_N_-methylpyrrol-2-yl)acetamide 33a

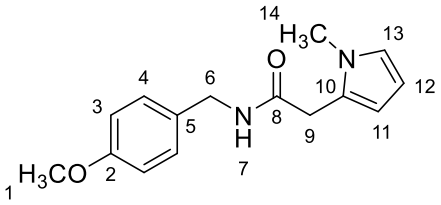

Prepared according to **General Procedure A** from a crude sample of *N*-methylpyrrole-2-yl acetic acid and 4-methoxybenzylamine (557 mg, 4.0 mmol) for 18 h. After heating, the reaction was diluted two-fold by transferring solvent from the Dean-Stark side-arm trap before being allowed to cool. The reaction mixture was concentrated under reduced pressure to leave a dark brown residue that was purified by flash column chromatography eluted with petroleum ether/EtOAC (90:10 – 70:30) to give **33a** as an orange solid (550 mg, 13% [yield for two steps]);

R_f 0.5 (petroleum ether/EtOAc 1:1);

m.p. 104 – 108 °C;

δ_H (700 MHz, $CDCl_3$) 7.11 (2H, d, *J* 8.7 Hz, H-4), 6.83 (2H, d, *J* 8.7 Hz, H-3), 6.60 (1H, dd, *J* 2.7 Hz, 1.9 Hz, H-13), 6.06 (1H, dd, *J* 3.5 Hz, 2.7 Hz, H-12), 6.03 (1H, dd, *J* 3.5 Hz, 1.9 Hz, H-11), 5.88 (1H, br s, H-7), 4.32 (2H, d, *J* 6.0 Hz, H-6), 3.78 (3H, s, H-1), 3.59 (2H, s, H-9), 3.49 (3H, s, H-14);

δ_C (176 MHz, $CDCl_3$) 170.1 (s, C-8), 159.1 (s, C-2), 130.5 (s, C-5), 129.0 (s, C-4), 125.8 (s, C-10), 123.3 (s, C-13), 114.2 (s, C-3), 109.5 (s, C-11), 107.5 (s, C-12), 55.4 (s, C-1), 43.0 (s, C-6), 35.0 (s, C-9), 33.9 (s, C-14);

ν_{max} (film/cm^{-1}) 3290 (N–H), 2937 (C–H), 1647 (C=O), 1511 (Ar), 1495 (Ar), 1463 (Ar);

LRMS (ES+) 539.3 ($[2M+Na]^+$, 100), 517.3 ($[2M+H]^+$, 90), 281.1 ($[M+Na]^+$, 30), 259.1 ($[M+H]^+$, 75);

HRMS Found (ES+): $[M+H]^+$ 259.1142 $[C_{15}H_{18}O_2N_2+H]^+$ requires 259.1447.

***N*-(4-Methoxybenzyl)-2-(5-(4,4,5,5-tetramethyl-1,3,2-dioxaborolan-2-yl)furan-2-yl)acetamide 32b** & **2-(3,5-bis(4,4,5,5-tetramethyl-1,3,2-dioxaborolan-2-yl)furan-2-yl)-*N*-(4-methoxybenzyl)acetamide 32c**

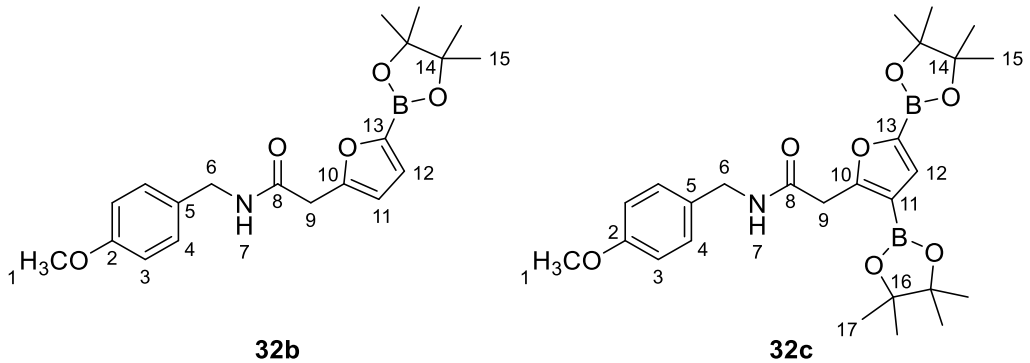

32b **32c**

(Inseparable mixture)

N-(4-Methoxybenzyl)-2-(furan-2-yl)acetamide **32a** (245 mg, 1.0 mmol, 1.0 eq.), B_2pin_2 (254 mg, 1.0 mmol, 1.0 eq.), $[Ir(COD)OMe]_2$ (10 mg, 15 µmol, 0.015 eq.) and tmphen (7 mg, 30 µmol, 0.03 eq.) were weighed into an oven-dried reaction tube and then sealed with a Teflon-lined screw cap. The tube was then evacuated and refilled with argon (three cycles) before 2 mL of dry THF was added *via* a syringe and the

mixture stirred at 85 °C for 18 h. Upon completion, the reaction mixture was concentrated leaving a residue that was purified by flash column chromatography eluted with CH_2Cl_2/MeOH (100:0 – 90:10) to give an inseparable mixture of **32b**/**32c** as an orange/yellow oil (119 mg, **32b**/**32c** 30:70; **32b** 8%, **32c** 18%);

R_f 0.5 (CH_2Cl_2/MeOH 95:5);

δ_H (700 MHz, $CDCl_3$) 7.22 (1H, s, **32c** H-12), 7.14 (2H, d, *J* 8.6 Hz, **32b** H-3), 7.11 (2H, d, *J* 8.6 Hz, **32c** H-3), 7.02 (1H, d, *J* 3.3 Hz, **32b** H-12), 6.83 (2H, d, *J* 8.6 Hz, **32b** H-4), 6.80 (2H, d, *J* 8.6 Hz, **32c** H-4), 6.40 (1H, br s, **32c** H-7), 6.29 (1H, d, *J* 3.3 Hz, **32b** H-11), 5.90 (1H, br s, **32b** H-7), 4.35 (2H, d, *J* 5.7 Hz, **32b** H-6), 4.30 (2H, d, *J* 5.5 Hz, **32c** H-6), 3.89 (3H, s, **32c** H-9), 3.77 (3H, s, **32b** H-1), 3.76 (3H, s, **32c** H-1), 3.71 (2H, s, **32b** H-9), 1.33 (12H, s, **32b** H-15), 1.31 (12H, s, **32c** H-15), 1.17 (12H, s, **32c** H-17);

δ_C (176 MHz, $CDCl_3$, C–B not visible) 168.1 (s, **32c** C-8), 168.1 (s, **32b** C-8), 163.2 (s, **32c** C-10), 159.1 (s, **32b**, C-2), 159.1 (s, **32c** C-2), 154.0 (s, **32b** C-10), 130.4 (s, **32c** C-5), 130.1 (s, **32b** C-5), 129.2 (s, **32c** C-12), 129.1 (s, **32c** C-3), 129.1 (s, **32b** C-3), 125.0 (s, **32b** C-12), 114.2 (s, **32b** C-4), 114.1 (s, **32c** C-4), 109.7 (s, **32b** C-11), 84.4 (s, **32b** C-14), 84.3 (s, **32c** C-14), 83.9 (s, **32c** C-16), 60.8 (s, **32c** C-9), 55.4 (s, **32c** C-1), 55.4 (s, **32b** C-1), 43.3 (s, **32b** C-6), 43.2 (s, **32c** C-6), 37.4 (s, **32c** C-9), 36.8 (s, **32b** C-9), 24.8 (s, **32b** C-15), 24.7 (s, **32c** C-15), 24.7 (s, **32c** C-17);

δ_B (225 MHz, $CDCl_3$) 29.0;

ν_{max} (film/cm^{-1}) 3300 (N–H), 2978 (C–H), 2933 (C–H), 1654 (C=O), 1612 (Ar), 1595 (Ar), 1531 (Ar), 1513vs (Ar), 1472 (Ar), 1454 (Ar), 1371, 1346vs, 1247vs (Ar–OCH_3), 1142vs (C–O);

HRMS **32b** Found (ES+): $[M+H]^+$ 371.2013 $[C_{20}H_{26}BNO_5+H]^+$ requires 371.2013, **32c** Found (ES+): $[M+H]^+$ 496.2904 $[C_{26}H_{37}B_2NO_7+H]^+$ requires 496.2902.

_N_-(4-Methoxybenzyl)-2-(5-(4,4,5,5-tetramethyl-1,3,2-dioxaborolan-2-yl)-_N_-methylpyrrol-2-yl)acetamide 33b & **_N_-(4-methoxybenzyl)-2-(bis-3,5-(4,4,5,5-tetramethyl-1,3,2-dioxaborolan-2-yl)-_N_-methylpyrrol-2-yl)acetamide 33c**

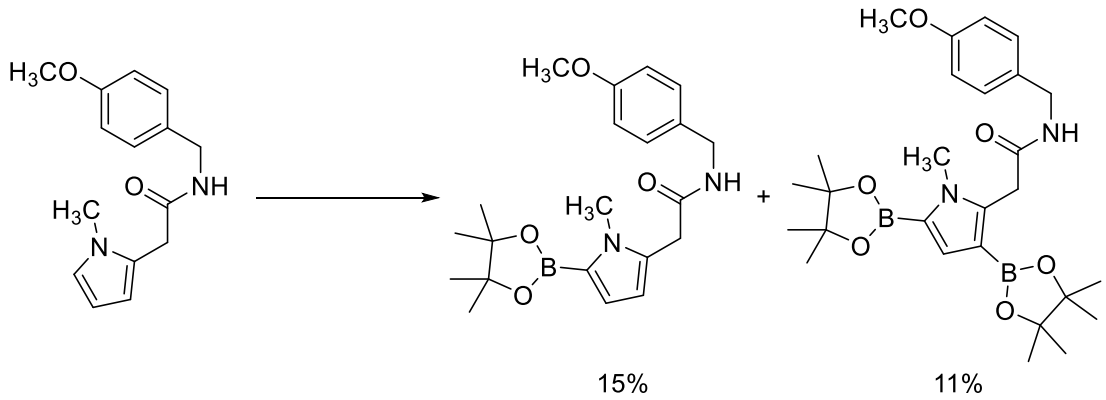

_N_-(4-Methoxybenzyl)-2-(_N_-methylpyrrol-2-yl)acetamide **33a** (258 mg, 1.0 mmol, 1.0 eq.), B_2pin_2 (254 mg, 1.0 mmol, 1.0 eq.), $[Ir(COD)OMe]_2$ (10 mg, 15 µmol, 0.015 eq.) and dtbpy (8 mg, 30 µmol, 0.03 eq.) were weighed into an oven-dried reaction tube and then sealed with a Teflon-lined screw cap. The tube was then evacuated and refilled with argon (three cycles) before 1 mL of dry THF was added *via* a syringe and the mixture stirred at 85 °C for 18 h. Upon completion, the reaction mixture was concentrated leaving a residue that was purified by flash column chromatography eluted with petroleum ether/EtOAc (95:5 – 15:85) to give a mixture of products. 39 mg (15%) **33a** was recovered from the reaction.

_N_-(4-Methoxybenzyl)-2-(5-(4,4,5,5-tetramethyl-1,3,2-dioxaborolan-2-yl)-_N_-methylpyrrol-2-yl)acetamide 33c

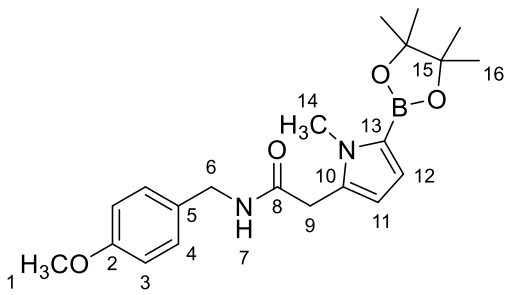

Orange/yellow oil (56 mg, 15%);

R_f 0.2 (petroleum ether/EtOAc 1:1);

δ_H (700 MHz, $CDCl_3$) 7.09 (2H, d, *J* 8.6 Hz, H-4), 7.04 (1H, d, *J* 1.7 Hz, H-12), 6.81 (2H, d, *J* 8.6 Hz, H-3), 6.34 (1H, d, *J* 1.7 Hz, H-11), 5.85 (1H, t, *J* 6.0 Hz, H-7), 4.30

(2H, d, *J* 6.0 Hz, H-6), 3.78 (3H, s, H-1), 3.58 (2H, s, H-9), 3.48 (3H, s, H-14), 1.29 (12H, s, H-16);

δ_C (176 MHz, $CDCl_3$) 169.8 (s, C-8), 159.1 (s, C-2), 132.5 (s, C-12), 130.4 (s, C-5), 129.0 (s, C-4), 127.2 (s, C-10), 115.3 (s, C-11), 114.2 (s, C-3), 108.4 (m, C-13), 83.1 (s, C-15), 55.4 (s, C-1), 43.0 (s, C-6), 35.0 (s, C-9), 34.0 (s, C-14), 24.9 (s, C-16);

δ_B (225 MHz, $CDCl_3$) 29.9;

ν_{max} (film/cm^{-1}) 3295 (N–H), 2976 (C−H), 2931 (C–H), 1650 (C=O), 1611 (Ar), 1561 (Ar), 1513vs (Ar), 1441 (Ar);

LRMS (EI) 407.2 ([M+Na]$^{+\bullet}$, 25), 385.2 ([M+H]$^{+\bullet}$, 100), 271.1 ([M−$C_6H_{12}O_2$+2H]$^{+\bullet}$, 10), 259.1 ([M−Bpin+H]$^{+\bullet}$, 40), 214.1 (15), 197.0 (10), 101.1 (10);

HRMS Found (ES+): [M+H]$^+$ 385.2296 [$C_{21}H_{29}BN_2O_4$+H]$^+$ requires 385.2299.

_N_-(4-Methoxybenzyl)-2-(5-(4,4,5,5-tetramethyl-1,3,2-dioxaborolan-2-yl)-_N_-methylpyrrol-2-yl)acetamide 33c

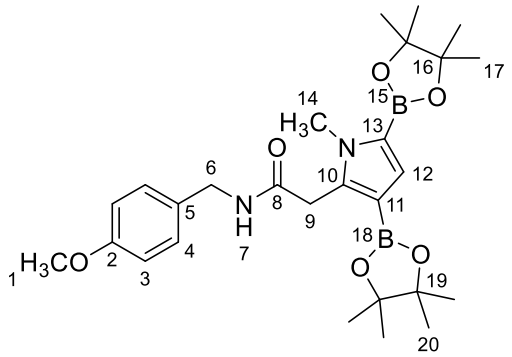

Orange/yellow oil (54 mg, 11%);

R_f 0.5 (petroleum ether/EtOAc 1:1);

δ_H (700 MHz, $CDCl_3$) 7.14 (1H, s, H-12), 7.10 (2H, d, *J* 8.8 Hz, H-4), 6.97 (1H, br s, H-7), 6.80 (2H, d, *J* 8.8 Hz, H-3), 4.26 (1H, d, *J* 5.5 Hz, H-6), 3.88 (3H, s, H-14), 3.78 (2H, s, H-9), 3.77 (3H, s, H-1), 1.28 (12H, s, H17), 1.12 (12H, s, H-20);

δ_C (176 MHz, $CDCl_3$) 169.8 (s, C-8), 159.1 (s, C-2), 141.6 (s, C-10), 130.5 (s, C-5), 129.2 (s, C-4), 128.2 (s, C-12), 126.0 – 127.1 (m, C-13), 114.1 (s, C-3),

108.1 – 108.9 (m, C-11), 83.3 (s, C-16), 83.1 (s, C-19), 55.4 (s, C-1), 43.2 (s, C-6), 35.4 (s, C-9), 33.8 (s, C-14), 24.9 (s, C-17), 24.7 (s, C-20);

δ_B (225 MHz, $CDCl_3$) 29.4 (B-15), 28.4 (B-16);

ν_{max} (film/cm^{-1}) 3326 (N–H), 2976 (C–H), 2933 (C–H), 1653 (C=O), 1513 (Ar), 1453 (Ar), 1317 (Ar), 1246 (Ar–OCH_3), 1135vs (C–O);

LRMS (EI) 1043.6 ($[2M+Na]^+$, 15), 637.4 (15), 511.3 ($[M+H]^+$, 100), 122.1 (5);

HRMS Found (ES+): $[M+H]^+$ 509.3219 $[C_{27}H_{40}B_2N_2O_6+H]^+$ requires 509.3218.

3,9-Dimethyl-1,2,3,4-tetrahydrocarbazole-4-one 40

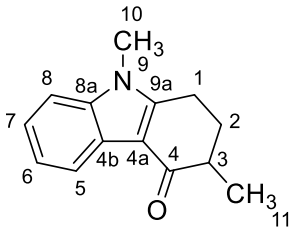

Ondansetron **39** (293 mg, 1.0 mmol, 1.0 eq.), B_2pin_2 (254 mg, 1.0 mmol, 1.0 eq.), $[Ir(COD)OMe]_2$ (10 mg, 15 µmol, 0.015 eq.) and dtbpy (8 mg, 30 µmol, 0.03 eq.) were weighed into an oven-dried reaction tube and sealed with a Teflon-lined screw cap. The tube was then evacuated and refilled with argon (three cycles) before 1 mL of dry dioxane was inserted *via* a syringe and the mixture stirred at 100 °C for 18 h. Afterwards, the crude mixture was purified by flash column chromatography eluted with petroleum ether/EtOAc (7:3) to give **40** as an orange solid (25 mg, 12%);

R_f 0.4 (petroleum ether/EtOAc 2:1);

m.p. 122 – 123 °C;

δ_H (700 MHz, $CDCl_3$) 8.24 – 8.27 (1H, m, H-5), 7.25 – 7.28 (3H, m, H-6-8), 3.66 (3H, s, H-10), 2.95 – 2.99 (1H, m, H-1), 2.87 – 2.92 (1H, m, H-1) 2.54 – 2.59 (1H, m, H-3), 2.29 – 2.33 (1H, m, H-2), 1.95 – 2.01 (1H, m, H-2) 1.28 (3H, d, *J* 7.0 Hz, H-11);

δ_C (176 MHz, $CDCl_3$) 196.5 (s, C-4), 151.4 (s, C-9a), 137.7 (s, C-8a), 125.1 (s, C-8), 123.0 (s, C-4b), 122.6 (s, C-6), 121.7 (s, C-5), 112.1 (s, C-4a), 109.2 (s, C-7), 41.2 (s, C-3), 31.4 (s, C-2), 29.8 (s, C-10), 21.5 (s, C-1), 15.5 (s, C-11);

LRMS (ES+) 662.2 ([3M+Na]$^+$, 30), 449.2 (2M+Na]$^+$, 15), 427.2 ([2M+H]$^+$, 70), 236.1 ([M+Na]$^+$, 5), 214.1 ([M+H]$^+$, 100);

Data consistent with the literature.[202]

1-Toluenesulfonyl-3-bromo-7-nitroindazole 43

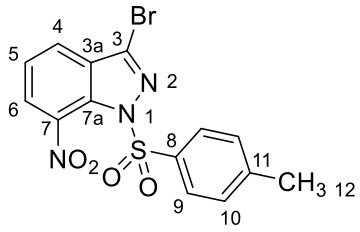

A flask was loaded with 3-bromo-7-nitro-1*H*-indazole **42** (896 mg, 3.70 mmol, 1.2 eq.), KOH (370 mg, 6.60 mmol, 2.2 eq.) and *p*-toluenesulfonyl chloride (581 mg, 3.05 mmol, 1.0 eq.). 25 mL dry THF was then inserted and the resulting mixture was stirred at 50 °C for 3 d. Afterwards, the reaction was concentrated under reduced pressure and added to 20 mL water then extracted with EtOAc (3 × 20 mL). The combined organic extracts were then washed with brine (20 mL), dried ($MgSO_4$), filtered and concentrated. The residue was then purified by column chromatography eluted with CH_2Cl_2/MeOH (100:0 – 90:10) to give **43** as a white solid (336 mg, 23%);

m.p. 147 – 149 °C;

R_f 0.6 (100% CH_2Cl_2);

δ_H (700 MHz, $CDCl_3$) 8.07 (2H, d, *J* 8.6 Hz, H-9), 7.99 (1H, dd, *J* 7.7 Hz, 1.0 Hz, H-6), 7.88 (1H, dd, *J* 8.0 Hz, 1.0 Hz, H-4), 7.51 (1H, t, *J* 7.8 Hz, H-5), 7.39 (2H, d, *J* 8.6 Hz, H-10), 2.46 (3H, s, H-12);

δ_C (176 MHz, $CDCl_3$) 146.5 (s, C-8), 138.1 (s, C-7), 134.1 (s, C-11), 131.5 (s, C-7a), 131.4 (s, C-3a), 130.0 (s, C-10), 129.3 (s, C-3), 128.7 (s, C-9), 125.9 (s, C-4), 125.8 (s, C-6), 124.7 (s, C-5), 22.0 (s, C-12);

ν_{max} (film/cm^{-1}) 3056 (C–H), 1614 (Ar), 1541 (N–O), 1376 (H_2C–H), 1358 (N–O), 1345 (N–O), 1317 (N–N), 1177 (S=O), 1057 (S=O), 531(C–Br);

LRMS (ES+) 814.9 ([2M+Na]$^+$, 50), 715.2 (5), 420.0 ([M+Na]$^+$, 25), 415.0 ([M+H_2O+H]$^+$, 85), 398.0 ([M+H]$^+$, 100), 254.2 (20), 155.0 ([Tos+H]$^+$, 30);

HRMS Found (ES+): $[M+H]^+$ 395.9653 $[C_{14}H_{10}BrN_3O_4S+H]^+$ requires 395.9648.

***m*-Xylyl-5-boronic acid pinacol ester 44b**

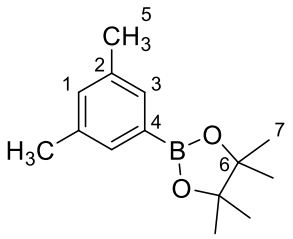

B_2pin_2 (254 mg, 1.0 mmol, 1.0 eq.), $[Ir(COD)OMe]_2$ (10 mg, 15 µmol, 0.015 eq.) and dtbpy (8 mg, 30 µmol, 0.03 eq.) were weighed into an oven-dried reaction tube and sealed with a Teflon-lined screw cap. The tube was then evacuated and refilled with nitrogen (three cycles) before dry, degassed *m*-xylene **44a** (123 µl, 1.0 mmol, 1.0 eq.) dissolved in 1 mL dry, degassed dioxane was inserted *via* a syringe and the mixture stirred at 100 °C for 18 h. Afterwards, the crude mixture was purified by flash column chromatography (SiO_2 12 g) eluted with cyclohexane/EtOAc (100:0 – 80:20) to give **44b** as a white crystalline solid (140 mg, 60%);

m.p. 98 – 100 °C;

R_f 0.6 (cyclohexane/EtOAc 95:5);

δ_H (700 MHz, $CDCl_3$) 7.44 (2H, s, H-3), 7.10 (1H, s, H-1), 2.32 (6H, s, H-5), 1.34 (12H, s, H-7);

δ_C (176 MHz, $CDCl_3$, C–B not visible) 137.3 (s, C-2), 133.1 (s, C-1), 132.5 (s, C-3), 83.8 (s, C-6), 25.0 (s, C-7), 21.3 (s, C-5);

δ_B (225 MHz, $CDCl_3$) 31.3;

LRMS (ES+) 233.2 ($[M+H]^+$, 5), 145.1 (5), 107.1 (5), 101.1 (100), 83.1 (20);

Data consistent with the literature.[203]

1-Toluenesulfonyl-3-bromoindazole 47a

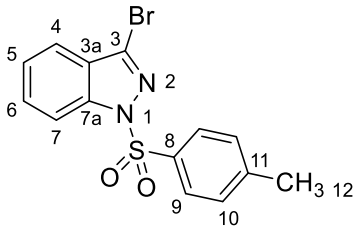

A flask was loaded with 3-bromo-1*H*-indazole **46a** (694 mg, 3.52 mmol, 1.0 eq.), KOH (378 mg, 6.74 mmol, 1.9 eq.) and *p*-toluenesulfonyl chloride (1.01 g, 5.30 mmol, 1.5 eq.). THF (15 mL) was then inserted and the resulting mixture was stirred at room temperature for 18 h. Afterwards, the reaction was concentrated under reduced pressure and added to 25 mL water then extracted with EtOAc (3 × 25 mL). The combined organic extracts were then washed with brine (20 mL), dried ($MgSO_4$) and filtered. The residue was then purified by silica gel column chromatography eluted with petroleum ether/EtOAc (100:0 – 90:10) to give **47a** as a colourless crystalline solid (1.07 g, 86%);

m.p. 124 – 126 °C;

R_f 0.3 (petroleum ether/EtOAc 95:5);

δ_H (700 MHz, $CDCl_3$) 8.18 (1H, dd, *J* 8.4 Hz, 0.8 Hz, H-4), 7.86 (2H, d, *J* 8.6 Hz, H-9), 7.60 (1H, ddd, *J* 8.4 Hz, 7.1 Hz, 1.1 Hz, H-5), 7.56 (1H, dd, *J* 8.2 Hz, 1.1 Hz, H-7), 7.37 (1H, ddd, *J* 8.2 Hz, 7.1 Hz, 0.8 Hz, H-6), 7.24 (2H, d, *J* 8.6 Hz, H-10), 2.34 (3H, s, H-12);

δ_C (176 MHz, $CDCl_3$) 146.0 (s, C-8), 141.1 (s, C-3), 134.2 (s, C-11), 131.5 (s, C-3a), 130.6 (s, C-5), 130.1 (s, C-10), 127.8 (s, C-9), 126.1 (s, C-7a), 125.0 (s, C-6), 121.0 (s, C-7), 113.5 (s, C-4), 21.8 (s, C-12);

LRMS (ES+) 726.9 ($[2M+Na]^+$, 15), 353.0 ($[M+H]^+$, 100);

Data consistent with the literature.[204]

tert-Butyl 3-bromo-1*H*-indazole-1-carboxylate 48a

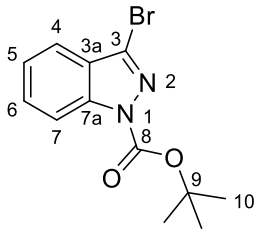

3-Bromo-1*H*-indazole **46a** (500 mg, 2.54 mmol, 1.0 eq.), di-*tert*-butyl dicarbonate (609 mg, 2.79 mmol, 1.1 eq.) and DMAP (31 mg, 250 µmol, 0.1 eq.) were dissolved in 10 mL dry THF and stirred at room temperature for 18 h. Afterwards, the reaction was diluted with water (10 mL) and extracted with EtOAc (3 × 10 mL). Combined organic extracts were washed with water (10 mL) and brine (10 mL) then dried ($MgSO_4$) and filtered. The filtrate was concentrated to leave a solid residue that was purified by flash column chromatography (SiO_2 12 g) eluted with cyclohexane/EtOAc (90:10 – 60:40) to deliver **48a** as a yellow oil (536 mg, 71%);

R_f 0.2 (100% cyclohexane);

δ_H (700 MHz, $CDCl_3$) 8.15 (1H, d, *J* 8.5 Hz, H-7), 7.63 (1H, dt, *J* 8.0 Hz, 1.1 Hz, H-4), 7.58 (1H, ddd, *J* 8.5 Hz, 7.1 Hz, 1.1 Hz, H-6), 7.37 (1H, dd, 8.0 Hz, 7.1 Hz, H-5), 1.72 (9H, s, H-10);

δ_C (176 MHz, $CDCl_3$) 148.6 (s, C-8), 140.5 (s, C-3a), 130.2 (s, C-6), 130.0 (s, C-3), 126.1 (s, C-7a), 124.4 (s, C-5), 120.8 (s, C-4), 114.9 (s, C-7), 85.7 (s, C-9), 28.3 (s, C-10);

ν_{max} (film/cm^{-1}) 2979 (C–H), 2933 (C–H), 1737 (C=O), 1492 (Ar), 1465 (H_2C–H), 1368 (H_2C–H), 1336 (C–H), 1239 (C–N), 1147, 1053, 972, 909 (Ar–H), 843 (Ar–H), 728vs (C–Br);

LRMS (ES+) 595.0 ($[2M+H]^+$, 10), 495.0 (15), 299.0 ($[M+H]^+$, 60), 297.0 ($[M+H]^+$, 60), 255.0 (15), 253.0 (15), 243.0 ($[M-{}^tBu+2H]^+$, 100), 241.0 ($[M-{}^tBu+2H]^+$ 100), 199.0 ($[M-Boc]^+$, 25), 197.0 $(M-Boc]^+$, 25), 118.0 ($[Boc+OH]^+$, 5);

HRMS Found (ES+): $[M+H]^+$ 297.0233 $[C_{12}H_{15}O_2N_2Br+H]^+$ requires 297.0244.

4.3.2.2 Investigation into the borylation of 4-substituted quinolines

Ethyl quinoline-4-carboxylate 51a

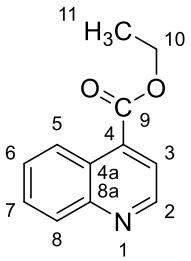

A round-bottomed flask was loaded with quinoline-4-carboxylic acid **53a** (1.00 g, 5.77 mmol), ethanol (75 mL) and *ca*. 500 µL conc H_2SO_4. The mixture was then heated to reflux and left to stir for 2 d. Afterwards, the reaction was left to cool and aq $NaHCO_3$ was added until the mixture was pH 7. The mixture was concentrated on the rotary evaporator and 25 mL water was added to the resulting residue. This was then extracted with EtOAc (3 × 25 mL), washed with brine, dried ($MgSO_4$), filtered and concentrated under reduced pressure to leave an oil. The residue was then purified by flash column chromatography eluted with petroleum ether/EtOAc (90:10 – 80:20) to give **51a** as an orange/yellow oil (800 mg, 69%);

R_f 0.4 (petroleum ether/EtOAc 8:2);

δ_H (600 MHz, $CDCl_3$) 8.98 (1H, d, *J* 4.4 Hz, H-2), 8.73 (1H, dd, *J* 8.5 Hz, 1.2 Hz, H-5), 8.14 (1H, d, *J* 8.5 Hz, H-8), 7.85 (1H, d, *J* 4.4 Hz, H-3), 7.72 (1H, ddd, *J* 8.4 Hz, 6.8 Hz, 1.4 Hz, H-7), 7.61 (1H, ddd, *J* 8.5 Hz, 6.8 Hz, 1.3 Hz, H-6), 4.47 (2H, q, *J* 7.2 Hz, H-10), 1.43 (3H, t, *J* 7.2 Hz, H-11);

δ_C (150 MHz, $CDCl_3$) 166.3 (s, C-9), 149.9 (s, C-2), 149.2 (s, C-8a), 135.3 (s, C-4a), 130.2 (s, C-8), 129.8 (s, C-7), 128.2 (s, C-6), 125.7 (s, C-5), 125.2 (s, C-4), 122.2 (s, C-3), 61.9 (s, C-10), 14.4 (s, C-11);

LRMS (ESI) 202.1 ($[M+H]^+$, 100);

Data consistent with the literature.[205]

***N*-[(4-Methoxyphenyl)methyl]quinoline-4-carboxamide 52a**

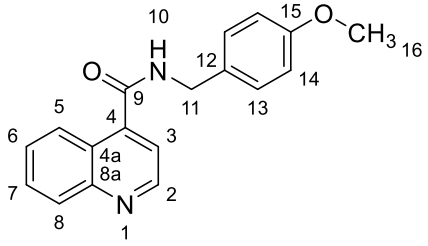

Prepared according to **General Procedure A** from quinoline-4-carboxylic acid **53a** (1.00 g, 5.77 mmol) and 4-methoxybenzylamine (790 µL, 6.1 mmol, 1.1 eq.). TAME (100 mL) was used as solvent and the reaction was stirred at reflux for 6 d. Upon cooling, an off-white precipitate crystallised out that was filtered and then washed with petroleum ether/diethyl ether (1:1). The resulting solid was isolated by Buchner filtration to give the desired product **52a** as an off-white solid (1.59 g, 92%);

R_f 0.3 (CH_2Cl_2/MeOH 3:1);

m.p. 141 – 143 °C;

δ_H (700 MHz, $CDCl_3$) 8.77 (1H, d, *J* 4.3 Hz, H-2), 8.44 (1H, d, *J* 8.4 Hz, H-8), 8.11 (1H, d, *J* 8.4 Hz, H-5), 7.68 (1H, td, *J* 7.1 Hz, 1.1 Hz, H-7), 7.42 (1H, t, *J* 7.1 Hz, H-6), 7.32 (1H, d, *J* 4.3 Hz, H-3), 6.94 (2H, d, *J* 8.5 Hz, H-14), 6.47 (2H, d, *J* 8.5 Hz, H-13), 3.74 (2H, s, H-11), 3.63 (3H, s, H-16);

δ_C (176 MHz, $CDCl_3$) 173.8 (s, C-9), 159.8 (s, C-15), 150.1 (s, C-2), 148.9 (s, C-8a), 144.1 (s, C-4a), 130.0 (s, C-14), 129.8 (s, C-5), 129.4 (s, C-7), 127.1 (s, C-6), 126.5 (s, C-8), 125.5 (s, C-12), 125.4 (s, C-4), 120.1 (s, C-3), 114.3 (s, C-13), 55.3 (s, C-16), 43.2 (s, C-11);

ν_{max} (film/cm^{-1}) 3587 (N–H), 2933 (C–H), 2640, 1612 (C=O), 1594 (Ar);

LRMS (ES+) 293.1 ($[M+H]^+$, 2);

HRMS Found (ES+): $[M+H]^+$ 293.1293 $[C_{18}H_{16}N_2O_2+H]^+$ requires 293.1290.

4-Chloroquinoline 55a

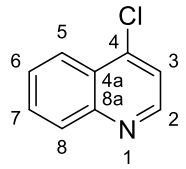

This method is based on a procedure by García-Mancheño and colleagues.[140] 4-Quinolinol **54a** (2.50 g, 17.2 mmol, 1.0 eq.) and $POCl_3$ (6.44 mL, 68.9 mmol, 4.0 eq.) were added to an oven-dried round-bottomed flask and the mixture was refluxed for 1 h. The reaction was allowed to cool before being transferred very slowly to 100 mL of cold water immersed in an ice bath. The mixture was then raised to pH 13 with the addition of NaOH pellets whilst still in an ice bath at 0 °C. It was then extracted with CH_2Cl_2 (3 × 50 mL), dried ($MgSO_4$), filtered and concentrated under reduced pressure to give **55a** (1.99 g, 71%) as an orange/brown oil which required no further purification;

δ_H (700 MHz, $CDCl_3$) 8.76 (1H, d, *J* 4.7 Hz, H-2), 8.21 (1H, dd, *J* 8.4 Hz, 1.3 Hz, H-8), 8.11 (1H, d, *J* 8.4 Hz, H-5), 7.75 (1H, dd, *J* 8.4 Hz, 6.9 Hz, H-7), 7.62 (1H, ddd, *J* 8.4 Hz, 6.9 Hz, 1.3 Hz, H-6), 7.47 (1H, d, *J* 4.7 Hz, H-3);

δ_C (176 MHz, $CDCl_3$) 150.0 (s, C-2), 149.3 (s, C-8a), 142.8 (s, C-4), 130.5 (s, C-7), 130.0 (s, C-5), 127.7 (s, C-6), 126.6 (s, C-4a), 124.3 (s, C-8), 121.4 (s, C-3);

LRMS (ESI) 164.0 ($[M+H]^+$, 100);

Data consistent with the literature.[140]

4-Methoxyquinoline 50a

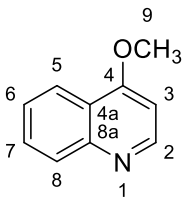

This method is a modified version of a procedure described by García-Mancheño and colleagues.[140] Methanol (100 mL) was added to an oven-dried three-necked round-bottomed flask and cooled to 0 °C in an ice-water bath. Whilst stirring, sodium (1.13 g, 49.2 mmol, 8.0 eq.) was added slowly in small portions over 30 min. Once

dissolved, 4-chloroquinoline **55a** (1.00 g, 6.11 mmol, 1.0 eq.) was added *via* a syringe and the mixture was heated to reflux and left to stir for 3 d. Afterwards, the reaction was left to cool then concentrated under reduced pressure to leave a yellow/brown residue. This was then dissolved in 25 mL water and extracted into CH_2Cl_2 (3 × 25 mL). The organic extracts were combined, dried ($MgSO_4$), filtered and concentrated under reduced pressure to leave an oil which was purified by flash column chromatography eluted with hexane/EtOAc (7:3) to provide **50a** as a yellow oil (515 mg, 52%);

R_f 0.3 (hexane/EtOAc 1:1);

δ_H (600 MHz, $CDCl_3$) 8.74 (1H, d, *J* 5.2 Hz, H-2), 8.19 (1H, ddd, *J* 8.4 Hz, 1.4 Hz, 0.4 Hz, H-5), 8.02 (1H, d, *J* 8.5 Hz, H-8), 7.68 (1H, ddd, *J* 8.5 Hz, 6.9 Hz, 1.4 Hz, H-7), 7.49 (1H, ddd, *J* 8.4 Hz, 6.9 Hz, 1.2 Hz, H-6), 6.72 (1H, d, *J* 5.2 Hz, H-3), 4.03 (3H, s, H-9);

δ_C (150 MHz, $CDCl_3$) 162.4 (s, C-4), 151.5 (s, C-2), 149.3 (s, C-8a), 129.9 (s, C-7), 129.0 (s, C-8), 125.7 (s, C-6), 121.9 (s, C-5), 121.5 (s, C-4a), 100.2 (s, C-3), 55.8 (s, C-9);

LRMS (ESI) 160.1 ($[M+H]^+$, 100), 145.1 ($[M-CH_3+H]^+$, 5);

Data consistent with the literature.[140]

4-Methyl-6-(4,4,5,5-tetramethyl-1,3,2-dioxaborolan-2-yl)quinoline 49b, **4-methyl-7-(4,4,5,5-tetramethyl-1,3,2-dioxaborolan-2-yl)quinoline 49c**, **4-methyl-1,2,3,4-tetrahydroquinoline 49d**, **4-methyl-6-(4,4,5,5-tetramethyl-1,3,2-dioxaborolan-2-yl)-1,2,3,4-tetrahydroquinoline 49e** & **4-methyl-7-(4,4,5,5-tetramethyl-1,3,2-dioxaborolan-2-yl)-1,2,3,4-tetrahydroquinoline 49f**

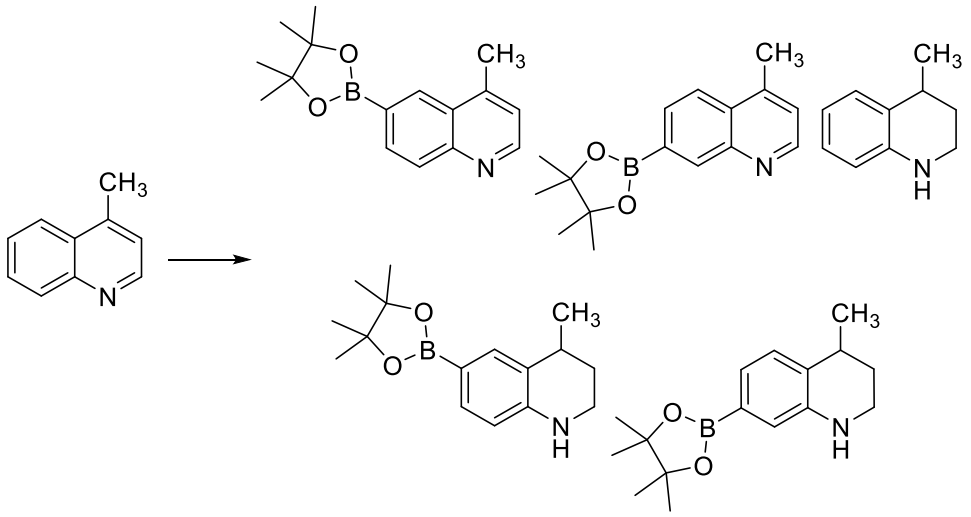

General Procedure B was followed with 4-methylquinoline **49a** (286 mg, 2.0 mmol) as the substrate. The reaction gave a mixture of products which were purified by column chromatography (petroleum ether/EtOAc 100:0 – 50:50).

4-Methyl-6-(4,4,5,5-tetramethyl-1,3,2-dioxaborolan-2-yl)-quinoline 49b & **4-methyl-7-(4,4,5,5-tetramethyl-1,3,2-dioxaborolan-2-yl)-quinoline 49c**

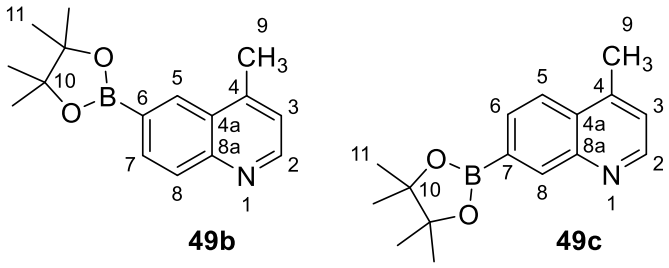

49b **49c**

(Inseparable mixture)

Yellow oil (178 mg, 33%, **49b**/**49c** 1.3:1);

R_f 0.2 (petroleum ether/EtOAc 8:2);

δ_H (700 MHz, $CDCl_3$) 8.78 (1H, d, *J* 4.2 Hz, **49b** & **49c** H-2), 8.59 (1H, s, **49b** H-8), 8.49 (1H, s, **49b** H-5), 8.06 (1H, d, *J* 8.5 Hz, **49b** H-8), 8.04 (1H, d, *J* 8.5 Hz,

49b H-7), 7.95 (1H, d, *J* 8.3 Hz, **49c** H-5), 7.90 (1H, d, *J* 8.3 Hz, **49c** H-6), 7.23 (1H, d, *J* 4.2 Hz, **49b** & **49c** H-3), 2.76 (3H, s, **49b** CH_3), 2.69 (3H, s, **49c** H-9), 1.39 (12H, s, **49b** H-11), 1.38 (12H, s, **49c** H-11);

δ_C (176 MHz, $CDCl_3$, C–B not visible) 151.1 (s, **49b** C-2), 150.2 (s, **49c** C-2), 149.5 (s, **49b** C-8a), 147.4 (s, **49c** C-8a**)** 145.5 (s, **49b** C-4), 144.3 (s, **49c** C-4) 138.0 (s, **49b** C-8), 134.2 (s, **49b** C-7), 132.1 (s, **49b** C-5), 131.1 (s, **49c** C-6), 130.1 (s, **49c** C-4a), 129.0 (s, **49b** C-8), 127.8 (s, **49b** C-4a), 123.1 (s, **49c** C-5), 122.7 (s, **49c** C-3), 122.1 (s, **49b** C-3), 84.3 (s, **49b** C-10), 84.2 (s, **49c** C-10), 25.0 (s, **49b** C-11), 25.0 (s, **49c** C-11), 19.0 (s, **49b** C-9), 18.8 (s, **49c** C-9);

δ_B (225 MHz, $CDCl_3$) 30.7 (**49b** and **49c**);

ν_{max} (film/cm^{-1}) 2977 (C–H), 2927 (C–H), 1618 (Ar);

LRMS (ES+) 411.3 ($[M+M-Bpin+H]^+$, 10), 410.3 ($[M+M-Bpin]^+$, 30), 270.2 ($[M+H]^+$, 100), 144.1 ($[M-Bpin+H]^+$, 15);

HRMS Found (ES+): $[M+H]^+$ 270.1669 $[C_{16}H_{20}NO_2B+H]^+$ requires 270.1665.

4-Methyl-1,2,3,4-tetrahydroquinoline 49d

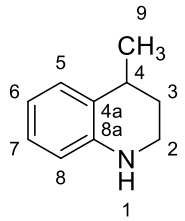

Yellow oil (14 mg, 5%);

R_f 0.3 (petroleum ether/EtOAc 95:5);

δ_H (700 MHz, $CDCl_3$) 7.06 (1H, d, *J* 7.7 Hz, H-5), 6.97 (1H, t, *J* 7.7 Hz, H-7), 6.64 (1H, t, *J* 7.7 Hz, H-6), 6.48 (1H, d, *J* 7.7 Hz, H-8), 3.86 (1H, br s, H-1), 3.32 – 3.35 (1H, m, H-2), 3.26 – 3.29 (1H, m, H-2), 2.90 – 2.94 (1H, m, H-4), 1.97 – 2.01 (1H, m, H-3), 1.66 – 1.71 (1H, m, H-3), 1.30 (3H, d, *J* 7.1 Hz, H-9);

δ_C (176 MHz, $CDCl_3$) 144.4 (s, C-8a), 128.6 (s, C-5), 126.9 (s, C-7), 126.7 (s, C-4a), 117.1 (s, C-6) 114.3 (s, C-8), 39.1 (s, C-2), 30.4 (s, C-4), 30.0 (s, C-3), 22.8 (s, C-9);

ν_{max} (film/cm^{-1}) 3405 (N–H), 2922 (C–H), 1606 (Ar), 1497;

LRMS (ES+) 148.2 ([M+H]$^+$, 100);

Data consistent with the literature.[145]

4-Methyl-6-(4,4,5,5-tetramethyl-1,3,2-dioxaborolan-2-yl)-1,2,3,4-tetrahydroquinoline 49e

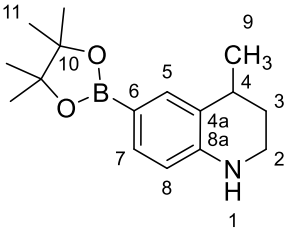

Yellow oil (7 mg, 1%);

R_f 0.6 (petroleum ether/EtOAc 80:20);

δ_H (700 MHz, $CDCl_3$, N–H not visible) 7.50 (1H, s, H-5), 7.42 (1H, dd, *J* 8.0 Hz, 1.2 Hz, H-7), 6.43 (1H, d, *J* 8.0 Hz, H-8), 3.34 – 3.37 (1H, m, H-2), 3.27 – 3.30 (1H, m, H-2), 2.89 – 2.94 (1H, m, H-4), 1.92 – 1.97 (1H, m, H-3), 1.65 – 1.69 (1H, m, H-3), 1.31 (6H, s, H-11), 1.31 (6H, s, H-11), 1.29 (3H, d, *J* 7.1 Hz, H-9);

δ_C (176 MHz, $CDCl_3$, C–B not visible) 147.1 (s, C-8a), 135.5 (s, C-5), 134.0 (s, C-7), 125.5 (s, C-4a), 113.3 (s, C-8), 83.2 (s, C-10), 38.7 (s, C-2), 30.2 (s, C-4), 29.5 (s, C-3), 25.0 (s, C-11), 24.9 (s, C-11) 22.6, (s, C-9);

δ_B (225 MHz, $CDCl_3$) 30.8;

ν_{max} (film/cm^{-1}) 3405 (N–H), 2925 (C–H), 1606 (Ar), 1499 (Ar);

LRMS (ES+) 274.3 ([M+H]$^+$, 100), 197.3 (5), 195.2 (15), 192.5 (10), 143.0 (10), 122.7 (10), 83.3 (10);

HRMS Found (ES+): [M+H]$^+$ 274.1980 [$C_{16}H_{24}NO_2B$+H]$^+$ requires 274.1978.

4-Methyl-7-(4,4,5,5-tetramethyl-1,3,2-dioxaborolan-2-yl)-1,2,3,4-tetrahydroquinoline 49f

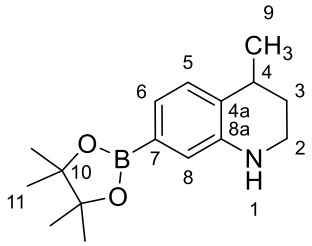

Orange oil, (1 mg, <1%);

R_f 0.7 (petroleum ether/EtOAc 7:3);

δ_H (700 MHz, $CDCl_3$) 7.08 (1H, d, *J* 7.4 Hz, H-6), 7.07 (1H, d, *J* 7.4 Hz, H-5), 6.93 (1H, s, H-8), 3.31 – 3.34 (1H, m, H-2), 3.25 – 3.28 (1H, m, H-2), 2.89 – 2.94 (1H, m, H-4), 1.95 – 2.00 (1H, m, H-3), 1.65 – 1.69 (1H, m, H-3), 1.31 (12H, s, H-11), 1.28 (3H, d, *J* 7.0 Hz, H-9);

δ_C (176 MHz, $CDCl_3$, C–B not visible) 143.9 (s, C-8a), 130.1 (s, C-4a), 128.1 (s, C-5), 123.4 (s, C-6), 120.5 (s, C-8), 83.6 (s, C-10), 39.1 (s, C-2), 30.6 (s, C-4), 29.9 (s, C-3), 25.0 (s, C-11), 24.9 (s, C-11), 22.7 (s, C-9);

δ_B (225 MHz, $CDCl_3$) 30.8;

ν_{max} (film/cm^{-1}) 3401 (N–H), 2925 (C–H), 1722;

LRMS (ES+) 274.2 ($[M+H]^+$, 100), 269.2 (35);

HRMS Found (ES+): $[M+H]^+$ 274.1981 $[C_{16}H_{24}NO_2B+H]^+$ requires 274.1978.

Ethyl 6-(4,4,5,5-tetramethyl-1,3,2-dioxaborolan-2-yl)-quinoline-4-carboxylate 51b, **ethyl-7-(4,4,5,5-tetramethyl-1,3,2-dioxaborolan-2-yl)-quinoline-4-carboxylate 51c**, **ethyl 1,2,3,4-tetrahydroquinoline-4-carboxylate 51d**, **ethyl 6-(4,4,5,5-tetramethyl-1,3,2-dioxaborolan-2-yl)-1,2,3,4-tetrahydroquinoline-4-carboxylate 51e** & **ethyl-7-(4,4,5,5-tetramethyl-1,3,2-dioxaborolan-2-yl)-1,2,3,4-tetrahydroquinoline-4-carboxylate 51f**

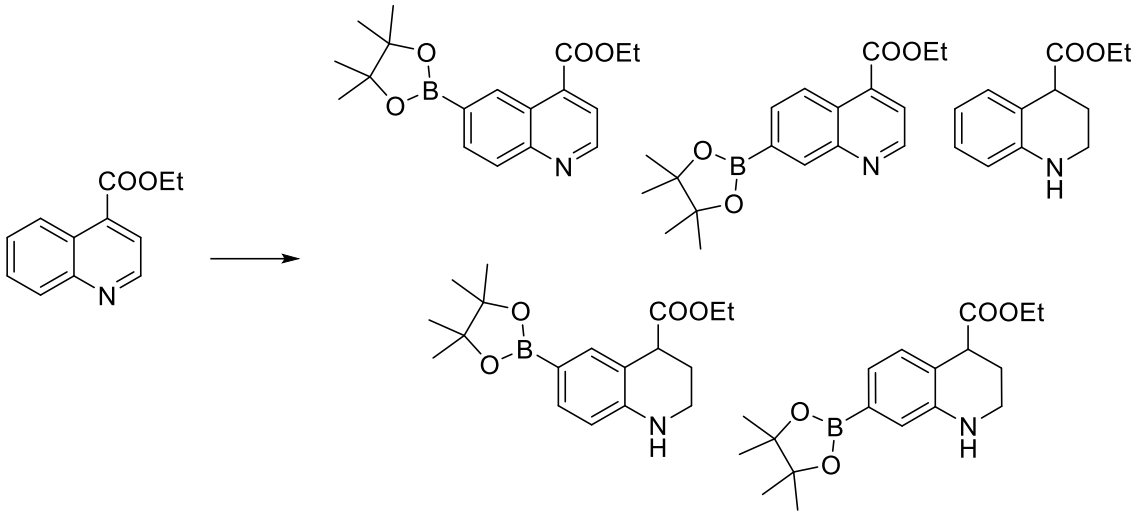

General Procedure B was followed with ethyl quinoline-4-carboxylate **51a** (402 mg, 2.00 mmol) as the substrate. The reaction gave a mixture of products which were purified by column chromatography (petroleum ether/EtOAc 100:0 – 40:60).

Ethyl 6-(4,4,5,5-tetramethyl-1,3,2-dioxaborolan-2-yl)-quinoline-4-carboxylate 51b & **ethyl-7-(4,4,5,5-tetramethyl-1,3,2-dioxaborolan-2-yl)-quinoline-4-carboxylate 51c**

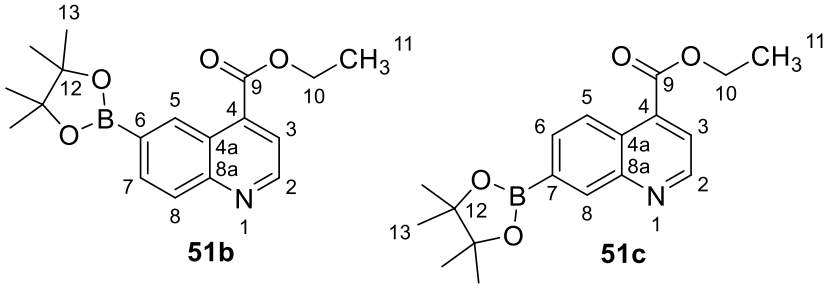

(Inseparable mixture)

Yellow oil (13 mg, 8%);

R_f 0.5 (petroleum ether/EtOAc 7:3);

δ_H (700 MHz, $CDCl_3$) 9.19 (1H, s, **51b** H-5), 9.03 (1H, d, *J* 4.3 Hz, **51b** & **51c** H-2), 8.73 (1H, d, *J* 8.5 Hz, **51c** H-5), 8.65 (1H, s, **51c** H-8), 8.13 (1H, d, *J* 8.5 Hz, **51c** H-7), 8.12 (1H, d, *J* 8.5 Hz, **51b** H-8), 7.99 (1H, d, *J* 8.5 Hz, **51c** H-6), 7.91 (1H, d, *J* 4.3 Hz, **51c** H-2), 7.86 (1H, d, *J* 4.3 Hz, **51b** H-2), 4.54 (2H, q, *J* 7.2 Hz, **51c** H-10), 4.51 (2H, q, *J* 7.2 Hz, **51b** H-10), 1.49 (3H, t, *J* 7.2 Hz, **51c** H-11), 1.47 (3H, t, *J* 7.2 Hz, **51b** H-11), 1.39 (12H, s, **51c** H-13), 1.39 (12H, s, **51b** H-13);

δ_C (176 MHz, $CDCl_3$, C–B not visible) 166.4 (s, **51b** & **51c**, C-9), 150.8 (s, **51b**, C-2), 150.6 (s, **51b**, C-8a), 149.9 (s, **51b**, C-2), 148.7 (s, **51c**, C-8a), 138.0 (s, **51c**, C-8), 136.2 (s, **51b**, C-4a), 135.1 (s, **51c**, C-4a), 134.6 (s, **51b**, C-8), 133.7 (s, **51b**, C-5), 132.8 (s, **51c**, C-6), 129.2 (s, **51b**, C-7), 126.9 (s, **51c**, C-4), 124.8 (s, **51b**, C-4), 124.5 (s, **51c**, C-5), 122.9 (s, **51c**, C-3), 122.1 (s, **51b**, C-3), 84.4 (s, **51b/c**, C-12), 84.4 (s, **51b/c**, C-12), 62.1 (s, **51c**, C-10), 62.0 (s, **51b**, C-10), 25.1 (s, **51b/c**, C-13), 25.1 (**51b/c**, C-13), 14.4 (**51b/c** C-11), 14.4 (**51b/c** C-11);

δ_B (225 MHz, $CDCl_3$) 30.9;

ν_{max} (film/cm^{-1}) 2978 (C–H), 2932 (C–H), 1723 (C=O), 1615 (Ar), 1582 (Ar), 1445 (Ar), 1423 (Ar);

LRMS (ES+) 328.2 ($[M+H]^+$, 100);

HRMS Found (ES+): $[M+H]^+$ 328.1721 $[C_{18}H_{22}BNO_4+H]^+$ requires 328.1720.

Ethyl 1,2,3,4-tetrahydroquinoline-4-carboxylate 51d

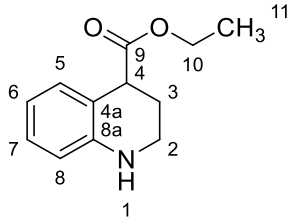

Orange oil (19 mg, 5%);

R_f 0.6 (petroleum ether/EtOAc 7:3);

δ_H (700 MHz, $CDCl_3$) 7.12 (1H, d, *J* 7.6 Hz, H-5), 7.02 (1H, t, *J* 7.6 Hz, H-7), 6.63 (1H, t, *J* 7.6 Hz, H-6), 6.51 (1H, d, *J* 7.6 Hz, H-8), 4.17 (2H, q, *J* 7.1 Hz, H-10), 3.95 (1H, br s, H-1), 3.76 (1H, t, *J* 4.9 Hz, H-4), 3.45 (1H, td, *J* 10.9, 2.5 Hz, H-2),

3.32 – 3.24 (1H, m, H-2), 2.25 – 2.28 (1H, m, H-3), 1.98 – 2.03 (1H, m, H-3), 1.27 (3H, t, *J* 7.1 Hz, H-11);

δ_C (176 MHz, $CDCl_3$) 174.4 (s, C-9), 144.6 (s, C-4a), 130.3 (s, C-5), 128.1 (s, C-6), 117.4 (s, C-8a), 117.1 (s, C-7), 114.9 (s, C-8), 60.9 (s, C-10), 41.8 (s, C-4), 39.0 (s, C-2), 24.8 (s, C-3), 14.4 (s, C-11);

ν_{max} (film/cm^{-1}) 3387 (N–H), 2978 (C–H), 2936 (C–H), 1726 (C=O), 1606 (Ar), 1504 (Ar), 1317 (Ar);

LRMS (ES+) 206.1 ($[M+H]^+$, 100);

HRMS Found (ES+): $[M+H]^+$ 206.1185 $[C_{12}H_{15}NO_2+H]^+$ requires 206.1181.

Ethyl 6-(4,4,5,5-tetramethyl-1,3,2-dioxaborolan-2-yl)-1,2,3,4-tetrahydroquinoline-4-carboxylate 51e & ethyl-7-(4,4,5,5-tetramethyl-1,3,2-dioxaborolan-2-yl)-1,2,3,4-tetrahydroquinoline-4-carboxylate 51f

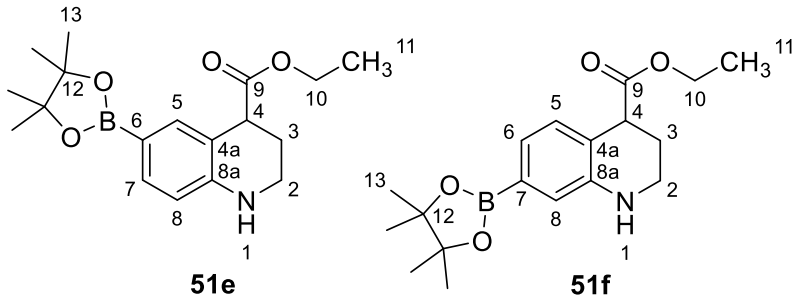

(Inseparable mixture)

Orange oil (17 mg, 3%);

R_f 0.6 (petroleum ether/EtOAc 7:3);

δ_H (700 MHz, $CDCl_3$, N–H not visible) 7.56 (1H, s, **51e** H-5), 7.47 (1H, d, *J* 8.0 Hz, **51e** H-7), 7.13 (1H, d, *J* 7.6 Hz, **51e** H-5), 7.07 (1H, d, *J* 7.6 Hz, **51e** H-6), 6.97 (1H, s, **51e** H-8), 6.47 (1H, d, *J* 8.0 Hz, **51e** H-8), 4.13 – 4.20 (2H, m, **51e** & **51f** H-10), 3.67 – 3.77 (1H, m, **51e** & **51f** H-4), 3.38 – 3.48 (1H, m, **51e** & **51f** H-2), 3.21 – 3.31 (1H, m, **51e** & **51f** H-2), 2.21 – 2.27 (1H, m, **51e** & **51f** H-3), 1.95 – 2.02 (1H, m, **51e** & **51f** H-3), 1.32 (12H, s, **51f** H-13), 1.31 (12H, s, **51e** H-13), 1.26 (3H, t, *J* 7.1 Hz, **51e** H-11), 1.24 (3H, t, 7.1 Hz, **51f** H-11);

δ_C (176 MHz, $CDCl_3$, C–B not visible) 174.4 (s, **51e** C-9), 174.2 (s, **51f** C-9), 147.1 (s, **51e** C-4a), 144.1 (s, **51f** C-4a), 137.5 (s, **51e** C-5), 135.1 (s, **51e** C-7), 129.8 (s, **51f** C-5), 123.3 (s, **51f** C-6), 121.2 (s, **51f** C-8), 120.5 (s, **51f** C-8a), 116.3 (s, **51e** C-8a), 113.8 (s, **51e** C-6), 83.8 (s, **51f** C-12), 83.3 (s, **51e** C-12), 61.0 (s, **51f** C-10), 60.9 (s, **51e** C-10), 42.0 (s, **51f** C-4), 41.7 (s, **51e** C-4), 39.1 (s, **51f** C-2), 38.6 (s, **51e** C-2), 24.7 (s, **51f** C-3), 24.6 (s, **51e** C-3), 14.3 (s, **51e** & **51f** C-11);

δ_B (225 MHz, $CDCl_3$) 30.8;

ν_{max} (film/cm^{-1}) 3404 (N–H), 2977 (C–H), 2933 (C–H), 1726 (C=O), 1608 (Ar), 1507 (Ar), 1472 (Ar);

LRMS (ES+) 663.4 ($[2M+H]^+$, 20), 537.3 ($[2M-Bpin+H]^+$, 25), 332.2 ($[M+H]^+$, 100), 206.1 ($[M-Bpin+H]^+$, 85);

HRMS Found (ES+): $[M+H]^+$ 332.2036 $[C_{18}H_{26}NO_4B+H]^+$ requires 332.2033.

4-Methyl-1,2,3,4-tetrahydroquinolin-3-ol 49i

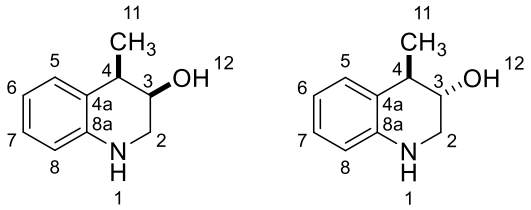

A reaction tube was loaded with 4-methylquinoline **49a** (293 mg, 2.05 mmol, 1.0 eq.), HBcat (1.20 g, 10.00 mmol, 4.9 eq.), $[Ir(COD)OMe]_2$ (20 mg, 30 μmol, 0.015 eq.) and dtbpy (16 mg, 60 μmol, 0.03 eq.) and sealed with a Teflon-lined screwcap. The tube was then evacuated and refilled with argon (three cycles) before 2 mL of dry dioxane was inserted *via* a syringe and the mixture was stirred at 100 °C for 18 h. The resulting mixture was then added to CH_2Cl_2 (25 mL) and washed with Na_2CO_3 (3 × 25 mL) and brine (25 mL). The organic phase was dried ($MgSO_4$), filtered and concentrated to leave a residue that was purified by column chromatography eluted with petroleum ether/EtOAc (80:20 – 40:60) to give a diastereomeric mixture of **49i** as an orange oil (19 mg, *syn*/*anti* 1:5, 5%);

R_f 0.1 (petroleum ether/EtOAc 7:3);

δ_H (700 MHz, $CDCl_3$, N–H & O–H not visible) 7.12 (1H, dt, *J* 7.7 Hz, 1.3 Hz, *syn* H-5), 7.07 (1H, d, *J* 7.6 Hz, *anti* H-5), 7.02 (1H, t, *J* 8.0 Hz, *syn* & *anti* H-7), 6.71 (1H, td, *J* 7.4 Hz, 1.2 Hz, *syn* & *anti* H-6), 6.55 (1H, dd, *J* 8.0 Hz, 1.2 Hz, *anti* H-8), 6.51 (1H, dd, *J* 8.0 Hz, 1.3 Hz, *syn* H-8), 4.01 – 4.04 (1H, m, *syn* H-3), 3.81 – 3.84 (1H, m, *anti* H-3), 3.31 – 3.38 (3H, m, *syn* H-2 (2H) & *anti* H-2 (1H)), 3.22 (1H, ddd, *J* 11.7 Hz, 4.2 Hz, 1.5 Hz, *anti* H-2), 3.00 – 3.06 (1H, m, *syn* H-4), 2.81 – 2.88 (1H, m, *anti* H-4), 1.38 (3H, d, *J* 7.1 Hz, *syn* H-11), 1.25 (3H, d, *J* 7.3 Hz, *anti* H-11);

δ_C (176 MHz, $CDCl_3$) 143.3 (s, *syn* C-8a), 142.9 (s, *anti* C-8a), 130.6 (s, *anti* C-5), 128.8 (s, *syn* C-5), 127.3 (s, *syn* C-7), 127.2 (s, *anti* C-7), 124.2 (s, *anti* C-4a), 124.1 (s, *syn* C-4a), 118.3 (s, *anti* C-6), 118.2 (s, *syn* C-6), 114.4 (s, *anti* C-8), 114.0 (s, *syn* C-8), 68.6 (s, *anti* C-3), 67.6 (s, *syn* C-3), 47.2 (s, *syn* C-2), 43.7 (s, *anti* C-2), 39.0 (s, *anti* C-4), 36.3 (s, *syn* C-4), 22.7 (s, *anti* C-11), 16.1 (s, *syn* C-11);

LRMS (ES+) 427.4 (20), 391.3 (15), 253.1 (20), 225.0 (30), 221.1 (40), 214.1 (100), 193.0 (70), 164.1 ($[M+H]^+$, 100), 146.1 ($[M-OH]^+$, 45), 144.1 (30);

Data consistent with the literature.[147]

4.3.2.3 Future work

1,8-Naphthalenediaminatoborane (HBdan) 58

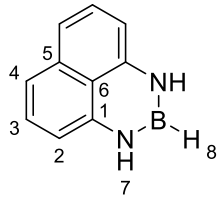

This procedure was adapted from a method described by Suginome.[152] 1,8-Diaminonaphthalene (1.58 g, 10 mmol, 1.0 eq.) was weighed into a flask and dissolved in CH_2Cl_2 (3 mL). The solution was cooled to 0 °C in an ice/water bath and stirred while BH_3•SMe_2 (948 µl, 10 mmol, 1.0 eq.) was added dropwise *via* a syringe over 15 min. The mixture was stirred at 0 °C for a further 30 min before being allowed to warm to room temperature and stirred for an additional 18 h. Then, compressed air was blown over the mixture to remove volatile materials and leave a dark red solid residue. The crude material was purified by vacuum distillation (158 °C, 6.2 mbar) to provide **58** as a white crystalline solid (937 mg, 56%);

m.p. 94 – 96 °C;

δ_H (700 MHz, $CDCl_3$) 7.12 (2H, dd, *J* 8.4 Hz, 7.3 Hz, H-3), 7.05 (2H, dd, *J* 8.4 Hz, 1.1 Hz, H-4), 6.30 (2H, dd, *J* 7.3 Hz, 1.1 Hz, H-2), 5.80 (2H, br s, H-7), 3.99 – 4.26 (1H, m, H-8);

δ_C (176 MHz, $CDCl_3$) 140.7 (s, C-1), 136.5 (s, C-5), 127.7 (s, C-3), 120.6 (s, C-6), 118.0 (s, C-4), 105.9 (s, C-2);

δ_B (225 MHz, $CDCl_3$) 26.7 (d, *J* 149.8 Hz);

LRMS (ES+) 169.1 ($[M+H]^+$, 100);

HRMS Found (ES+): $[M+H]^+$ 168.0968 $[C_{10}H_9N_2B+H]^+$ requires 168.0968;

Data consistent with the literature.[152,206]

4.3.3 Electrophilic aromatic C–H borylation mediated with copper and gold

4.3.3.1 Copper-mediated C–H borylation

tert-Butyl 3-(4,4,5,5-tetramethyl-1,3,2-dioxaborolan-2-yl)propanoate 59

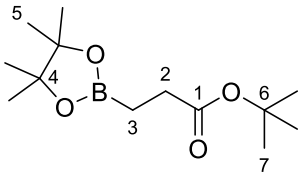

This method mimics a procedure described by Santos and colleagues.[117] An oven-dried flask was purged with nitrogen and loaded with copper(I) chloride (3.71 mg, 38 µmol, 0.05 eq.). CH_2Cl_2 was then added (500 µL) and the suspension was stirred for 2 min. PDIPA diboron **25** (403 mg, 1.50 mmol, 2 eq.) in CH_2Cl_2 (12 mL) was added *via* a syringe and the suspension was stirred for a further 10 min. The mixture was then cooled in an ice bath and *tert*-butyl acrylate (110 µl, 750 µmol, 1 eq.) followed by MeOH (121 µl, 3.00 mmol, 4 eq.) were added *via* a syringe. The reaction was allowed to warm to room temperature and stirred for 18 h. Afterwards, the reaction mixture was filtered through a pad of Celite (10 g) and then concentrated under reduced pressure to leave a white solid residue. Purification of this material by flash column chromatography (SiO_2 10 g) eluted with

cyclohexane/[EtOAc/EtOH 3:1] (100:0 – 0:100) gave **59** as a pale yellow oil (74 mg, 39%);

R_f 0.6 (cyclohexane/EtOAc/EtOH 4:3:1);

δ_H (700 MHz, $CDCl_3$) 2.32 (2H, t, *J* 7.3 Hz, H-2), 1.41 (9H, s, H-7), 1.21 (12H, s, H-5), 0.94 (2H, t, *J* 7.3 Hz, H-3);

δ_C (176 MHz, $CDCl_3$, C–B not visible) 173.9 (s, C-1), 83.0 (s, C-4), 80.0 (s, C-6), 29.9 (s, C-2), 28.1 (s, C-7), 24.7 (s, C-5);

δ_B (225 MHz, $CDCl_3$) 33.8;

LRMS (ES+) 297.2 ($[M+C_3H_5]^+$, 30), 279.2 ($[M+Na]^+$, 100), 243.1 (5), 238.1 (40);

Data consistent with the literature.[117]

***N*-(*ortho*-Tolyl)pivalamide 60**

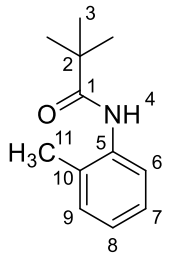

This method is based on a procedure described by Houlihan and colleagues.[207] 2-Methylaniline (3.52 g, 32.8 mmol, 1.00 eq.) and Et_3N (5.04 mL, 36.1 mmol, 1.10 eq.) were added to 50 mL dry toluene and stirred. Pivaloyl chloride (4.24 mL, 34.5 mmol, 1.05 eq.) was then added slowly and the mixture warmed to reflux. After stirring for 3 h, the reaction was allowed to cool and left to stand for 18 h. Then, the mixture was filtered and the recovered solids were added to 50 mL H_2O and stirred at room temperature for 1.5 h. A second filtration provided **60** as a white crystalline solid (3.14 g, 50%);

m.p. 106 – 107 °C;

δ_H (700 MHz, $CDCl_3$) 7.86 (1H, d, *J* 8.0 Hz, H-6), 7.23 (1H, br s, H-4), 7.21 (1H, t, *J* 8.0 Hz, H-7), 7.18 (1H, d, *J* 7.5 Hz, H-9), 7.06 (1H, t, *J* 7.5 Hz, H-8), 2.25 (3H, s, H-11), 1.34 (9H, s, H-3);

δ_C (176 MHz, $CDCl_3$) 176.6 (s, C-1), 136.0 (s, C-5), 130.5 (s, C-9), 128.8 (s, C-10), 127.0 (s, C-7), 125.0 (s, C-8), 122.9 (s, C-6), 39.9 (s, C-2), 27.9 (s, C-3), 17.8 (s, C-11);

LRMS (ES+) 405.3 ($[2M+Na]^+$, 50), 383.3 ($[2M+H]^+$, 25), 192.1 ($[M+H]^+$, 100);

Data consistent with the literature.[207]

_N_-(4-Methylbiphenyl-3-yl)pivalamide 61

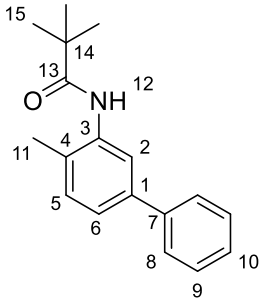

This method is based on a procedure described by Gaunt and colleagues.[153] *N*-(*o*-tolyl)pivalamide (48 mg, 250 µmol, 1.0 eq.) was weighed into a reaction tube and dissolved in 1,2-dichloroethane (1.25 mL). Whilst stirring at room temperature, diphenyliodonium triflate (215 mg, 500 µmol, 2.0 eq.) and $Cu(OTf)_2$ (9 mg, 25 µmol, 0.1 eq.) were added in one charge and the tube was sealed. The mixture was then warmed to 70 °C and stirred for a further 18 h. Afterwards, the reaction was allowed to cool to room temperature and transferred to a separating funnel. CH_2Cl_2 (15 mL) was added followed by sat aq $NaHCO_3$ (15 mL) and the phases were separated. The aqueous layer was then extracted with CH_2Cl_2 (2 × 15 mL) and the combined extracts were dried ($MgSO_4$), filtered and concentrated under reduced pressure to leave a white residue. The crude material was then purified by flash column chromatography eluted with cyclohexane/CH_2Cl_2 (50:50 – 0:100) to provide **61** as a white solid (35 mg, 52%);

R_f 0.5 (cyclohexane/EtOAc 7:3);

m.p. 112 – 114 °C;

δ_H (700 MHz, $CDCl_3$) 8.20 (1H, d, *J* 2.0 Hz, H-2), 7.61 (2H, dd, *J* 7.9 Hz, 1.2 Hz, H-8), 7.40 (2H, t, *J* 7.9 Hz, H-9), 7.28 – 7.33 (3H, m, H-6, H-10 & H-12), 7.24 (1H, d, *J* 7.9 Hz, H-5), 2.29 (3H, s, H-11), 1.36 (9H, s, H-15);

δ_C (176 MHz, $CDCl_3$) 176.6 (s, C-13), 140.8 (s, C-7), 140.1 (s, C-1), 136.4 (s, C-3), 130.9 (s, C-5), 128.8 (s, C-9), 127.5 (s, C-4), 127.3 (s, C-8), 127.2 (s, C-10), 123.5 (s, C-6), 121.5 (s, C-2), 40.0 (s, C-14), 27.9 (s, C-15), 17.4, (s, C-11);

LRMS (ES+) 285.3 ($[M+NH_4]^+$, 10), 269.4 (30), 268.4 ($[M+H]^+$, 100);

Data consistent with the literature.[208]

_N_-Methyl-3-(4,4,5,5-tetramethyl-1,3,2-dioxaborolan-2-yl)-1_H_-indole 62

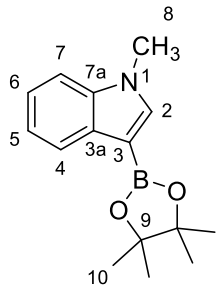

This procedure is based on a procedure described by Tanaka and colleagues.[86] A 1 M solution of BBr_3 in CH_2Cl_2 (30.5 mL, 30.5 mmol, 4 eq.) and 2,6-lutidine (3.27 mL, 30.5 mmol, 4 eq.) were added to an oven-dried flask under nitrogen in an ice/water bath. *N*-Methyl-1*H*-indole (1.00 g, 7.62 mmol, 1 eq.) was then added dropwise and the mixture was allowed to warm to room temperature and stirred for 1 h. Afterwards, the reaction was cooled again in an ice/water bath and a solution of pinacol (3.60 g, 30.5 mmol, 4 eq.) in DIPEA (20.0 mL, 115 mmol, 15 eq.) was added *via* a syringe before the mixture was allowed to warm to room temperature and stirred for a further 1 h. The mixture was then dissolved by the addition of CH_2Cl_2 (100 mL), dried ($MgSO_4$), filtered and concentrated under reduced pressure. Purification of the crude residue by flash column chromatography (SiO_2 80 g; cyclohexane/EtOAc 100:0 – 50:50) gave **62** as a yellow/brown crystalline solid (1.35 g, 69%);

R_f 0.5 (cyclohexane/EtOAc 95:5);

m.p. 111 – 113 °C;

δ_H (700 MHz, $CDCl_3$) 8.03 (1H, d, *J* 8.0 Hz, H-4), 7.52 (1H, s, H-2), 7.30 (1H, d, *J* 8.0 Hz, H-7), 7.23 (1H, t, *J* 8.0 Hz, H-6), 7.18 (1H, t, *J* 8.0 Hz, H-5), 3.80 (3H, s, H-8), 1.36 (12H, s, H-10);

δ_C (176 MHz, $CDCl_3$, C–B not visible) 138.6 (s, C-2), 138.0 (s, C-3a), 132.6 (s, C-7a), 122.8 (s, C-4), 121.9 (s, C-6), 120.3 (s, C-5), 109.3 (s, C-7), 82.8 (s, C-8), 33.1 (s, C-9), 25.0 (s, C-10);

δ_B (225 MHz, $CDCl_3$) 30.2;

LRMS (ES+) 257.2 ($[M+H]^+$, 25);

Data consistent with the literature.[86]

3-Chloro-*N*-methyl-1*H*-indole 63

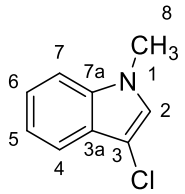

This method mimics a procedure described by Liégault and colleagues.[154] *N*-Methyl-1*H*-indole (244 µl, 1.91 mmol, 1.00 eq.) was dissolved in 6 mL THF and *N*-chlorosuccinimide (264 mg, 1.98 mmol,1.04 eq.) was added at once. The reaction mixture was then stirred at 20 °C for 5 h. Afterwards, the reaction mixture was washed with brine (15 mL) and extracted with EtOAc (3 × 15 mL). The combined organic extracts were then dried ($MgSO_4$), filtered and concentrated under reduced pressure to leave an orange residue that was purified by reverse phase flash column chromatography (SiO_2 C_{18}) eluted with MeCN/H_2O (70:30 – 15:85). This gave **63** as a pale yellow oil (175 mg, 56%);

δ_H (700 MHz, $CDCl_3$) 7.62 (1H, dt, *J* 7.8 Hz, 1.0 Hz, H-4), 7.31 – 7.36 (2H, m, H-6 & H-7), 7.22, (1H, t, *J* 7.8 Hz, H-5), 7.03 (1H, s, H-2), 3.75 (3H, s, H-8);

δ_C (176 MHz, $CDCl_3$) 136.1 (s, C-7a), 125.9 (s, C-3a), 125.5 (s, C-2), 122.9 (s, C-6), 120.1 (s, C-5), 118.5 (s, C-4), 109.7 (s, C-7), 104.7 (s, C-3);

LRMS (ES+) 165.1 ($[M+H]^+$, 100), 130.1 ($[M-Cl]^+$, 15), 89.0 (10), 51.0 (5);

Data consistent with the literature.[154]

2-(4,4,5,5-Tetramethyl-1,3,2-dioxaborolan-2-yl)-2,3-dihydro-1*H*-naphtho[1,8-*de*][1,3,2]diazaborine (pinB-Bdan) 67

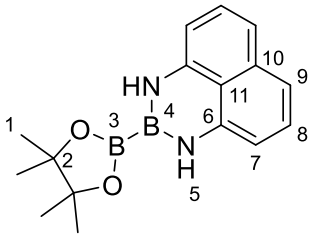

This method mimics a procedure described by Suginome and colleagues.[158] A round-bottomed flask was loaded with tetrakis(dimethylamido)diboron (10.90 mL, 51.0 mmol, 1.0 eq.) and dissolved in CH_2Cl_2 (102 mL). 1,8-Diaminonaphthalene (8.07 g, 51.0 mmol, 1.0 eq.) and pinacol (6.10 g, 51.6 mmol, 1.0 eq.) were subsequently added and the mixture was cooled in an ice bath at 0 °C. Whilst stirring, 1 M ethereal HCl (500 µL) was then added dropwise over the course of 15 min before being stirred for a further 30 min. The reaction was then allowed to warm to room temperature and stirred for 2 d. Afterwards, the mixture's volatile materials were removed on the rotary evaporator leaving a solid residue that was washed with hot toluene (3 × 300 mL). The washings were combined and concentrated under reduced pressure to leave a residue that was washed with hexane (3 × 100 mL). The solid material was then purified by column chromatography eluted with cyclohexane/CH_2Cl_2 (1:1) to give **67** as a pale red solid (6.12 g, 41%);

R_f 0.3 (cyclohexane/CH_2Cl_2 1:1);

m.p. 181 – 182 °C;

δ_H (700 MHz, $CDCl_3$) 7.07 (2H, dd, *J* 8.1 Hz, 7.3 Hz, H-8), 6.98 (2H, dd, *J* 8.1 Hz, 0.7 Hz, H-9), 6.26 (2H, dd, *J* 7.3 Hz, 0.7 Hz, H-7), 6.20 (2H, br s, H-5), 1.29 (12H, s, H-1);

δ_C (176 MHz, $CDCl_3$) 140.7 (s, C-6), 136.6 (s, C-10), 127.7 (s, C-8), 121.3 (s, C-11), 117.8 (s, C-9), 105.6 (s, C-7), 83.5 (s, C-2), 25.2 (s, C-1);

δ_B (225 MHz, $CDCl_3$) 32.3 (s, B-3), 27.9 (s, B-4);

LRMS (ES+) 295.2 ([M+H]$^+$, 100), 294.2 ([M]$^+$, 50);

Data consistent with the literature.[158]

(2*R*,2'*R*)-1,1'-(Benzylazanediyl)bis(propan-2-ol) 68

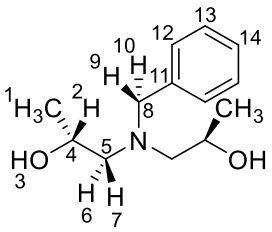

This method is based on a procedure described by Santos and colleagues.[118] Benzylamine (1.64 mL, 15.0 mmol, 1.0 eq.) and (*R*)-(+)-propylene oxide (2.31 mL, 33.0 mmol, 2.2 eq.) were added to a flask containing MeOH (10 mL). The resulting solution was stirred at 60 °C for 16 h and monitored by TLC. Following completion, the reaction was concentrated under reduced pressure to leave an oil. The crude residue was purified by silica gel chromatography eluted with 100% EtOAc to provide amine **68** as a yellow oil (3.16 g, 94%);

R_f 0.5 (100% EtOAc);

δ_H (700 MHz, $CDCl_3$) 7.21 – 7.36 (5H, m, H-12, H-13 & H-14), 3.78 – 3.91 (3H, m, H-2 & H-9 or H-10), 3.50 (1H, d, *J* 13.6 Hz, H-9 or H-10), 3.18 (2H, br s, H-3), 2.43 (4H, m, H-6 & H-7), 1.08 (6H, d, *J* 6.2 Hz, H-1);

δ_C (176 MHz, $CDCl_3$) 138.6 (s, C-11), 129.2 (s, C-12), 128.6 (s, C-13), 127.4 (s, C-14), 64.2 (s, C-4), 62.2 (s, C-5), 60.0 (s, C-8), 20.5 (s, C-1);

LRMS (ES+) 246.2 ([M+Na]$^+$, 5), 225.2 (15), 224.2 ([M+H]$^+$, 100);

Data consistent with the literature.[118]

(2*R*,2'*R*)-1,1'-Azanediylbis(propan-2-ol) 69

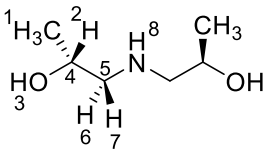

This method is based on a procedure described by Santos and colleagues.[118] Amine **68** (2.66 g, 11.91 mmol, 1.0 eq.) and 10% Pd/C (63 mg, 600 µmol, 0.05 eq.) were weighed into a flask, before MeOH (13 mL) was added. The resulting suspension was stirred under an atmosphere of hydrogen for 16 h at room temperature and monitored by TLC. Once completed, the reaction was filtered through a pad of Celite and concentrated under reduced pressure to provide spectroscopically pure **69** as a pale yellow oil (1.60 g, 100%);

δ_H (700 MHz, $CDCl_3$) 3.86 – 3.93 (2H, m, H-2), 2.66 (2H, dd, *J* 12.4 Hz, 2.9 Hz, H-7), 2.58 (2H, dd, *J* 12.4 Hz, 9.3 Hz, H-6), 1.14 (6H, d, *J* 6.5 Hz, H-1);

δ_C (176 MHz, $CDCl_3$) 63.9 (s, C-4), 55.3 (s, C-5), 21.0 (s, C-1);

LRMS (ES+) 189.2 ($[M+CH_2CH(OH)CH_3]^+$, 5), 146.1 (10), 134.1 ($[M+H]^+$, 100), 116.1 ($[M-OH]^+$, 10), 98.1 ($[M-H_2O-OH]^+$, 5), 74.1 ($[M-CH_2CH(OH)CH_3]^+$, 15);

Data consistent with the literature.[118]

4-Tolyl(triphenylphosphine)gold(I) 70

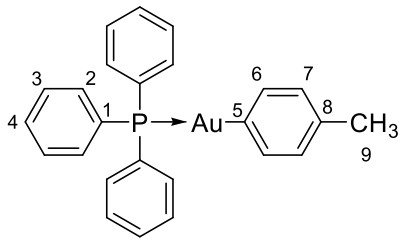

A reaction tube was loaded with 4-tolylboronic acid pinacol ester (55 mg, 250 µmol, 1.5 eq.) and Cs_2CO_3 (89 mg, 270 µmol, 1.6 eq.). The reaction tube was evacuated and refilled with argon (four cycles) before dry ^{i}PrOH (2.5 mL) was inserted and the mixture stirred vigorously. To this suspension was added bromo(triphenylphosphine)gold(I) (92 mg, 170 µmol, 1.0 eq.) suspended in 2.5 mL dry ^{i}PrOH. The reaction was then warmed to 50 °C and stirred for a further 24 h. The

reaction was then cooled to room temperature and evaporated to dryness to leave a solid residue that was extracted with benzene (3 × 5 mL). The combined extracts were filtered through a pad of Celite, and the filtrate was concentrated and washed with pentane (3 × 5 mL). Remaining solid material was re-extracted into the minimum amount of benzene, filtered and pentane vapour was diffused into the saturated solution to crystallise a colourless solid, which was washed with cold MeOH (2 × 1 mL) and cold pentane (2 × 1 mL) before being dried under high vacuum to give **70** as a white crystalline solid (4 mg, 4%);

m.p. Melting point analysis could not be carried out due to an insufficient quantity of material;

δ_H (700 MHz, C_6D_6) 8.07 (2H, dd, *J* 7.3 Hz, 5.5 Hz, H-6), 7.42 – 7.45 (6H, m, H-2), 7.37 (2H, d, *J* 7.3 Hz, H-7), 6.96 – 6.98 (3H, m, H-4), 6.91 – 6.94 (6H, m, H-3), 2.34 (3H, s, H-9);

δ_C (176 MHz, C_6D_6) 170.1 (d, *J* 170.1 Hz, C-5), 140.2 (s, C-6), 135.0 (s, C-8), 134.7 (d, *J* 13.7 Hz, C-2), 131.9 (d, *J* 48.1 Hz, C-1), 131.0 (d, *J* 2.2 Hz, C-4), 129.2 (d, *J* 10.6 Hz, C-3), 128.9 (d, *J* 6.5 Hz, C-7), 21.7 (s, C-9);

δ_P {^{1}H} (283 MHz, $CDCl_3$) 43.6;

LRMS (ES+) 551.1 ([M+H]$^+$, 10), 263.1 ([Ph_3P+H]$^+$, 100);

Data consistent with the literature.[209]

(IPr)AuBpin 71

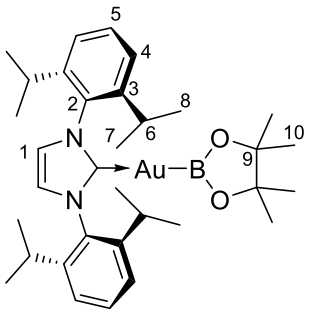

Chloro[1,3-bis(2,6-diisopropylphenyl)imidazol-2-ylidene]gold(I) (124 mg, 200 µmol, 1.0 eq.), B_2pin_2 (76 mg, 300 µmol, 1.5 eq.) and Cs_2CO_3 (110 mg, 338 µmol, 1.7 eq.) were weighed into a reaction tube. The vessel was sealed, then evacuated and refilled with nitrogen (three cycles). Dry, degassed isopropanol (5 mL) was then

added *via* a syringe and the suspension was stirred vigorously for 1 h at room temperature. Afterwards, the reaction was filtered and the solvent was removed under a current of nitrogen to leave pure **71** as an off-white solid (118 mg, 83%);

m.p. Accurate melting point analysis was not obtained due to product decomposition;

δ_H (500 MHz, CD_2Cl_2) 7.56 (2H, t, *J* 7.6 Hz, H-5), 7.36 (4H, d, *J* 7.6 Hz, H-4), 7.11 (2H, s, H-1), 2.63 (4H, sept, *J* 6.9 Hz, H-6), 1.34 (12H, d, *J* 6.9 Hz, H-7), 1.21 (12H, d, *J* 6.9 Hz, H-8), 1.01 (12H, s, H-10);

δ_C (126 MHz, CD_2Cl_2, carbene C not visible) 145.9 (s, C-2), 134.7 (s, C-3), 130.0 (s, C-5), 123.9 (s, C-4), 123.2 (s, C-1), 79.8 (s, C-9), 28.7 (s, C-6), 25.1 (s, C-10), 24.3 (s, C-7), 23.6 (s, C-8);

δ_B (160 MHz, CD_2Cl_2) 48.4;

ν_{max} (film/cm^{-1}) 2961 (C–H), 2927 (C–H), 2868 (C–H), 1459 (C–H), 1363, 1174 (C–O), 1040vs (C–N), 908 (Ar–H), 803 (Ar–H), 757 (Ar–H);

Data consistent with the literature.[160]

Acetoxy(1,3-bis(2,6-diisopropylphenyl)-2,3-dihydro-1*H*-imidazol-2-yl)gold 72

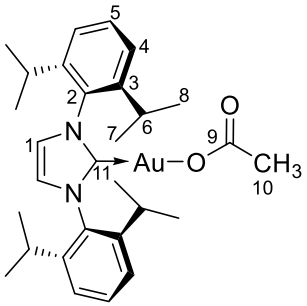

Chloro[1,3-bis(2,6-diisopropylphenyl)imidazol-2-ylidene]gold(I) (50 mg, 81 µmol, 1.00 eq.) and silver acetate (14.1 mg, 85 µmol, 1.05 eq.) were weighed into a scintillation vial followed by the addition of 800 µL CH_2Cl_2. The bottle was then sealed with a screwcap, wrapped in aluminium foil and stirred vigorously for 1 h at room temperature. After being left to stand overnight, the reaction was then filtered through Celite and rinsed through with small portions of CH_2Cl_2. Compressed air was then blown over the resulting solution to evaporate off volatile material and leave **72** as a white solid (38 mg, 73%);

m.p. Decomposes at *ca.* 190 °C;

δ_H (700 MHz, $CDCl_3$) 7.50 (2H, t, *J* 7.8 Hz, H-5), 7.29 (4H, d, *J* 7.8 Hz, H-4), 7.17 (2H, s, H-1), 2.55 (4H, sept, *J* 6.9 Hz, H-6), 1.77 (3H, s, H-10), 1.37 (12H, d, *J* 6.9 Hz, H-7), 1.22 (12H, d, *J* 6.9 Hz, H-8);

δ_C (176 MHz, $CDCl_3$) 176.5 (s, C-11), 168.9 (s, C-9), 145.8 (s, C-3), 134.2 (s, C-2), 130.8 (s, C-5), 124.4 (s, C-4), 123.2 (s, C-1), 29.0 (s, C-6), 24.5 (s, C-7), 24.2 (s, C-8), 24.0 (s, C-10);

LRMS (ES−) 700.3 (30), 680.2 ($[M-H+K]^-$, 5), 676.2 (90), 670.2 (80), 643.2 ($[M-H]^-$,100), 249.0 (10), 170.1 (15);

Data consistent with the literature.[160]

Trifluoroacetoxy(1,3-bis(2,6-diisopropylphenyl)-2,3-dihydro-1*H*-imidazol-2-yl)gold 73

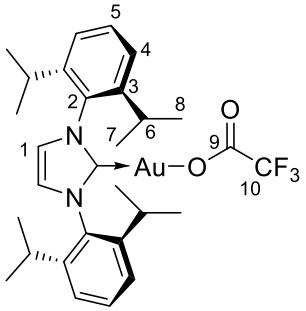

Chloro[1,3-bis(2,6-diisopropylphenyl)imidazol-2-ylidene]gold(I) (155 mg, 25 µmol, 1.0 eq.) and silver trifluoroacetate (61 mg, 280 µmol, 1.1 eq.) were weighed into a scintillation vial. CH_2Cl_2 (2.5 mL) was then added and the tube was sealed with a screwcap and wrapped in foil. The reaction was then stirred vigorously in the dark for 2 h before being left to stand overnight. Afterwards, the reaction was filtered through a pad of Celite and the filtrate was concentrated to provide **73** as a white crystalline solid (173 mg, 99%) that needed no further purification;

m.p. Decomposes at *ca.* 180 °C;

δ_H (700 MHz, $CDCl_3$) 7.53 (2H, t, *J* 7.8 Hz, H-5), 7.31 (4H, d, *J* 7.8 Hz, H-4), 7.21 (2H, s, H-1), 2.54 (4H, sept, *J* 6.9 Hz, H-6), 1.35 (12H, d, *J* 6.9 Hz, H-7), 1.22 (12H, d, *J* 6.9 Hz, H-8);

δ_C (176 MHz, $CDCl_3$, carbene C not visible) 166.4 (s, C-9), 161.0 (q, *J* 36.6 Hz, C-10), 145.7 (s, C-2), 133.9 (s, C-3), 131.0 (s, C-5), 124.5 (s, C-4), 123.5 (s, C-1), 29.0 (s, C-6), 24.5 (s, C-7), 24.3 (s, C-8);

δ_F (659 MHz, $CDCl_3$) −74.1;

LRMS (ES−) 745.2 (5), 729.2 (10), 713.2 (70), 697.2 ($[M-H^+]^-$, 100), 671.2 (45), 537.1 ($[M-(IPr)^+]^-$, 5), 232.1 (5);

HRMS Found (ES−): $[M-H^+]^-$ 697.2324 $[C_{29}H_{36}AuF_3N_2O_2-H]^-$ requires 697.2322.

Data consistent with the literature.[210]

Heptafluorobutoxy(1,3-bis(2,6-diisopropylphenyl)-2,3-dihydro-1*H*-imidazol-2-yl)gold 74

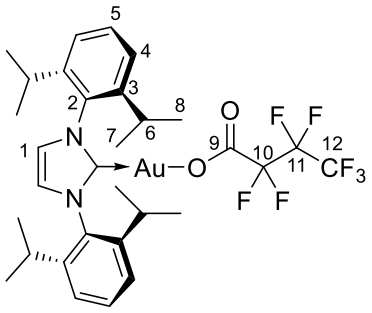

Chloro[1,3-bis(2,6-diisopropylphenyl)imidazol-2-ylidene]gold(I) (124 mg, 20 μmol, 1.0 eq.) and silver heptafluorobutyrate (65.5 mg, 204 μmol, 1.02 eq.) were weighed into a scintillation vial. CH_2Cl_2 (2 mL) was then added and the tube was sealed with a screwcap and wrapped in foil. The reaction was then stirred vigorously in the dark for 1 h before being left to stand for 16 h. Afterwards, the reaction was filtered through a pad of Celite and the filtrate was concentrated to provide **74** as an off-white crystalline solid (143 mg, 90%) that needed no further purification;

m.p. Decomposes at *ca.* 215 °C;

δ_H (700 MHz, $CDCl_3$) 7.52 (2H, t, *J* 7.8 Hz, H-5), 7.31 (4H, d, *J* 7.8 Hz, H-4), 7.21 (2H, s, H-1), 2.53 (4H, sept, *J* 6.9 Hz, H-6), 1.34 (12H, d, *J* 6.9 Hz, H-7), 1.22 (12H, d, *J* 6.9 Hz, H-8);

δ_C (176 MHz, $CDCl_3$) 166.3 (s, C-9), 161.2 (s, C-12), 145.7 (s, C-10), 133.8 (s, C-11), 131.0 (s, C-5), 124.5 (s, C-4), 123.5 (s, C-1), 29.0 (s, C-6), 24.4 (s, C-7), 24.3 (s, C-8);

δ_F (659 MHz, $CDCl_3$) −81.0 (t, *J* 8.4 Hz, F-10), −117.6 (q, *J* 8.4 Hz, F-12), −127.4 (s, F-11);

ν_{max} (film/cm^{-1}) 2963 (C–H), 2928 (C–H), 2871 (C–H), 1712 (C=O), 1470 (C–H), 1326 (C–O), 1226 (C–F), 1208 (C–F), 1075 (C–O), 964, 807, 758, 743;

LRMS (ES−) 829.2 (5), 813.2 ($[M+CH_3]^-$ 30), 797.2 ($[M-H^+]^-$, 100), 771.2 (20), 697.2 (5), 637.1 (10), 213.0 ($[CF_3CF_2CF_2COO]^-$, 10), 169.0 (5);

HRMS Found (ES−): $[M-H]^-$ 797.2259 $[C_{31}H_{36}AuF_7N_2O_2-H]^-$ requires 797.2258.

1-Hydroxy-1,2-benziodoxol-3(1*H*)-one (HBX) 76 & **1-pivaloyloxy-1,2-benziodoxol-3(1*H*)-one (PBX) 77**

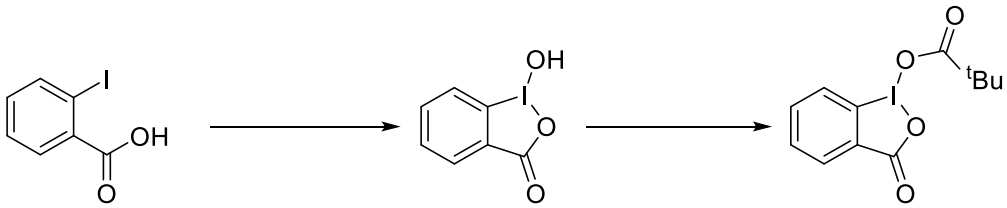

76 **77**

This procedure was carried out according to a method described by Larrosa and colleagues.[166] A suspension of 2-iodobenzoic acid (3.22 g, 13.0 mmol, 1.00 eq.) and KIO_4 (3.15 g, 13.7 mmol, 1.05 eq.) in 30% aq AcOH (20 mL) was heated to reflux and stirred for 4 h. Afterwards, the mixture was allowed to cool to room temperature and then diluted with ice-cold water (20 mL). Then, the mixture was cooled further to 0 °C in an ice/water bath and allowed to settle for 2 h. The mixture was then filtered, and the filtrate was washed thoroughly with cold water (4 × 25 mL) and acetone (3 × 10 mL). A current of air was then blown over the resulting solution to leave a white crystalline solid **76** that was dried further under high vacuum.

77 (2.50 g, 9.5 mmol, 1.0 eq.) was weighed into a round-bottomed flask followed by the addition of pivalic anhydride (8 mL). The mixture was then stirred vigorously at 150 °C until complete dissolution of the starting material (~1 h). The reaction was allowed to cool to room temperature, then left to settle for 18 h in a freezer (−18 °C),

allowing colourless needles to form. The solid material was then vacuum filtered, washed with Et_2O (6 × 5 mL) and dried, affording **77** as a white crystalline solid.

1-Hydroxy-1λ^3-benzo[*d*][1,2]iodaoxol-3(1*H*)-one (HBX) 76

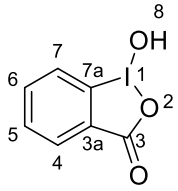

White solid (3.12 g, 91%);

m.p. Accurate melting point analysis was not obtained due to product decomposition;

δ_H (700 MHz, DMSO-d_6) 8.01 (1H, br s, H-8), 8.00 (1H, dd, *J* 7.4 Hz, 1.5 Hz, H-4), 7.95 (1H, ddd, *J* 8.4 Hz, 7.4 Hz, 1.5 Hz, H-6), 7.83 (1H, dd, *J* 8.4 Hz, 1.0 Hz, H-7), 7.69 (1H, dd, *J* 7.4 Hz, 1.0 Hz, H-5);

δ_C (176 MHz, DMSO-d_6) 167.7 (s, C-3), 134.5 (s, C-6), 131.6 (s, C-7a), 131.1 (s, C-4), 130.4 (s, C-5), 126.3 (s, C-7), 120.5 (s, C-3a);

LRMS (ES+) 524.9 ([2M+H]$^+$, 10), 316.9 (25), 302.9 (20), 279.0 (65), 264.9 ([M+H]$^+$, 100);

Data consistent with the literature.[166]

1-Pivaloyloxy-1,2-benziodoxol-3(1*H*)-one (PBX) 77

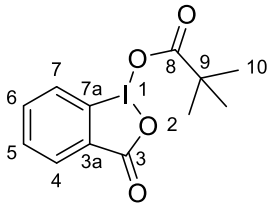

White solid (2.83 g, 86%; 78% overall yield);

m.p. Decomposes at *ca.* 165 °C;

δ_H (700 MHz, $CDCl_3$) 8.27 (1H, ddd, *J* 7.6 Hz, 1.6 Hz, 0.4 Hz, H-4), 7.97 (1H, ddd, *J* 8.4 Hz, 1.1 Hz, 0.4 Hz, H-7), 7.93 (1H, ddd, *J* 8.4 Hz, 7.1 Hz, 1.6 Hz, H-6), 7.72 (1H, ddd, *J* 7.6 Hz, 7.1 Hz, 1.1 Hz, H-5), 1.32 (9H, s, H-10);

δ_C (176 MHz, $CDCl_3$) 184.0 (s, C-8), 168.3 (s, C-3), 136.3 (s, C-6), 133.4 (s, C-4), 131.4 (s, C-5), 129.4 (s, C-7), 129.3 (s, C-3a), 118.7 (s, C-7a), 39.7 (s, C-9), 27.9 (s, C-10);

LRMS (ES+) 350.0 (15), 349.0 ($[M+H]^+$, 100);

Data consistent with the literature.[166]

(IPr)Au(Bdan) 78

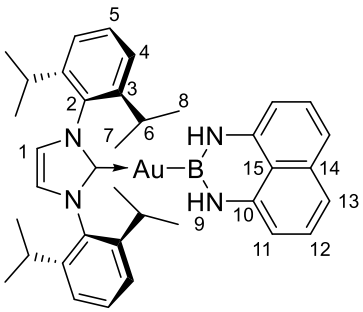

Chloro[1,3-bis(2,6-diisopropylphenyl)imidazol-2-ylidene]gold(I) (62 mg, 100 µmol, 1.0 eq.), pinB–Bdan **67** (44 mg, 150 µmol, 1.5 eq.) and Cs_2CO_3 (52 mg, 160 µmol, 1.6 eq.) were weighed into a reaction tube. The vessel was sealed then evacuated and refilled with argon (three cycles). Dry, degassed isopropanol (2.5 mL) was then inserted *via* a syringe and the suspension stirred vigorously for 1 h at room temperature. Afterwards, the reaction was filtered and grey, solid material intercepted was found to be spectroscopically pure **78** (4 mg, 5%);

Due to product instability, only ^1H and ^{11}B NMR data are reported.

δ_H (500 MHz, CD_2Cl_2) 7.54 (2H, t, *J* 7.8 Hz, H-4), 7.35 (4H, d, *J* 7.8 Hz, H-5), 7.16 (2H, s, H-1), 6.91 (2H, dd, *J* 8.3 Hz, 7.4 Hz, H-12), 6.73 (2H, dd, *J* 8.3 Hz, 1.0 Hz, H-13), 5.99 (2H, dd, *J* 7.4 Hz, 1.0 Hz, H-11), 5.59 (2H, br s, H-9), 2.65 (4H, sept, *J* 7.0 Hz, H-6), 1.39 (12H, d, *J* 6.9 Hz, H-7), 1.22 (12H, d, *J* 6.9 Hz, H-8);

δ_B (225 MHz, CD_2Cl_2) 40.3;

ν_{max} (film/cm^{-1}) 3439 (N–H), 2963 (C–H), 2927 (C–H), 1625 (Ar), 1592vs (C–N), 1481 (Ar), 1390 (Ar), 1105, 760;

LRMS (ES+) 753.3 ($[M+H]^+$, 5), 626.3 (100), 389.3 ($[IPr+H]^+$, 5), 199.1 (30);

HRMS Found (ES+): $[M+H]^+$ 752.3417 $[C_{37}H_{44}AuBN_4+H]^+$ requires 752.3433.

2,6-Dinitrophenyl(tri-*tert*-butylphosphine)gold(I) 79

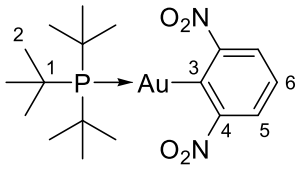

General procedure C was carried out with (P^tBu_3)AuCl (43.5 mg, 100 µmol, 1 eq.), 1,3-dinitrobenzene (67.0 mg, 400 µmol, 4 eq.) and NaO^tBu (38.0 mg, 400 µmol, 4 eq.) in DMF at 75 °C for 5 h. Flash column chromatography (SiO_2 12 g) eluted with cyclohexane/EtOAc (100:0 – 95:5) provided **79** as a yellow solid (52 mg, 92%);

R_f 0.4 (cyclohexane/EtOAc 9:1);

m.p. 218 – 221 °C;

δ_H (700 MHz, $CDCl_3$) 8.19 (2H, dd, *J* 8.0 Hz, 1.3 Hz, H-5), 7.33 (1H, t, *J* 8.0 Hz, H-6), 1.56 (27H, d, *J* 13.2 Hz, H-2);

δ_C (176 MHz, $CDCl_3$) 162.9 (d, *J* 93.3 Hz, C-3), 159.0 (d, *J* 2.7 Hz, C-4), 127.6 (d, *J* 2.7 Hz, C-5), 126.2 (s, C-6), 39.1 (d, *J* 17.5 Hz, C-1), 32.5 (d, *J* 4.1 Hz, C-2);

δ_P {^{1}H} (283 MHz, $CDCl_3$) 91.4;

LRMS (ES−) 581.1 (10), 566.2 ([M]$^-$, 5), 509.1 ([M−^{t}Bu]$^-$, 100);

HRMS Found (ES−): [M]$^-$ 566.1611 $[C_{18}H_{30}AuN_2O_4P]^-$ requires 566.1614;

Data consistent with the literature.[172]

2,4,6-Trifluorophenyl(tri-*tert*-butylphosphine)gold(I) 80

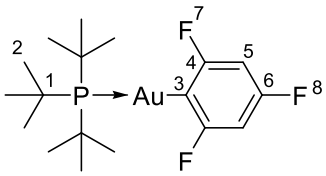

General Procedure C was carried out with (P^tBu_3)AuCl (86.9 mg, 200 µmol, 1 eq.), 1,3,5-trifluorobenzene (82.6 µl, 800 µmol, 4 eq.) and NaO^tBu (76.9 mg, 400 µmol, 4 eq.) in DMF at 75 °C for 5 h. Flash column chromatography (SiO_2 12 g) eluted with

cyclohexane/EtOAc (100:0 – 95:5) provided **80** as a white crystalline solid (84 mg, 79%);

R_f 0.3 (100% cyclohexane);

m.p. 127 – 131 °C;

δ_H (700 MHz, $CDCl_3$) 6.54 – 6.59 (2H, m, H-5), 1.56 (27H, d, *J* 13.1 Hz, H-2);

δ_C (176 MHz, $CDCl_3$) 168.4 (dddd, *J* 231.0 Hz, 28.9 Hz, 15.0 Hz, 3.6 Hz, C-4), 161.8 (dt, *J* 242.1 Hz, 13.9 Hz, C-6), 137.1 – 137.8 (m, C-3), 98.2 – 99.0 (m, C-5), 39.3 (d, *J* 16.4 Hz, C-1), 32.6 (d, *J* 4.9 Hz, C-2);

δ_P {^{1}H} (283 MHz, $CDCl_3$) 92.3;

δ_F (659 MHz, $CDCl_3$) −85.6 – −86.6 (m, F-8), −114.9 (tt, *J* 9.4 Hz, 6.9 Hz, F-7);

LRMS (ES+) 547.2 (2), 531.2 ([M+H]$^+$, <1), 440.2 (100), 417.2 ([(P^tBu_3)Au+NH_4]$^+$, 55), 399.2 ([(P^tBu_3)Au]$^+$, 30), 219.2 (5), 203.2 ([(P^tBu_3+H]$^+$, 20), 147.1 ([(P^tBu_2+2H]$^+$, 3);

Data consistent with the literature.[172]

2,6-Difluorophenyl(tri-*tert*-butylphosphine)gold(I) 81

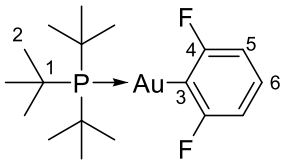

General procedure C was carried out with (P^tBu_3)AuCl (86.9 mg, 200 µmol, 1 eq.), 1,3-difluorobenzene (78.5 µl, 800 µmol, 4 eq.) and NaO^tBu (76.9 mg, 400 µmol, 4 eq.) in DMF at 75 °C for 5 h. Flash column chromatography (SiO_2 12 g) eluted with cyclohexane/EtOAc (100:0 – 95:5) provided **81** as a white crystalline solid (70 mg, 68%);

R_f 0.3 (cyclohexane/EtOAc 9:1);

m.p. 123 – 128 °C;

δ_H (700 MHz, $CDCl_3$) 7.01 (1H, tt, *J* 8.1 Hz, 7.0 Hz, H-6), 6.80 – 6.85 (2H, m, H-5), 1.57 (27H, d, *J* 13.1 Hz, H-2);

δ_C (176 MHz, $CDCl_3$) 168.8 (ddd, *J* 231.0 Hz, 24.5 Hz, 3.7 Hz, C-4), 142.7 (dt, 94.2 Hz, 61.2 Hz, C-3), 127.5 (d, *J* 8.2 Hz, C-5), 109.9 (t, *J* 3.2 Hz, C-6), 39.3 (d, *J* 16.4 Hz, C-1), 32.6 (d, *J* 4.5 Hz, C-2);

δ_P {^{1}H} (283 MHz, $CDCl_3$) 92.3;

δ_F (659 MHz, $CDCl_3$) −88.3 (d, *J* 5.3 Hz);

LRMS (ES+) 617.3 (5), 542.2 (5), 513.2 ([M+H]$^+$, 1), 456.2 ([(M−^{t}Bu)+H]$^+$, 1), 440.2 (100), 417.2 (75), 399.2 ([M−2^{t}Bu+H]$^+$, 20), 219.2 (5), 203.2 ([^{t}Bu+H]$^+$, 10);

Data consistent with the literature.[172]

4.3.4 Mono-*N*-alkylation of primary amines and activation of nitriles *via* halomethyl boronates

_N_-Methyl-4-methoxybenzylamine 86 & **4-methoxybenzylamine 86**

General Procedure D was carried out with 4-methoxybenzylamine (261 µl, 2.0 mmol, 2.0 eq.) as the amine and pivalonitrile (2 mL) as the nitrile. Silica gel column chromatography eluted with EtOAc/MeOH/Et_3N (90:8:2 – 85:13:2) delivered an inseparable mixture of **86** and **85** as a pale yellow oil (104 mg, **86**/**85** 55:45; **86** 39%);

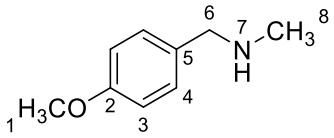

86

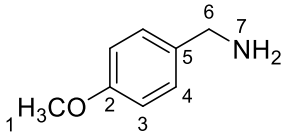

85

(Inseparable mixture)

R_f 0.2 (EtOAc/MeOH/Et_3N 90:8:2);

δ_H (700 MHz, $CDCl_3$) 7.22 – 7.25 (4H, m, **86** H-4 & **85** H-4), 6.85 – 6.88 (4H, m, **86** H-3 & **85** H-3), 3.80 (2H, s, **85** H-6), 3.80 (3H, s, **85** H-1), 3.79 (3H, s, **86** H-1), 3.69 (2H, s, **86** H-6), 2.44 (3H, s, **86** H-8), 2.15 (2H, s, **85** H-6), 1.78 (3H, br s, **86** H-7 & **85** H-7);

δ_C (176 MHz, $CDCl_3$,) 158.8 (s, **86** C-2), 158.7 (s, **85** C-2), 135.7 (s, **85** C-5) 132.2 (s, **86** C-5), 129.5 (s, **85** C-4), 128.4 (s, **85** C-4), 114.1 (s, **85** C-3), 113.9 (s, **86** C-3), 55.5 (s, **86** C-6), 55.4 (s, **85** C-6), 55.4 (s, **86** & **85** C-1), 46.1 (s, **85** C-6), 35.9 (s, **86** C-8);

LRMS (ES+) 151.1 ([**86** M]$^+$, 10), 121.1 ([4-(OMe)Bn]$^+$, 100);

Data consistent with the literature.[211,212]

3-(4-Methoxybenzyl)-2,7,7,8,8-pentamethyl-6,9-dioxa-1λ^4,3-diaza-5λ^4-boraspiro[4.4]non-1-ene 87

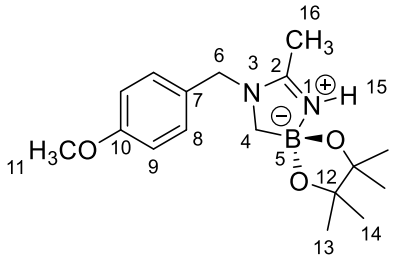

A 1 M solution of 4-methoxybenzylamine (130.5 µl, 1.00 mmol, 2.0 eq.) in CH_3CN was added to a 1 M solution of $ClCH_2Bpin$ (129.7 µl, 750 µmol, 1.5 eq.) in CH_3CN. The resulting mixture was stirred at room temperature for 16 h (white precipitate develops after a few minutes). Afterwards, the suspension was added to a sat aq $NaHCO_3$ (20 mL) and extracted with CH_2Cl_2 (3 × 15 mL). Combined organic extracts were then washed with brine (20 mL), dried ($MgSO_4$), filtered and concentrated. Column chromatography (SiO_2) eluted with EtOAc/MeOH/Et_3N (90:8:2) delivered diazaborole **87** as a pale yellow oil (19 mg, 8%);

R_f 0.4 (EtOAc/MeOH/Et_3N 90:8:2);

δ_H (700 MHz, $CDCl_3$) 7.06 (2H, d, *J* 8.7 Hz, H-8), 6.83 (2H, d, *J* 8.7 Hz, H-9), 5.70 (1H, br s, H-15), 4.35 (2H, s, H-6), 3.78 (3H, s, H-11), 2.38 (2H, s, H-4), 2.11 (3H, s, H-16), 1.13 (6H, s, H-14), 1.06 (6H, s, H-13);

δ_C (176 MHz, $CDCl_3$,) 166.6 (s, C-2), 159.4 (s, C-10), 128.7 (s, C-8), 127.6 (s, C-7), 114.4 (s, C-9), 78.8 (s, C-12), 55.5 (s, C-11), 52.1 (s, C-6), 46.0 – 47.5 (m, C-4), 25.3 (s, C-14), 25.1 (s, C-13), 15.7 (s, C-16);

δ_B (225 MHz, $CDCl_3$) 7.6;

ν_{max} (film/cm^{-1}) 3251 (N–H), 2965 (C–H), 2926 (C–H), 1599 (Ar), 1557 (Ar), 1512 (Ar), 1242 (H_2C–H), 1161 (C–N), 1048 (C–N);

LRMS (ES+) 319.2 ([M+H]$^+$, 100), 233.1 (10), 219.1 (15), 121.1 (30), 79.1 (5), 65.1 (10);

HRMS Found (ES+): [M+H]$^+$ 318.2225 [$C_{17}H_{27}O_3N_2B$+H]$^+$ requires 318.2224.

2-Ethyl-3-(4-methoxybenzyl)-7,7,8,8-tetramethyl-6,9-dioxa-1,3-diaza-5λ^4-boraspiro[4.4]non-1-ene 88

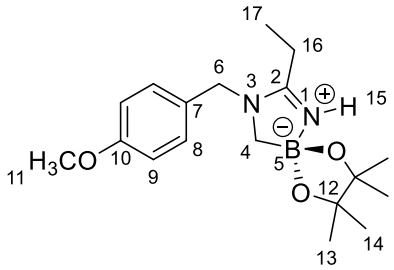

General Procedure D was carried out with 4-methoxybenzylamine (261 µl, 2.0 mmol, 2.0 eq.) as the amine and propionitrile (2 mL) as the nitrile. Silica gel column chromatography eluted with EtOAc/MeOH/Et_3N (90:8:2) delivered **88** as a pale yellow oil (25 mg, 8%);

R_f 0.4 (EtOAc/MeOH/Et_3N 90:8:2);

δ_H (700 MHz, $CDCl_3$) 7.05 (2H, d, *J* 8.6 Hz, H-8), 6.82 (2H, d, *J* 8.6 Hz, H-9), 5.73 (1H, br s, H-15), 4.34 (2H, s, H-6), 3.77 (3H, s, H-11), 2.38 – 2.41 (4H, m, H-4 & H-16), 1.21 (3H, t, *J* 7.5 Hz, H-17), 1.13 (6H, s, H-14), 1.06 (6H, s, H-13);

δ_C (176 MHz, $CDCl_3$,) 170.9 (s, C-2), 159.3 (s, C-10), 128.6 (s, C-8), 127.7 (s, C-7), 114.4 (s, C-9), 78.8 (s, C-12), 55.4 (s, C-11), 51.5 (s, C-6), 46.4 – 47.8 (m, C-4), 25.3 (s, C-14), 25.1 (s, C-13), 21.7 (s, C-16), 9.9 (s, C-17);

δ_B (225 MHz, $CDCl_3$) 7.7;

ν_{max} (film/cm^{-1}) 3263 (N–H), 2967 (C–H), 2930 (C–H), 1583 (C=N), 1513 (Ar), 1235 (Ar–OCH_3), 1162vs (C–O), 1053vs (C–O);

LRMS (ES+) 333.2 ([M+H]$^+$, 100), 315.2 (5), 233.1 (65), 214.1 (15), 195.1 (50), 147.1 (75), 124.1 (15);

HRMS Found (ES+): $[M+H]^+$ 332.2382 $[C_{18}H_{29}O_3N_2B+H]^+$ requires 332.2380.

3-Cyclohexyl-2,7,7,8,8-pentamethyl-6,9-dioxa-1,3-diaza-5λ⁴-boraspiro[4.4]non-1-ene 90

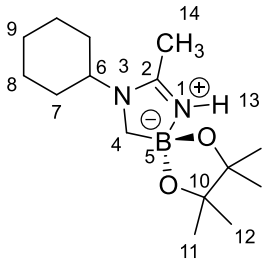

General Procedure D was carried out with cyclohexylamine (229 µl, 2.0 mmol, 2.0 eq.) as the amine and MeCN (2 mL) as the nitrile. Silica gel column chromatography eluted with EtOAc/MeOH/Et_3N (98:0:2 – 94:4:2) delivered **90** as a colourless oil (107 mg, 38%);

R_f 0.4 (EtOAc/MeOH/Et_3N 90:8:2);

δ_H (700 MHz, $CDCl_3$) 5.50 (1H, br s, H-13), 3.27 – 3.31 (1H, m, H-6), 2.29 (2H, s, H-4), 2.02 (3H, s, H-14), 1.79 – 1.83 (2H, m, H-8), 1.61 – 1.65 (1H, m, H-9), 1.52 – 1.60 (4H, m, H-7), 1.21 – 1.28 (3H, m, H-8 (2H) & H-9 (1H)), 1.12 (6H, s, H-12), 1.09 (6H, s, H-11);

δ_C (176 MHz, $CDCl_3$,) 165.4 (s, C-2), 78.7 (s, C-10), 56.1 (s, C-6), 39.0 – 40.4 (m, C-4), 31.0 (s, C-7), 25.6 (s, C-8), 25.3 (s, C-12), 25.3 (s, C-9), 25.2 (s, C-11), 15.5 (s, C-14);

δ_B (225 MHz, $CDCl_3$) 7.6;

ν_{max} (film/cm^{-1}) 3270 (N–H), 2965 (C–H), 2932 (C–H), 2857 (C–H), 1592s (C=N), 1163vs (C–O),1052vs (C–O);

LRMS (ES+) 361.3 ($[M+Cy]^+$, 15), 281.2 ($[M+H]^+$, 15), 199.2 ($[M-Cy+2H]^+$, 100), 181.2 (80), 158.1 (15), 101.1 (10);

HRMS Found (ES+): $[M+H]^+$ 280.2433 $[C_{19}H_{25}O_2N_2B+H]^+$ requires 280.2431.

3-Cyclohexyl-2-ethyl-7,7,8,8-tetramethyl-6,9-dioxa-1λ⁴,3-diaza-5λ⁴-boraspiro[4.4]non-1-ene 91

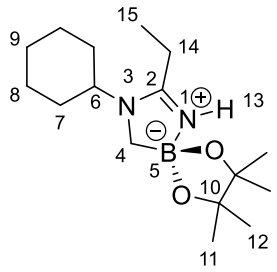

General Procedure D was carried out with cyclohexylamine (229 µl, 2.0 mmol, 2.0 eq.) as the amine and MeCN (2 mL) as the nitrile. Silica gel column chromatography eluted with EtOAc/MeOH/Et_3N (98:0:2 – 90:8:2) delivered **91** as a colourless oil (39 mg, 13%);

R_f 0.4 (EtOAc/MeOH/Et_3N 90:8:2);

δ_H (700 MHz, $CDCl_3$) 5.54 (1H, br s, H-13), 3.28 – 3.33 (1H, m, H-6), 2.31 – 2.35 (4H, m, H-4 & H-14), 1.79 – 1.83 (2H, m, H-8), 1.62 – 1.66 (1H, m, H-9), 1.55 – 1.61 (4H, m, H-7), 1.22 – 1.29 (3H, m, H-8 (2H) & H-9 (1H)), 1.20 (3H, t, *J* 7.5 Hz, H-15), 1.14 (6H, s, H-12), 1.10 (6H, s, H-11);

δ_C (176 MHz, $CDCl_3$,) 169.7 (s, C-2), 78.7 (s, C-10), 55.6 (C-6), 39.3 – 40.7 (m, C-4), 31.0 (s, C-7), 25.7 (s, C-8), 25.3 (s, C-12), 25.3 (s, C-9), 25.2 (s, C-11), 21.8 (s, C-14), 10.1 (s, C-15);

δ_B (225 MHz, $CDCl_3$) 7.6;

ν_{max} (film/cm^{-1}) 3263 (N–H), 2966 (C–H), 2934 (C–H), 2858 (C–H), 1588 (C=N), 1165vs, (C–O), 1054vs (C–O);

LRMS (ES+) 611.5 ($[2M+Na]^+$, 5), 565.5 (10), 417.3 (5), 389.3 (35), 213.2 ($[M-Cy+2H]^+$, 100), 195.2 (85);

HRMS Found (ES+):$[M+H]^+$ 295.2542 $[C_{16}H_{31}O_2N_2B+H]^+$ requires 295.2551.

3-(4-Methoxyphenyl)-2,7,7,8,8-pentamethyl-6,9-dioxa-1λ⁴,3-diaza-5λ⁴-boraspiro[4.4]non-1-ene 92

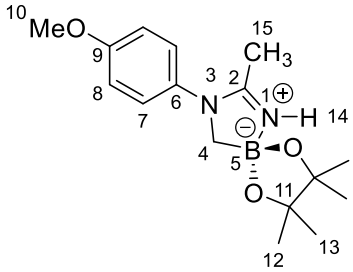

General Procedure D was carried out with *p*-anisidine (246 mg, 2.0 mmol, 2.0 eq.) as the amine and MeCN (2 mL) as the nitrile. Silica gel column chromatography eluted with EtOAc/MeOH/Et_3N (98:0:2 – 96:2:2) delivered an impure mixture of **92** and pinacol (6:1). This residue was dissolved in CH_2Cl_2 (20 mL) and washed with 1 M NaOH (4 × 20 mL) and brine (20 mL). Remaining organic material was then dried ($MgSO_4$), filtered and concentrated to give pure **92** as a brown oil (59 mg, 19%);

R_f 0.3 (EtOAc/MeOH/Et_3N 90:8:2);

δ_H (700 MHz, $CDCl_3$) 7.03 (2H, d, *J* 8.8 Hz, H-7), 6.86 (2H, d, *J* 8.8 Hz, H-8), 5.95 (1H, br s, H-14), 3.79 (3H, s, H-10), 2.81 (2H, s, H-4), 1.92 (3H, s, H-15), 1.16 (6H, s, H-13), 1.11 (6H, s, H-12);

δ_C (176 MHz, $CDCl_3$,) 167.0 (s, C-2), 158.9 (s, C-6), 134.5 (s, C-9), 127.1 (s, C-7), 114.8 (s, C-8), 78.9 (s, C-11), 55.6 (s, C-10), 51.2 – 52.8 (m, C-4), 25.3 (s, C-13), 25.2 (s, C-12), 16.2 (s, C-15);

δ_B (225 MHz, $CDCl_3$) 7.8;

ν_{max} (film/cm^{-1}) 3252 (N–H), 2967 (C–H), 2930 (C–H), 1591 (C=N), 1513vs (Ar), 1247 (Ar–OCH_3), 1164 (C–O), 1055 (C–O);

LRMS (ES+) 305.2 ($[M+H]^+$, 100), 205.1 (15), 165.1 (5);

HRMS Found (ES+): $[M+H]^+$ 304.2063 $[C_{16}H_{25}O_3N_2B+H]^+$ requires 304.2067.

2,7,7,8,8-Pentamethyl-3-propyl-6,9-dioxa-1λ⁴,3-diaza-5λ⁴-boraspiro[4.4]non-1-ene 94

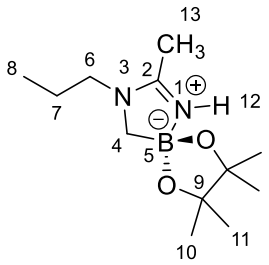

General Procedure D was carried out with propylamine (164 µl, 2.0 mmol, 2.0 eq.) as the amine and MeCN (2 mL) as the nitrile. Silica gel column chromatography eluted with EtOAc/MeOH/Et_3N (90:8:2) delivered **94** as a colourless oil that crystallised on standing as the monohydrate (62 mg, 26%);

R_f 0.4 (EtOAc/MeOH/Et_3N 90:8:2);

m.p. 132 – 133 °C (as the monohydrate);

δ_H (700 MHz, $CDCl_3$) 5.52 (1H, br s, H-12), 3.12 (2H, t, *J* 7.4 Hz, H-6), 2.35 (2H, s, H-4), 1.99 (3H, s, H-13), 1.56 (2H, sext, *J* 7.4 Hz, H-7), 1.10 (6H, s, H-11), 1.07 (6H, s, H-10), 0.84 (3H, t, *J* 7.4 Hz, H-8);

δ_C (176 MHz, $CDCl_3$,) 166.2 (s, C-2), 78.7 (s, C-12), 50.3 (s, C-6), 44.9 – 46.5 (m, C-4), 25.3 (s, C-11), 25.1 (s, C-10), 21.0 (s, C-7), 15.4 (s, C-13), 11.3 (s, C-8);

δ_B (225 MHz, $CDCl_3$) 7.6;

ν_{max} (film/cm^{-1}) 3275 (N–H), 2965 (C–H), 2924 (C–H), 2876 (C–H), 2853 (C–H), 1600 (C=N), 1160 (C–O), 1049 (C–O);

LRMS (ES+) 241.2 ($[M+H]^+$, 100);

HRMS Found (ES+):$[M+H]^+$ 240.2116 $[C_{12}H_{25}O_2N_2B+H]^+$ requires 240.2118.

4.3.5 Miscellaneous compounds

The following compounds **103 – 109** were synthesised, isolated and characterised during the course of this project, but are not discussed in this thesis.

N-(4-(Triethylsilyl)phenyl)acetamide 103

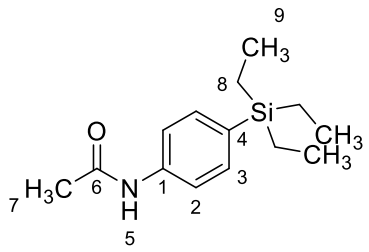

This method is based on a procedure described by Liu and colleagues.[213] An oven-dried flask was charged with *N*-phenylacetamide (135 mg, 1.0 mmol, 1.0 eq.), Cu_2O (7.2 mg, 50 µmol, 0.05 eq.), triethylsilane (2.9 mL, 18 mmol, 18 eq.), di-*tert*-butyl peroxide (2.2 mL, 12 mmol, 12 eq.) and *tert*-amyl alcohol (5 mL). The mixture was then stirred at 120 °C for 12 h before further portions of triethylsilane (2.9 mL, 18 mmol, 18 eq.) and di-*tert*-butyl peroxide (2.2 mL, 12 mmol, 12 eq.) were added and the solution was heated for a further 12 h. Afterwards, the mixture was evaporated under reduced pressure and the residue was purified by flash column chromatography (petroleum ether/EtOAc 3:1) to afford **103** as a white solid (88 mg, 33%);

m.p. 44 – 47 °C;

R_f 0.2 (petroleum ether/EtOAc 3:1);

δ_H (700 MHz, $CDCl_3$) 7.81 (1H, br s, H-5), 7.50 (2H, d, *J* 7.8 Hz, H-3), 7.42 (2H, d, *J* 7.8 Hz, H-2), 2.15 (3H, s, H-7), 0.95 (9H, t, *J* 7.9 Hz, H-9), 0.76 (6H, q, *J* 7.9 Hz, H-8);

δ_C (176 MHz, $CDCl_3$) 168.3 (C-6), 138.4 (C-1), 135.2 (C-2), 133.2 (C-4), 119.4 (C-3), 24.8 (C-7), 7.5 (C-9), 3.5 (C-8);

LRMS (EI) 249.18 ($[M]^+$, 25), 220.12 ($[M-Et]^+$, 100), 192.10 ($[M-CH_3CONH]^+$, 55), 164.07 (75), 122.06 (25).

Data consistent with the literature.[213]

2,2'-Bi(1,3,6,2-dioxazaborocane) 104 & **2,2'-oxybis(1,3,6,2-dioxazaborocane) 105**

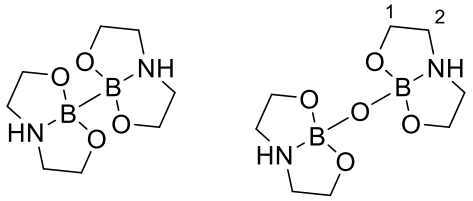

104 **105**

This compound was prepared according to a procedure described by Skrydstrup and colleagues.[214] A flame-dried flask was loaded with tetrahydroxydiboron (2.30 g, 25.7 mmol, 1.0 eq.) followed by 175 mL of CH_2Cl_2. Diethanolamine (5.76 g, 54.8 mmol, 2.1 eq.) was then added and the mixture was stirred at room temperature for 30 min. The reaction mixture was vacuum filtered and washed with copious amounts of EtOAc to give the title compound as a white solid (4.65 g, 80%). As **104** was found to be insoluble in a range of common NMR solvents, the compound was reacted with D_2O to give diboraxane **105**, which remained in solution in D_2O.

δ_H (700 MHz, D_2O, N–H not visible) 3.77 (8H, t, *J* 5.3 Hz, H-1), 3.05 (8H, t, *J* 5.3 Hz, H-2);

δ_C (176 MHz, D_2O) 58.1 (s, C-1), 49.7 (s, C-2);

δ_B (225 MHz, D_2O) 15.7;

LRMS (ES+) 245.2 ($[M+H]^+$, 100);

Data consistent with the literature.[214]

Triphenylphosphinegold(I) acetate 106

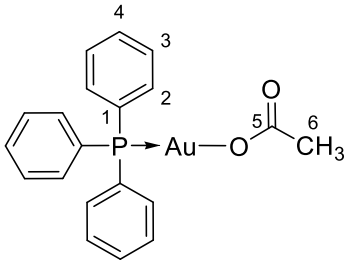

$(PPh_3)AuCl$ (100 mg, 202 μmol, 1.00 eq.) and AgOAc (35.1 mg, 210 μmol, 1.04 eq.) were weighed into a scintillation vial, followed by the addition of 2 mL CH_2Cl_2. The vial was then sealed with a screwcap, wrapped in aluminium foil and stirred vigorously for 1 h at room temperature. After being left to stand overnight, the reaction was then filtered through Celite and rinsed through with small portions of CH_2Cl_2. Concentration of CH_2Cl_2 washings under a current of air gave **106** as a white solid (102 mg, 98%);

m.p. Decomposes at *ca.* 115 °C;

δ_H (500 MHz, CD_2Cl_2) 7.42 – 7.50 (9H, m, H-2 and H-4), 7.35 – 7.41 (6H, m, H-3), 1.86 (3H, s, H-6);

δ_C (126 MHz, CD_2Cl_2) 176.2 (s, C-5), 134.1 (d, *J* 13.7 Hz, C-2), 132.0 (d, *J* 3.1 Hz, C-4), 129.2 (d, *J* 12.2 Hz, C-3), 128.8 (d, *J* 64.1 Hz, C-1), 23.5 (s, C-6);

δ_P $\{^1H\}$ (202 MHz, CD_2Cl_2) 27.6;

ν_{max} (film/cm^{-1}) 3442, 3053 (C–H), 2926 (C–H), 1625 (C=O), 1481 (Ar), 1435 (Ar), 1305vs (C–O), 1101 (C–O), 692vs (Ar–H), 548vs, 508;

Data consistent with the literature.[215]

2,2'-Oxybis(4,4,5,5-tetramethyl-1,3,2-dioxaborolane) (pinB-O-Bpin) 107

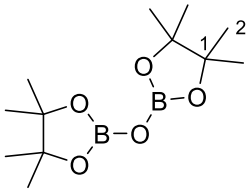

B_2pin_2 (254 mg, 1.0 mmol, 1.00 eq.) and trimethylamine-*N*-oxide (79 mg, 1.05 mmol, 1.05 eq.) were weighed into a scintillation vial. CH_3Cl (1 mL) was added slowly and the reaction was stirred at room temperature for 18 h. Volatile material was removed *in vacuo* to give **107** as a white solid that require no further purification (154 mg, 57%);

m.p. 59 – 60 °C;

δ_H (700 MHz, $CDCl_3$) 1.27 (24H, s);

δ_C (176 MHz, $CDCl_3$) 83.4 (s, C-1), 24.7 (s, C-2);

δ_B (225 MHz, $CDCl_3$) 22.5;

LRMS (ES+) 270.3 ($[M+H]^+$, 5), 255.2 ($[M-CH_3]^+$, 45), 170.2 (45), 129.1 (100), 101.2 (40), 89.1 (45), 83.2 (95), 69.2 (35), 59.1 (55), 57.1 (50), 55.1 (45), 43.1 (90), 41.1 (85);

Data consistent with the literature.[216]

2,4-Dimethoxyphenyl boronic acid pinacol ester 108

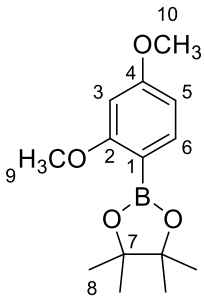

2,4-Dimethoxyphenylboronic acid (364 mg, 2.0 mmol, 1.00 eq.) and pinacol (248 mg, 2.1 mmol, 1.05 eq.) were weighed into round-bottomed flask. Benzene (4 mL) was added to the mixture and Dean-Stark apparatus was fitted to the flask (side-arm filled

with benzene). After stirring the reaction at reflux for 18 h, the mixture was allowed to cool and water (10 mL) was added before extraction with EtOAc (3 × 20 mL). Combined organic extracts were washed with brine (25 mL), dried (Na_2SO_4) and filtered. Concentration of the resulting solution under reduced pressure gave **108** as a colourless oil which required no further purification (453 mg, 86%);

δ_H (600 MHz, $CDCl_3$) 7.63 (1H, d, *J* 8.2 Hz, H-6), 6.47 (1H, dd, *J* 8.2 Hz, 2.2 Hz, H-5), 6.40 (1H, d, *J* 2.2 Hz, H-3), 3.81 (3H, s, H-10), 3.81 (3H, s, H-9), 1.33 (12H, s, H-8);

δ_C (150 MHz, $CDCl_3$) 166.1 (s, C-2), 163.8 (s, C-4), 138.5 (s, C-6), 108.7 – 111.1 (m, C-1), 104.5 (s, C-5), 98.2 (s, C-3), 83.3 (s, C-7), 55.9 (s, C-10), 55.4 (s, C-9), 25.0 (s, C-8);

δ_B (225 MHz, $CDCl_3$) 30.8;

LRMS (ES+) 265.2 ($[M+H]^+$, 90), 197.1 (30), 183.1 (60), 145.1 (40), 139.1 ($[M-Bpin+H]^+$, 100);

HRMS Found (ES+): $[M+H]^+$ 264.1641 $[C_{14}H_{21}BO_4+H]^+$ requires 264.1642;

Data consistent with the literature.[217]

2-(2,4-Dimethoxyphenyl)-2,3-dihydro-1*H*-naphtho[1,8-*de*][1,3,2]diazaborinine 109

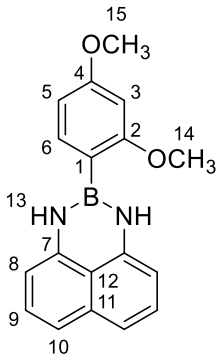

2,4-Dimethoxyphenyl boronic acid (315 mg, 1.73 mmol, 1.00 eq.) and 1,8-diaminonaphthalene (288 mg, 1.82 mmol, 1.05 eq.) were weighed into a round-bottomed flask. Fluorobenzene (3.5 mL) was added and the mixture was stirred at reflux for 18 h. Afterwards, the reaction was allowed to cool and water (10 mL) was added before extraction with EtOAc (3 × 20 mL). Combined organic

extracts were washed with brine (25 mL), dried ($MgSO_4$) and filtered. Concentration of the resulting solution under reduced pressure left a solid residue that was purified by flash column chromatography (SiO_2 25 g) eluted with cyclohexane/EtOAc (100:0 – 75:25) to provide **109** as a pale red solid (367 mg, 70%);

R_f 0.3 (cyclohexane/EtOAc 8:2);

m.p. 158 – 160 °C;

δ_H (500 MHz, $CDCl_3$) 7.46 (1H, d, *J* 8.4 Hz, H-6), 7.12 (1H, dd, *J* 8.4 Hz, 7.3 Hz, H-9), 7.01 (2H, dd, *J* 8.4 Hz, 0.9 Hz, H-10), 6.58 (1H, dd, *J* 8.4 Hz, 2.2 Hz, H-5), 6.48 – 6.51 (3H, m, H-3 & H-13), 6.38 (2H, d, *J* 7.3 Hz, H-8), 3.90 (3H, s, H-14), 3.86 (3H, s, H-15);

δ_C (126 MHz, $CDCl_3$, C–B not visible) 165.7 (s, C-2), 163.1 (s, C-4), 141.7 (s, C-7), 136.5 (s, C-11), 134.6 (s, C-6), 127.7 (s, C-9), 119.9 (s, C-12), 117.3 (s, C-10), 105.8 (s, C-8), 105.1 (s, C-5), 98.5 (s, C-3), 55.5 (s, C-14), 55.5 (s, C-15);

δ_B (225 MHz, $CDCl_3$) 28.3;

ν_{max} (film/cm^{-1}) 3410 (N–H), 3383 (N–H), 3052 (C–H), 2933 (C–H), 2830 (C–H), 1595 (N–H), 1493 (Ar), 1402 (Ar), 1250 (C–O), 1198, 1122, 1033 (C–O), 819 (Ar–H), 763 (Ar–H), 688 (Ar–H);

LRMS (ES+) 305.1 ($[M+H]^+$, 100), 243.1 (5), 171.1 (15), 159.1 (25), 127.1 (20), 113.1 (45);

HRMS Found (ES+): $[M+H]^+$ 304.1493 $[C_{18}H_{17}BN_2O_2+H]^+$ requires 304.1492.

5 References

1. Davies, D. T. *Aromatic Heterocyclic Chemistry*. (Oxford University Press, 1992).

2. Taylor, R. D., Maccoss, M. & Lawson, A. D. G. Rings in drugs. *J. Med. Chem.* **57**, 5845–5859 (2014).

3. Rogge, T. *et al.* C–H activation. *Nat. Rev. Methods Prim.* **1**, (2021).

4. Cernak, T., Dykstra, K. D., Tyagarajan, S., Vachal, P. & Krska, S. W. The medicinal chemist's toolbox for late stage functionalization of drug-like molecules. *Chem. Soc. Rev.* **45**, 546–576 (2016).

5. Guillemard, L., Kaplaneris, N., Ackermann, L. & Johansson, M. J. Late-stage C–H functionalization offers new opportunities in drug discovery. *Nat. Rev. Chem.* **5**, 522–545 (2021).

6. Khotinsky, E. & Melamed, M. Die wirkung der magnesiumorganischen verbindungen auf die borsäureester. *Ber. Dtsch. Chem. Ges.* **42**, 3090–3096 (1909).

7. Clary, J. W. & Singaram, B. Synthesis of boronic esters and boronic acids using grignard reagents. (2016).

8. Suzuki, A. Recent advances in the cross-coupling reactions of organoboron derivatives with organic electrophiles, 1995–1998. *J. Organomet. Chem.* **576**, 147–168 (1999).

9. Vantourout, J. C., Law, R. P., Isidro-Llobet, A., Atkinson, S. J. & Watson, A. J. B. Chan–Evans–Lam amination of boronic acid pinacol (BPin) esters: overcoming the aryl amine problem. *J. Org. Chem.* **81**, 3942–3950 (2016).

10. Litvinas, N. D., Fier, P. S. & Hartwig, J. F. A general strategy for the perfluoroalkylation of arenes and arylbromides by using arylboronate esters and [(phen)CuR(F)]. *Angew. Chem., Int. Ed.* **51**, 536–539 (2012).

11. Webb, K. S. & Levy, D. A facile oxidation of boronic acids and boronic esters. *Tetrahedron Lett.* **36**, 5117–5118 (1995).

12. Murphy, J. M., Liao, X. & Hartwig, J. F. Meta halogenation of 1,3-disubstituted arenes via iridium-catalyzed arene borylation. *J. Am. Chem. Soc.* **129**, 15434–15435 (2007).

13. Liskey, C. W., Liao, X. & Hartwig, J. F. Cyanation of arenes via iridium-catalyzed borylation. *J. Am. Chem. Soc.* **132**, 11389–11391 (2010).

14. Ishiyama, T. *et al.* Mild iridium-catalyzed borylation of arenes. High turnover numbers, room temperature reactions, and isolation of a potential intermediate. *J. Am. Chem. Soc.* **124**, 390–391 (2002).

15. Takagi, J., Sato, K., Hartwig, J. F., Ishiyama, T. & Miyaura, N. Iridium-catalyzed C–H coupling reaction of heteroaromatic compounds with bis(pinacolato)diboron: Regioselective synthesis of heteroarylboronates. *Tetrahedron Lett.* **43**, 5649–5651 (2002).

16. Ishiyama, T., Takagi, J., Yonekawa, Y., Hartwig, J. F. & Miyaura, N. Iridium-catalyzed direct borylation of five-membered heteroarenes by bis(pinacolato)diboron: Regioselective, stoichiometric, and room temperature reactions. *Adv. Synth. Catal.* **345**, 1103–1106 (2003).

17. Ishiyama, T., Nobuta, Y., Hartwig, J. F. & Miyaura, N. Room temperature borylation of arenes and heteroarenes using stoichiometric amounts of pinacolborane catalyzed by iridium complexes in an inert solvent. *Chem. Commun.* 2924–2925 (2003).

18. Mkhalid, I. A. I., Barnard, J. H., Marder, T. B., Murphy, J. M. & Hartwig, J. F. C−H Activation for the construction of C−B bonds. *Chem. Rev.* **110**, 890–931 (2009).

19. Preshlock, S. M. *et al.* High-throughput optimization of Ir-catalyzed C–H borylation: A tutorial for practical applications. *J. Am. Chem. Soc.* **135**, 7572–7582 (2013).

20. Larsen, M. A. & Hartwig, J. F. Iridium-catalyzed C–H borylation of heteroarenes: Scope, regioselectivity, application to late-stage functionalization, and mechanism. *J. Am. Chem. Soc.* **136**, 4287–4299 (2014).

21. Zhou, Y.-G. Asymmetric hydrogenation of heteroaromatic compounds. *Acc. Chem. Res.* **40**, 1357–1366 (2007).

22. Stahl, T., Ohki, Y., Tatsumi, K. & Oestreich, M. Catalytic generation of borenium ions by cooperative B–H bond activation: The elusive direct electrophilic borylation of nitrogen heterocycles with pinacolborane. *J. Am. Chem. Soc.* **135**, 10978–10981 (2013).

23. Esteruelas, M. A., Oliván, M. & Vélez, A. POP–Rhodium-promoted C–H and B–H bond activation and C–B bond formation. *Organometallics* **34**, 1911–1924 (2015).

24. Furukawa, T., Tobisu, M. & Chatani, N. C–H Functionalization at sterically congested positions by the platinum-catalyzed borylation of arenes. *J. Am. Chem. Soc.* **137**, 12211–12214 (2015).

25. Obligacion, J. V, Semproni, S. P. & Chirik, P. J. Cobalt-catalyzed C–H borylation. *J. Am. Chem. Soc.* **136**, 4133–4136 (2014).

26. Dombray, T., Werncke, C. G., Jiang, S., Grellier, M. & Vendier, L. Iron-catalyzed C−H borylation of arenes. *J. Am. Chem. Soc.* **137**, 4062–4065 (2015).

27. Furukawa, T., Tobisu, M. & Chatani, N. Nickel-catalyzed borylation of arenes and indoles via C–H bond cleavage. *Chem. Commun.* **51**, 6508–6511 (2015).

28. Bose, S. K. *et al.* Zinc-catalyzed dual C–X and C–H borylation of aryl halides. *Angew. Chem., Int. Ed.* **54**, 11843–11847 (2015).

29. Ingleson, M. A perspective on direct electrophilic arene borylation. *Synlett* **23**, 1411–1415 (2012).

30. De Vries, T. S., Prokofjevs, A. & Vedejs, E. Cationic tricoordinate boron intermediates: Borenium chemistry from the organic perspective. *Chem. Rev.* **112**, 4246–4282 (2012).

31. Yan, G., Huang, D. & Wu, X. Recent advances in C–B bond formation through a free radical pathway. *Adv. Synth. Catal.* **360**, 1040–1053 (2017).

32. Friese, F. W. & Studer, A. New avenues for C–B bond formation via radical intermediates. *Chem. Sci.* **10**, 8503–8518 (2019).

33. Xu, L. *et al.* Recent advances in catalytic C−H borylation reactions. *Tetrahedron* **73**, 7123–7157 (2017).

34. Waltz, K. M., He, X., Muhoro, C. & Hartwig, J. F. Hydrocarbon functionalization by transition metal boryls. *J. Am. Chem. Soc.* **117**, 11357–11358 (1995).

35. Cho, J. Y., Iverson, C. N. & Smith, M. R. Steric and chelate directing effects in aromatic borylation. *J. Am. Chem. Soc.* **122**, 12868–12869 (2000).

36. Cho, J. Y., Tse, M. K., Holmes, D., Maleczka, R. E. & Smith, M. R. Remarkably selective iridium catalysts for the elaboration of aromatic C–H bonds. *Science* **295**, 305–308 (2002).

37. Kuivila, H. G. & Nahabedian, K. V. Electrophilic displacement reactions. X. General acid catalysis in the protodeboronation of areneboronic acids. *J. Am. Chem. Soc.* **83**, 2159–2163 (1961).

38. Kuivila, H. G., Nahabedian, K. V. Electrophilic displacement reactions. XI. Solvent isotope effects in the protodeboronation of areneboronic acids. *J. Am. Chem. Soc.* **83**, 2164–2166 (1961).

39. Nahabedian, K. V. & Kuivila, H. G. Electrophilic displacement reactions. XII. Substituent effects in the protodeboronation of areneboronic acids. *J. Am. Chem. Soc.* **83**, 2167–2174 (1961).

40. Kuivila, H. G., Reuwer Jr., J. F. & Mangravite, J. A. Electrophilic displacement reactions: XV. Kinetics and mechanism of the base-catalyzed protodeboronation of areneboronic acids. *Can. J. Chem.* **41**, 3081–3090 (1963).

41. Cox, P. A., Leach, A. G., Campbell, A. D. & Lloyd-Jones, G. C. Protodeboronation of heteroaromatic, vinyl, and cyclopropyl boronic acids: pH−Rate profiles, autocatalysis, and disproportionation. *J. Am. Chem. Soc.* **138**, 9145–9157 (2016).

42. Tamura, H., Yamazaki, H., Sato, H. & Sakaki, S. Iridium-catalyzed borylation of benzene with diboron. Theoretical elucidation of catalytic cycle including unusual iridium(V) intermediate. *J. Am. Chem. Soc.* **125**, 16114–16126 (2003).

43. Boller, T. M. *et al.* Mechanism of the mild functionalization of arenes by diboron reagents catalyzed by iridium complexes. Intermediacy and chemistry of bipyridine-ligated iridium trisboryl complexes. *J. Am. Chem. Soc.* **127**, 14263–14278 (2005).

44. Press, L. P., Kosanovich, A. J., Mcculloch, B. J. & Ozerov, O. V. High-turnover aromatic C–H borylation catalyzed by POCOP-type pincer complexes of iridium. *J. Am. Chem. Soc.* **138**, 9487–9497 (2016).

45. Scott, J. S. *et al.* Optimisation of aqueous solubility in a series of G protein coupled receptor 119 (GPR119) agonists. *Med. Chem. Commun.* **4**, 95–100 (2013).

46. Lee, J. *et al.* Synthesis and structure-activity relationship of aminopyridines with substituted benzoxazoles as c-Met kinase inhibitors. *Bioorg. Med. Chem. Lett.* **22**, 4044–4048 (2012).

47. Marks, T. J. Surface-bound metal hydrocarbyls. Organometallic connections between heterogeneous and homogeneous catalysis. *Acc. Chem. Res.* **25**, 57–65 (1992).

48. Yang, X., Stern, C. L. & Marks, T. J. Cationic zirconocene olefin polymerization catalysts based on the organo-Lewis acid tris(pentafluorophenyl)borane. A synthetic, structural, solution dynamic, and polymerization catalytic study. *J. Am. Chem. Soc.* **116**, 10015–10031 (1994).

49. Erker, G. Tris(pentafluorophenyl)borane: a special boron Lewis acid for special reactions. *Dalton Trans.* 1883–1890 (2005).

50. Sabatini, M. T., Boulton, L. T. & Sheppard, T. D. Borate esters: Simple catalysts for the sustainable synthesis of complex amides. *Sci. Adv.* **3**, 1–9 (2017).

51. Burwell Jr, R. L. The cleavage of ethers. *Chem. Rev.* **54**, 615–685 (1954).

52. Noth, H. & Kolle, P. The chemistry of borinium and borenium ions. *Chem. Rev.* **85**, 399–418 (1985).

53. Olah, G. A. & Klumpp, D. A. *Superelectrophiles and Their Chemistry*. (Wiley, 2008).

54. Nöth, H., Staudigl, R. & Wagner, H. U. Contributions to the chemistry of boron. 121. Dicoordinate amidoboron cations. *Inorg. Chem.* **21**, 706–716 (1982).

55. Schneider, W. F., Bursten, B. E., Narula, C. K. & Nöth, H. Structure and bonding trends in two- and three-coordinate boron cations. *Inorg. Chem.* **30**, 3919–3927 (1991).

56. Courtenay, S., Mutus, J. Y., Schurko, R. W. & Stephan, D. W. The extended borinium cation: $[(tBu_3PN)_2B]^+$. *Angew. Chem., Int. Ed.* **41**, 498–501 (2002).

57. Shitov, O. P., Ioffe, S. L., Tartakovskii, V. A. & Novikov, S. S. Cationic boron complexes. *Russ. Chem. Rev.* **39**, 905–922 (1970).

58. Rudolph, R. W. *Boron hydride chemistry*. (Elsevier, 1975).

59. Prokofjevs, A., *et al.* Borenium ion catalyzed hydroboration of alkenes with N-heterocyclic carbene-boranes. *J. Am. Chem. Soc.* **134**, 12281–12288 (2012).

60. Pan, X., Boussonnière, A. & Curran, D. P. Molecular iodine initiates hydroborations of alkenes with N-heterocyclic carbene boranes. *J. Am. Chem. Soc.* **135**, 14433–14437 (2013).

61. Brauer, D. J., Bürger, H., Pawelke, G., Weuter, W. & Wilke, J. The reaction of (trifluoromethyl)dialkylaminoboranes with HF, HCl and HBr. X-ray structure investigation of the amineboranes $(CF_3)_2B(X)NHMe_2$, X = F and OH. *J. Organomet. Chem.* **329**, 293–304 (1987).

62. Piers, W. E., Bourke, S. C. & Conroy, K. D. Borinium, borenium, and boronium ions: synthesis, reactivity, and applications. *Angew. Chem., Int. Ed.* **44**, 5016–5036 (2005).

63. Kotz, J. C. & Post, E. W. Ferrocenylboranes. I. Preparation and properties of ferrocenyldichloroborane. *Inorg. Chem.* **9**, 1661–1669 (1970).

64. Ruf, W., Fueller, M. & Siebert, W. Metallocenborane. I. Zur reakton von ferrocen mit trihalogenboranen. *J. Organomet. Chem.* **64**, C45–C47 (1974).

65. Paetzold, P. & Hoffmann, J. Eine neue methode zur borylierung von alkylbenzol und polystyrol. *Chem. Ber.* **113**, 3724–3733 (1980).

66. Vedejs, E., Nguyen, T., Powell, D. R. & Schrimpf, M. R. Generation of reactive borenium ions in the 2,3-benzazaborolidine series. *Chem. Commun.* **4**, 2721–2722 (1996).

67. De Vries, T. S. & Vedejs, E. Electrophilic activation of Lewis base complexes of borane with trityl tetrakis(pentafluorophenyl)borate. *Organometallics* **26**, 3079–3081 (2007).

68. De Vries, T. S., Prokofjevs, A., Harvey, J. N. & Vedejs, E. Superelectrophilic intermediates in nitrogen-directed aromatic borylation. *J. Am. Chem. Soc.* **131**, 14679–14687 (2009).

69. Del Grosso, A., Pritchard, R. G., Muryn, C. A. & Ingleson, M. J. Chelate restrained boron cations for intermolecular electrophilic arene borylation. *Organometallics* **29**, 241–249 (2010).

70. Del Grosso, A., Singleton, P. J., Muryn, C. A. & Ingleson, M. J. Pinacol boronates by direct arene borylation with borenium cations. *Angew. Chem., Int. Ed.* **50**, 2150–2154 (2011).

71. Del Grosso, A., Helm, M. D., Solomon, S. A., Caras-Quintero, D. & Ingleson, M. J. Simple inexpensive boron electrophiles for direct arene borylation. *Chem. Commun.* **47**, 12459–12461 (2011).

72. Hurd, D. T. The reactions of diborane with hydrocarbons. *J. Am. Chem. Soc.* **70**, 2053–2055 (1948).

73. Muetterties, E. L. Synthesis of aryldichloroboranes. *J. Am. Chem. Soc.* **81**, 2597 (1959).

74. Muetterties, E. L. & Tebbe, F. N. Dichloroboronation of aromatic hydrocarbons. mechanistic aspects. *Inorg. Chem.* **7**, 2663–2664 (1968).

75. Depuy, C. H. *et al.* The gas phase ion chemistry of BH_2^+. *J. Am. Chem. Soc.* **120**, 5086–5092 (1998).

76. Narula, C. K. & Noth, H. Preparation and characterization of salts containing cations of tricoordinate boron. *Inorg. Chem.* **23**, 4147–4152 (1984).

77. Beckett, M. A., Brassington, D. S., Coles, S. J. & Hursthouse, M. B. Lewis acidity of tris(pentafluorophenyl) borane: crystal and molecular structure of $B(C_6F_5)_3$•$OPEt_3$. *Inorg. Chem. Commun.* **3**, 530–533 (2000).

78. Lambert, J. B., Zhang, S., Stern, C. L. & Huffman, J. C. Crystal structure of a silyl cation with no coordination to anion and distant coordination to solvent. *Science* **260**, 1917–1918 (1993).

79. Reed, C. A., Xie, Z., Bau, R. & Benesi, A. Closely approaching the silylium ion (R_3Si^+). *Science* **262**, 402–404 (1993).

80. Shapland, P. & Vedejs, E. Intramolecular hydroboration of unsaturated phosphine boranes. *J. Org. Chem.* **69**, 4094–4100 (2004).

81. Welch, G. C., Masuda, J. D. & Stephan, D. W. Phosphonium-borate zwitterions, anionic phosphines, and dianionic phosphonium-dialkoxides via tetrahydrofuran ring-opening reactions. *Inorg. Chem.* **45**, 478–480 (2006).

82. Noth, H. & Narula, C. K. Competition between adduct and cation formation in reactions between diorganylborane derivatives and pyridine or lutidines. *Inorg. Chem.* **24**, 2532–2539 (1985).

83. Ishiyama, T. & Miyaura, N. Metal-catalyzed reactions of diborons for synthesis of organoboron compounds. *Chem. Rec.* **3**, 271–280 (2004).

84. Ishida, N., Moriya, T., Goya, T. & Murakami, M. Synthesis of pyridine-borane complexes via electrophilic aromatic borylation. *J. Org. Chem.* **75**, 8709–8712 (2010).

85. Prokofjevs, A., Kampf, J. W. & Vedejs, E. A boronium ion with exceptional electrophilicity. *Angew. Chem., Int. Ed.* **50**, 2098–2101 (2011).

86. Tanaka, S., Saito, Y., Yamamoto, T. & Hattori, T. Electrophilic borylation of terminal alkenes with BBr_3/2,6-disubstituted pyridines. *Org. Lett.* **20**, 1828–1831 (2018).

87. Oda, S., Ueura, K., Kawakami, B. & Hatakeyama, T. Multiple electrophilic C–H borylation of arenes using boron triiodide. *Org. Lett.* **22**, 700–704 (2020).

88. Grundy, M. E., Yuan, K., Nichol, G. S. & Ingleson, M. J. Zinc catalysed electrophilic C–H borylation of heteroarenes. *Chem. Sci.* **12**, 8190–8198 (2021).

89. Ishiyama, T., Murata, M. & Miyaura, N. Palladium(0)-catalyzed cross-coupling reaction of alkoxydiboron with haloarenes: a direct procedure for arylboronic esters. *J. Org. Chem.* **60**, 7508–7510 (1995).

90. Chen, H., Schlecht, S., Semple, T. C. & Hartwig, J. F. Thermal, catalytic, regiospecific functionalization of alkanes. *Science* **287**, 1995–1997 (2000).

91. Ishiyama, T., Takagi, J., Hartwig, J. F. & Miyaura, N. A stoichiometric aromatic C–H borylation catalysed by iridium(I)/2,2'-bipyridine complexes at room temperature. *Angew. Chem., Int. Ed.* **41**, 3056–3058 (2002).

92. Zhang, L. & Jiao, L. Pyridine-catalyzed radical borylation of aryl halides. *J. Am. Chem. Soc.* **139**, 607–610 (2017).

93. Pinet, S., Liautard, V., Debiais, M. & Pucheault, M. Radical metal-free borylation of aryl iodides. *Synthesis* **49**, 4759–4768 (2017).

94. Atack, T. C. & Cook, S. P. Manganese-catalyzed borylation of unactivated alkyl chlorides. *J. Am. Chem. Soc.* **138**, 6139–6142 (2016).

95. Qiu, D. *et al.* Synthesis of pinacol arylboronates from aromatic amines: a metal-free transformation. *J. Org. Chem.* **78**, 1923–1933 (2013).

96. Liu, W., Yang, X., Gao, Y. & Li, C.-J. Simple and efficient generation of aryl radicals from aryl triflates: synthesis of aryl boronates and aryl iodides at room temperature. *J. Am. Chem. Soc.* **139**, 8621–8627 (2017).

97. Marciasini, L. D., Richy, N., Vaultier, M. & Pucheault, M. Iron-catalysed borylation of arenediazonium salts to give access to arylboron derivatives via aryl(amino)boranes at room temperature. *Adv. Synth. Catal.* **355**, 1083–1088 (2013).

98. Studer, A. & Curran, D. P. Organocatalysis and C–H activation meet radical- and electron-transfer reactions. *Angew. Chem., Int. Ed.* **50**, 5018–5022 (2011).

99. Sun, C.-L. *et al.* An efficient organocatalytic method for constructing biaryls through aromatic C–H activation. *Nat. Chem.* **2**, 1044–1049 (2010).

100. Liu, W. *et al.* Organocatalysis in cross-coupling: DMEDA-catalyzed direct C–H arylation of unactivated benzene. *J. Am. Chem. Soc.* **132**, 16737–16740 (2010).

101. Shirakawa, E., Itoh, K.-I., Higashino, T. & Hayashi, T. tert-Butoxide-mediated arylation of benzene with aryl halides in the presence of a catalytic 1,10-phenanthroline derivative. *J. Am. Chem. Soc.* **132**, 15537–15539 (2010).

102. Wang, G. *et al.* Homolytic cleavage of a B–B bond by the cooperative catalysis of two Lewis bases: computational design and experimental verification. *Angew. Chem., Int. Ed.* **55**, 5985–5989 (2016).

103. Viehe, H. G., Janousek, Z. & Merényi, R. The Captodative Effect. *Acc. Chem. Res.* **18**, 148–154 (1985).

104. Zhang, J., Wu, H.-H. & Zhang, J. Cesium carbonate mediated borylation of aryl iodides with diboron in methanol. *Eur. J. Org. Chem.* **2013**, 6263–6266 (2013).

105. Bose, S. K., Deiβsenberger, A., Eichhorn, A., Steel, P. G., Lin, Z. & Marder, T. B. Zinc-catalyzed dual C–X and C–H borylation of aryl halides. *Angew. Chem., Int. Ed.* **54**, 11843–11847 (2015).

106. Nguyen, V. D., Nguyen, V. T., Jin, S., Dang, H. T. & Larionov, O. V. Organoboron chemistry comes to light: recent advances in photoinduced synthetic approaches to organoboron compounds. *Tetrahedron* **75**, 584–602 (2019).

107. Mella, M. *et al.* Photoinduced, ionic meerwein arylation of olefins. *J. Org. Chem*. **66**, 6344–6352 (2001).

108. Budén, M. E., Guastavino, J. F. & Rossi, R. A. Room-temperature photoinduced direct C–H-arylation via base-promoted homolytic aromatic substitution. *Org. Lett.* **15**, 1174–1177 (2013).

109. Lu, S. C. *et al.* Intramolecular photochemical cross-coupling reactions of 3-acyl-2-haloindoles and 2-chloropyrrole-3-carbaldehydes with substituted benzenes. *Adv. Synth. Catal.* **351**, 2839–2844 (2009).

110. Mfuh, A. M., Doyle, J. D., Chhetri, B., Arman, H. D. & Larionov, O. V. Scalable, metal- and additive-free, photoinduced borylation of haloarenes and quaternary arylammonium salts. *J. Am. Chem. Soc.* **138**, 2985–2988 (2016).

111. Luo, Y.-R. *Comprehensive handbook of chemical bond energies*. (CRC Press, 2007).

112. Ollivier, C. & Renaud, P. Organoboranes as a source of radicals. *Chem. Rev.* **101**, 3415–3434 (2001).

113. Chen, K., Zhang, S., He, P. & Li, P. Efficient metal-free photochemical borylation of aryl halides under batch and continuous-flow conditions. *Chem. Sci.* **7**, 3676–3680 (2016).

114. Salami, J. & Crews, C. M. Waste disposal – an attractive strategy for cancer therapy. *Science* **355**, 1163–1167 (2017).

115. Gu, S., Cui, D., Chen, X., Xiong, X. & Zhao, Y. PROTACs: an emerging targeting technique for protein degradation in drug discovery. *BioEssays* **40**, 1700247 (2018).

116. Churcher, I. Protac-induced protein degradation in drug discovery: breaking the rules or just making new ones? *J. Med. Chem.* **61**, 444–452 (2018).

117. Gao, M., Thorpe, S. B. & Santos, W. L. sp^2-sp^3 Hybridized mixed diboron: synthesis, characterization, and copper-catalyzed β-boration of α,β-unsaturated conjugated compounds. *Org. Lett.* **11**, 3478–3481 (2009).

118. Gao, M. *et al.* Structure and reactivity of a preactivated sp^2-sp^3 diboron reagent: catalytic regioselective boration of α,β-unsaturated conjugated compounds. *J. Org. Chem.* **76**, 3997–4007 (2011).

119. Minisci, F., Vismara, E. & Fontana, F. Recent developments of free-radical substitutions of heteroaromatic bases. *Heterocycles* **28**, 489–519 (1989).

120. Minisci, F. Novel applications of free-radical reactions in preparative organic chemistry. *Synthesis* **1973**, 1–24 (1973).

121. Minisci, F., Bernardi, R., Bertini, F., Galli, R. & Perchinijmmo, M. Nucleophilic character of alkyl radicals—VI: a new convenient selective alkylation of heteroaromatic bases. *Tetrahedron* **27**, 3575–3579 (1971).

122. Duncton, M. A. J. Minisci reactions: versatile CH-functionalizations for medicinal chemists. *Med. Chem. Commum.* **2**, 1135–1161 (2011).

123. Bose, S. K. *et al.* First-row d-block element-catalyzed carbon-boron bond formation and related processes. *Chem. Rev.* **121**, 13238–13341 (2021).

124. Zhang, L. & Jiao, L. Super electron donors derived from diboron. *Chem. Sci.* **9**, 2711–2722 (2018).

125. Murphy, J. A. Discovery and development of organic super-electron-donors. *J. Org. Chem.* **79**, 3731–3746 (2014).

126. Kim, J. H. *et al.* A radical approach for the selective C–H borylation of azines. *Nature* **595**, 677–684 (2021).

127. Takagi, J., Sato, K., Hartwig, J. F., Ishiyama, T. & Miyaura, N. Iridium-catalyzed C–H coupling reaction of heteroaromatic compounds with bis(pinacolato)diboron: regioselective synthesis of heteroarylboronates. *Tetrahedron Lett.* **43**, 5649–5651 (2002).

128. Chotana, G. A., Kallepalli, V. A., Maleczka, R. E. & Smith, M. R. Iridium-catalyzed borylation of thiophenes: versatile, synthetic elaboration founded on selective C–H functionalization. *Tetrahedron* **64**, 6103–6114 (2008).

129. Ishiyama, T., Isou, H., Kikuchi, T. & Miyaura, N. ortho-C–H Borylation of benzoate esters with bis(pinacolato)diboron catalyzed by iridium-phosphine complexes. *Chem. Commun.* **46**, 159–161 (2010).

130. Morris, J., Steel, P. G. & Marder, T. B. A one-pot, single-solvent process for tandem, catalyzed C–H borylation–Suzuki-Miyaura cross-coupling sequences. *Synlett* 147–150 (2009).

131. Tan, Y. & Ghandi, K. Kinetics and mechanism of pyrrole chemical polymerization. *Synth. Met.* **175**, 183–191 (2013).

132. Reddy, L. A. *et al.* Synthesis and process optimization of amtolmetin: an antiinflammatory agent. *Org. Process. Res. Dev.* **14**, 362–368 (2010).

133. Sadler, S. A. *et al.* Multidirectional synthesis of substituted indazoles via iridium-catalyzed C–H borylation. *J. Org. Chem.* **80**, 5308–5314 (2015).

134. Michael, J. P. Quinoline, quinazoline and acridone alkaloids. *Nat. Prod. Rep.* **25**, 166–187 (2008).

135. Iwai, T. & Sawamura, M. Transition-metal-catalyzed site-selective C–H functionalization of quinolines beyond C2 selectivity. *ACS Catal.* **5**, 5031–5040 (2015).

136. Stephens, D. E. & Larionov, O. V. Recent advances in the C–H-functionalization of the distal positions in pyridines and quinolines. *Tetrahedron* **71**, 8683–8716 (2015).

137. Tajuddin, H. *et al.* Iridium-catalyzed C–H borylation of quinolines and unsymmetrical 1,2-disubstituted benzenes: insights into steric and electronic effects on selectivity. *Chem. Sci.* **3**, 3505–3515 (2012).

138. Harrisson, P., Morris, J., Marder, T. B. & Steel, P. G. Microwave-accelerated iridium-catalyzed borylation of aromatic C–H Bonds. *Org. Lett.* **11**, 3586–3589 (2009).

139. Fischer Emil & Speier, A. Darstellung der Ester. *Ber. Dtsch. Chem. Ges.* **28**, 3252–3258 (1895).

140. Zurro, M., Asmus, S., Beckendorf, S., Mück-Lichtenfeld, C. & Mancheño, O. G. Chiral helical oligotriazoles: New class of anion-binding catalysts for the asymmetric dearomatization of electron-deficient N-heteroarenes. *J. Am. Chem. Soc.* **136**, 13999–14002 (2014).

141. Sadler, S. A. *et al.* Iridium-catalyzed C–H borylation of pyridines. *Org. Biomol. Chem.* **12**, 7318–7327 (2014).

142. Wang, W.-B., Lu, S.-M., Yang, P.-Y., Han, X.-W. & Zhou, Y.-G. Highly enantioselective iridium-catalyzed hydrogenation of heteroaromatic compounds, quinolines. *J. Am. Chem. Soc.* **125**, 10536–10537 (2003).

143. Dobereiner, G. E. *et al.* Iridium-catalyzed hydrogenation of N-heterocyclic compounds under mild conditions by an outer-sphere pathway. *J. Am. Chem. Soc.* **133**, 7547–7562 (2011).

144. Wang, D.-S., Chen, Q.-A., Lu, S.-M. & Zhou, Y.-G. Asymmetric hydrogenation of heteroarenes and arenes. *Chem. Rev.* **112**, 2557–2590 (2011).

145. Murahashi, S.-I., Imada, Y. & Hirai, Y. Rhodium catalyzed hydrogenation of quinolines and isoquinolines under water-gas shift conditions. *Bull. Chem. Soc. Jpn.* **62**, 2968–2976 (1989).

146. Wu, J. *et al.* Robust cyclometallated Ir(III) catalysts for the homogeneous hydrogenation of N-heterocycles under mild conditions. *Chem. Commun.* **49**, 7052–7054 (2013).

147. Kim, E., Jeon, H. J., Park, S. & Chang, S. Double hydroboration of quinolines via borane catalysis: diastereoselective one pot synthesis of 3-hydroxytetrahydroquinolines. *Adv. Synth. Catal.* **362**, 308–313 (2020).

148. Altiti, A. S., Cheng, K. F., He, M. & Al-Abed, Y. β-Hydroxy-tetrahydroquinolines from quinolines using chloroborane: synthesis of the peptidomimetic FISLE-412. *Chem. Eur. J.* **23**, 10738–10743 (2017).

149. Cook, X. A. F., de Gombert, A., McKnight, J., Pantaine, L. R. E. & Willis, M. C. The 2-pyridyl problem: challenging nucleophiles in cross-coupling arylations. *Angew. Chem., Int. Ed.* **60**, 11068–11091 (2021).

150. Yoshida, H., Takemoto, Y., Kamio, S., Osaka, I. & Takaki, K. Copper-catalyzed direct borylation of alkyl, alkenyl and aryl halides with B(dan). *Org. Chem. Front.* **4**, 1215–1219 (2017).

151. Li, J., Seki, M., Kamio, S. & Yoshida, H. Transition metal-free B(dan)-installing reaction (dan: naphthalene-1,8-diaminato): H–B(dan) as a B(dan) electrophile. *Chem. Commun.* **56**, 6388–6391 (2020).

152. Iwadate, N. & Suginome, M. Synthesis of masked haloareneboronic acids via iridium-catalyzed aromatic C–H borylation with 1,8-naphthalenediaminatoborane (danBH). *J. Organomet. Chem.* **694**, 1713–1717 (2009).

153. Phipps, R. J. & Gaunt, M. J. A meta-selective copper-catalyzed C–H bond arylation. *Science* **323**, 1593–1597 (2009).

154. Liégault, B., Petrov, I., Gorelsky, S. I. & Fagnou, K. Modulating reactivity and diverting selectivity in palladium-catalyzed heteroaromatic direct arylation through the use of a chloride activating/blocking group. *J. Org. Chem.* **75**, 1047–1060 (2010).

155. Noguchi, H., Hojo, K. & Suginome, M. Boron-masking strategy for the selective synthesis of oligoarenes via iterative Suzuki-Miyaura coupling. *J. Am. Chem. Soc.* **129**, 758–759 (2007).

156. Cid, J., Carbõ, J. J. & Fernández, E. A clear-cut example of selective Bpin–Bdan activation and precise Bdan transfer on boron conjugate addition. *Chem. Eur. J.* **20**, 3616–3620 (2014).

157. Pubill-Ulldemolins, C., Bonet, A., Gulyás, H., Bo, C. & Fernández, E. Essential role of phosphines in organocatalytic β-boration reaction. *Org. Biomol. Chem.* **10**, 9677–9682 (2012).

158. Iwadate, N. & Suginome, M. Differentially protected diboron for regioselective diboration of alkynes: internal-selective cross-coupling of 1-alkene-1,2-diboronic acid derivatives. *J. Am. Chem. Soc.* **132**, 2548–2549 (2010).

159. Segawa, Y., Yamashita, M. & Nozaki, K. Boryl anion attacks transition-metal chlorides to form boryl complexes: syntheses, spectroscopic, and structural studies on group 11 borylmetal complexes. *Angew. Chem., Int. Ed.* **46**, 6710–6713 (2007).

160. Zinser, C. M. *et al.* Synthesis and reactivity of [Au(NHC)(Bpin)] complexes. *Chem. Commun.* **55**, 6799–6802 (2019).

161. Hopkinson, M. N., Gee, A. D. & Gouverneur, V. Au^{I}/Au^{III} catalysis: an alternative approach for C–C oxidative coupling. *Chem. Eur. J.* **17**, 8248–8262 (2011).

162. Nijamudheen, A. & Datta, A. Gold-catalyzed cross-coupling reactions: an overview of design strategies, mechanistic studies, and applications. *Chem. Eur. J.* **26**, 1442–1487 (2020).

163. Ball, L. T., Lloyd-Jones, G. C. & Russell, C. A. Gold-catalyzed direct arylation. *Science* **337**, 1644–1648 (2012).

164. Cambeiro, X. C., Boorman, T. C., Lu, P. & Larrosa, I. Redox-controlled selectivity of C–H activation in the oxidative cross-coupling of arenes. *Angew. Chem., Int. Ed.* **52**, 1781–1784 (2013).

165. Ball, L. T., Lloyd-Jones, G. C. & Russell, C. A. Gold-catalyzed oxidative coupling of arylsilanes and arenes: origin of selectivity and improved precatalyst. *J. Am. Chem. Soc.* **136**, 254–264 (2014).

166. Cambeiro, X. C., Ahlsten, N. & Larrosa, I. Au-catalyzed cross-coupling of arenes via double C−H activation. *J. Am. Chem. Soc.* **137**, 15636–15639 (2015).

167. Corrie, T. J. A., Ball, L. T., Russell, C. A. & Lloyd-Jones, G. C. Au-catalyzed biaryl coupling to generate 5- to 9-membered rings: turnover-limiting reductive elimination versus π-complexation. *J. Am. Chem. Soc.* **139**, 245–254 (2017).

168. Hofer, M., Genoux, A., Kumar, R. & Nevado, C. Gold-catalyzed direct oxidative arylation with boron coupling partners. *Angew. Chem., Int. Ed.* **56**, 1021–1025 (2017).

169. Liu, J.-R. *et al.* C−H acidity and arene nucleophilicity as orthogonal control of chemoselectivity in dual C−H bond activation. *Org. Lett.* **21**, 2360–2364 (2019).

170. Anastasia, L. & Negishi, E. Palladium-catalysed Aryl-Aryl Coupling. in *Handbook of Organopalladium Chemistry for Organic Synthesis* (ed. Negishi, E.) 311–334 (John Wiley & Sons, 2002).

171. Alberico, D., Scott, M. E. & Lautens, M. Aryl−aryl bond formation by transition-metal-catalyzed direct arylation. *Chem. Rev.* **107**, 174–238 (2007).

172. Lu, P., Boorman, T. C., Slawin, A. M. Z. & Larrosa, I. Gold(I)-mediated C–H activation of arenes. *J. Am. Chem. Soc.* **132**, 5580–5581 (2010).

173. Gaillard, S., Cazin, C. S. J. & Nolan, S. P. N-Heterocyclic carbene gold(I) and copper(I) complexes in C–H bond activation. *Acc. Chem. Res.* **45**, 778–787 (2012).

174. Ahlsten, N., Perry, G. J. P., Cambeiro, X. C., Boorman, T. C. & Larrosa, I. A silver-free system for the direct C–H auration of arenes and heteroarenes from gold chloride complexes. *Catal. Sci. Technol.* **3**, 2892–2897 (2013).

175. Kharasch, M. S. & Isbell, H. S. The chemistry of organic gold compounds. III. Direct introduction of gold into the aromatic nucleus. *J. Am. Chem. Soc.* **53**, 3053–3059 (1931).

176. Hashmi, A. S. K., Schwarz, L., Choi, J.-H. & Frost, T. M. A new gold-catalyzed C–C bond formation. *Angew. Chem., Int. Ed.* **39**, 2285–2288 (2000).

177. Partyka, D. V., Zeller, M., Hunter, A. D. & Gray, T. G. Relativistic functional groups: aryl carbon-gold bond formation by selective transmetalation of boronic acids. *Angew. Chem., Int. Ed.* **45**, 8188–8191 (2006).

178. Miyaura, N. & Suzuki, A. Palladium-catalyzed cross-coupling reactions of organoboron compounds. *Chem. Rev.* **95**, 2457–2483 (1995).

179. Pfennig, V. S., Villella, R. C., Nikodemus, J. & Bolm, C. Mechanochemical grignard reactions with gaseous CO_2 and sodium methyl carbonate. *Angew. Chem., Int. Ed.* **61**, e202116514 (2022).

180. Feng, Q. & Song, Q. Aldehydes and ketones formation: copper-catalyzed aerobic oxidative decarboxylation of phenylacetic acids and α-hydroxyphenylacetic acids. *J. Org. Chem.* **79**, 1867–1871 (2014).

181. Bernardo, J. R. & Fernandes, A. C. Deoxygenation of carbonyl compounds using an alcohol as an efficient reducing agent catalyzed by oxo-rhenium complexes. *Green Chem.* **18**, 2675–2681 (2016).

182. Lawrence, S. A. *Amines: Synthesis, Properties and Applications*. (Cambridge University Press, 2008).

183. Harrison, I. R. *et al.* 1,3,5-Triazapenta-1,4-dienes: chemical aspects of a new group of pesticides. *Pestic. Sci.* **4**, 901–910 (1973).

184. Wu, L. & Burgess, K. Fluorescent amino- and thiopyronin dyes. *Org. Lett.* **10**, 1779–1782 (2008).

185. Irons, J. Fluvoxamine in the treatment of anxiety disorders. *Neuropsychiatr. Dis. Treat.* **1**, 289–99 (2005).

186. Dopheide, J. A. & Pliszka, S. R. Attention-deficit–hyperactivity disorder: an update. *Pharmacotherapy* **29**, 656–679 (2009).

187. Hofmann, A. W. Von. V. Researches regarding the molecular constitution of the volatile organic bases. *Phil. Trans. R. Soc.* **140**, 93–131 (1850).

188. Abdel-Magid, A. F., Carson, K. G., Harris, B. D., Maryanoff, C. A. & Shah, R. D. Reductive amination of aldehydes and ketones with sodium triacetoxyborohydride. Studies on direct and indirect reductive amination procedures. *J. Org. Chem.* **61**, 3849–3862 (1996).

189. Salvatore, R. N., Yoon, C. H. & Jung, K. W. Synthesis of secondary amines. *Tetrahedron* **57**, 7785–7811 (2001).

190. Basu, B., Jha, S., Bhuiyan, M. M. H. & Das, P. A simple protocol for direct reductive amination of aldehydes and ketones using potassium formate and catalytic palladium acetate. *Synlett* **4**, 555–557 (2003).

191. Guillena, G., Ramón, D. J. & Yus, M. Hydrogen autotransfer in the N-alkylation of amines and related compounds using alcohols and amines as electrophiles. *Chem. Rev.* **110**, 1611–1641 (2010).

192. Bhattacharyya, S., Pathak, U., Mathur, S., Vishnoi, S. & Jain, R. Selective N-alkylation of primary amines with R-NH_2•HBr and alkyl bromides using a competitive deprotonation/protonation strategy. *RSC Adv.* **4**, 18229–18233 (2014).

193. Choi, G. & Hong, S. H. Selective monomethylation of amines with methanol as the C_1 source. *Angew. Chem., Int. Ed.* **57**, 6166–6170 (2018).

194. Coomber, C. E. & Diorazio, L. J. N-Alkylation of α-amino esters and amides through hydrogen borrowing. *Eur. J. Org. Chem.* e202200152, (2022).

195. Dowsell, R., Graff, T. A. & Sheppard, T. D. Unpublished work.

196. Xie, Q. & Dong, G. Aza-Matteson reactions via controlled mono- and double-methylene insertions into nitrogen−boron bonds. *J. Am. Chem. Soc.* **143**, 14422–14427 (2021).

197. Biedrzycki, M., Scouten, W. H. & Biedrzycka, Z. Derivatives of tetrahedral boronic acids. *J. Organomet. Chem.* **431**, 255–270 (1992).

198. Nizioł, J. *et al.* Synthesis, reactivity and biological activity of N(4)-boronated derivatives of 2′-deoxycytidine. *Bioorg. Med. Chem.* **22**, 3906–3912 (2014).

199. Miura, W., Hirano, K. & Miura, M. Rhodium-catalyzed C6-selective C–H borylation of 2-pyridones. *Org. Lett.* **18**, 3742–3745 (2016).

200. Ming, W., Liu, X., Friedrich, A., Krebs, J. & Marder, T. B. The Borono-Strecker reaction: synthesis of α-aminoboronates via a multicomponent reaction of carbonyl compounds, amines, and B_2pin_2. *Org. Lett.* **22**, 365–370 (2020).

201. Matteson, D. S. & Majumdar, D. α-Chloro boronic esters from homologation of boronic esters. *J. Am. Chem. Soc.* **102**, 7588–7590 (1980).

202. Gulle, S. & Ergun, Y. Synthesis of new precursors for the carbazole alkaloids. *Asian J. Chem.* **22**, 5517–5522 (2010).

203. Yang, C. *et al.* Alkylboronic esters from copper-catalyzed borylation of primary and secondary alkyl halides and pseudohalides. *Angew. Chem., Int. Ed.* **51**, 528–532 (2012).

204. Xu, Y., Gao, C., Andreásson, J. & Grøtli, M. Synthesis and photophysical characterization of azoheteroarenes. *Org. Lett.* **20**, 4875–4879 (2018).

205. Ono, I. & Hata, N. Photochemical reactions of ethoxycarbonyl-substituted quinolines. *Bull. Chem. Soc. Jpn.* **60**, 2891–2897 (1987).

206. Caserío Jr, F. F., Cavallo, J. J. & Wagner, R. I. Preparation of 8-bora-7,9-diazaro-peri-naphthene and derivatives. *J. Org. Chem.* **26**, 2157–2158 (1961).

207. Houlihan, W. J., Parrino, V. A., Uike, Y. Lithiation of N-(2-alkylphenyl)alkanamides and related compounds. A modified Madelung indole synthesis *J. Org. Chem.* **46**, 4511–4515 (1981).

208. Gemoets, H. P. L., Laudadio, G., Verstraete, K., Hessel, V. & Noël, T. A modular flow design for the meta-selective C−H arylation of anilines. *Angew. Chem., Int. Ed.* **56**, 7161–7165 (2017).

209. Roth, K. E. & Blum, S. A. Relative kinetic basicities of organogold compounds. *Organometallics* **29**, 1712–1716 (2010).

210. Nicholls, L. D. M. & Wennemers, H. Synergistic peptide and gold catalysis: enantioselective addition of branched aldehydes to allenamides. *Chem. Eur. J.* **27**, 17559–17564 (2021).

211. Chakrabarti, K., Mishra, A., Panja, D., Paul, B. & Kundu, S. Selective synthesis of mono- and di-methylated amines using methanol and sodium azide as C1 and N1 sources. *Green Chem.* **20**, 3339–3345 (2018).

212. Buonomo, J. A., Cole, M. S., Eiden, C. G. & Aldrich, C. C. 1,3-Diphenyldisiloxane enables additive-free redox recycling reactions and catalysis with triphenylphosphine. *Synthesis* **52**, 3583–3594 (2020).

213. Xu, Z., Chai, L. & Liu, Z. Free-radical-promoted site-selective C−H silylation of arenes by using hydrosilanes. *Org. Lett.* **19**, 5573–5576 (2017).

214. Flinker, M. *et al.* Efficient water reduction with sp^3-sp^3 diboron(4) compounds: application to hydrogenations, H–D exchange reactions, and carbonyl reductions. *Angew. Chem., Int. Ed.* **56**, 15910–15915 (2017).

215. Barron, P. P., Engelhardt, L. M., Healy, P. C., Oddy, J. & White, A. H. Lewis-base adducts of group 11 metal(I) compounds. XXVI. Solid-state cross-polarization magic-angle-spinning ^{31}P N.M.R. and structural studies on 1:1 adducts of triphenylphosphine with gold(I) salts. *Aust. J. Chem.* **40**, 1545–1555 (1987).

216. Li, N., Shen, J. & Liu, X. Hydrolysis of B_2pin_2 over Pd/C catalyst: high efficiency, mechanism, and in situ tandem reaction. *Eur. J. Inorg. Chem.* 2797–2800 (2021).

217. Tse, M. K., Cho, J.-Y. & Smith, M. R. Regioselective aromatic borylation in an inert solvent. *Org. Lett.* **3**, 2831–2833 (2001).

6 Appendix

6.1 Single crystal X-ray diffraction measurements

The diffraction data for **94** were collected on a four-circle *Agilent SuperNova* (Dual Source) single crystal X-ray diffractometer using a micro-focus CuK_α X-ray beam (λ = 1.54184 Å) and an *Atlas* CCD detector. The sample temperatures were controlled with an *Oxford Instruments* cryojet.

All data were processed using the *CrysAlis*^{Pro}.[I] The crystal structures were solved with the *SHELXT* programme,[II] used within the *Olex2* software suite,[III] and refined by least squares on the basis of F^2 with the *SHELXL*[IV] programme using the *ShelXle* graphical user interface.[V] All non-hydrogen atoms were refined anisotropically by the full-matrix least-squares method. Hydrogen atoms associated with carbon atoms were refined isotropically [U_{iso}(H) = 1.2U_{eq}(C)] in geometrically constrained positions.

Table 6.1. Crystallographic information and refinement parameters for **94.**

94 (SCXRD)	
empirical formula	$C_{24}H_{28}N_6O_7$
M_r / g mol^{-1}	512.52
crystal system	orthorhombic
space group	*Pnma*
a / Å	7.2385(4)
b / Å	9.9560(6)
c / Å	10.9548(7)
α / °	76.357(5)
β / °	89.805(5)
γ / °	84.418(5)
V / Å^3	763.40(8)
Z	2
ρ_{calc} / g cm^{-3}	1.123
T / K	150.0(1)
μ / mm^{-1}	0.628
F(000)	284
crystal size / mm^3	0.19 × 0.14 × 0.04
radiation	CuK_α (λ = 1.54184 Å)
2*θ* range for data collection / °	4.154−66.569
index ranges	−8 ≤ *h* ≤ 8 −11 ≤ *k* ≤ 11 −12 ≤ *l* ≤ 13
number of collected reflections	10940
unique reflections	2694
number of unique	2156 [$I > 2\sigma(I)$]

reflections	
R_{int}	0.0402
$R(F)$, $F > 2\sigma(F)$	0.0393
$wR(F^2)$, $F > 2\sigma(F)$	0.1001
$R(F)$, all data	0.0514
$wR(F^2)$, all data	0.1076
Δ_r (max., min.) e Å^{-3}	0.263/−0.197

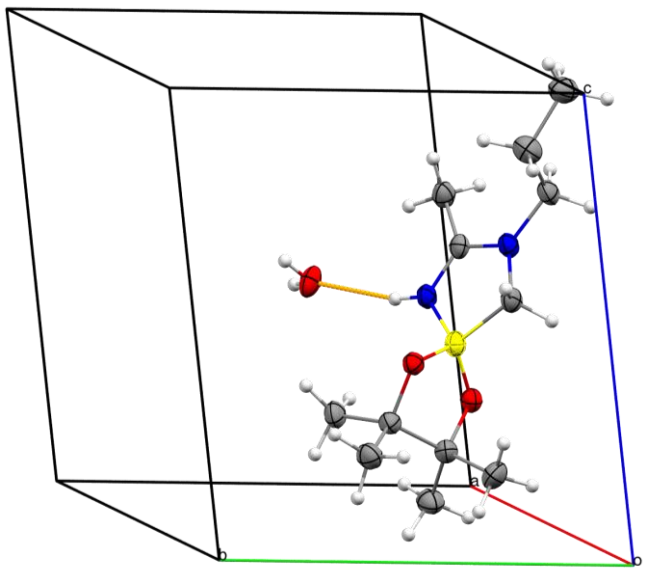

Figure 6.1: The asymmetric unit of compound **94**. The thermal ellipsoids are drawn at the 50% probability level. Colour scheme: carbon – dark grey, hydrogen – white, boron – yellow, nitrogen – blue, oxygen – red.

References

I. *CrysAllisPro*, *Agilent Technologies Inc.* (2014).

II. Sheldrick, G. M. SHELXT – Integrated space-group and crystal-structure determination. *Acta Crystallogr. A.* **64**, 3–8 (2015).

III. Dolomanov, O. V., Bourhis, L. J., Gildea, R. J., Howard, J. A. K. & Puschmann, H. OLEX2: a complete structure solution, refinement and analysis program. *J. Appl. Cryst.* **42**, 339–341 (2009).

IV. Sheldrick, G. M. Crystal structure refinement with SHELXL. *Acta Crystallogr. C.* **71**, 3–8 (2015).

V. Hübschle, C. B., Sheldrick, G. M. & Dittrich, B. ShelXle: a Qt graphical user interface for SHELXL. *J. Appl. Cryst.* **44**, 1281–1284 (2011).